Semisynthetic Pincer Metalloenzymes:

A Match between Organometallic and Protein Building Blocks

Birgit Wieczorek

Semisynthetic Pincer Metalloenzymes: A Match between Organometallic and Protein Building Blocks

Semisynthetische Pincer Metaalenzymen: Het Samenpassen van Organometaal- en Proteinbouwstenen

(met een samenvatting in het Nederlands)

(with a summary in English)

Proefschrift

ter verkrijging van de graad van doctor aan de Universiteit Utrecht op gezag van de rector magnificus, prof. dr. J.C. Stoof, ingevolge het besluit van het college voor promoties in het openbaar te verdedigen op woensdag 7 oktober 2009 des ochtends te 10.30 uur

door

Birgit Wieczorek

geboren op 4 maart 1980 te Mainz, Duitsland

Promotoren: Prof. dr. G. van Koten
Prof. dr. R. J. M. Klein Gebbink
Prof. dr. M. R. Egmond

Semisynthetic Pincer Metalloenzymes:

A Match between Organometallic and Protein Building Blocks

Colofon

Wieczorek, Birgit

Title: Semisynthetic Pincer Metalloenzymes: A Match between Organometallic and Protein Building Blocks

Utrecht, Utrecht University, Faculty of Science

Ph.D. thesis Utrecht University – with ref. – with summary in Dutch

ISBN: 978-90-393-51734

Circulation: 350

Printer: Ipskamp Drukkers

The work described in this Ph.D. thesis was carried out at the Chemical Biology and Organic Chemistry Group, Workgroup Organic Chemistry, Faculty of Science, Utrecht University, the Netherlands.

TABLE OF CONTENTS

PREFACE

Aim and Scope of this Thesis

Recently, the synthetic modification of proteins by transition metal complexes has gained a lot of attention.[1-4] By combining the special properties of transition metal complexes (rich coordination chemistry, subtle tuning of reactivities, versatile applicability) with those of proteins (chiral molecules with high selectivity, reactivity and versatility) novel hybrid transition metal-protein constructs have been synthesized. These semisynthetic biometal materials can be used in various applications in such diverse areas as *e.g.* catalysis,[5-9] protein labeling, profiling studies[2, 3, 10, 11] and medical research.[1, 4] In these attractive and relevant fields of research new biomaterials with unique properties are created aided by an efficient merger of expertise in coordination chemistry, organometallic chemistry and biochemistry.

Due to recent advances in protein chemistry, synthetic chemists can use the detailed knowledge of protein structure and function to modify the protein of choice with a desired synthetic moiety. In principle, many protein modification strategies are feasible, based on the chemical modification step and the structural features of the protein. In the literature, different covalent and non-covalent protein modification strategies have been reported, which will be highlighted here in some detail (*vide infra*).

A very popular target for the application of the non-covalent method for protein modification is the biotin-avidin system, in which the strong interaction between biotin and (strept)avidin is used for the introduction of various organometallic complexes by using a functionalized biotin molecule (Figure 1a). The resulting semisynthetic metalloproteins have been used, *e.g.* in hydrogenation catalysis,[12] and luminescent protein labelling.[13]

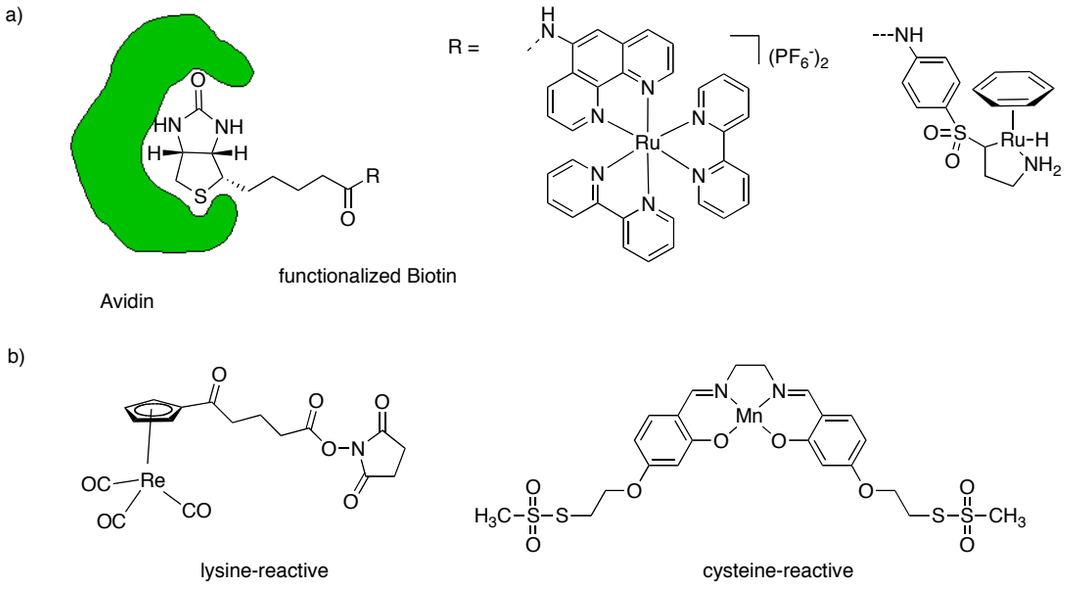

Figure 1: a) Semisynthetic metalloproteins based on the biotin-avidin technology,[12, 13] b) examples of transition metal complexes with lysine-[14] and cysteine-reactive[15] functional groups for covalent anchoring to specific amino acid residues in proteins.

Several other non-covalent protein modification strategies have been reported as well, such as the reconstitution of apo-myoglobin, haemoglobin or horseradish peroxidase by chemically modified co-factors with the aim to generate enantioselective oxidation catalysts.[8, 9] Antibody proteins as hosts for synthetic hapten molecules containing a transition metal complex have also been used successfully to obtain oxidation catalysts for various substrates.[16]

The covalent modification of proteins by synthetic transition metal complexes has mainly been based on functional groups reacting with specific amino acids residues, like *e.g.* cysteine, lysine or tyrosine residues.[17] An example of a lysine-reactive rhenium complex for diagnostic protein labeling[14] is shown in Figure 1b. A synthetic salen co-factor with two cysteine-reactive groups for the covalent reconstitution of apo-myoglobin (Figure 1b) has been successfully applied to make a hybrid catalyst for an enantioselective sulfoxidation reaction.[15]

Because often more than one amino acid residue in a protein is available for modification, in some cases the site-specific attachment of synthetic molecules to proteins via this approach appeared problematic. Therefore, several groups have made use of a site-directed approach, in which the catalytically active site of an enzyme is addressed to covalently anchor a transition metal complex to an enzyme. A very popular target enzyme in this respect is papain, which possesses a highly nucleophilic, catalytically active cysteine residue in the active site. Various transition metal complexes have been attached to the papain active site, including several

cyclopentadienyl metal complexes as heavy atom probes for proteases[1] and a rhodium hydrogenation[18] and a manganese salen oxidation catalyst.[19]
The fact that serine proteases are inhibited by aryl sulfonyl fluorides that covalently bind to the active site serine has been exploited by several groups. Already in the late 1960s several mercury sulfonyl fluorides for heavy atom labeling were developed.[20, 21]
All serine hydrolases, such as lipases, esterases and proteases, are known to possess a catalytic triad consisting of an Asp/Glu, His and a Ser residue, and they are known to be irreversibly and covalently inhibited by various phosphonate esters.[22] The groups of Reetz[19] and Van Koten[23, 24] have developed different phosphonate inhibitors containing a transition metal complex which have specific properties as catalysts,[19, 25] building blocks in supramolecular chemistry and sensoring materials.[25] A typical example is the organometallic ECE-pincer metal phosphonate inhibitor (Figure 2), which is also the subject of study in this thesis.[23]

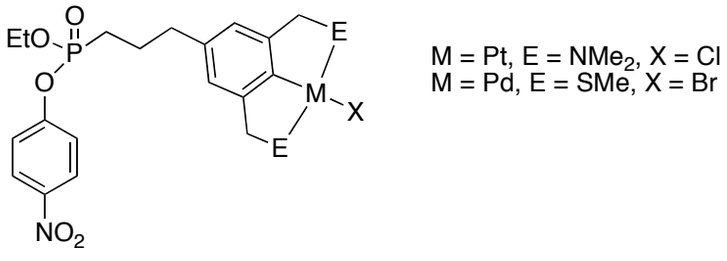

Figure 2: Structure of an ECE-pincer metal phosphonate complex as an irreversible inhibitor of serine hydrolases.[23]

The ECE-pincer metal complexes are a class of very well-studied, stable transition metal complexes with high stabilities and a wide range of applications. Among others they have been used for the modification of polymers, dendrimers, carbohydrates, peptides and, very recently, proteins.[23-25] Due to their high stabilities and their successful use as catalysts, building blocks in coordination chemistry and heavy metal atom labels,[25] ECE-pincer metal complexes were expected to be the ideal target molecules for the modification of various proteins. This thesis gives a description of the synthesis of several transition metal complex-lipase hybrids and shows their application as structural probes and building blocks in coordination chemistry, as catalysts, and heavy metal atom labels.

In *Chapter 1* an overview of the reported chemistry of bioorganometallic pincer complexes is given, which highlights the high stability and the versatility of ECE-pincer metal complexes as catalysts, supramolecular building blocks, biomarkers and sensors in a biological setting.
The analysis of the structural features of various ECE-pincer metal cutinase hybrids in the solid state is presented in *Chapter 2*. Several crystal structures demonstrate that

the pincer metal complex is situated at the surface of the protein. This structural information is used as a starting point for the coordination and catalytic studies reported in *Chapters 4-5*. The molecular geometries of the hybrids in the resolved crystal structures reveal that, depending on their structural features, very similar ECE-pincer metal phosphonate inhibitors can bind to the active site of cutinase with opposite stereochemistry. A kinetic study, which investigates the differences in inhibitory activity for the enantiomers of two different ECE-pincer metal complexes is presented in *Chapter 3*.

Chapter 4 describes a study of the coordination chemistry between a cutinase-embedded cationic NCN-pincer platinum complex and various phosphine ligands. ES-mass spectrometry and NMR spectroscopy indicate that several phosphines do coordinate to the protein-embedded NCN-pincer platinum centre thus showing that the metal centre is still accessible for ligands or substrate molecules. This feature is used in the study of an abiotic C-C coupling reaction in aqueous media that is catalyzed by a semisynthetic pincer palladoenzyme (*Chapter 5*).

In *Chapter 6* the synthesis, spectroscopic and protein labeling studies of a novel luminescent organometallic NCN-pincer platinum phosphonate complex are discussed. This complex proved to be a successful inhibitor and stable label for various lipases and could be used as a diagnostic protein agent.

In *Chapter 7* the coordination chemistry of a luminescent stilbazole molecule to the platinum center of a cationic NCN-pincer platinum complexes is described. The influence of the metal coordination on the spectroscopic properties of the stilbazole molecule is studied and the red-shift of the absorption and emission spectra upon metal coordination is described.

Chapter 8 deals with the synthesis and site-specific immobilization of a ruthenium racemisation catalyst onto lipase-beads. The novel heterogeneous catalytic material obtained was successfully applied in a dynamic kinetic resolution cascade reaction of a secondary alcohol.

References

1. Salmain, M.; Jaouen, G., *C. R. Chimie* **2003,** 6, 249-258 and references mentioned therein.
2. Lo, K. K.-W., *Struct. Bond.* **2007,** 123, 205-245 and references mentioned therein.
3. Lo, K. K.-W.; Hui, W.-K.; Chung, C.-K.; Tsang, K. H.-K.; Ng, C. H.-C.; Zhu, N.; Cheung, K.-K., *Coord. Chem. Rev.* **2005,** 249, 1434-1450 and references mentioned therein.
4. Meggers, E., *Curr. Opin. Chem. Biol.* **2007,** 11, 287-292.
5. Pordea, A.; Ward, T. R., *Chem. Comm.* **2008**, 4239-4249.
6. Steinreiber, J.; Ward, T. R., *Coord. Chem. Rev.* **2008,** 252, 751-766.
7. Letondor, C.; Ward, T. R., *ChemBioChem* **2006,** 7, 1845-1852.
8. Ueno, T.; Yokoi, N.; Abe, S.; Watanabe, Y., *J. Inorg. Biochem.* **2007,** 101, 1667-1675.
9. Ueno, T.; Abe, S.; Yokoi, N.; Watanabe, Y., *Coord. Chem. Rev.* **2007,** 251, 2717-2731.
10. Cravatt, B. F.; Wright, A. T.; Kozarich, J. W., *Annu. Rev. Biochem.* **2008,** 77, 383-414.
11. Schmidinger, H.; Hermetter, A.; Birner-Gruenberger, R., *Amino Acids* **2006,** 30, 333-350.
12. Creus, M.; Pordea, A.; Rossel, T.; Sardo, A.; Letondor, C.; Ivanova, A.; LeTrong, I.; Stenkamp, R. E.; Ward, T. R., *Angew. Chem. Int. Ed.* **2008,** 47, 1400-1404.
13. Slim, M.; Sleiman, H. F., *Bioconjugate Chem.* **2004,** 15, 949-953.
14. Salmain, M.; Gunn, M.; Gorfti, A.; Top, S.; Jaouen, G., *Bioconjugate Chem.* **1993,** 4, 425-433.
15. Carey, J. R.; Ma, S. K.; Pfister, T. D.; Garner, D. K.; Kim, H. K.; Abramite, J. A.; Wang, Z.; Guo, Z.; Lu, Y., *J. Am. Chem. Soc.* **2004,** 126, 10612-10813.
16. Cochran, A. G.; Schultz, P. G., *J. Am. Chem. Soc.* **1990,** 112, 9414-9415.
17. Thordarson, P.; Le Droumaguet, B.; Velonia, K., *Appl. Mircobiol. Biotechnol.* **2006,** 73, 243-254 and references mentioned therein.
18. Panella, L.; Broos, J.; Jin, J.; Fraaije, M. W.; Janssen, D. B.; Jeronimus-Stratingh, M.; Feringa, B. L.; Minnaard, A. J.; de Vries, J. G., *Chem. Commun.* **2005**, 5656-5658.
19. Reetz, M. T.; Rentzsch, M.; Pletsch, A.; Maywald, M., *Chimia* **2002,** 56, 721-723.
20. Powers, J. C.; Asgian, J. L.; Ekici, O. D.; James, K. E., *Chem. Rev.* **2002,** 102, 4639-4750 and references mentioned therein.
21. Fenselau, A.; Koenig, D.; Kosland Jr., D. E.; Latham Jr., G. H.; Weiner, H., *Proc. Natl. Acad. Sci. USA* **1967,** 57, 1670-1673.
22. Kraut, J., *Annu. Rev. Biochem.* **1977,** 46, 331-358.
23. Kruithof, C. A.; Casado, M. A.; Guillena, G.; Egmond, M. R.; van der Kerk-van Hoof, A.; Heck, A. J. R.; Klein Gebbink, R. J. M.; van Koten, G., *Chem. Eur. J.* **2005,** 11, 6869-6877.
24. Kruithof, C. A.; Casado, M. A.; Guillena, G.; Egmond, M. R.; van der Kerk-van Hoof, A.; Heck, A. J. R.; Klein Gebbink, R. J. M.; van Koten, G., *Eur. J. Inorg. Chem.* **2008,** 27, 4425-4432.
25. Albrecht, M.; van Koten, G., *Angew. Chem. Int. Ed.* **2001,** 40, 3750-3781.

CHAPTER 1

Incorporating ECE-Pincer Metal Complexes as Functional Building Blocks in Semisynthetic Metalloenzymes, Supramolecular Polypeptide Hybrids, Tamoxifen Derivatives, Biomarkers and Sensors

This chapter was published as a contribution to a special issue on bioorganometallic chemistry in the *Journal of Organometallic Chemistry* (*J. Organomet. Chem.* **2009**, 694, 812-822) and based on a lecture given at the '4th International Symposium on Bioorganometallic Chemistry' in Missoula, MT, USA on July 7th, 2008.

ECE-pincer metal compounds often have excellent thermal and chemical stability, which makes these organometallics attractive for use as building blocks in bioorganometallic chemistry. This account highlights different applications of hybrids involving covalent or non-covalent assemblies of ECE-pincer building blocks as, in anticarcinogenic agents (*e.g.* tamoxifen derivatives), carbohydrates (surface plasmon resonance enhancers), polypeptides (supramolecular synthons) and solid supports (organometallic peptide-labels) or lipases (bio-catalysts). The design, synthesis and potential applications of semisynthetic pincer-metalloenzymes are also discussed.

Introduction

The field of bioorganometallic chemistry comprises the synthesis and application of organometallics, *i.e* of metal complexes with at least one covalent metal-carbon bond, in biological systems and in chemical biology.[1, 2] The properties of the resulting bioorganometallic systems and compounds have been studied in a variety of applications as potential anticarcinogenics,[3-8] antibiotic or antiviral drugs,[9, 10] as *in vitro* and *in vivo* diagnostics or radiopharmaceutical agents,[11, 12] as biosensors[13] and electrochemical probes,[14-16] as metallo-immunoassays,[17-19] as active site mimics of metalloenzymes,[19-22] as structural probes[23, 24] or as semisynthetic metalloenzymes for catalytic purposes.[5, 25, 26]
In naturally occurring bioorganometallics, for example Vitamine B_{12},[27] the steric and electronic properties of the transition metal ion are tuned to realize preferential geometrical arrangements, folding of the protein or porphyrin backbone, or to tune the accessibility and activity of the metal centre, *e.g.* for catalytic reactions.[28, 29] The synthetic chemistry of transition metal complexes in biological media is often hampered by the sensitivity and instability of these complexes and/or their ligands in aqueous or aerobic media. Furthermore, lability of bioorganometallics towards biomolecules other than the targeted ones or aspecific binding to the metal centre is often observed. Several anticancer drugs, for instance, cause severe and sometimes toxic side effects when administered to patients, which is often due to the decomposition of the original organometallic or coordination complexes.[30] Recent advances in bioorganometallic chemistry concerning the design of more stable organometallic building blocks have led to the synthesis and application of a whole range of bioorganometallic complexes which are compatible with biological media.[1] Some metallocenes, like substituted ferrocene complexes, are an interesting example of a class of stable, biocompatible organometallic building blocks, which possess interesting redox and electrochemical properties.[2, 31, 32]

Another well-studied class of organometallics, some members of which have considerable thermal and chemical stability, are the so-called ECE-pincer metal complexes. These contain a terdentate, monoanionic ligand of the general formula $[2,6\text{-}(ECH_2)_2C_6H_3]^-$, where E is a neutral, two-electron heteroatom donor, like $N(R)_2$, PR_2, or SR. Figure 1 shows the general structure of an ECE-pincer metal complex in which M(II) is a divalent transition metal ion, for example from the d^8 metal series, and X is an anion.[33] In these complexes, the bis-*ortho*-chelation of the metal ion by the two E-donating groups provides further stability to the central M—C bond, making some ECE-pincer metal complexes even compatible with aqueous solvent media (acidic, neutral, basic), aerobic conditions and elevated temperatures.

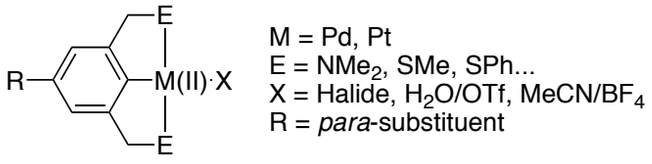

Figure 1: General structure of an ECE-pincer metal(II) complex.[33]

Due to their specific structural features[34, 35] and remarkable stability, ECE-pincer metal-complexes have found numerous applications, ranging from their uses such as catalysts, organometallic switches, and heavy atom probes to sensoring applications.[33] Different types of ECE-pincer metal complexes have been attached as building blocks to polymers,[36] dendrimers[37] and solid supports (*e.g.* silica surfaces).[38] Those hybrid materials were successfully used as catalytic materials in both homogeneous and immobilised "homogeneous" (*i.e.,* heterogeneous) catalysis. Due to their robustness, ECE-pincer metal complexes are suitable building blocks for the modification of biomolecules, as they are known to be compatible with a variety of operations common in synthetic (bio)-organic and –inorganic chemistry working under aqueous and aerobic conditions.

The use of ECE-pincer metal complexes as potential anticarcinogenic agents, as Surface Plasmon Resonance enhancers and as supramolecular synthons will be described. In addition, pincer substituted oligopeptides have been successfully applied as peptide biomarkers and bio-organometallic peptide catalysts. Finally, the design of semisynthetic pincer-metalloenzymes will be illustrated.

Bioorganometallic ECE-pincer metal complexes

Pincercifen as a new tamoxifen derivative

The pioneering work of Jaouen et al.[39-43] demonstrated unambiguously that organometallic complexes can be successfully combined with selective estrogen receptor modulators (SERM)[41] affording organometallic tamoxifen derivatives like ferrocifen (**1**) and hydroxyferrocifen (**2**, Figure 2)[39, 40, 42, 43] with good cytotoxic and antiestrogenic (for **2**) activities. In both **1** and **2** it is the phenyl group originally present in hydroxy-tamoxifen, which is replaced by either a ferrocenyl or an oxaliplatin-derived group, respectively. The cytotoxic activities of **1** and **2** were attributed to the redox properties of the ferrocene functionality. In comparison to hydroxy-tamoxifen, the binding affinity of hydroxy-ferrocifen **2** to the estrogen receptor protein was slightly lower, which is most probably caused by the increased steric bulk of the ferrocene moiety when compared to the phenyl ring.[43] Other tamoxifen derivatives containing an oxaliplatin-derived coordination complex (**3** and **4**, Figure 2) have been developed by Jaouen and co-workers as well.[44] Interestingly, the (poor) stability of platinum coordination complexes under physiological conditions can be used to selectively deliver the cytotoxic metal moiety to its target, however

also toxic side effects due to aselective decomposition of the coordination complex can occur.[30]

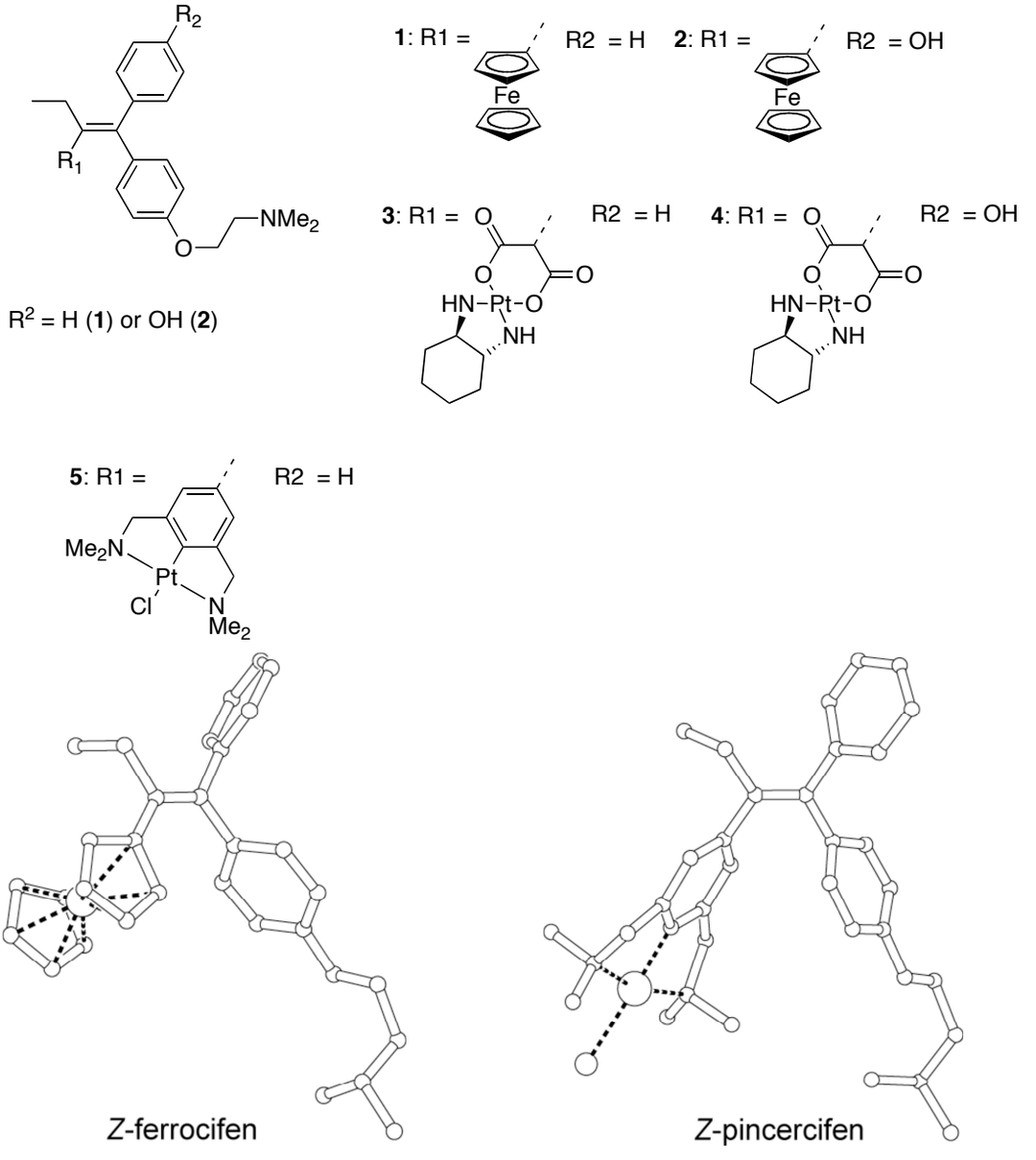

Figure 2: Different metal-containing tamoxifen analogues and the crystal structures of *Z*-ferrocifen **1** and *Z*-pincercifen **5**.[39-46]

Inspired by these elegant studies, our group designed NCN-pincer platinum(II) containing analogues (coined 'pincercifens' **5**, Figure 2).[45, 46] As the NCN-pincer platinum halide unit possesses a covalent platinum-carbon bond, it was anticipated that compound **5** would be more stable under physiological conditions and show less toxic side-effects upon transport and delivery towards the cancer cells than common commercial anticancer drugs. Comparison of the crystal structures of *Z*-ferrocifen **1**

and *Z*-pincercifen **5** (Figure 2) shows that the steric bulk of pincercifen **5** is different from ferrocifen **1**, which might result in different binding affinities and strengths of the two complexes to the target molecules. Furthermore, the redox properties of ferrocenyl and NCN-pincer platinum(II) units are different, which could result in altered cytotoxic activities of **5** when compared to **1**. Currently, the biological activities of pincercifen **5** are under investigation.[46, 47]

NCN-pincer platinum(II) complexes as SPR enhancers for the study of carbohydrate-protein interactions

For the studies of biomolecular interactions in real time, biosensors based on surface plasmon resonance (SPR) have become an increasingly popular tool.[48, 49] SPR has been proven to be an emerging technique for the qualitative and quantitative study of nucleic acid-protein, protein-protein, carbohydrate-carbohydrate and carbohydrate-protein interactions.[50-55] As the SPR response is proportional to the accumulation of mass on the sensor surface, a serious constraint of SPR concerns the dimensions of the analyte-molecules. Especially in the study of the generally weak carbohydrate-protein interactions, the low availability of high-molecular mass oligosaccharides hampers the wide applicability of this technique.

As NCN-pincer platinum complexes are small in size and contain a platinum ion as heavy metal, these complexes were suitable candidates for the enhancement of the SPR signal.[56] For this purpose different low-molecular mass mono- and disaccharides labelled with a NCN-pincer platinum unit were used to assay the carbohydrate-protein interactions with the immobilized lectins RCA_{120} and ConA, being standard proteins for the study of carbohydrate-protein interactions (Figure 3).[56]

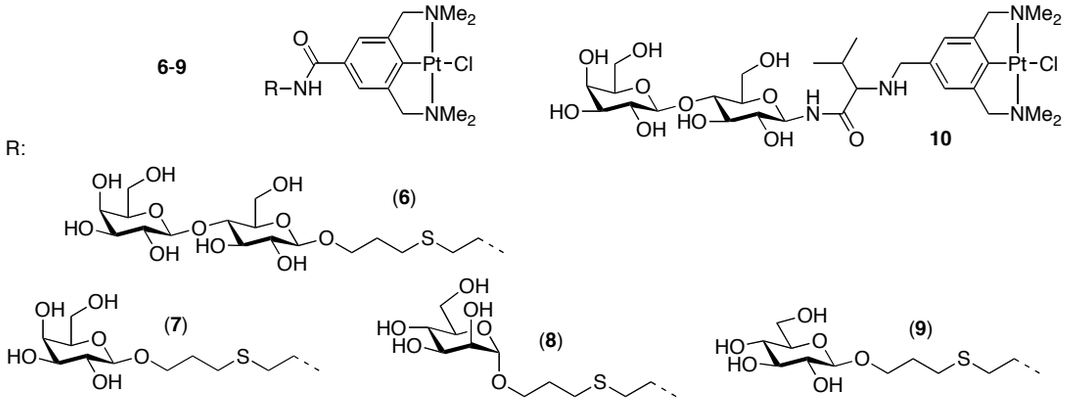

Figure 3: NCN-pincer platinum unit labelled lactose (**6**, **10**), D-galactose (**7**), D-mannose (**8**), D-glucose (**9**), which were used as SPR sensitizers in carbohydrate-protein interaction studies.[56]

The studies showed that specific binding of the NCN-pincer platinum unit labelled saccharides led to a strong detectable SPR signal enhancement as compared to the

pincer-free saccharides, even at low analyte concentrations (9 μM). This interaction was only specific for the intact protein and not for its denatured species (Figure 4).

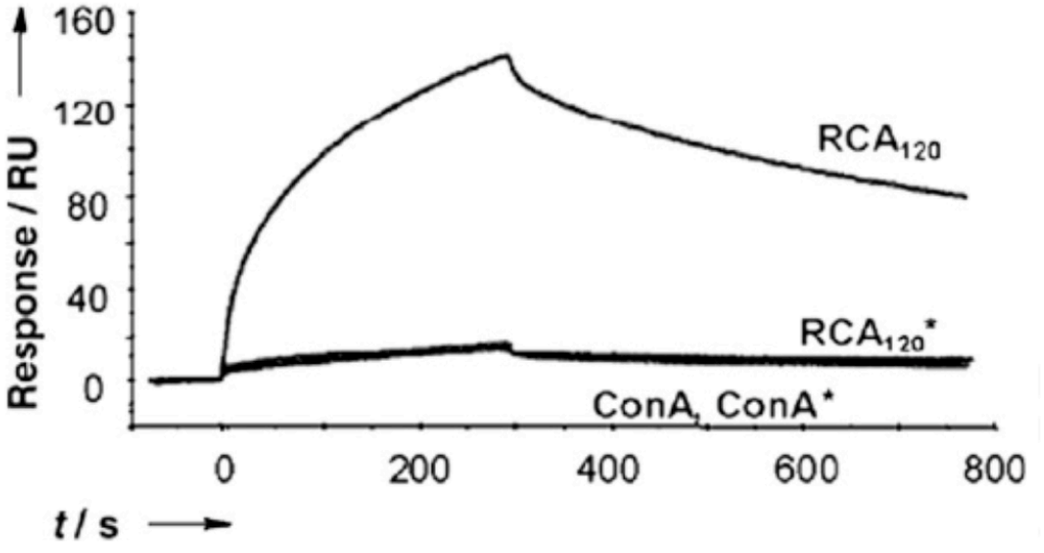

Figure 4: Sensorgrams of NCN-pincer platinum unit labelled **6** (9 μM) flowing across RCA_{120}, denatured RCA_{120}^{*}, ConA and denatured $ConA^{*}$ (RCA_{120} is known to be specific for galactose/lactose, ConA specific for mannose).[56]

As saccharides without NCN-pincer platinum labels did not show any detectable binding affinities in the SPR studies, despite their well-known selectivity for the used lectins, the signal enhancement is purely attributed to the NCN-pincer platinum label. Control studies showed that signal enhancement occurred exclusively upon incorporation of the NCN-pincer platinum(II) label and not in the presence of the NCN-pincer ligand only (*i.e.* without platinum), which proves that the sensitivity increase is only due to the heavy atom effect of the platinum(II) ion.[56] It is believed that not only the mass increase by the Pt(II) ion contributes to the observed beneficial labelling properties, but that also a significant interaction between the platinum electrons and the evanescent wave produced in proximity of the sensorchip surface is responsible for the observed phenomenon.[56]
Interestingly, variation of the linker length between the NCN-pincer platinum label and the carbohydrate, as for complexes **6** and **10** (Figure 4), did not influence the response significantly, which indicates that the signal enhancement is not influenced by the bond distance between the label and the saccharide. In comparison to other SPR enhancers, the NCN-pincer platinum labels described here are small in size, possess a lower molecular weight and do not have a negative influence on the carbohydrate-protein interaction, making them unique, powerful detection tools for SPR. It also highlights the full biocompatibility of the NCN-pincer platinum moiety.

Supramolecular assemblies involving ECE-pincer palladium(II) complexes and biomolecules

The groups of Weck[57] and Reinhoudt[58] elegantly used the well-established properties of cationic ECE-pincer metal(II) complexes coordinating to (substituted) pyridines[59-72] to construct supramolecular assemblies involving these pincer cations and pyridine-modified peptides[57] and carbohydrates,[58] thereby constructing bio-coordination complexes with special properties.

For this purpose, Weck et al. investigated the coordination strengths of different pyridyl glycine (**12**, **13**) and pyridyl alanine (**14**, **15**) tripeptides with a 3-pyridyl (**13**, **15**) or 4-pyridyl (**12**, **14**) functionality to the *p*-methoxy-substituted SCS-pincer palladium(II) cation **11** (Figure 5). The formation of the Pd-N coordination bonds was studied by ^{1}H NMR spectroscopy, ES-MS and isothermal titration calorimetry (ITC). In this case, ITC also allowed for the determination of K_a's for the binding of peptides **12**-**15** to the cationic pincer complex **11**.

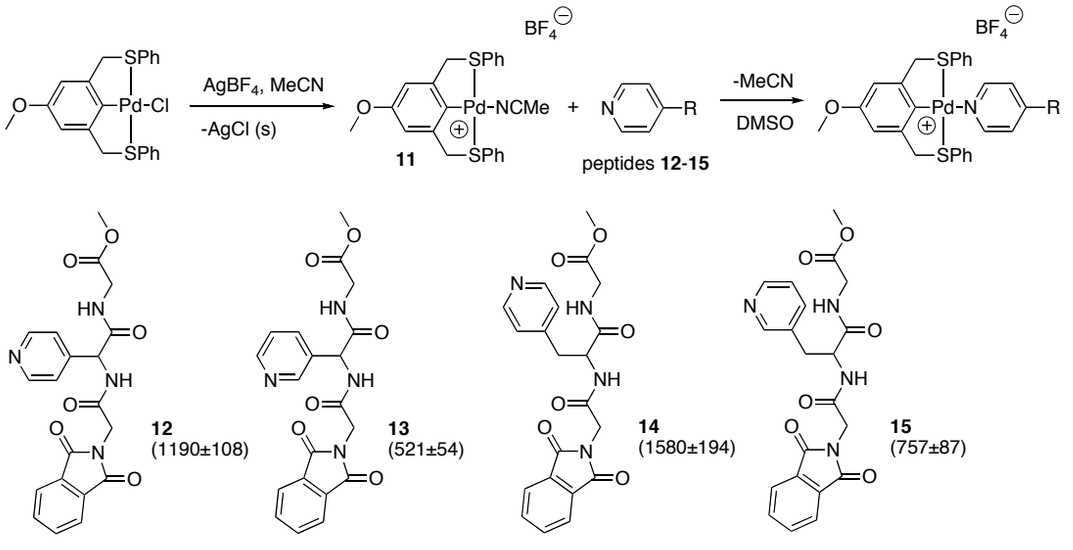

Figure 5: Coordination of different pyridyl-modified peptides to SCS-pincer palladium(II) cations. The ITC K_a values of peptides **12**-**15** binding to the cationic pincer complex **11** are given in brackets.[57]

According to the different analysis methods used, the metal-pyridine coordination to peptides **12**-**15** was quantitative in all cases and no competitive coordination by other heteroatoms present in the peptide backbone was observed. The latter preference for monodentate coordinating ligands underlines the unique features of the tridentate binding of the SCS-manifold to the central d^8 metal atom. The investigation of the bond strength with ITC (Figure 5) showed that the 4-pyridyl peptides **12** and **14** form a stronger coordination bond with the SCS-pincer palladium centre than the 3-pyridyl peptides **13** and **15**, which was attributed to steric reasons. The stronger coordination of the alanyl derived peptides **14** and **15** in comparison to

the glycyl derived peptides **12** and **13** was explained by electronic activation of the pyridyl moiety via a methylene spacer.[34, 66]
The bioorganometallic coordination complexes described here can be used as biological synthons for the design of biocompatible metal-coordination materials. The next step in these studies will be the design of cyclic peptides and their self-assembly with bifunctional metallated pincer complexes for the creation of novel supramolecular systems.[57]

The group of Reinhoudt has held a long tradition in studying the formation of non-covalent metal-induced self-assemblies, for which they also used ECE-pincer metal complexes immobilized onto dendrimers as coordination scaffolds.[66, 67, 73, 74] In one example,[58] they tried to mimic the solubility properties of water-soluble globular proteins, where the hydrophobic core of the protein is decorated with hydrophilic amino acids on the surface. As core-mimics they used hydrophobic dendrimers, which were functionalized with cationic SCS-palladium(II) pincer groups at the periphery (Figure 6).

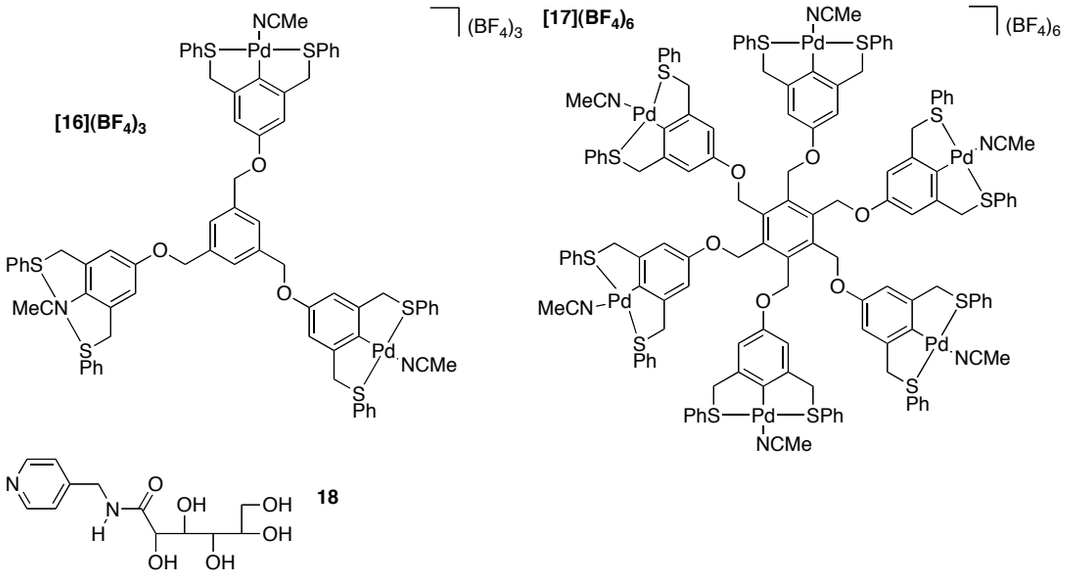

Figure 6: Tri- and hexa-cationic SCS-pincer palladium(II) dendrimers **[16](BF$_4$)$_3$** and **[17](BF$_4$)$_6$** to which 4-pyridyl-substituted carbohydrate **18** was coordinated.[58]

To these hydrophobic tri- and hexa-pincer cationic dendrimers **[16]$^{3+}$** and **[17]$^{6+}$** (Figure 6) dissolved in MeCN were added three (for **[16]$^{3+}$**) or six (for **[17]$^{6+}$**) equivalents of a linear 4-pyridine-functionalized carbohydrate **18**. Solution NMR analysis showed that the resulting coordination complexes **[16·3*(18)](BF$_4$)$_3$** and **[17·6*(18)](BF$_4$)$_6$** were formed quantitatively in d_6-DMSO and CD_3CN/d_3-MeOD, respectively. However, complex **[16·3*(18)](BF$_4$)$_3$** appeared to be insoluble in D_2O. The hexanuclear coordination complex **[17·6*(18)](BF$_4$)$_6$** dissolved well in hot D_2O,

but upon cooling to room temperature an aqueous gel was formed. This study shows that the coordination of functionalized sugar molecules to dendritic cationic SCS-pincer palladium molecules is successful in polar solvents, showing the suitability of SCS pincer palladium dendrimers as building blocks for the construction of new bioorganometallic hybrid materials.

Pincer platinum(II) complexes as peptide biomarkers

Organometallic complexes attached to peptides have been successfully used in immunoassay[19] and in biomedical studies due to their anti-bacterial and anti-proliferative properties.[10] Ferrocene amino acids[23, 24] have also been used as structural probes, e.g. as turn inducers. NCN-pincer platinum(II) complexes are well known for their properties as sensor materials, *e.g.* for the sensing of SO_2 and diiodine.[33, 75] The formation of the pentacoordinate SO_2 or I_2 adducts induces a change in the visible part of the UV-VIS spectrum, which enables detection of the coordination complexes by the naked eye (Scheme 1).

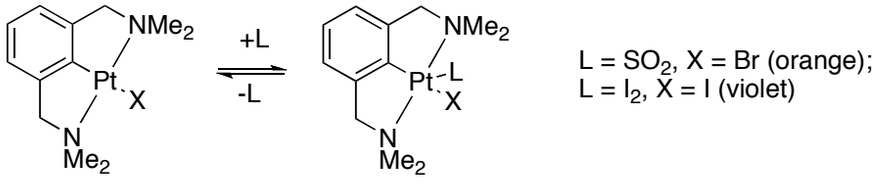

Scheme 1: Reversible formation of the pentacoordinated SO_2 and I_2 NCN pincer platinum(II) coordination complexes.[33, 75]

The exceptionally high stability of NCN-pincer platinum(II) complexes in aqueous media and in air enabled Van Koten and co-workers to investigate their use as organometallic peptide labels. For this purpose, NCN-pincer platinum(II) units were covalently bonded to the N-[76, 77] and C-termini[77] and to the α-carbon atom[77, 78] of different amino acids (Table 1). The pincer sensing moieties were introduced at different stages during the syntheses using various organic transformations. In all cases the covalent platinum-carbon bond remained intact, which allowed the use of this NCN-pincer-platinum unit as a low-molecular weight biomarker for peptides.[76, 77]

Table 1: NCN-pincer platinum complexes bonded to the N- (**19**-**24**) and C- (**25**-**31**) termini and to the α-carbon atom (**32**-**34**) of different diprotected amino acids; the ^{195}Pt NMR data for pincer diprotected amino acids **19**-**34** and the corresponding SO_2-coordination complexes are given.

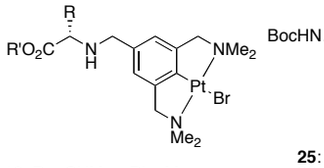

19: R = $CHMe_2$, R' = Me;
20: R = $CHMe_2$, R' = H;
21: R = CH_2Ph, R' = Me;
22: R = CH_2Ph, R' = H;
23: R = CH_2COOH, R' = Me;
24: R = CH_2Ph, R' = -NH-$CHMe_2$-CO_2Me

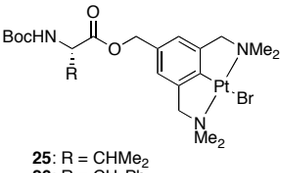

25: R = $CHMe_2$
26: R = CH_2Ph
27: R = H
28: R = CH_2COOH

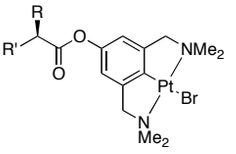

29: R = $CHMe_2$, R' = NHBoc;
30: R = CH2Ph, R' = NHBoc;
31: R = CHMe, R' = NH_3Br

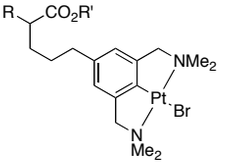

32: R = NHBoc, R' = Me;
33: R = NHBoc, R' = H;
34: R = NH_3Br, R' = H

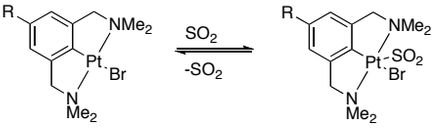

(orange)

Compound	R-group	Solvent	δ(Pt)	δ(Pt/SO_2-adduct)	Δδ
19	CH_2-L-Val-OMe	$CDCl_3$	-1982	-751	1231
20	CH_2-L-Val-OH	CD_3OD	-1972	-1170	802
21	CH_2-L-Phe-OMe	$CDCl_3$	-1973	-732	1241
22	CH_2-L-Phe-OMe	CD_3OD	-1973	-1170	803
23	CH_2-L-Asp-OMe	$CDCl_3$	-1983	-954	1029
24	CH_2-L-Phe-L-Val-OMe	$CDCl_3$	-1983	-954	1029
25	CH_2-L-Val-Boc	$CDCl_3$	-1964	-870	1094
26	CH_2-L-Phe-Boc	$CDCl_3$	-1963	-1219	744
27	CH_2-Gly-Boc	$CDCl_3$	-1964	-776	1188
28	CH_2-L-Asp-Boc	$CDCl_3$	-1964	-1152	812
29	L-Val-Boc	$CDCl_3$	-1967	-790	1177
30	L-Phe-Boc	$CDCl_3$	-1967	-883	1084
31	L-Val-NH_3Br	CD_3OD	-1982	-	-
32	BocHN{$CH(CH_2)_3$}CO_2Me	$CDCl_3$	-1997	-1078	919
33	BocHN{$CH(CH_2)_3$}CO_2H	$CDCl_3$	-1982	-998	984
34	BrH_3N{$CH(CH_2)$}CO_2H	DMSO	-1980	-	-

Due to the characteristic NMR/MRI activity of the ^{195}Pt nucleus (natural abundance 33.8%, I = ½), the NCN-pincer platinum units can also be used as biomarkers for peptides. The chemical shifts for the N-terminus derivatives **19**-**24** range from δ = -1983 to -1972 ppm, for the C-terminus derivatives **25**-**31** from δ = -1963 to -1967 ppm and for the α-carbon atom derivatives **32**-**34** from δ = -1997 to -1980 ppm. The characteristic range of the resonances suggests that a distinction between N-, C- and

α-carbon labelled peptides based on the resonance of the ^{195}Pt nucleus is possible, making the NCN-pincer platinum(II) moiety a site-specific metal probe.

SO_2 binds instantaneously and reversibly to NCN-pincer platinum(II) halides with a concomitant diagnostic colour change from colourless to orange (Scheme 1, Table 1), resulting in detection limits in the ppm range. This SO_2-Pt bond formation, which can occur in the solid state as well,[79] is also reflected in large ^{195}Pt NMR downfield shifts for the modified peptides **19**-**34**. These shifts range from δ = 744-1241 ppm and are fully reversible. As soon as the SO_2 atmosphere is removed, the original pincer peptides are recovered unchanged. Moreover, the formation of the SO_2 adduct is insensitive to other atmospheric gases, like CO, HCl and to humidity.[33] As SO_2 is a physiologically important gas,[80] the use of these very stable NCN-pincer platinum(II) halide labels as sensitive sensors in biochemical and medicinal applications is open for further studies, both *in vitro* and *in vivo*.
The reversible coordination of I_2 to NCN-pincer platinum(II) halide complexes could be used to label peptides in solid-phase synthesis. The two different NCN-pincer platinum(II) iodide complexes **35** and **36** were used as colour biomarkers in the solid-phase peptide synthesis of the oligopeptides **35**-GPPFPF and **36**-XGPPFPF (with X being any of the naturally occurring α-amino acids, Figure 7). Firstly, both NCN-pincer platinum labelled oligopeptides on resin showed the characteristic reversible orange coloration upon exposure to SO_2, which disappeared after removal of the beads from the SO_2 containing atmosphere.

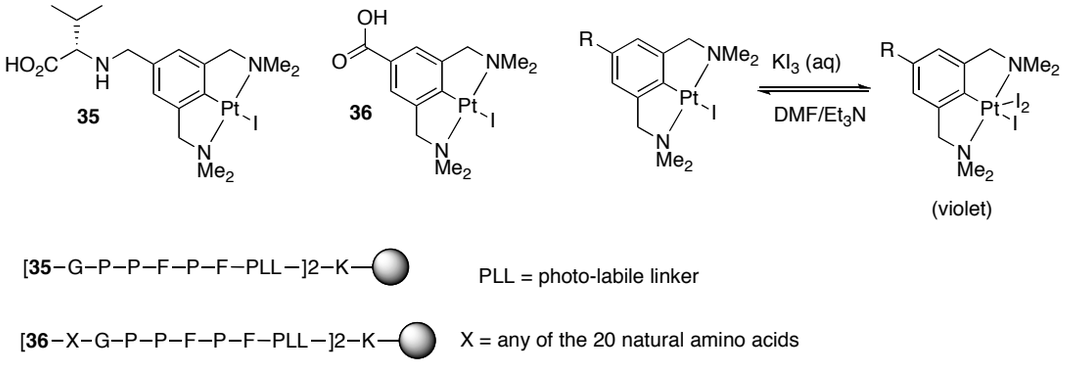

Figure 7: The solid-phase peptide biomarkers **35** and **36**, their attachment onto oligopeptides and the reversible coloring of the NCN-pincer platinum halide labels by KI_3.[81]

Secondly, when the oligopeptides **35**-GPPFPF and **36**-XGPPFPF on resin were treated with an aqueous solution of KI_3, a persistent purple/black coloration of the beads was observed. This coloration was due to the formation of an η^1-I_2 coordination complex[75] (Figure 7) from which the I_2 could easily be removed (decoordinated) by washing the beads with a DMF/Et_3N solution. As biomarker **36**, lacking the labile secondary amine

function present in **35**, was more stable towards acidic peptide deprotection protocols, the deprotection, photocleavage and analysis of the peptides labelled with **36** was investigated in detail. For **36**-XGPPFPF on resin first the side chain protecting groups *t*-Bu, Boc and Trt were removed by treatment with TFA/tri-isopropylsilane/H_2O (90/5/5), after which the metal-labelled peptides were removed from the support by UV-irradiation. Subsequent mass spectrometric analysis of the 20 different **36**-XGPPFPF metal-labelled oligopeptides showed that in all cases the biomarker **36** had been introduced quantitatively (the characteristic Pt pattern was well-visible in the MALDI-TOF mass spectra in all cases) and that no degradation of the NCN platinum moiety had occurred under the acidic deprotection conditions applied, again emphasizing the remarkable stability of this moiety under many reaction conditions.

As the mild coloration method with KI_3 was reversible and easily detectable, but more persistent (removal of coloration only after treatment with DMF/Et_3N or DMF/morpholine) than the coloration with SO_2, it appeared to be a very convenient assay for the analysis of different polypeptides. An investigation of the sensitivity of the coloration process on beads also showed that only capping of 6% of the amine termini with **36** already resulted in differently coloured resins, which could be distinguished by the eye.[81] The coloration process did not interfere with the polypeptide backbone and as the coloration was stable in water and could repeatedly be switched on and off, the NCN-pincer platinum(II) moiety proved to be a very useful solid-phase peptide label.

Pincer palladium(II) complexes as catalytically active artificial peptides

Peptides substituted by phosphines have been used successfully as chiral backbones for transition metal catalysts in asymmetric hydrogenation, alkylation and allylic substitution reactions.[82-86] ECE-pincer palladium complexes, which have been broadly applied as homogeneous catalysts, *e.g.* in Suzuki, Heck and aldol condensation reactions,[33] could also be attached to different peptides and applied as organometallic peptide catalysts (Figure 8).[78, 87]

For the purpose of preparing catalytically active artificial peptides, protocols were developed to couple appropriately functionalized NCN-ligands to peptide chains. This was done by coupling the N- or C-termini or the α-carbon atom of the respective mono- or di-peptides to the NCN-bromide ligand and subsequent metallation with [$Pd_2(dba)_3 \bullet CHCl_3$]. Interestingly, palladation of the NCN-bromide peptide ligands was relatively straightforward, and even the hydrolysis of the protected NCN-pincer palladium(II) peptide **37** to the free acid **38**, which was performed using LiOH, could be pursued without any problems, as the Pd-C bond remained intact under the deprotection conditions applied.

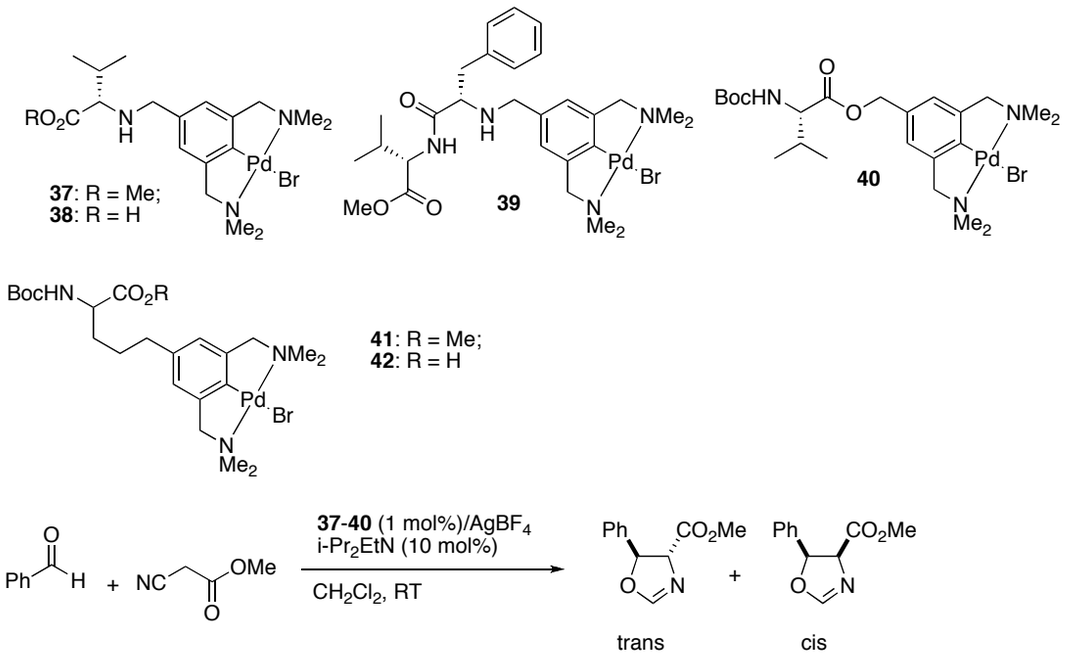

Entry	Catalyst	Time (h)	TOF	Conversion (%)	*trans:cis*
1	None	5	0	0	-
2	[PdCl(NCN)]	7	43	83	62:38
3	BnValOH	24	1	18	80:20
4	**37**	7	52	96	62:38
5	**38**	3	62	>99	64:36
6	**39**	7	40	97	68:32
7	**40**	7	30	94	62:38

Figure 8: NCN-pincer palladium complexes bonded to the N- (**37**-**39**) and C- (**40**) termini and to the α-carbon atoms (**41**-**42**) of different peptides; **37**-**40** were used as catalysts in the aldol condensation of methyl isocyanate and benzaldehyde.[87]

Subsequently, the NCN pincer palladium(II) substituted amino acids **37**-**40** were used as catalysts in the aldol condensation reaction of methyl isocyanate and benzaldehyde to give either the *cis* or the *trans* product. To do so, the organometallic pincer peptides **37**-**40** were first activated with $AgBF_4$ to form their cationic analogues, and after thorough removal of the residual silver salt by filtration, they were used in catalysis.

All activated analogues of **37**-**40** were catalytically active and gave ≥94% conversion after the indicated time (Figure 8). However, no significant stereoselective influence of the pincer peptide catalysts on the product formation was observed. This is probably due to the short lengths of the peptides used. As the stereocentres of the peptides are too far away from the catalytically active Pd(II) centre, the chiral

induction of the peptide backbone is too low. To induce chirality, the introduction of NCN pincer palladium(II) complexes into longer peptide chains is necessary.

ECE-pincer metal(II) protein hybrids

Recently, the bioorganometallic research of the Van Koten group has gradually shifted its focus from the modification of carbohydrates and oligopeptides to the modification of entire proteins by ECE-pincer metal complexes. As illustrated for sugars and oligopeptides (*vide infra*), pincer complexes could be successfully applied as biosensors or artificial biocatalysts. Therefore, it was interesting to explore whether the obtained knowledge could be applied to more complex biological systems, *i.e.* proteins. Since the pioneering work of Whitesides et al.[88], different groups have been working on the modification of proteins with transition metal complexes already, with very popular examples being the non-covalent biotin-(strept)avidin[26, 89-92] system and apo-myoglobin, which had been modified covalently by *e.g.* salen complexes.[25, 93]

For the development of a general and selective anchoring strategy of organometallic ECE-pincer complexes to proteins it was decided to not only address one specific type of protein, but a whole protein class. As the serine hydrolases are a very large and well-studied class of proteins with a very pronounced and broad activity and substrate profile,[94] we focused on the site-selective modification of serine hydrolases. A common feature of serine hydrolases is their irreversible and covalent inhibition by phosphonate inhibitors, which is due to a covalent bond formation between the catalytically active serine residue and the phosphorous atom of the phosphonate (Figure 9).

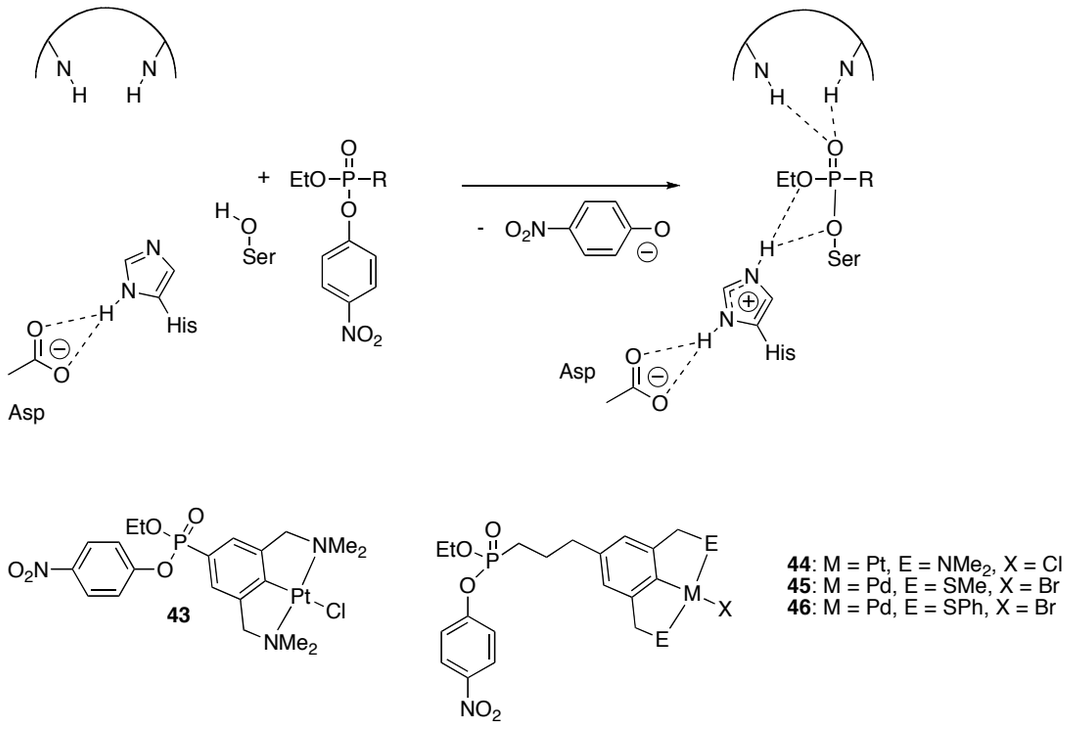

Figure 9: Irreversible inhibition of a serine hydrolase by a phosphonate inhibitor and the different ECE-pincer metal phosphonate inhibitors developed with a C0- (**43**) and a C3-tether (**44**-**46**).[95, 96]

Because of these interesting features, new synthesis protocols were developed to couple various pincer palladium and platinum complexes to reactive phosphonate moieties. The designed ECE-pincer metal phosphonate inhibitors **43**-**46** all possess one *para*-nitrophenolate leaving group, which makes the inhibitors less susceptible to autohydrolysis in aqueous media when compared to other phosphonate inhibitors.[97] Furthermore, the release of the *para*-nitrophenolate anion (PNP) during inhibition allowed us to follow the inhibition reaction profile spectrophotometrically, since the PNP anion is brightly yellow coloured in solution and thus easily detectable with UV-VIS spectroscopy at 400 nm. After irreversible binding, the active site of the serine hydrolase is blocked and therefore no residual hydrolytic activity of the serine hydrolase is observed anymore. This feature can be used to verify and quantify the inhibition, by assaying the remaining hydrolytic activity of a serine hydrolase after (partial) inhibition with a test substrate (should be lacking upon full inhibition).[95, 96] In a preliminary study, it was found that several different serine hydrolases, *e.g.* CALB, patatine, *chromobacterium viscosum* lipase and cutinase could be inhibited with different phosphonates.[94]

Using this methodology, the serine hydrolase cutinase was successfully modified with phosphonate-pincer adducts **43**-**46**. Comparing the inhibition reactions of the various phosphonates (**43**-**46**) a large difference in reaction speed between the C0-tethered **43**,[95] and the C3-tethered pincer phosphonates **44**-**46**[96] was observed. For pincer

phosphonates **44** and **45** for instance, the inhibition with 2 equivalents of inhibitor was complete after 5 minutes, whereas the complete inhibition of cutinase with **43** took overnight. The slow inhibition of cutinase by **43** causes most probably more steric constraints by the bulk of the pincer head group than for **44** and **45** when it approaches the active site of the protein.

Conclusions

The many different examples of the use of ECE-pincer metal complexes in bioorganometallic chemistry, highlighted in this review, show clearly that pincer complexes are versatile building blocks with diverse and broad applicabilities. Moreover, these ECE-pincer metal complexes display exceptional stability and robustness in biological media, which enables their use in the study of biomolecules and biological interactions. Their applications range from anticarcinogenic agents, SPR enhancers, supramolecular assemblies for the generation of new hybrid-biomaterials, peptide biomarkers and catalysts to building blocks for new semisynthetic metalloenzymes. The recent shift of the research focus towards the modification of whole proteins by ECE-pincer metal complexes shows that larger systems can be addressed, which will enable us to study the behaviour of more complex biological systems with metal complexes further[98] and provide us with a useful tool in chemical biology.

References

1. Jaouen, G., *Bioorganometallics: Biomolecules, Labeling, Medicine*. Wiley-VCH Verlag: Weinheim, 266; p 444.
2. Kraatz, H.-B.; Metzler-Nolte, N., *Concepts and Models in Bioinorganic Chemistry*. Wiley-VCH Verlag: Weinheim, 2006; p 1-469.
3. Atilla-Gokcumen, G. E.; Williams, D. S.; Bregman, H.; Pagano, N.; Meggers, E., *ChemBioChem* **2006,** 7, 1443-1450.
4. Williams, D. S.; Carroll, P. J.; Meggers, E., *Inorg. Chem.* **2007,** 46, 2944-2946.
5. Dougan, S. J.; Habtemariam, A.; McHale, S. E.; Parsons, S.; Sadler, P. J., *Proc. Natl. Acad. Sci. USA* **2008,** 105, 11628-11633.
6. Aird, R. E.; Cumminds, J.; Ritchie, A. A.; Muir, M.; Morris, R. E.; Chen, H.; Sadler, P. J.; Jodrell, D. I., *Brit. J. Canc.* **2002,** 86, 1652-1657.
7. Pigeon, P.; Top, S.; Vessieres, A.; Huche, M.; Hillard, E. A.; Salomon, E.; Jaouen, G., *J. Med. Chem.* **2005,** 48, 2814-2821.
8. Allard, E.; Passirani, C.; Garcion, E.; Pigeon, P.; Vessieres, A.; Jaouen, G.; Benoit, J.-P., *J. Controlled Release* **2008,** 130, 146-153.
9. Allardyce, C. S.; Dyson, P. J., *Top. Organomet. Chem.* **2006,** 17, 177-210.
10. Metzler-Nolte, N., *Chimia* **2007,** 61, 736-741.
11. Alberto, R., *Radiopharmaceuticals*. Wiley-VCH Verlag: Weinheim, 2006; p 97-124.
12. Alberto, R., *Top. Curr. Chem.* **2005,** 252, 1-44.
13. Fish, R. H., *Supramolecular host recognition processes with biological compounds, organometalli pharmaceuticals, and alkali-metal ions as guests*. Wiley-VCH Verlag: Weinheim, 2006; p 321-352.
14. Maurer, A.; Kraatz, H.-B.; Metzler-Nolte, N., *Eur. J. Inorg. Chem.* **2005,** 16, 3207-3210.
15. Schatzschneider, U.; Metzler-Nolte, N., *Angew. Chem. Int. Ed.* **2006,** 45, 1504-1507.
16. Li, C.-Z.; Long, Y.-T.; Sutherland, T.; Lee, J. S.; Kraatz, H.-B., *Front. Biochip Technology* **2006**, 274-291.
17. Fischer-Durand, N.; Salmain, M.; Rudolf, B.; Vessieres, A.; Zakrzweski, J.; Jaouen, G., *ChemBioChem* **2004,** 5, 519-525.
18. Heldt, J.-M.; Fischer-Durand, N.; Salmain, M.; Vessieres, A.; Jaouen, G., *J. Organomet. Chem.* **2004,** 689, 4775-4782.
19. Severin, K.; Bergs, R.; Beck, W., *Angew. Chem. Int. Ed.* **1998,** 37, 1635-1654.
20. Aguirre de Carcer, I.; Di Pasquale, A.; Rheingold, A. L.; Heinekey, D. M., *Inorg. Chem.* **2006,** 45, 8000-8002.
21. Rampersad, M. V.; Jeffery, S. P.; Reibenspies, J. H.; Ortiz, C. G.; Darensbourg, D. J.; Darensbourg, M. Y., *Angew. Chem. Int. Ed.* **2005,** 44, 1217-1220.
22. Green, K. N.; Jeffery, S. P.; Reibenspies, J. H.; Darensbourg, M. Y., *J. Am. Chem. Soc.* **2006,** 128, 6493-6498.
23. Barisic, L.; Dropucic, M.; Rapic, V.; Pritzkow, H.; Kirin, S.; Metzler-Nolte, N., *Chem. Comm.* **2004**, 2004-2005.
24. Barisic, L.; Mojca, M.; Khaled, A.; Liu, Y.; Kraatz, H.-B.; Pritzkow, H.; Kirin, S. I.; Metzler-Nolte, N.; Rapic, V., *Chem. Eur. J.* **2006,** 12, 4965-4980.
25. Ueno, T.; Koshiyama, T.; Ohashi, M.; Kondo, K.; Kono, M.; Suzuki, A.; Yamane, T.; Watanabe, Y., *J. Am. Chem. Soc.* **2005,** 127, 6556-6562.
26. Creus, M.; Pordea, A.; Rossel, T.; Sardo, A.; Letondor, C.; Ivanova, A.; LeTrong, I.; Stenkamp, R. E.; Ward, T. R., *Angew. Chem. Int. Ed.* **2008,** 48, 1400-1404.
27. Randaccio, L.; Geremia, S.; Wuerges, J., *J. Organomet. Chem.* **2007,** 693, 1198-1215.
28. Arnesano, F.; Banci, L.; Bertini, I.; Ciofi-Baffoni, S., *Eur. J. Inorg. Chem.* **2004,** 8, 1583-1593.
29. Arnesano, F.; Banci, L.; Bertini, I.; Capozzi, F.; Ciofi-Baffoni, S.; Ciurli, S.; Luchinat, C.; Mangani, S.; Rosato, A.; Turano, P.; Viezzoli, M. S., *Coord. Chem. Rev.* **2006,** 250, 1419-1450.
30. Allardyce, C. S.; Dorcier, A.; Scolaro, C.; Dyson, P. J., *Appl. Organomet. Chem.* **2005,** 19, 1-10.
31. Tebben, L.; Bussmann, K.; Hegemann, M.; Kehr, G.; Frohlich, R.; Erker, G., *Organometallics* **2008,** 27, 4269-4272.
32. Gasser, G.; Husken, N.; Koster, S. D.; Metzler-Nolte, N., *Chem. Comm.* **2008**, 3675-3677.

33. Albrecht, M.; van Koten, G., *Angew. Chem. Int. Ed.* **2001,** 40, 3750-3781.
34. Slagt, M. Q.; Rodriguez, G.; Grutters, M. M. P.; Klein Gebbink, R. J. M.; Klopper, W.; Jenneskens, L. W.; Lutz, M.; Spek, A. L.; van Koten, G., *Chem. Eur. J.* **2004,** 10, 1331-1344.
35. Stiriba, S.-E.; Slagt, M. Q.; Kautz, H.; Klein Gebbink, R. J. M.; Thomann, R.; Frey, H.; van Koten, G., *Chem. Eur. J.* **2004,** 10, 1267-1273.
36. Slagt, M. Q.; Stiriba, S.-E.; Klein Gebbink, R. J. M.; Kautz, H.; Frey, H.; van Koten, G., *Macromolecules* **2002,** 35, 5734-5737.
37. Kleij, A. W.; Gossage, R. A.; Jastrzebski, J. T. B. H.; Boersma, J.; van Koten, G., *Angew. Chem. Int. Ed.* **2000,** 39, 176-178.
38. Mehendale, N. C.; Sietsma, J. R. A.; de Jong, K. P.; van Walree, C. A.; Klein Gebbink, R. J. M.; van Koten, G., *Adv. Synth. Catal.* **2007,** 349, 2619-2630.
39. Jaouen, G.; Top, S.; Vessieres, A.; Alberto, R., *J. Organomet. Chem.* **2000,** 600, 23-26.
40. Top, S.; Dauer, B.; Vaissermann, J.; Jaouen, G., *J. Organomet. Chem.* **1997,** 541, 355-361.
41. Top, S.; Tang, J.; Vessieres, A.; Carrez, D.; Provot, C.; Jaouen, G., *Chem. Comm.* **1996**, 955-956.
42. Top, S.; Vessieres, A.; Leclercq, G.; Quivy, J.; Tang, J.; Vaissermann, J.; Huche, M.; Jaouen, G., *Chem. Eur. J.* **2003,** 9, 5223-5236.
43. Vessieres, A.; Top, S.; Beck, W.; Hillard, E.; Jaouen, G., *J. Chem. Soc., Dalton Trans.* **2006**, 529-541.
44. Top, S.; Kaloun, E. B.; Vessieres, A.; Leclercq, G.; Laios, I.; Ourevitch, M.; Deuschel, C.; McGlinchey, M. J.; Jaouen, G., *ChemBioChem* **2003,** 4, 754-761.
45. *As presented at the IVth International Symposium on Bioorganometallic Chemistry* **2008**.
46. Batema, G. D.; Korstanje, T. J.; Guillena, G.; Rodriguez, G.; Lutz, M.; Kooijman, H.; Spek, A. L.; van Klink, G. P. M.; van Koten, G., **2008**, manuscript in preparation.
47. *The cytotoxic studies are currently performed*.
48. Green, R. J.; Frazier, R. A.; Shakesheff, K. M.; Davies, M. C.; Roberts, C. J.; Tendler, S. J. B., *Biomaterials* **2000,** 21, 1823-1835.
49. Rich, R. L.; Myszka, D. G., *Curr. Opin. Biotechnol.* **2000,** 11, 54-61.
50. Rich, R. L.; Myszka, D. G., *J. Mol. Recognit.* **2003,** 16, 351-382.
51. Rich, R. L.; Myszka, D. G., *J. Mol. Recognit.* **2002,** 15, 352-376.
52. Rich, R. L.; Myszka, D. G., *J. Mol. Recognit.* **2001,** 14, 273-294.
53. Rich, R. L.; Myszka, D. G., *J. Mol. Recognit.* **2000,** 13, 388-407.
54. Lopper, M. E.; Keck, J. L., *Handbook of Proteins* **2007,** 2, 1259-1265.
55. Huber, W.; Mueller, F., *Current Pharmaceutical Design* **2006,** 12, 3999-4021.
56. Beccati, D.; Halkes, K. M.; Batema, G. D.; Guillena, G.; Carvalho de Souza, A.; van Koten, G.; Kamerling, J. P., *ChemBioChem* **2005,** 6, 1196-1203.
57. Gerhardt, W. W.; Weck, M., *J. Org. Chem.* **2006,** 71, 6333-6341.
58. van Manen, H.-J.; Fokkens, R. H.; van Veggel, F. C. J. M.; Reinhoudt, D. N., *Eur. J. Org. Chem.* **2002**, 3189-3197.
59. Jude, H.; Krause Bauer, J. A.; Connick, W. B., *Inorg. Chem.* **2004,** 43, 725-733.
60. Hall, J.; Loeb, S. J.; Shimizu, G. K. H.; Yap, G. P. A., *Angew. Chem. Int. Ed.* **1998,** 37, 121-123.
61. Jude, H.; Krause Bauer, J. A.; Connick, W. B., *J. Am. Chem. Soc.* **2003,** 125, 3446-3447.
62. South, C. R.; Weck, M., *Langmuir* **2008,** 24, 7506-7511.
63. Gerhardt, W. W.; Zucchero, A. J.; Wilson, J. N.; South, C. R.; Bunz, U. H. F.; Weck, M., *Chem. Commun.* **2006,** 20, 2141-2143.
64. van Manen, H.-J.; Auletta, T.; Dordi, B.; Schonherr, H.; Vancso, G. J.; van Veggel, F. C. J. M.; Reinhoudt, D. N., *Adv. Funct. Mater.* **2002,** 12, 811-818.
65. van Manen, H.-J.; Fokkens, R. H.; Nibbering, N. M. M.; van Veggel, F. C. J. M.; Reinhoudt, D. N., *J. Org. Chem.* **2001,** 66, 4643-4650.
66. van Manen, H.-J.; Nakashima, K.; Shinkai, S.; Kooijman, H.; Spek, A. L.; van Veggel, F. C. J. M.; Reinhoudt, D. N., *Eur. J. Inorg. Chem.* **2000,** 12, 2533-2540.
67. Huck, W. T. S.; Prins, L. J.; Fokkens, R. H.; Nibbering, N. M. M.; van Veggel, F. C. J. M.; Reinhoudt, D. N., *J. Am. Chem. Soc.* **1998,** 120, 6240-6246.
68. Suijkerbuijk, B. M. J. M.; Aerts, B. N. H.; Dijkstra, H. P.; Lutz, M.; Spek, A. L.; van Koten, G.; Klein Gebbink, R. J. M., *Dalton Trans.* **2007,** 13, 1273-1276.
69. Chuchuryukin, A. V.; Chase, P. A.; Miils, A. M.; Lutz, M.; Spek, A. L.; van Klink, G. P. M.; van Koten, G., *Inorg. Chem.* **2006,** 45, 2045-2054.

70. Amijs, C. H. M.; Berger, A.; Soulimani, F.; Visser, T.; van Klink, G. P. M.; Lutz, M.; Spek, A. L.; van Koten, G., *Inorg. Chem.* **2005,** 44, 6567-6578.
71. Chuchuryukin, A. V.; Dijkstra, H. P.; Klein Gebbink, R. J. M.; van Klink, G. P. M.; van Koten, G., *Polym. Prepr. (Am. Chem. Soc., Div. Polym. Chem.)* **2004,** 45, 343-344.
72. Chuchuryukin, A. V.; Dijkstra, H. P.; Suijkerbuijk, B. M. J. M.; Klein Gebbink, R. J. M.; van Klink, G. P. M.; Mills, A. M.; Spek, A. L.; van Koten, G., *Russ. J. Org. Chem.* **2003,** 39, 422-429.
73. Huck, W. T. S.; van Veggel, F. C. J. M.; Kropman, B. L.; Blank, D. H. A.; Keim, E. G.; Smithers, M. M. A.; Reinhoudt, D. N., *J. Am. Chem. Soc.* **1995,** 117, 8293-8294.
74. Huck, W. T. S.; Snellink-Rueel, B.; van Veggel, F. C. J. M.; Reinhoudt, D. N., *Organometallics* **1997,** 16, 4287-4291.
75. Gossage, R. A.; Ryabov, A. D.; Spek, A. L.; Stufkens, D. J.; van Beek, J. A. M.; van Eldik, R.; van Koten, G., *J. Am. Chem. Soc.* **1999,** 121, 2488-2497.
76. Albrecht, M.; Rodriguez, G.; Schoenmaker, J.; van Koten, G., *Org. Lett.* **2000,** 2, 3461-3464.
77. Guillena, G.; Rodriguez, G.; Albrecht, M.; van Koten, G., *Chem. Eur. J.* **2002,** 8, 5368-5376.
78. Guillena, G.; Kruithof, C. A.; Casado, M. A.; Egmond, M. R.; van Koten, G., *J. Organomet. Chem.* **2003,** 668, 3-7.
79. Albrecht, M.; Lutz, M.; Schreurs, A. M. M.; Lutz, E. T. H.; Spek, A. L.; van Koten, G., *Dalton Trans.* **2000,** 21, 3797-3804.
80. Okpodu, C. M.; Alscher, R. G.; Grabau, E. A.; Cramer, C. L., *J. Plant Physiol.* **1996,** 148, 309-316.
81. Guillena, G.; Halkes, K. M.; Rodriguez, G.; Batema, G. D.; van Koten, G.; Kamerling, J. P., *Org. Lett.* **2003,** 5, 2021-2024.
82. Greenfield, S. J.; Agarkov, A.; Gilbertson, S. R., *Org. Lett.* **2003,** 5, 3069-3072.
83. Agarkov, A.; Greenfield, S. J.; Ohishi, T.; Collibee, S. E.; Gilbertson, S. R., *J. Org. Chem.* **2004,** 69, 8077-8085.
84. Agarkov, A.; Greenfield, S. J.; Xie, D.; Pawlick, R.; Starkey, G.; Gilbertson, S. R., *Biopolymers* **2006,** 84, 48-73.
85. Benito, J. M.; Christensen, C. A.; Meldal, M. A., *Org. Lett.* **2005,** 7, 581-584.
86. Christensen, C. A.; Meldal, M. A., *Chem. Eur. J.* **2005,** 11, 4121-4131.
87. Guillena, G.; Rodriguez, G.; van Koten, G., *Tetrahedron Lett.* **2002,** 43, 3895-3898.
88. Wilson, M. E.; Whitesides, G. M., *J. Am. Chem. Soc.* **1978,** 100, 306-307.
89. Letondor, C.; Humbert, N.; Ward, T. R., *Proc. Natl. Acad. Sci. USA* **2005,** 102, 4683-4687.
90. Pierron, J.; Malan, C.; Creus, M.; Gradinaru, J.; Hafner, I.; Ivanova, A.; Sardo, A.; Ward, T. R., *Angew. Chem. Int. Ed.* **2008,** 47, 701-705.
91. Steinreiber, J.; Ward, T. R., *Coord. Chem. Rev.* **2008,** 252, 751-766.
92. Pordea, A.; Creus, M.; Panek, J.; Duboc, C.; Mathis, D.; Novic, M.; Ward, T. R., *J. Am. Chem. Soc.* **2008,** 130, 8085-8088.
93. Satake, Y.; Abe, S.; Okazaki, S.; Ban, N.; Hikage, T.; Ueno, T.; Nakajima, H.; Suzuki, A.; Yamane, T.; Nishiyama, H.; Watanabe, Y., *Organometallics* **2007,** 26, 4904-4908.
94. Dijkstra, H. P.; Sprong, H.; Aerts, B. N. H.; Kruithof, C. A.; Egmond, M. R.; Klein Gebbink, R. J. M., *Org. Biomol. Chem.* **2008,** 6, 523-531.
95. Kruithof, C. A.; Casado, M. A.; Guillena, G.; Egmond, M. R.; van der Kerk-van Hoof, A.; Heck, A. J. R.; Klein Gebbink, R. J. M.; van Koten, G., *Eur. J. Inorg. Chem.* **2008,** 27, 4425-4432.
96. Kruithof, C. A.; Casado, M. A.; Guillena, G.; Egmond, M. R.; van der Kerk-van Hoof, A.; Heck, A. J. R.; Klein Gebbink, R. J. M.; van Koten, G., *Chem. Eur. J.* **2005,** 11, 6869-6877.
97. Reetz, M. T.; Rentzsch, A.; Pletsch, M.; Maywald, M., *Chimia* **2002,** 56, 721-723.
98. *The structural, coordination, catalytic and luminescence studies of these pincer-protein hybrids are described in chapters 2-6 and 8 of this thesis.*

CHAPTER 2

Solid State Structural Characterization of ECE-Pincer Metal-Cutinase Hybrids

This chapter was published in *Chemistry – A European Journal* (*Chem. Eur. J.* **2009**, 15, 4270-4280).

The first crystal structures of lipases, covalently modified by site selective inhibition by different organometallic pincer-metal phosphonate complexes, are described. Two "ECE" pincer-type d^8-metal-complexes, *i.e.* platinum (**1**) or palladium (**2**), phosphonate esters (ECE = $[(EtO)\text{-}(O{=})P(\text{-}O\text{-}C_6H_4\text{-}(NO_2)\text{-}4)(\text{-}C_3H_6\text{-}4\text{-}(C_6H_2\text{-}(CH_2E)_2)]^-$ with E = NMe_2 or SMe) have been introduced prior to crystallization and have been shown to bind selectively to the Ser120 residue in the active site of the lipase cutinase. For all five presented crystal structures, the ECE-pincer platinum or palladium head group sticks out of cutinase and is exposed to the solvent. Depending on the nature of the ECE metal head group, the ECE pincer platinum (**cut-1**) and palladium (**cut-2**) phosphonate guests occupy different pockets in the active site of cutinase, with concomitant different stereochemistries on the phosphorous atom for the **cut-1** (S_P) and **cut-2** (R_P) structures. When **cut-1** was crystallized under halide-poor conditions, a novel metal-induced dimeric structure was formed between two cutinase-bound pincer platinum head groups, which are interconnected via a single μ-Cl bridge. This halide-bridged metal dimer shows that coordination chemistry is possible with protein modified pincer metal complexes. Furthermore, we could use NCN-pincer platinum complex **1** as site-selective tool for the phasing of raw protein diffraction data, which shows the potential use of pincer platinum complex **1** as heavy-atom derivative in protein crystallography.

Introduction

The modification of proteins with synthetic molecules has become an important strategy in the newly emerging area of chemical biology. Since the pioneering work of Kaiser[1] and Whitesides[2] many different protein modification strategies have been developed in order to facilitate protein identification, to change their structural characteristics, and to study their biological functionalities and activities. The synthetic modification of biological compounds with transition metal complexes plays a special role in this case. Through the presence of a transition metal several novel spectroscopic and reactivity properties can be added to those a protein intrinsically already has. Transition metal complexes attached to biomolecules have, for example, been used as anticancer agents,[3, 4] as radioactive[4-9] or luminescent labels,[10-12] as paramagnetic NMR probes,[13] or as semisynthetic metalloenzymes in catalysis.[14-28]
The incorporation of transition metal complexes into proteins can be accomplished by a variety of different methods, among which the non-covalent anchoring of metal complexes to both apo-myoglobin[14, 29, 30] and the biotin-(strept)avidin system[2, 18, 20-22, 28, 31, 32] are well known. Transition metal complexes can also be covalently attached to proteins, *e.g.* by binding ligands or complexes to amino acid functional groups.[15, 17, 33] By doing so, different functional domains and specific sites in a protein can be addressed. In this way new hybrid systems are obtained, which possess not only interesting structural and catalytic properties but also have favorable solubility characteristics. Transition metal catalysts, for example, can now be used in environmentally friendly aqueous media and the chiral protein environment can positively influence the stereoselectivity and enantioselectivity of the bound transition metal catalyst.[28]
Versatile probes for the modification of different biomolecules have been the so-called 'pincer' complexes.[9, 34] Pincer metal complexes consist of a mono-anionic, bis-*ortho*-chelating ECE ligand (ECE = $[C_6H_3(CH_2E)_2\text{-}2,6]^-$), where the binding of the two electron-donating *ortho*-substituents complement the central carbon-metal bond (E = *e.g.* NMe_2, PPh_2 and SMe). Pincer-platinum complexes have, among others, been bound to carbohydrates as Surface Plasmon Resonance (SPR) sensitizers,[35] as well as to peptides[36] and lipolytic enzymes.[37] Due to their high stability, excellent properties as sensors,[38] heavy metal atom labels and catalysts,[34] pincer-metal molecules are ideal candidates for the modification of biomolecules.

Recently, we have been able to attach pincer metal-d^8 complexes to the lipase cutinase in a covalent manner by active site-directed inhibition.[37] Cutinase (21kDa) is a member of the lipase family (subfamily of the serine hydrolases) with an exposed catalytic triad (Ser120-Asp175-His188).[39, 40] As the structure and activity of this stable enzyme have been well studied, we envisioned cutinase as being the ideal candidate for the study of semisynthetic pincer-metal/enzyme hybrids. From different studies it is known that lipases can be inhibited by phosphonate esters,[41, 42] which function as transition state analogues of fatty acid ester substrates. Therefore, a

pincer-metal complex linked to a phosphonate moiety would be an ideal compound to become covalently bonded to cutinase. Two different phosphonate pincer complexes, namely NCN-pincer platinum complex **1** and SCS-pincer palladium complex **2**, were attached to the active site Ser120 of cutinase, resulting in complexes in which the pincer-metal complexes become irreversibly immobilized to the lipase (Scheme 1).[37] We linked inhibitors **1** and **2** to the protein via a covalent bond between the active site serine of cutinase (Ser120) and the inhibitor phosphonate group, which is attached by a spacer to the *para* position of the pincer-phenyl ring (Scheme 1). This was done by addition of a racemic mixture of pincer-metal complexes *rac*-**1** or *rac*-**2** to cutinase, as it was known from earlier studies[37, 39, 43, 44] that the reaction of cutinase with phosphonates proceeds with high enantioselectivity. By doing so, it was anticipated that only the fast reacting enantiomer of the pincer-metal phosphonate complex would bind to cutinase.

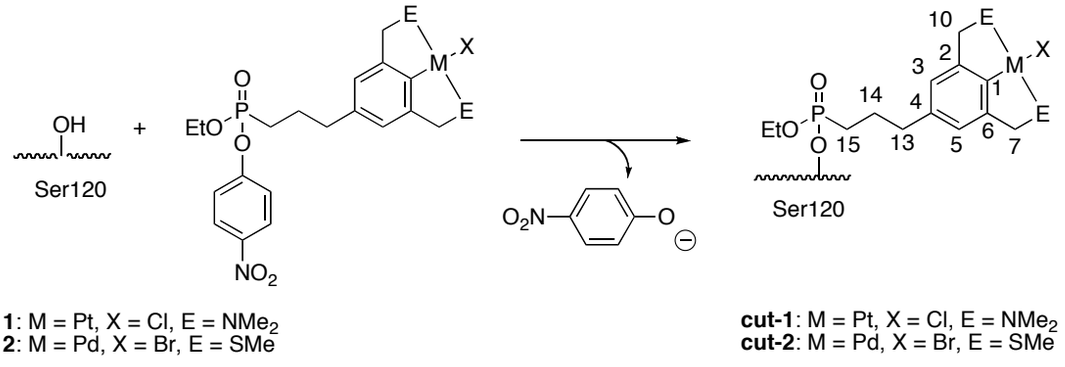

1: M = Pt, X = Cl, E = NMe_2
2: M = Pd, X = Br, E = SMe

cut-1: M = Pt, X = Cl, E = NMe_2
cut-2: M = Pd, X = Br, E = SMe

Scheme 1: Binding of the pincer-metal phosphonate complexes *rac*-**1** and *rac*-**2** to Ser120 of cutinase; the numbering scheme for **1** and **2** is shown.

Cutinase has another advantage over other lipases in that it lacks interfacial activation, because of an exposed active site and a preformed oxyanion hole consisting of two main chain nitrogens (Ser 42 N and Gln121 N) and the Oγ of Ser 42.[39] Cutinase is a well-studied enzyme, which is reflected by the many crystal structures that are known of the free protein, of mutants and of cutinase-inhibitor complexes, like different phosphonate[39, 45-47] inhibitors.

Here we report on single crystal X-ray structure determinations of cutinase hybrids having bound in its active site either pincer-platinum complex **1** or pincer-palladium complex **2**, respectively, (Scheme 1), i.e. three structures of the **cut-1** (cutinase-pincer **1**) complex and two structures of the **cut-2** (cutinase-pincer **2**) complex. To the best of our knowledge, these are the first organometallic palladium- and platinum-protein crystal structures reported to date. The molecular structures of **cut-1** and **cut-2** (Scheme 1) revealed a detailed picture of the various binding modes of the pincer-metal complexes to the protein and the aggregation of two pincer-metal

lipase hybrids around a bridging halide anion in the solid state. These results, moreover, show that the different pincer-metal inhibitor molecules occupy different binding pockets in the active site of the enzyme (pockets 1 and 2, respectively).

Results

Inhibition, crystallization, data collection and structure determinations

The pincer-metal inhibitor complexes *rac*-**1** and *rac*-**2** (3 equivalents) were added to a buffered solution of cutinase (1 mM). By adding an excess of phosphonate inhibitor, the binding of the fast-reacting phosphonate enantiomer of **1** or **2** to cutinase was assured. After overnight incubation, excess inhibitor was removed by dialysis and the mixture was concentrated and crystallized (see Experimental Section for details). To obtain crystals of the pincer cutinase hybrids, the literature conditions for the crystallization of cutinase[39] had to be changed in order to obtain suitable crystals. Interestingly, we did not find the crystal forms of free cutinase and other cutinase inhibitor complexes known from the literature,[39] but found five new cutinase packing motifs instead. Moreover, the arrangement of the pincer molecules with respect to each other is different (*vide infra*).

Three different crystal structures of **cut-1** (**cut-1a**, **cut-1b** and **cut-1c**) and two of **cut-2** (**cut-2a** and **cut-2b**) pincer-cutinase hybrids are described. The molecular structures were solved by Molecular Replacement methods using the coordinates of a previously solved cutinase structure[45] and of two different pincer metal structures.[48, 49] A selection of data processing and refinement statistics is shown in Table 1.

Table 1: Selection of the data processing and refinement statistics for the different resolved **cut-1** (Pt) and **cut-2** (Pd) structures (all data deposited at www.pdb.org).

	cut-1a	**cut-1b**	**cut-1c**	**cut-2a**	**cut-2b**
PDB-code	3EF3	3ESA	3ESB	3ESC	3ESD
Space group	I222	$P2_1$	$P3_121$	$P6_3$	R3(H3)
Unit cell					
A	59.3	34.0	70.0	83.9	72.4
B	89.8	71.9	70.0	83.9	72.4
C	97.5	68.6	100.7	55.8	110.8
β	90.0	96.9	90.0	120.0	120
Solvent content (%)	56	32	60	50	49
Total oscillation[c]	120	180	120	120	120
Radiation	ID14-EH1	ID14-EH1	ID14-EH1	ID29	ID29
Wavelength[a]	0.934	0.940	0.934	0.9792	1.0332

Exposure time[d]	5.0	1.0	10.0	0.5	0.5
Mol./ASU	1	1	1	1	1
Resolution[a] (outer shell)	29-1.5 (1.58-1.5)	36-2.0 (2.11-2.0)	39-2.3 (2.42-2.3)	44-1.2 (1.26-1.2)	41-1.22 (1.29-1.22)
R-merge (%) (outer shell)	7.5 (60.3)	8.9 (41.0)	7.8 (52.1)	10.0 (71.3)	12.5 (80.5)
R-pim(%)	4.3 (33.2)	8.9 (41.0)	7.8 (52.1)	10.0 (71.3)	12.5 (80.5)
Data processing program	MOSFLM	MOSFLM	MOSFLM	XDS	XDS
Refinement program	REFMAC	REFMAC	REFMAC	SHELXL	SHELXL
Completeness (%) (outer shell)	99.7 (100)	99.5 (99.5)	97.0 (100)	100 (100)	97.1 (100)
I/σI (outer shell)	13.2 (2.5)	13.6 (2.4)	14.6 (3.3)	13.6 (2.3)	5.7 (1.2)
No. observations	198777 (28810)	78072 (11532)	91501 (13883)	500894 (72004)	220922 (19794)
No. unique observations	41835 (6064)	22076 (3202)	12784 (1903)	69883 (10146)	61949 (7679)
Multiplicity (outer shell)	4.8 (4.8)	3.5 (3.6)	7.2 (7.3)	7.2 (7.1)	3.6 (2.6)
Refinement statistics					
R_{work} (%)	15.9	19.9	22.2	16.6	19.9
R_{free} (%)	17.8	25.3	24.5	19.4	22.2
r.m.s.d. bond lengths[a]	0.01	0.01	0.01	0.02	0.02
r.m.s.d. bond angles[b]	1.45	1.60	1.45	0.03	0.04
average B-factor[e]	19.4	37.7	39.5	17.2	22.8

[a] in Å; [b, c] in [O]; [d] in s; [e] in Å^2.

*Crystal packing of **cut-1** structures*

The different **cut-1** crystal structures were all obtained after inhibition of cutinase with pincer platinum complex **1** (Scheme 1). The crystal structures **cut-1a** (space group I222) and **cut-1c** ($P3_121$) both contained one molecule in the asymmetric unit, whereas **cut-1b** ($P2_1$) contained two independent molecules (Table 1). In all three **cut-1** molecular structures the (neutral) NCN-pincer platinum chloride entity is

situated in pocket 1 and in all cases the *S*-enantiomer of the phosphonate is bound to Ser120.

The crystal structure of **cut-1a**, which was determined at 1.5 Å resolution, showed a 'head-to-head' packing of the pincer-cutinase hybrid molecule, where the 'heads' of two symmetry related molecules are in mutual proximity (Figure 1a). The intermolecular Pt…Pt^{i} distance is 8.9 Å (i: 1-x, y, -z) and the platinum-coordinated chlorides are located in the region of the bulk solvent. The Pt1…Cl1 bond length is 2.4 Å, which is in agreement with the crystal structure data of a small molecular analogue pincer-platinum complex (Pt…Cl = 2.407(1) Å).[48]

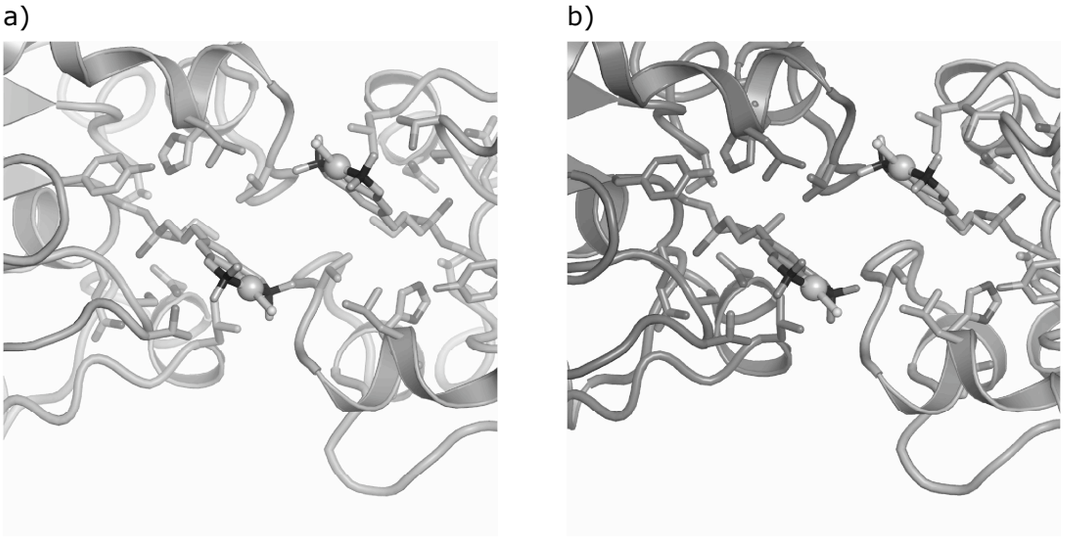

Figure 1: a) The structure of **cut-1a** viewed along the twofold rotation axis; b) The two molecules in the asymmetric unit in **cut-1b** (molecule A is represented in lighter tones than molecule B).

Similarly, in **cut-1b** the pincer-enzyme hybrids are also packed 'head to head' resulting in an intermolecular Pt1…Pt2 distance of 8.7 Å (Figure 1b). The Pt1…Cl1 and Pt2…Cl1 bond lengths are 2.4 Å, the same values as for the **cut-1a** molecular structure. For both **cut-1a** and **cut-1b** the electron density of the platinum and the chloride have ellipsoidal shapes (Figure 2).

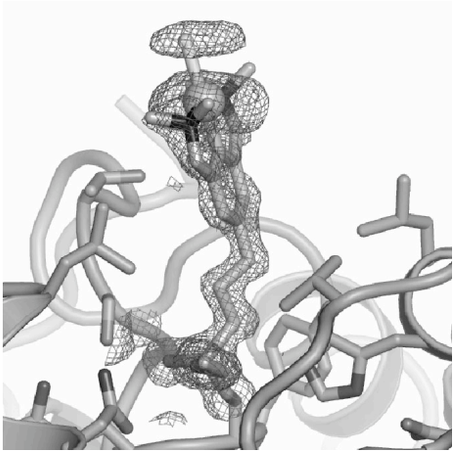

Figure 2: Ellipsoidal shape of the electron density around platinum and chloride of the (neutral) pincer entity in **cut-1a.**

In **cut-1b**, the coordinated chloride of molecule B is located in the region of the bulk solvent, but the one of molecule A is closer to a symmetry related molecule A in the crystal packing. The shortest distances are 5.7 Å and 5.7 Å, between the chloride and $Gly_{212}C$ and the chloride and $Arg_{208}C\beta$, respectively.
Due to the head-to-head packing observed for both **cut-1a** and **cut-1b**, the hydrophobic areas of the pincer-cutinase hybrids, consisting of the pincer-metal moiety embedded in the substrate binding region, are shielded from the aqueous solvent. This feature has been observed before for several other cutinase crystal structures with and without inhibitor molecules in the active site.[39, 45, 46]

When **cut-1** was crystallized under halide-poor conditions (2% PEG-1000, 100 mM Hepes pH 6.0), a dinuclear pincer-platinum/cutinase hybrid was formed. This surprising molecular structure for **cut-1** ($P3_121$) was observed with a different crystal packing than for mononuclear **cut-1a** and **cut-1b**. In **cut-1c**, two cationic pincer-platinum/cutinase hybrids share one chloride anion, forming a $\{[Pt]\text{-}Cl\text{-}[Pt]\}^+$ bridge, which results in a monocation dinuclear species (Figure 3). The bridging μ-chloride is located on a crystallographic two-fold rotation axis.

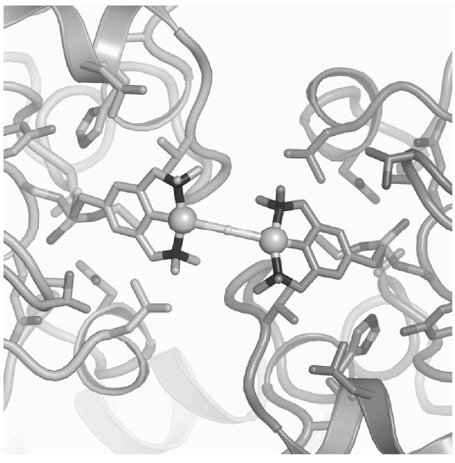

Figure 3: Crystallographic symmetry related molecules that bridge via a μ-chloride in **cut-1c** (view along the two-fold rotation axis).

X-ray data of **cut-1c** were obtained up to a resolution of 2.3 Å. The position of the platinum atom is quite well-defined due to its high scattering factor. The Pt…Pt^i distance is 5.2 Å, which is significantly shorter in comparison to **cut-1a** (Pt…Pt^i = 8.9 Å) and **cut-1b** (Pt1…Pt2 = 8.69 Å). Due to the coordination bonds of platinum to the bridging chloride, the electron density around platinum has a spherical shape. This indicates that the molecular motion is significantly smaller for **cut-1c** than for the **cut-1a** or **cut-1b** molecular structures. The Pt-Cl-Pt^i angle is 179.5° with a Pt-Cl and Pt^i-Cl distance of 2.7 Å, which is slightly longer than the distance for the mononuclear pincer-metal structures (2.4 Å, *vide infra*). The torsion angle between the aromatic planes of the pincer-platinum moieties (C2C6-C2C6$_{sym}$) is -23.0°.
As outlined above the overall charge of the dinuclear molecular structure for **cut-1c** is +1. The second chloride that is present in the pincer-cutinase hybrid **cut-1** prior to crystallization could neither be located in the difference Fourier maps nor in anomalous dispersion maps (low anomalous scattering power at the given wavelength). Due to this, the second chloride is assumed to be disordered in the bulk solvent region. It is important to note that the formation of μ-halide bridged, dinuclear pincer-metal complexes has been observed for small molecule analogues before[50, 51] and was found to be an intrinsic property of the NCN-pincer-metal cationic moieties (metal is platinum or palladium) under halide-poor reaction conditions. The corresponding, small molecule structures of $[\{Pd(C_6H_3(CH_2NMe_2)_2\text{-}2,6\}_2(\mu\text{-}Cl)]^+$ dinuclear NCN-pincer palladium complexes have slightly different Pd2-Cl1-Pd1 angles (134.80°[50] and 121.11°[51]) and torsion angles (-95.78°[50] and -61.32°[51]). These observations show that the μ-halide bridged dimer formation can also occur with pincer-cutinase hybrids in which the covalently anchored cutinase enzyme molecules act as giant *para*-substituents for each of the NCN-pincer platinum cations. The low concentration (high dilution) of halide ions may be the driving force for the formation of cationic, dinuclear species in this case. Under the chloride-poor crystallization

conditions (*vide infra*), the equilibrium between neutral pincer-platinum chloride and cationic pincer-platinum moieties caused by Pt-Cl bond dissociation will shift to the side of the cationic species. This view is substantiated by the fact that reaction of the small molecule equivalent, $[\{M(C_6H_3(CH_2NMe_2)_2\text{-}2,6\}_2(\mu\text{-}Cl)]^+$ (M = Pt or Pd) with excess chloride leads to the formation of neutral NCN-pincer platinum chloride.[52, 53]
Superposition of the three **cut-1** structures shows that the orientation of the linker atoms C15-C14-C13 is basically the same for all structures. For the dinuclear structure **cut-1c** the plane of the aromatic pincer ring is rotated ~90º, with respect to **cut-1a** and the two independent molecules of **cut-1b** as can be seen Figure 4.

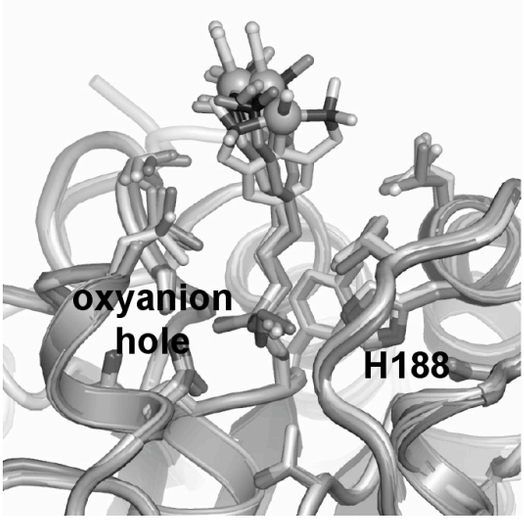

Figure 4: Superposition of **cut-1a**, **cut-1b** and **cut-1c**.

*Crystal packing of **cut-2** structures*
The **cut-2** hybrid complexes in are formed by inhibition of cutinase with the SCS-pincer palladium bromide complex **2** (Scheme 1). The **cut-2a** complex crystallized in space group $P6_3$ and **cut-2b** in spacegroup R3 (hexagonal setting). Both asymmetric unit cells contain one SCS-pincer palladium bromide/cutinase hybrid. In both **cut-2** molecular structures the SCS-pincer palladium bromide entity is situated in pocket 2 and for both structures the *R*-enantiomer of the phosphonate is bound to Ser120. The **cut-2** pincer-cutinase hybrids are packed 'head-to-head' with three pincer-modified cutinase entities oriented towards each other (Figure 5).
In the **cut-2a** structure the pincer-palladium complexes of the hybrid molecules are located in proximity of the 6_3-screw axis. The electron density map clearly shows two positions for palladium, which indicates positional disorder, i.e. two conformations for the pincer-palladium complex. The minor disorder component has an occupancy of 1/3 and the corresponding bromide is located on the symmetry axis, where we observe electron density. The major disorder component has its Br atom on a general position away from the axis and the occupancy of this entity is 2/3. Because in the X-ray diffraction experiment only the average over the whole crystal is observed, our

disorder model means that 1/3 of all molecules at the symmetry axis have one orientation while 2/3 have the second orientation (Figure 5).

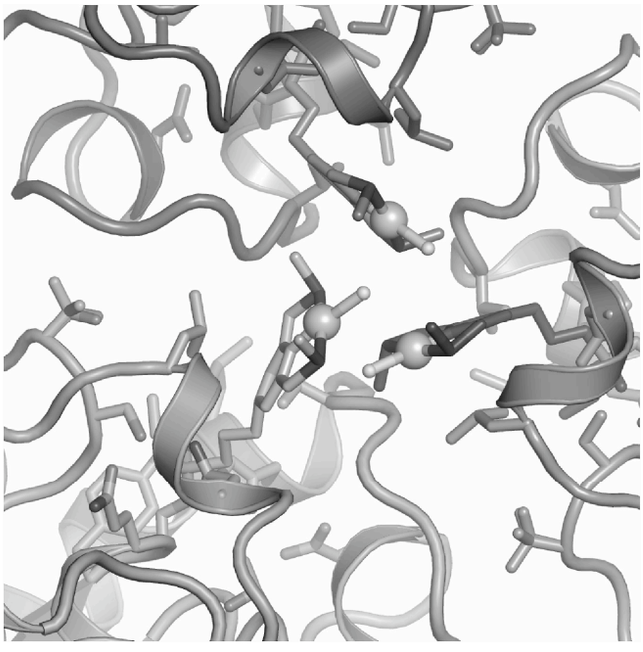

Figure 5: Disordered crystallographic trimer of **cut-2a** viewed along the symmetry axis. The pincer moiety with its bromide at the threefold rotation axis (1/3 occupancy) is shown in lighter tones than the other pincer moiety.

The Pd1…Pd1^{i} distance is 4.0 Å between the major and minor component, while the distance between the major Pd positions is 5.6 Å. By using the same data as for the refinement (wavelength 0.98 Å), an anomalous difference map was calculated. The split Pd positions were clearly detectable, but no anomalous signal for the bromides was observed. Therefore, the bromide positions were exclusively derived from the 2Fo-Fc Fourier map. The Pd…Br distance is 2.4 Å in both the minor and the major disorder components.

The packing of the pincer-palladium bromide moieties in **cut-2b** was quite similar to **cut-2a**, except that we did not observe disorder. The pincer-cutinase hybrid complexes were packed in layers parallel to the crystallographic a,b-plane as shown in Figure 6.

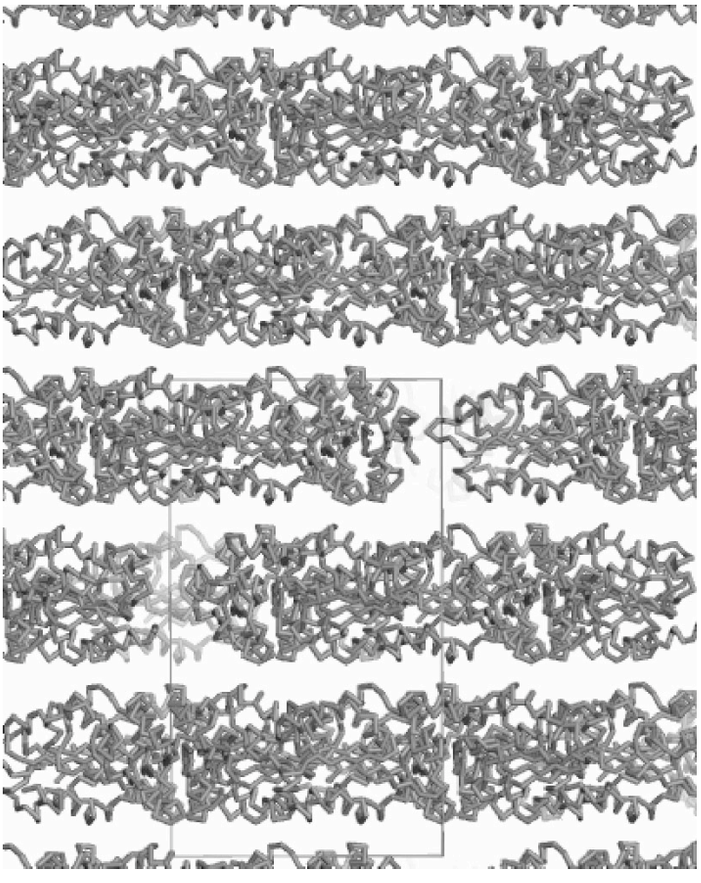

Figure 6: Crystal packing of R3 **cut-2b** molecules. The layer packing could explain the observed twinning. The cell axes are shown (The view is along the a-axis. The c-axis is vertical.)

This layer packing motive makes merohedral twinning possible with a twofold rotation about the a-axis as twin operation. This twinning was indeed observed in the present crystal and refined with SHELXL using the TWIN instruction,[54] resulting in a twin fraction of 0.5. The point group 3 of the crystal lattice can be obtained via a coset decomposition of point group 32 of the twin lattice.[55] The twofold twin axis cannot be a real crystallographic operation because this would result in only half a molecule in the asymmetric unit. For this structure, the pincer entity is located in proximity to symmetry related molecules and thus is shielded from the bulk solvent. In **cut-2b** the Pd1…Pd1^{i} distance is 5.3 Å (Figure 7). The Pd…Br distance is 2.5 Å.

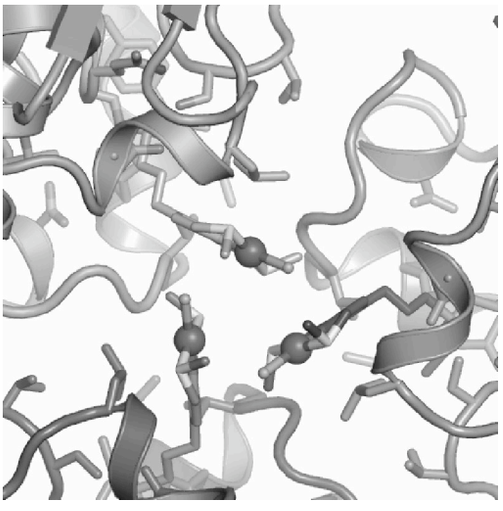

Figure 7: Crystallographic trimer of **cut-2b**, viewed along the three-fold rotation axis.

For one of the pincer arms we do not observe electron density for the methyl group. This is most probably due to disorder, as the methyl groups of the SCS-pincer palladium complex can adopt two different configurations (axial or equatorial) resulting in different diastereomers.[56] The axial or equatorial configurations of the thiomethoxy groups of SCS-pincer palladium complexes as observed previously[56] could not be accurately refined for **cut-2a** and **cut-2b** due to the resolution of the diffraction data.

Discussion

Influence of the pincer-metal phosphonates on cutinase and vice versa

To determine the influence of the pincer-metal guest complexes on the molecular structure of cutinase, we compared the molecular structures of the pincer-enzyme hybrids in the five different crystal structures with free, uninhibited cutinase.[45] Table 2 shows the root mean square deviation, the average deviation and the maximum deviation for the Cα-atoms.

Table 2: Comparison of **cut-1** and **cut-2** structures with uninhibited cutinase[45] (a) for the whole molecule and (b) for 10 Å around active site phosphorous.

(a) Whole molecule						
	rmsd[a] Cα	av.[b] Cα	max.[c] Cα	rmsd[a] all	av.[b] all	max.[c] all
cut-1a	0.37	0.31	1.83	0.97	0.51	8.77
cut-1b	0.37	0.29	2.25	0.86	0.47	8.20
(mol A)						
cut-1b	0.44	0.33	2.91	0.89	0.49	8.96
(mol A)						
cut-1c	0.71	0.37	7.95	1.04	0.55	10.45
cut-2a	0.42	0.31	2.445	0.947	0.50	10.59
cut-2b	0.40	0.32	1.96	0.83	0.48	9.46

(b) 10 Å around active site phosphorous						
	rmsd[a] Cα	av.[b] Cα	max.[c] Cα	rmsd[a] all	av.[b] all	max.[c] all
cut-1a	0.26	0.22	0.53	0.49	0.32	2.91
cut-1b	0.28	0.24	0.54	0.60	0.39	3.15
(mol A)						
cut-1b	0.28	0.25	0.46	0.53	0.36	2.95
(mol A)						
cut-1c	0.32	0.28	0.74	0.52	0.37	2.62
cut-2a	0.36	0.28	0.84	0.52	0.37	2.54
cut-2b	0.38	0.31	0.78	0.54	0.40	2.56

[a] root mean square deviation; [b] average deviation; [c] maximum deviation.

Additionally, the same quantities are given with respect to all atoms within 10 Å around the phosphorus of the active site and for all atoms in the whole protein. Especially in the calculation for the 10 Å sphere it becomes evident that the deviations are small. For example, the root mean square deviation for the Cα-atoms is less than 0.4 Å. From these numbers we conclude that no major changes occur within the active site by binding of the pincer-metal complex. Thus, similar to other cutinase-inhibitor structures,[39, 40] the pincer molecules only have a minor effect on the active site conformation. The exposed position and the freedom to move of the C3 pincer-metal complexes observed here is complementary to another study by our group, where C0 linked pincer-metal complexes have been bound to cutinase.[49] Contrary to the C3 linked structures, modelling studies for the C0 linked pincer-metal complexes shows that the pincer-metal moieties are immersed in the periphery of cutinase.

To get insight into how the protein environment can influence the embedded pincer-metal complex, the distances of the metal sites to atoms of the protein are of great importance (Table 3). In **cut-1a** the nearest residue to the metal is threonine 44 with

a distance of 4.8 Å between Oγ and the platinum atom. In Table 3 the distances of the platinum and palladium ions to the closest amino acid atoms and to chiral carbon atoms of the protein backbone are given.

Table 3: Shortest distances of metal to protein atoms (a) and metal to chiral carbon atoms of the backbone (b).

Structure	Distances (Å)			
	(a)		(b)	
cut-1a	Pt- Thr_{44} Oγ	4.8	Pt- Thr_{44} Cβ	5.6
cut-1b (mol. A)	Pt- Thr_{44} Oγ	4.4	Pt- Thr_{44} Cβ	5.6
cut-1b (mol. B)	Pt- Thr_{44} Oγ	5.4	Pt- Thr_{44} Cβ	6.2
cut-1c	Pt- Val_{184} Cγ	6.1	Pt- Val_{184} Cα	7.6
cut-2a (conf. 1)	Pd1- Leu_{81} Cγ	4.0	Pd1-Leu81Cα	5.7
cut-2a (conf. 2)	Pd2- Leu_{81} Cγ	5.2	Pd2-Leu81Cα	6.7
cut-2b	Pd- Leu_{81} Cγ	3.9	Pd-Leu81Cα	5.4

The shortest distances to the protein atoms vary from 4.0 Å to 6.1 Å, the shortest distances to chiral carbon atoms range from 5.7 Å to 7.6 Å. The ellipsoidal shape of the electron density of the metal atoms in **cut-1a** (Figure 2) and **cut-1b** and the disorder of the complete pincer entities in **cut-2a** (Figure 5) indicate a large degree of freedom for molecular movements in the active site. In **cut-1c** the motion of the pincer is significantly smaller due to the pincer-platinum induced formation of monocationic dinuclear species in the crystal. Also due to crystal packing in **cut-2b** the motion of the pincer is restricted by the proximity of symmetry related molecules. The different arrangements of the **cut-1** and **cut-2** structures are only possible because of the large degrees of freedom of the pincer in the active site. A great advantage of this freedom to move is that the metal centre of the pincer guest complex is exposed to the solvent and is well available for ligand coordination. This will allow us to perform supramolecular coordination chemistry at the metal centre.

Due to the large distances of the metal centre to the chiral carbon atoms of the protein backbone, a significant chiral induction of the protein backbone onto the metal centre with these particular inhibitors is less likely. The latter is of importance when these semisynthetic metalloenzymes will be applied as catalysts in organic transformations, where chiral induction might be desirable in some cases.

Binding modes of the pincer-metal complexes

When the different **cut-1** and **cut-2** structures are compared with each other, different spatial orientations of the SCS-pincer palladium and NCN-pincer platinum moieties in the active site of cutinase are observed (Figure 8a, b). NCN-pincer platinum complexes of all three **cut-1** structures occupy one pocket ('pocket 1') of

the cutinase active site, whereas the SCS-pincer palladium moieties of the two **cut-2** structures occupy the second pocket ('pocket 2'), as depicted in Figure 8a, b.

a) b)

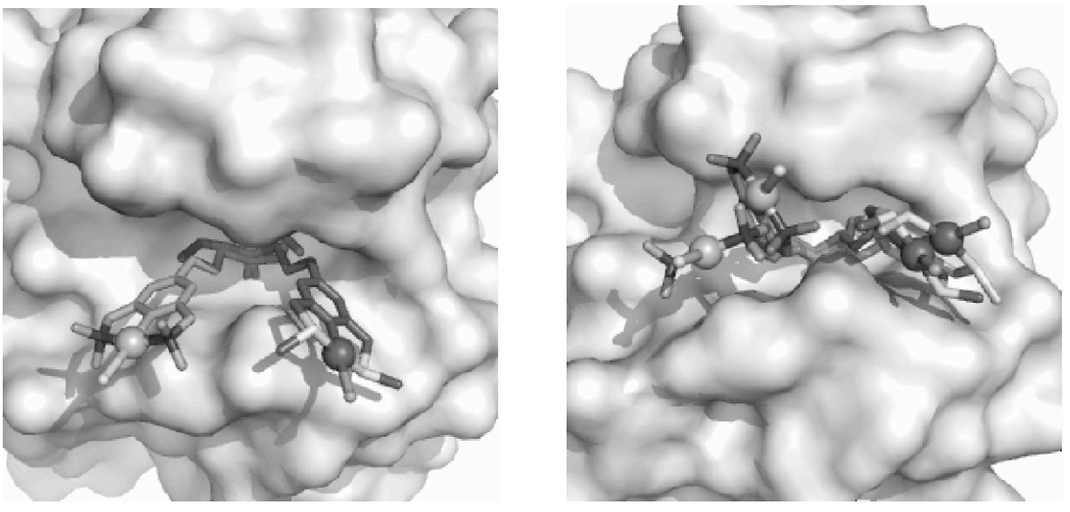

Figure 8: Surface representation of the cutinase active site with superposed cutinase molecules: a) **cut-1** (shown in light grey) and **cut-2** (shown in dark grey) pincer-metal entities occupy different pockets in the active site of cutinase; only the pincer-metal complexes of **cut-1b** and **cut-2b** are shown as representatives; b) variety of orientations of the pincer-metal entities in the active site of cutinase.

A closer look at the binding of the different phosphonates to cutinase reveals that for all NCN-pincer platinum **cut-1** structures the S_P-enantiomer of the phosphonate is bound to cutinase, whereas for the two SCS-pincer palladium-containing **cut-2** structures the R_p-enantiomer is bound. In Figure 8a the different stereochemical orientations on phosphorous are well visible, with the two C15-C14-C13 linkers of the pincer platinum and palladium moiety positioned in the two different pockets. Similar to other phosphonate inhibitors known from literature,[39, 40] the phosphonate moieties in the **cut-2** palladium structure form an additional hydrogen bond between the ethoxy O2 (Scheme 1) and the imidazole-bound (Nε2) hydrogen atom of His188 in pocket 1. Due to binding of the other enantiomer, this hydrogen bond is lacking for the **cut-1** platinum structures, as the ethoxy O2 is situated in pocket 2.
The different spatial orientation of the pincer platinum and palladium phosphonates bound to cutinase (Figure 8) and their different stereochemistry on phosphorous is a rather unexpected observation. The platinum (*rac*-**1**) and palladium (*rac*-**2**) phosphonate inhibitor molecules (Scheme 1) have similar structures and a similar kinetic inhibition behaviour,[37] and therefore spatial orientation of metal inhibitors **1** and **2** into different pockets in the active site of cutinase is surprising.

Although the structures of **1** and **2** (Scheme 1) resemble each other, the pincer platinum phosphonate complex **1** is slightly more bulky around the metal centre than complex **2**. The dimethylamino groups of **1** are larger than the thiomethoxy groups of **2**. As for all **cut-1** and **cut-2** structures the metal centres are situated close to the surface at the rim of the cutinase active site, the subtle differences in steric bulk between **1** and **2** could play a decisive role when the inhibitor molecule approaches the active site and diffuses towards the Ser120 residue. The crystal structural data of the cutinase backbone show that binding pocket 2, the pocket in which the pincer palladium complex is present (**cut-2**), is slightly narrower than binding pocket 1 of the pincer platinum complex (**cut-1**). Due to the slightly enhanced bulk of **1**, the pincer platinum phosphonate complex can probably approach the active site faster via pocket 1 and can therefore mainly yield the pincer-metal complex with *S* stereochemistry on phosphorous, as observed for the **cut-1** structures. Apparently, the smaller palladium inhibitor **2** fits well into pocket 2 and therefore binds to cutinase with the preferred R_P stereochemistry. If diffusion to Ser120 via pocket 1 or 2 is considered as being the rate-determining step of the inhibition process, then the binding of the NCN-pincer platinum inhibitor in pocket 1 could be explained.
We do not know whether for inhibitor **1** also the other enantiomer (*R*) binds to cutinase in solution or that it just does not crystallize under the conditions applied. However, as the inhibition speed of cutinase by complexes **1** and **2** is comparable[37] and as we added three equivalents of the racemic inhibitor each time, we propose that the binding of the *S*-enantiomer in the **cut-1** structures is caused by slight differences in steric bulk between inhibitors **1** and **2**.
Currently, we are investigating the inhibition kinetics of *rac*-**1** and *rac*-**2** further in order to obtain information about the relative inhibition rates of the *R* and *S* enantiomers of **1** and **2**.

Matching of the hydrophobic sites
When the packing of the structures described above is studied in more detail, the shielding of the hydrophobic active site regions from the solvent region is a feature observed for all five crystal structures. For the **cut-1a**-**c** structures, the pincer-modified hydrophobic active sites of two cutinase molecules are oriented towards each other, whereas for **cut-2a**/**b** three active sites are packed head-to-head. This matching of the hydrophilic and hydrophobic regions of cutinase in the crystal structure packing has been observed earlier for native cutinase and cutinase modified with different inhibitors[39, 40] and is also common for the crystal structure packing of other lipases.[41] This hydrophobic site matching positions the pincer-metal phosphonate complexes in a hydrophobic environment. Due to the dimeric (for **cut-1**) or trimeric (for **cut-2**) aggregates, the accessibility of the pincer-metal centres for *e.g.* solvent molecules or substrates can be limited and controlled by the presence of (an)other cutinase or pincer metal molecule(s). As it is not clear whether the hydrophobic shielding observed here also occurs in solution, we are currently investigating this phenomenon with different techniques (*e.g.* NMR) in aqueous

media. If head-to-head packing motives occur in solution as well, this can play an important role when different processes, like *e.g.* ligand binding to or reactions at the metal centre of the semisynthetic metalloproteins are investigated.

The observed dinuclear pincer-platinum/cutinase hybrid **cut-1c** is formed by the coordination of two NCN-pincer platinum monocations to a bridging μ-chloride anion. The dinuclear structure of **cut-1c** shows that the coordination chemistry, which is observed for small-molecular transition metal complexes, can also be performed with transition metal complexes attached to biomolecules. Since we are interested in using the described enzyme modification strategy to construct novel semi-synthetic metallo-proteins with special properties, this was a very important finding, as it revealed that non-natural metal complexes still exhibited classical coordination chemistry behaviour.

Phasing with platinum

One of the applications of the pincer-metal complexes discussed here is to use them as a heavy atom derivative for phasing in the process of structure determination of serine hydrolases. Obtaining crystals of proteins with heavy atom derivatives can be very laborious, as a straightforward general method for an easy and selective incorporation of anomalous scatterers is still lacking in protein crystallography.[57] Traditionally, the introduction of heavy metals into protein crystals is accomplished by soaking the protein crystal with a solution of a suitable salt of the heavy metal or a more advanced heavy metal species as, for example, metal complexes or metal clusters. These methods have in common that there are only weak interactions between the protein and the heavy metal species, which often result in the aspecific labelling or even the destruction of the protein crystals. Other methods for the site-specific introduction of anomalous scatterers, like the substitution of natural methionines by seleno-methionines, are limited to *in vitro* protein expression systems only.

In the present study the covalent attachment of a pincer-metal complex to a protein has several advantages as the heavy metal label can be attached to a specific serine residue of the protein prior to crystallization. In this study we used the pincer platinum complex **1** (Scheme 1) as a heavy atom derivative for obtaining phases for the structure determination of **cut-1a**. Since platinum is a strong anomalous scatterer at the wavelength used for data collection, we successfully used the anomalous signal for single wavelength anomalous dispersion (SAD) phasing with SHELXD to 1.5 Å resolution. Figure 9 shows a part of the obtained electron density map, clearly showing its high quality.

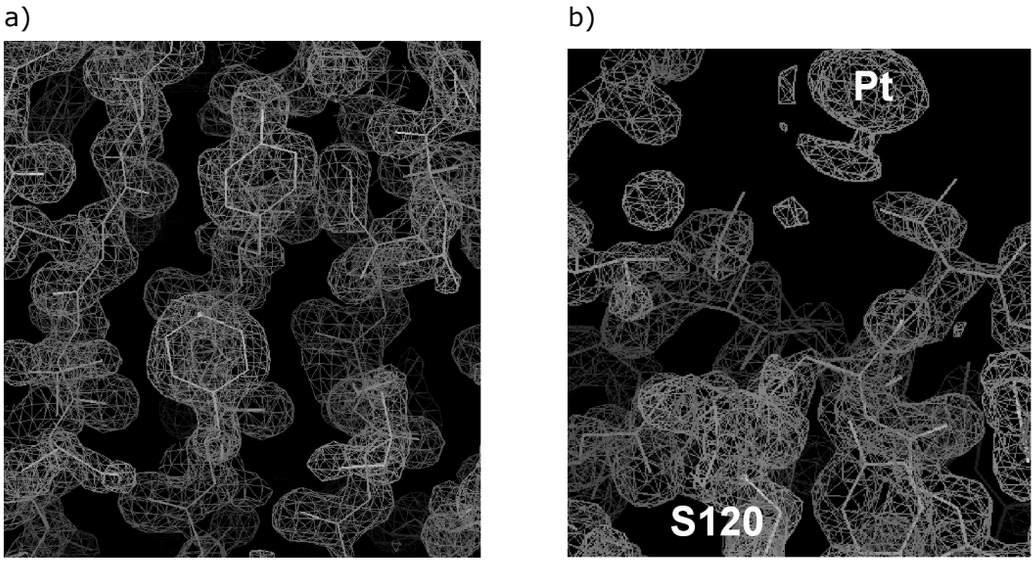

Figure 9: The use of platinum as site-selective phasing tool for **cut-1a** a) part of the cutinase backbone b) the active site of cutinase Ser120; the electron density shown as chicken wire is contoured at 1.0 σ.

We also calculated an anomalous difference electron density map for each of the structures. In **cut-1a** and **cut-1b** structures, this density, like in the 2Fo-Fc density map, showed an ellipsoidal electron density map for the platinum atom. In **cut-1a** this elongation is perpendicular to the two-fold symmetry axis. In **cut-1c** the anomalous difference map shows a spherical shape for the platinum. In **cut-2a** the anomalous map helped to clarify the disorder situation (*vide supra*).

The use of pincer-metal phosphonate inhibitors as heavy atom derivatives for the phasing of raw protein diffraction data has several advantages over conventional phasing label methods. As the anomalous scatterer is covalently attached to one unique site, i.e. the active site, its position can be used for the tracing of the protein sequence. The transition metal label is introduced prior to crystallization, which means that it does not destroy crystals, its binding can be quantified and it always leads to a 1:1 addition adduct. As phosphonates are known to bind covalently to lipases and serine hydrolases, one of the largest enzyme superfamilies, this phasing label can be used for the structure elucidation of many different enzymes.
The phasing method applied (Figure 9) yielded high quality electron density maps for the protein backbone and the cutinase active site, which shows the strength of this methodology. In the future we intend to expand this phasing methodology and use our heavy atom labels for the elucidation of the structures of novel lipolytic enzymes and as reactivity probe for other serine hydrolases. These studies are ongoing and will be published elsewhere.

Conclusions

Different pincer-metal complexes attached to the lipase cutinase have been crystallized and five different crystal structures have been solved with high-resolution data. This study shows that pincer-metal complexes have been covalently and site-specifically bound to the enzyme cutinase. These molecular structures in the solid state are the first examples of pincer-metal complexes embedded into a protein and give a detailed insight into the exact positioning of the pincer groups in the cutinase protein structure. Interestingly, the pincer *platinum* inhibitors (**cut-1**) bind all in the same pocket with the same (S_P) configuration at the phosphorus centre. However, the pincer *palladium* inhibitors (**cut-2**) emerge exclusively in the second binding pocket with the opposite stereochemistry (R_P) at the former phosphonate P center. This binding mode and stereochemistry for the **cut-1** structures is surprising, as the bound phosphonate does not mimic the tetrahedral transition state, which is usually observed for phosphonates bound to lipases and was expected at the beginning of this study.[37] This different binding to the cutinase active site is most probably caused by the differences in steric bulk of the pincer-metal complexes **1** and **2**. We are currently investigating the inhibition behaviour of racemic **1** and **2** with different lipases further.
When halide-poor crystallization conditions were applied, a novel metal-induced μ-chloride bridged dinuclear coordination complex was formed, showing that coordination chemistry with protein-substituted pincer-metal complexes is an exciting new possibility.

The distance of the metal center of the pincer entity to the (chiral) protein environment is quite large, which is apparent from the freedom the pincer entity has to move about its average position and to adapt different orientations. Consequently large chiral induction in catalytic reactions of the pincer-metal complex can hardly be expected. Recently, we prepared hybrids in which the C3 linker is absent, *i.e.* the pincer-metal unit is directly attached to the phosphonate grouping;[49] for these pincer-metal cutinase hybrids a closer contact of the pincer-metal group to the chiral protein environment is established.
The exposed position of the pincer-metal centre for the structures described here can also be used in other systems, like as diagnostic tool in NMR spectroscopy (^{195}Pt is a NMR active nucleus) or in activity-based protein-profiling applications for example. Currently, these applications are investigated by our group.

Finally, the present results show that binding of a pincer-platinum or palladium phosphonate complex to the active site of an enzyme facilitates to obtain readily phases from anomalous scattering of the heavy atoms for the structure determination, *e.g.* of **cut-1a**. In the future the use of pincer-metal complexes as phasing tools for protein diffraction data may simplify the structure elucidation of other hydrolases as well.

The intrinsic power of pincer-metal complexes lies in their easy modification by a wide variety of *para*-substituents,[34] which enables the binding of pincer-metal complexes to a wide variety of biomolecules like proteins,[37, 49] peptides,[36] and carbohydrates.[35] Currently, we are expanding this approach of covalent and specific biomolecule modification by phosphonates to other protein families, like, *e.g.* other serine hydrolases.[58] Moreover, these different semisynthetic metalloenzymes are currently used in coordination and catalytic studies, where the specific properties of a protein-embedded transition metal complex are explored further.

Experimental Section

General comments: Tris(hydroxylmethyl)aminomethane was purchased from J.T. Baker, aqueous HCl from Interchema and MeCN from Acros Organics. MeCN was distilled over CaH_2 prior to use. Purification of water for buffer solutions was performed with the Milli-Q filtration system (Millipore, Quantum Ultrapure). The dialysis membranes were purchased from Pierce. Centrion YM-3 modules were provided by Amicon (Millipore). Cutinase mutant N172K was provided by Unilever. The synthesis of metalloinhibitors **1** and **2** has been described previously.[37]

Inhibition of Cutinase N172K with pincer-metal complex 1:–The published inhibition protocol[37] was slightly modified: A solution of **1** in MeCN (41.2 μL, 40 mM, 1.6477 μmol, 3 eq.) was added to a buffer solution (100 mM TrisHCl, pH8) of cutinase mutant N172K (1.098 mM, 0.549 μmol, 500 μL, 1 eq.). The yellow solution was left at room temperature during 8 hours and then stored at 4 °C overnight. Prior to crystallization, the pincer-cutinase hybrids were dialysed using a 3.5 kDa cut-off, against a five hundred–fold volume excess of 5 mM Tris-HCl pH 8.0. The hybrid was then concentrated to ~10 mg/ml using Centricon YM-3 modules (Amicon, Millipore).

Inhibition of Cutinase N172K with pincer-metal complex 2: The published inhibition protocol[37] was slightly modified: A solution of **2** in MeCN (16.5 μL, 40 mM, 0.659 μmol, 3 eq.) was added to a buffer solution (100 mM TrisHCl, pH8) of cutinase mutant N172K (1.098 mM, 0.220 μmol, 200 μL, 1 eq.). The yellow solution was stored in the fridge overnight. Prior to crystallization, the pincer-cutinase hybrids were dialysed using a 3.5 kDa cut-off, against a five hundred–fold volume excess of 5 mM Tris-HCl pH 8.0. The hybrid was then concentrated to ~10 mg/ml using Centricon YM-3 modules (Amicon, Millipore).

Tris buffer: Tris (100 mmol, 12.1140g) was dissolved in MilliQ-H_2O (1L) and acidified with aqueous HCl (30%, technical grade) to pH 8.

Crystallization: Crystallization screens were set up using the Honeybee 961 (Genomic Solutions) automated fluid-handling system. More than 600 conditions were screened at 18° C. The crystallization screens used were Crystal Screen 1 & 2,

PEG-Ion, PACT, JCGS and Wizard 1 & 2 (Hampton Research) as well diluted variants of these screens. The latter screens were diluted 1:1 with ultra pure water. The hanging drops consisted of equal volumes (150 nl) of mother liquor and protein solution and were equilibrated against 50 μl of mother liquor. These trials yielded approximately twenty promising conditions for pincer-cutinase hybrids **cut-1** and **cut-2**, which were then further optimized manually. For this purpose we used the hanging drop vapor diffusion method. Droplets containing 0.5 μl of protein solution and 0.5 μl of mother liquor were equilibrated against a reservoir containing 500 μl of mother liquor. Finally, we obtained well-diffracting single-crystals of **cut-1** in three different space groups, and **cut-2** in two space groups. **cut-1a** (space group I222) was obtained using 20% (w/v) PEG-6000, 100 mM sodium, acetate pH 4.5 and 200 mM sodium chloride. Crystals of **cut-1b** ($P2_1$) were obtained using 22% (w/v) PEG-6000, 100 mM sodium acetate pH5.0 and 200 mM sodium chloride. **cut-1c** ($P3_121$) was obtained using 2% (w/v) PEG-1000, 100 mM 4-(2-hydroxyethyl)-1-piperazineethanesulfonic acid (Hepes) pH 6.0. The cryo-condition contained additionally 20 % (v/v) glycerol. **cut-2a (**$P6_3$) grew with 10% (w/v) PEG-3350, 25% (v/v) glycerol, 100 mM 2-(bis(2-hydroxyethyl)amino)-2-(hydroxymethyl)propane-1,3-diol (BisTrisP) pH 6.5, 200 mM sodium citrate. Crystals of **cut-2b** (R3) appeared with the condition 6% (w/v) PEG-3350, 30% (v/v) glycerol, 50 mM BisTrisP 8.5, 100 mM potassium thiocyanate. All crystals were collected from their drop using crystal-loops (Hampton and Mitogen) and were either directly flash-cooled (**cut-1a**, **cut-1b**, **cut-2a**, and **cut-2b**) or transferred to a cryo-solution prior to flash-cooling (**cut-1c**) in liquid nitrogen.

Data Collection: X-ray diffraction data of **cut-1** and **cut-2** crystals were collected at 100K on ID14-1, ID14-4 or ID29 beam lines at the European Synchrotron Radiation Facility (ESRF) in Grenoble (France). The obtained diffraction images were integrated using MOSFLM[59] or XDS,[60] see Table S1. The obtained reflections were scaled using SCALA as provided in the CCP4 program suite version 6.0.1.[61] In SCALA 5% of the data were assigned as Rfree set and not used for structure refinement.[62]

Structure Determination: cut-1a, **cut-2a** and **cut-2b** were solved by Molecular Replacement with the program PHASER[63] using the 1.8 Å resolution structure of cutinase-N172K (PDB-code: 1CUA). **cut-1b** and **cut-1c** were solved by molecular replacement based on **cut-1a**. Model building was performed using the program COOT.[64] The **cut-1** structures were refined with REFMAC5.[65] For refinement of **cut-1a** in REFMAC, we used the TLS option, with the protein and the pincer as separate groups. Using this TLS option gave a large improvement in the R-factor and yielded a better 2Fo-Fc electron density map. In **cut-1a** residues S30, S57, S61, T80, S92, D111, S129, R138, D139 and R158 were refined with double conformations. In residues R78A and R78B of **cut-1b** and none of **cut-1c** were refined with double conformations. The **cut-2** structures were refined with SHELXL97.[54] **cut-2a** structure was refined with double conformations for residues I24, S30, T43, S57, S61, R78,

S78, S92, K108, S129 and R196. Furthermore, the pincer entity was refined with a double conformation. The minor component has an occupancy of 1/3 and the corresponding bromide is located on the symmetry axis. The major component has an occupancy of 2/3. **cut-2b** was refined with anisotropic displacement parameters for Pd and Br and as a merohedral twin with (1,0,0/-1,-1,0/0,0,-1) as twin matrix resulting in a twin fraction of 0.5. The relatively high agreement factors for **cut-2b** are a consequence of the relatively weak data in the highest resolution shell. Nevertheless the residual electron density in **cut-2b** is extraordinarily small.

The distance and angle restraints for the refinement of the pincer-metal molecules were derived from the corresponding small-molecule variants, ($C_{12}H_{19}ClN_2Pt$)[48] for **cut-1** and ($C_{10}H_{13}BrPdS_2$)[49] for **cut-2**, respectively.

As a proof of concept that covalently bound organometallic species can be useful for the phase determination of macromolecular protein structures we used the single-wavelength anomalous dispersion (SAD) phasing method with **cut-1a** as an example. 1.5 Å resolution data were used for the calculation of phases using the programs SHELXC, SHELXD and SHELXE as implemented in CCP4.

References

1. Kaiser, E. T.; Lawrence, D. S., *Science* **1984,** 226, 505-511.
2. Wilson, M. E.; Whitesides, G. M., *J. Am. Chem. Soc.* **1978,** 100, 306-307.
3. Chen, H.; Parkinson, J. A.; Morris, R. E.; Sadler, P. J., *J. Am. Chem. Soc.* **2003,** 125, 173-186.
4. Jaouen, G., *Bioorganometallics: Biomolecules, Labelling, Medicine*. Wiley-VCH: Weinheim, 2006; p 1-472.
5. James, S.; Maresca, K. P.; Babich, J. W.; Valliant, J. F.; Doering, L.; Zubieta, J., *Bioconjugate Chem.* **2006,** 17, 590-596.
6. Pak, J. K.; Benny, P.; Spingler, B.; Ortner, K.; Alberto, R., *Chem. Eur. J.* **2003,** 9, 2053-2061.
7. Agorastos, N.; Borsig, L.; Renard, A.; Antoni, P.; Viola, G.; Spingler, B.; Kurz, P.; Alberto, R., *Chem. Eur. J.* **2007,** 13, 3842-3852.
8. Alberto, R., *Bioorganometallics*. Wiley-VCH: Weinheim, 2006; p 97-124.
9. Morales Morales, D.; Jensen, C., *The Chemistry of Pincer Compounds*. Elsevier: Amsterdam, 2007; p 1-467.
10. Poupart, S.; Boudou, C.; Peixoto, P.; Massonneau, M.; Renard, P.-Y.; Romieu, A., *Org. Biomol. Chem.* **2006,** 4, 4165-4177.
11. Yang, X.-J.; Drepper, F.; Wu, B.; Sun, W.-H.; Haehnel, W.; Janiak, C., *Dalton Trans.* **2005**, 256-267.
12. Kam-Wing Lo, K.; Hui, W.-K., *Inorg. Chem.* **2005,** 44, 1992-2002.
13. Pintacuda, G.; John, M.; Su, X.-C.; Otting, G., *Acc. Chem. Res.* **2007,** 40, 206-212.
14. Ohashi, M.; Koshiyama, T.; Ueno, T.; Yanase, M.; Fujii, H.; Watanabe, Y., *Angew. Chem. Int. Ed.* **2003,** 42, 1005-1008.
15. Carey, J. R.; Ma, S. K.; Pfister, T. D.; Garner, D. K.; Kim, H. K.; Abramite, J. A.; Wang, Z.; Guo, Z.; Lu, Y., *J. Am. Chem. Soc.* **2004,** 126, 10812-10813.
16. Gallagher, J.; Zelenko, O.; Walts, A. D.; Sigman, D. S., *Biochemistry* **1998,** 37, 2096-2104.
17. Davies, R. R.; Distefano, M. D., *J. Am. Chem. Soc.* **1997,** 119, 11643-11652.
18. Collot, J.; Gradinaru, J.; Humbert, N.; Skander, M.; Zocchi, A.; Ward, T. R., **2003,** 125, 9030.
19. Panella, L.; Broos, J.; Jin, J.; Fraaije, M. W.; Janssen, D. B.; Jeronimus-Stratingh, M.; Feringa, B. L.; Minnaard, A. J.; De Vries, J. G., *Chem. Commun.* **2005,** 45, 5656-5658.
20. Steinreiber, J.; Ward, T. R., *Coord. Chem. Rev.* **2008,** 252, 751-766.
21. Creus, M.; Pordea, A.; Rossel, T.; Sardo, A.; Letondor, C.; Ivanova, A.; LeTrong, I.; Stenkamp, R. E.; Ward, T. R., *Angew. Chem. Int. Ed.* **2008,** 47, 1400-1404.
22. Pierron, J.; Malan, C.; Creus, M.; Gradinaru, J.; Hafner, I.; Ivanova, A.; Sardo, A.; Ward, T. R., *Angew. Chem. Int. Ed.* **2008,** 47, 701-705.
23. Norihiko, Y.; Ueno, T.; Unno, M.; Matsui, T.; Ikeda-Sato, M.; Watanabe, Y., *Chem. Comm.* **2008**, 229-231.
24. Ueno, T.; Norihiko, Y.; Abe, S.; Watanabe, Y., *J. Inorg. Biochem.* **2007,** 101, 1667-1675.
25. Ueno, T.; Abe, S.; Yokoi, N.; Watanabe, Y., **2007,** 251, 2717.
26. Satake, Y.; Abe, S.; Okazaki, S.; Ban, N.; Hikage, T.; Ueno, T.; Nakajima, H.; Suzuki, A.; Yamane, T.; Nishiyama, H.; Watanabe, Y., *Organometallics* **2007,** 26, 4904-4908.
27. Ueno, T.; Abe, S.; Yokoi, N.; Watanabe, Y., *Coord. Chem. Rev.* **2007,** 251, 2717-2731.
28. Collot, J.; Gradinaru, J.; Humbert, N.; Skander, M.; Zocchi, A.; Ward, T. R., *J. Am. Chem. Soc.* **2003,** 125, 9030-9031.
29. Ueno, T.; Koshiyama, T.; Abe, S.; Yokoi, N.; Ohashi, M.; Nakajima, H.; Watanabe, Y., *J. Organomet. Chem.* **2007,** 692, 142-147.
30. Yokoi, N.; Ueno, T.; Unno, M.; Matsui, T.; Ikeda-Sato, M.; Watanabe, Y., *Chem. Commun.* **2008**, 229-231.
31. Thomas, C. M.; Letondor, C.; Humbert, N.; Ward, T. R., *J. Organomet. Chem.* **2005,** 690, 4488-4491.
32. Lin, C.-C.; Lin, C.-W.; Chan, A. S. C., *Tet. Asymm.* **1999,** 10, 1887-1893.
33. McNae, I. W.; Fishburne, K.; Habtemariam, A.; Hunter, T. M.; Melchart, M.; Wang, F.; Walkinshaw, M. D.; Sadler, P. J., *Chem. Commun.* **2004**, 1786-1787.
34. Albrecht, M.; van Koten, G., *Angew. Chem. Int. Ed.* **2001,** 40, 3750-3781.

35. Beccati, D.; Halkes, K. M.; Batema, G. D.; Guillena, G.; Carvalho de Souza, A.; van Koten, G.; Kamerling, J. P., *ChemBioChem* **2005,** 6, 1196-1203.
36. Guillena, G.; Rodriguez, G.; Albrecht, M.; van Koten, G., *Chem. Eur. J.* **2002,** 8, 5368-5376.
37. Kruithof, C. A.; Casado, M. A.; Guillena, G.; Egmond, M. R.; van der Kerk-van Hoof, A.; Heck, A. J. R.; Klein Gebbink, R. J. M.; van Koten, G., *Chem. Eur. J.* **2005,** 11, 6869-6877.
38. Albrecht, M.; Gossage, R. A.; Lutz, M.; Spek, A. L.; van Koten, G., *Chem. Eur. J.* **2000,** 6, 1431-1445.
39. Longhi, S.; Mannesse, M. L. M.; Verheij, H. M.; De Haas, G. H.; Egmond, M.; Knoops-Mouthuy, E.; Cambillau, C., *Protein Sci.* **1997,** 6, 275-286.
40. Jelsch, C.; Longhi, S.; Cambillau, C., *Proteins: Structure, Function and Genetics* **1998,** 31, 320-333.
41. Cambillau, C.; Longhi, S.; Nicolas, A.; Martinez, C., *Curr. Opin. Struct. Biol.* **1996,** 6, 449-456.
42. Schmidinger, H.; Birner-Gruenberger, R.; Riesenhuber, G.; Saf, R.; Susani-Etzerodt, H.; Hermetter, A., *ChemBioChem* **2005,** 6, 1776-1781.
43. Mannesse, M. L. M.; de Haas, G. H.; van der Heijden, H. T. W. M.; Egmond, M. R.; Verheij, H. M., *Biochem. Soc. Trans.* **1997,** 25, 165-170.
44. Cavalier, J.-F.; Buono, G., *Acc. Chem. Res.* **2000,** 33, 579-589.
45. Longhi, S.; Nicolas, A.; Creveld, L.; Egmond, M.; Verrips, C. T.; de Vlieg, J.; Martinez, C.; Cambillau, C., *Proteins* **1996,** 26, 442-458.
46. Longhi, S.; Cambillau, C., *Biochim. Biophys. Acta* **1999,** 1441, 185-196.
47. Martinez, C.; Nicolas, A.; van Tilbeurgh, H.; Egloff, M. P.; Cudrey, C.; Verger, R.; Cambillau, C., *Biochemistry* **1994,** 33, 83-89.
48. Albrecht, M.; Lutz, M.; Schreurs, A. M. M.; Lutz, E. T. H.; Spek, A. L.; van Koten, G., *J. Chem. Soc., Dalton Trans.* **2000**, 3797-3804.
49. Kruithof, C. A.; Dijkstra, H. P.; Lutz, M.; Spek, A. L.; Egmond, M. R.; Klein Gebbink, R. J. M.; van Koten, G., *Eur. J. Inorg. Chem.* **2008**, 4425-4432.
50. Terheijden, J.; Van Koten, G.; Grove, D. M.; Vrieze, K., *J. Chem. Soc. Dalton Trans.* **1987**, 1359-1366.
51. van den Broeke, J.; Heeringa, J. J. H.; Chuchuryukin, A. V.; Kooijman, H.; Mills, A. M.; Spek, A. L.; van Lenthe, J. H.; Ruttink, P. J. A.; Deelman, B.-J.; van Koten, G., *Organometallics* **2004,** 23, 2287-2294.
52. Chuchuryukin, A.; Chase, P. A.; Dijkstra, H. P.; Suijkerbuijk, B. M. J. M.; Mills, A. M.; Spek, A. L.; van Klink, G. P. M.; van Koten, G., *Adv. Synth. Catal.* **2005,** 347, 447-462.
53. Dijkstra, H. P.; Chuchuryukin, A.; Suijkerbuijk, B. M. J. M.; van Klink, G. P. M.; Mills, A. M.; Spek, A. L.; van Koten, G., *Adv. Synth. Catal.* **2002,** 344, 770-780.
54. Herbst-Irmer, R.; Sheldrick, G. M., *Acta Cryst.* **1998,** B54, 443.
55. Flack, H. D., *Acta Cryst.* **1987,** A43, 564.
56. Kruithof, C. A.; Dijkstra, H. P.; Lutz, M.; Spek, A. L.; Klein Gebbink, R. J. M.; van Koten, G., *Organometallics* **2008,** 27, 4928-4937.
57. Pompidor, G.; D'Aléo, A.; Vicat, J.; Toupet, L.; Giraud, N.; Kahn, R.; Maury, O., *Angew. Chem. Int. Ed.* **2008,** 47, 3388-3391.
58. Dijkstra, H. P.; Sprong, H.; Aerts, B. N. H.; Kruithof, C. A.; Egmond, M. R.; Klein Gebbink, R. J. M., *Org. Biomol. Chem.* **2008,** 6, 523-531.
59. Leslie, A. G., *Acta Cryst.* **1999,** D55, 1696-1702.
60. Kabsch, W., *J. Appl. Cryst.* **1993,** 26, 795-800.
61. CCP4, *Acta Cryst.* **1994,** D50, 760-763.
62. Kabsch, W., *J. Appl. Cryst.* **1988,** 21, 916-924.
63. McCoy, A. J.; Grosse-Kunstleve, R. W.; Adams, P. D.; Winn, M. D.; Storoni, L. C.; Read, R. J., *J. Appl. Cryst.* **2007,** 40, 658-674.
64. Emsley, P.; Cowtan, K., *Acta Cryst.* **2004,** D60, 2126-2132.
65. Murshudov, G. N.; Vagin, A. A.; Dodson, E. J., *Acta Cryst.* **1997,** D53, 240-255.

CHAPTER 3

Study on the Chiral Preference of Cutinase in the Reaction with ECE-Pincer Metal Phosphonate Inhibitors

Previously resolved crystal structures of cutinase inhibited by either NCN-pincer platinum phosphonate **1** or SCS-pincer palladium phosphonate **2** showed opposite stereochemistry at the phosphorus centre for each of the covalently bonded inhibitor molecules, *i.e. S* for **1** and *R* for **2.** Moreover, these structures showed that the respective ECE-pincer metal head groups occupy different cavities in the inhibited cutinase hybrid. In the present study, the covalent binding process of these inhibitor molecules **1** and **2** in solution was studied by ^{31}P NMR spectroscopy and kinetic inhibition experiments. ^{31}P NMR showed that after addition of one equivalent of the racemic phosphonate inhibitor (*rac*-**1** or *rac*-**2**, respectively), two phosphorous resonance signals were observed pointing to the presence of two different diastereomers formed upon inhibition of either one of the enantiomers to cutinase. Upon addition of 2.5 equivalents of *rac*-**1** or -**2**, respectively, only one resonance signal was observed, most likely corresponding to the diastereoisomer of the cutinase hybrid formed on inhibition of the faster reacting enantiomer of the inhibitor, *i.e. S* for **1** and *R* for **2**. Inhibitors **1** and **2** showed different kinetic inhibition behaviour with **1** exhibiting a more pronounced stereopreference than **2**. The obtained results suggest that the opposite stereochemistries at the respective phosphorus centres of the inhibited molecules **1** and **2** found in the solid state is not a crystallization artefact, but is in concord with the conclusions from the present solution studies. Possible reasons for the observed stereoselectivity of the inhibition process are discussed and, most likely, originate from a difference in steric bulk of the pincer head groups, *i.e.* of NMe_2 *vs.* SMe.

Introduction

Lipolytic enzymes (EC 3.1.1.3) play an increasingly important role as catalysts in the detergent industry, the food and flavour sector and in the preparation of enantio-pure chemicals, pharmaceuticals and polymers.[1-13] The high enantio-selectivities of various lipases, for example, have made them beneficial catalysts in the synthesis of various enantio-pure drugs and drug precursors.[6, 14-16] Due to their robustness and their high catalytic activities in both aqueous (micellar) and organic media, lipases have gained importance as environmentally benign, cheap catalysts operating under mild conditions and temperatures.[1, 5, 6] Lipases possess a common catalytic triad consisting of Ser-His-Asp/Glu and the active site of various lipases is covered by a lid, which is displaced when the enzyme assumes its active site conformation at the water-lipid interface.[17, 18] The structural and mechanistic details of their activities and (enantio)selectivities have been elucidated with the aid of various active site-directed inhibitor molecules, which covalently bind to the active site Ser residue and which function as transition state analogues. An important class of these transition state analogues are various chiral phosphonate inhibitors,[19] which often have a structural similarity with triglycerides (Figure 1a).

Often, these phosphonate suicide inhibitors possess a *para*-nitrophenolate leaving group, which gets released upon binding to the Ser residue of the lipase, enabling monitoring of the inhibition process by UV-vis spectroscopy (at 400 nm). Other leaving groups, like *e.g.* fluoride[20] or fluorescent 4-methylumbelliferone[21] (Figure 1a) have been reported as well.

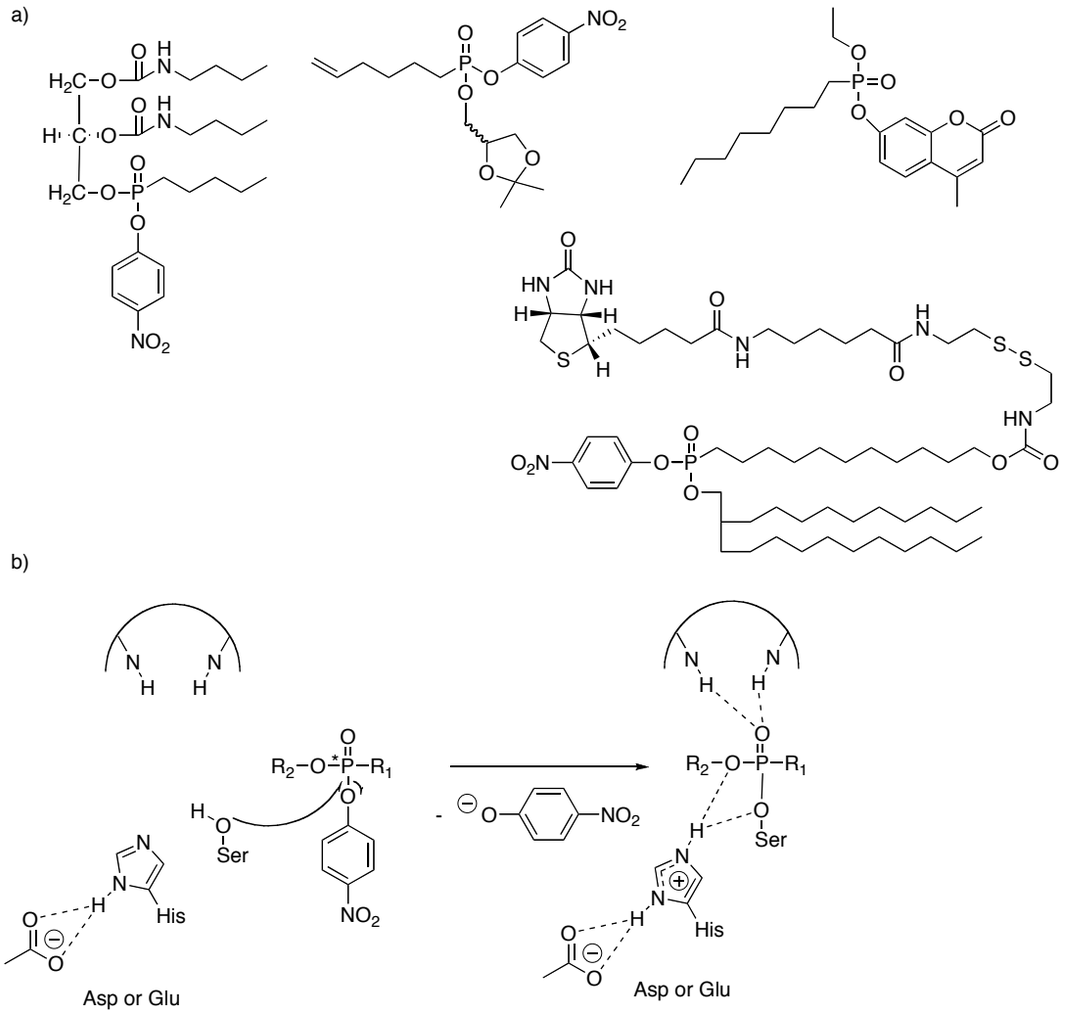

Figure 1: a) Various chiral phosphonate lipase inhibitors known from literature and b) binding of a phosphonate transition state analogue to the active site of a lipase.[21-25]

For a typical inhibition procedure, either an excess of a racemic phosphonate inhibitor (two equivalents or more) or an enantiopure phosphonate (one equivalent) are added to the target lipase in buffer containing a surfactant at basic pH, after which the release of the leaving group (*e.g. para*-nitrophenolate, Figure 1b) is measured over time. After completion of the inhibition, the mixture is dialysed to remove excess inhibitor and the released leaving group. Several crystal structures of lipases inhibited by phosphonates have been known to date,[17, 22, 26-34] with a typical binding mode and hydrogen bond pattern as depicted in Figure 1b. The chiral phosphorous atom forms a covalent bond with the oxygen atom of the Ser residue. The oxygen atom of the OR^2-group forms a hydrogen bond with the His residue in the active site, whereas the phosphoryl oxygen atom forms hydrogen bonds with the oxyanion hole, thereby stabilizing the covalent phosphorous-oxygen bond to the Ser residue of the lipase further.

In our laboratory novel phosphonate inhibitors have been developed recently, where the alkyl tail of a phosphonate moiety has been functionalized by different organometallic ECE-pincer metal complexes (Figure 2a).[35]

a) b)

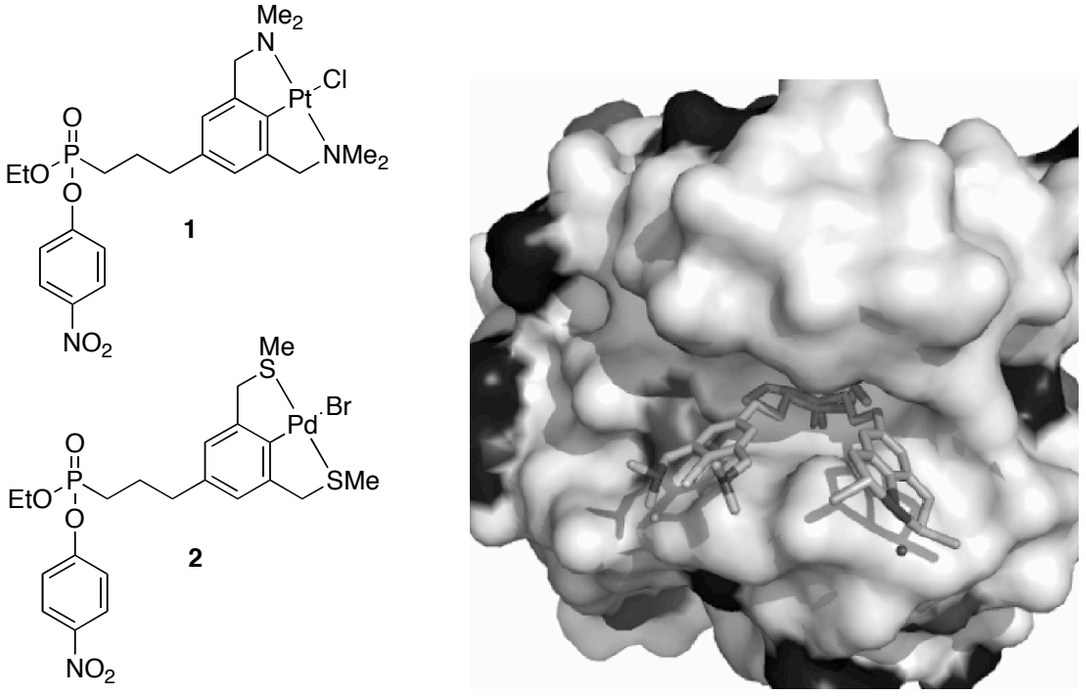

Figure 2: a) NCN-pincer platinum phosphonate and SCS-pincer palladium phosphonate inhibitors **1** and **2** developed by our group;[35] b) superposition of the crystal structures of **cut-1** and **cut-2** showing the opposite stereochemistry on phosphorous and the different spatial orientation of the pincer head groups.

By substituting ECE-pincer metal complexes with protein-reactive phosphonate groups, it was anticipated that the well-established chemistry of pincer complexes (*e.g.* their use as catalysts, building blocks in supramolecular chemistry and sensor materials)[36] could be expanded to biological systems. These ECE-pincer metal phosphonates (Figure 2a) have been used in the inhibition of the lipase cutinase[35] and the resulting pincer-cutinase hybrid systems were successfully used in structural and coordination studies and as catalysts.[37-39] As cutinase is a relatively small (21 kDa), stable and highly active lipase lacking the lid covering the hydrophobic active site,[40] it is an ideal model enzyme for inhibition studies with ECE-pincer metal phosphonates **1** and **2**.
For a typical inhibition study of cutinase with inhibitors **1** or **2**, two or more equivalents of *rac*-**1** or *rac*-**2** are added to cutinase (1 equivalent). After incubation overnight, the mixture is dialysed to obtain the pure pincer-cutinase hybrid.[35, 39] As the prior separation of the enantiomers of both *rac*-**1** and *rac*-**2** proved unsuccessful,[35] this approach with an excess of the racemic inhibitor was chosen to assure that only the faster reacting enantiomer would bind to the cutinase active site and give the preferred stereochemistry.

Recently, several crystal structures of cutinase inhibited by ECE-pincer phosphonates **1** and **2** were resolved.[39] In all of these structures, the pincer metal moiety of the pincer-cutinase hybrid is situated at the surface of the protein, with the pincer head group being in proximity to the hydrophilic rim of the cutinase active site.

Interestingly, the spatial orientation and the stereochemistry of the pincer-cutinase hybrids with inhibitors **1** and **2** are different, with the two different inhibitors occupying different cavities in the active site (Figure 2b). For cutinase inhibited by SCS-pincer palladium complex **2**, the *R*-enantiomer is bonded to the Ser residue, with the hydrogen bonds between the phosphonate and the cutinase backbone being very similar to other phosphonate-lipase crystal structures known (Figure 1a).[22, 29] For cutinase inhibited by NCN-pincer platinum complex **1**, the *S*-enantiomer binds to Ser and the hydrogen bond between the ethoxy oxygen atom and His is lacking. Furthermore, the SCS-pincer palladium inhibitor **2** binds to Ser^{120} via a slightly smaller pocket than NCN-pincer platinum phosphonate **1**. Due to the similarity of the organometallic groupings of **1** and **2**, this difference in stereochemistry and spatial orientation is rather surprising. As the described structures might well be "crystallization artefacts", it was decided to study the cutinase inhibition behaviour of ECE-pincer metal phosphonates **1** and **2** in solution, to elaborate whether any differences between the rather similar inhibitors **1** and **2** could be observed.

Here, the binding of different equivalents of inhibitors *rac*-**1** and *rac*-**2** to the lipase cutinase is studied by ^{31}P NMR spectroscopy and by a kinetic inhibition experiment. It was found that phosphonates **1** and **2** show slightly but distinctly different inhibition kinetics, pointing towards a stereoselective inhibition process for both inhibitors, which can explain the opposite stereochemistry observed in the crystal structures.

Results & Discussion

NMR studies

To establish that both S_P and R_P enantiomers of *rac*-**1** and *rac*-**2** bind to cutinase and that the formed diastereoisomeric cutinase hybrids **cut-1** and **cut-2**, respectively, are detectable with ^{31}P NMR spectroscopy, inhibition experiments with different amounts of the inhibitors *rac*-**1** and *rac*-**2** were performed. For this purpose, cutinase (1.0 equivalent) was inhibited with either 1.0 or 2.5 equivalents of *rac*-**1** or *rac*-**2** (incubation overnight), after which the excess of inhibitor and *para*-nitrophenolate were removed by dialysis (2 x 400 mL, 24 h). Subsequent analysis by ^{31}P NMR spectroscopy during 60 h showed that addition of 1.0 equivalent of either *rac*-**1** or *rac*-**2** to cutinase results in two phosphorous resonance signals (41.8 and 35.8 ppm for **cut-1**, and 41.4 and 35.5 ppm for **cut-2**), corresponding to the different diastereomers formed (Figure 3). These results show, that upon addition of only one equivalent of either *rac*-**1** or *rac*-**2**, both phosphonate-cutinase diastereomers, **cut-1** and **cut-2,** respectively are formed and can be observed by ^{31}P NMR spectroscopy with a difference in chemical shift of 6 ppm. Moreover, the results confirm that the active site of cutinase is open and exposed enough to accommodate the *R*- as well as the *S*-enantiomer of the ECE-pincer metal phosphonate grouping.

When an excess (2.5 equivalents) of the racemic inhibitor *rac*-**1** or *rac*-**2** was added to cutinase, almost exclusively the faster reacting enantiomer was bonded, which is reflected by the appearance of the resonance with the higher ppm value (41.9 ppm for **cut-1**, 41.3 ppm for **cut-2**) as the only signal in the ^{31}P NMR spectrum. In conclusion, in both cases it is the resonance above 41 ppm that corresponds to the faster formed

diastereomer after an excess (2.5 equivalents) of the racemic phosphonate had been added during inhibition.

a)

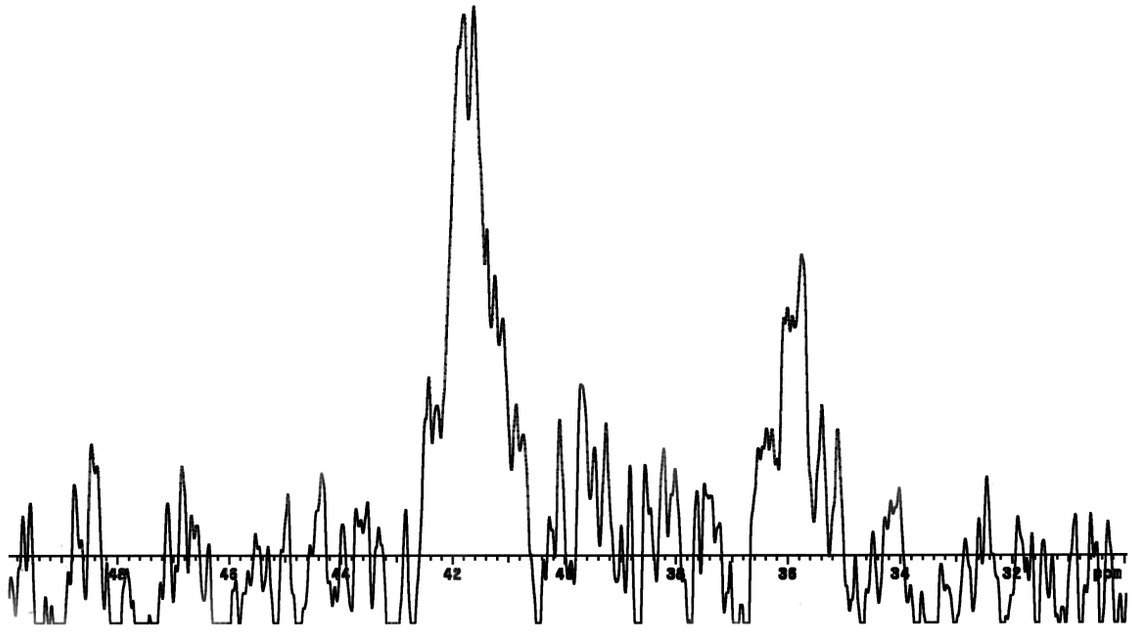

b)

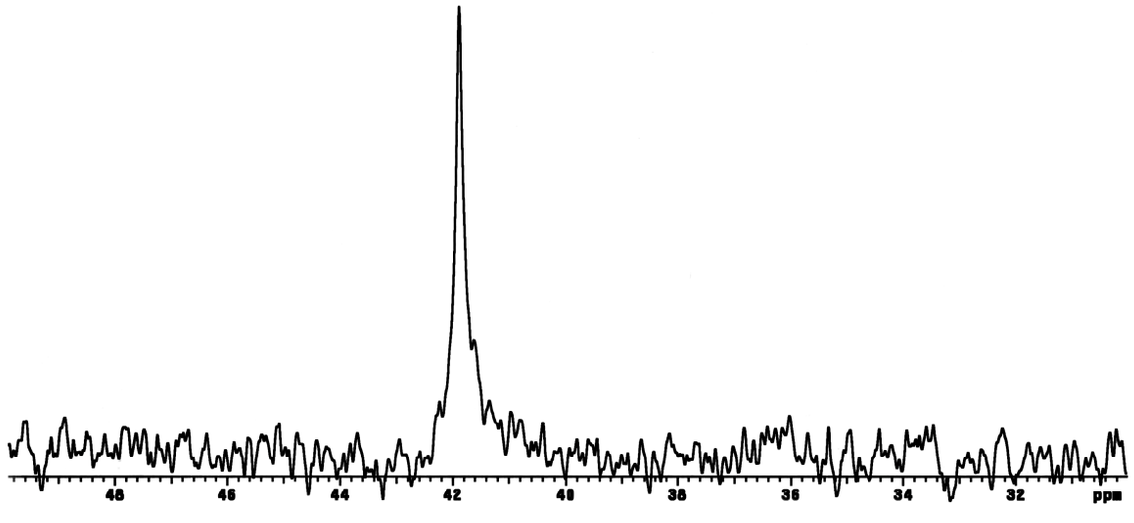

c)

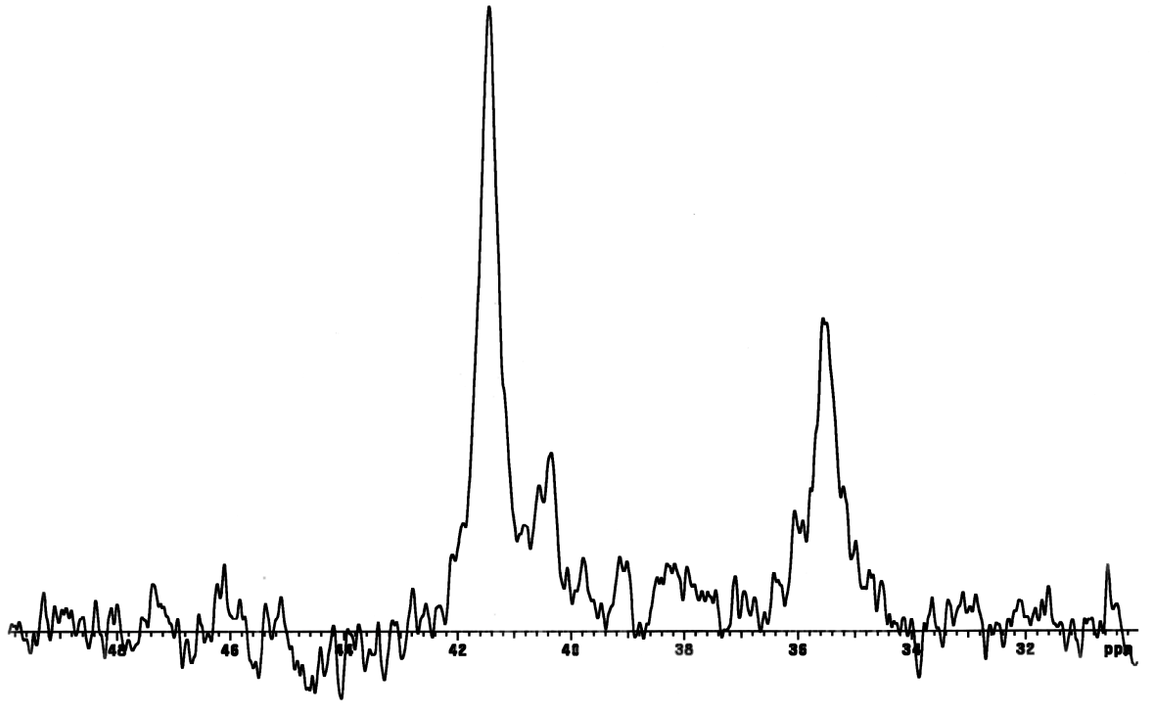

d)

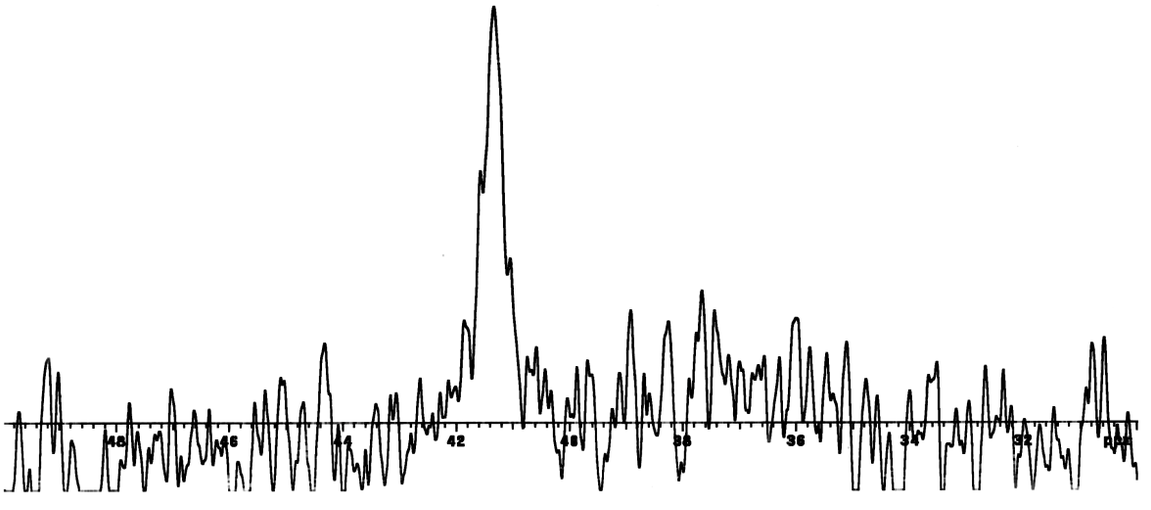

Figure 3: ^{31}P NMR spectra of cutinase inhibited with a) 1.0 eq. of **1** b) 2.5 eq. of **1** c) 1.0 eq. of **2** d) 2.5 eq. of **2** (all spectra were measured after dialysis).

Kinetic studies

In the kinetic experiments, a concentrated solution of cutinase (0.0250 μmol, 2 mM, 1.0 eq.) was used to mimic the conditions used in the NMR experiments (*vide supra*) and in previous crystallization studies.[39] To allow for both enantiomers to fully react with the enzyme, *rac*-**1** and *rac*-**2** respectively, were added to cutinase in amounts at or preferably below 1 eq. Subsequently, the release of *para*-nitrophenolate was followed spectrophotometrically at 400 nm over time. The data obtained could not be

fitted to single exponential curves, which is in accord with the view that both enantiomers had reacted indeed. However, as shown in Figure 4, a double exponential function fits the data very well. From the function: $OD_{400nm} = a_0 - a_1 \exp[-k_1t] - a_2 \exp[-k_2t]$ the reaction constant k_1 and k_2 can be obtained by non-linear regression. Time is indicated by the symbol t and is measured in minutes. The constants a_0 and $\{a_0 - (a_1+a_2)\}$ are the final and initial absorbance levels, respectively. Under the conditions used a_1 equals a_2 ($a_1 = a_2$), as both enantiomers fully react with the enzyme.

Table 1: Rate constants calculated after incubation of cutinase with NCN-pincer platinum inhibitor **1** and SCS-pincer palladium inhibitor **2**, respectively.

Inhibitor	Equivalents[a]	k_1 (min^{-1})	k_2 (min^{-1})	E^{*b}
1	0.50	0.12	2.84	24
2	0.50	0.16	0.93	6

[a] 1.0 equivalent of cutinase was used in both cases; [b] E^* = Enantioselectivity (k_2/k_1).

a)

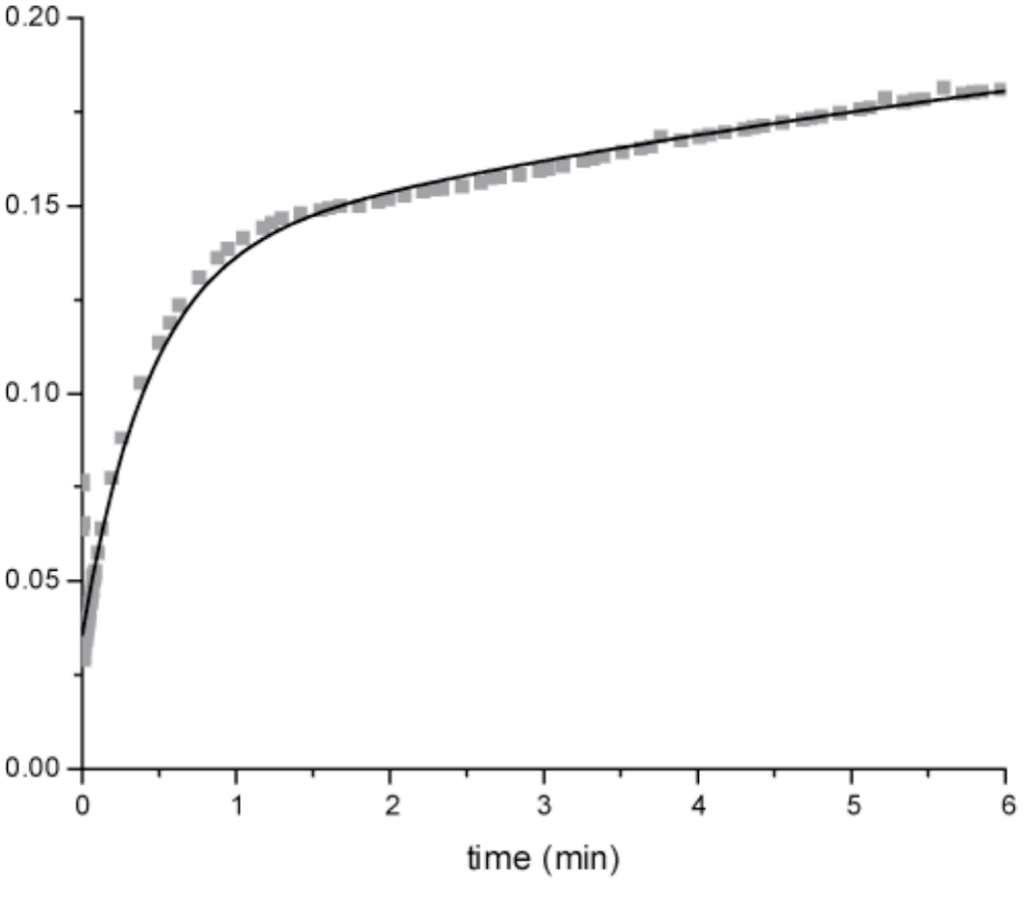

b)

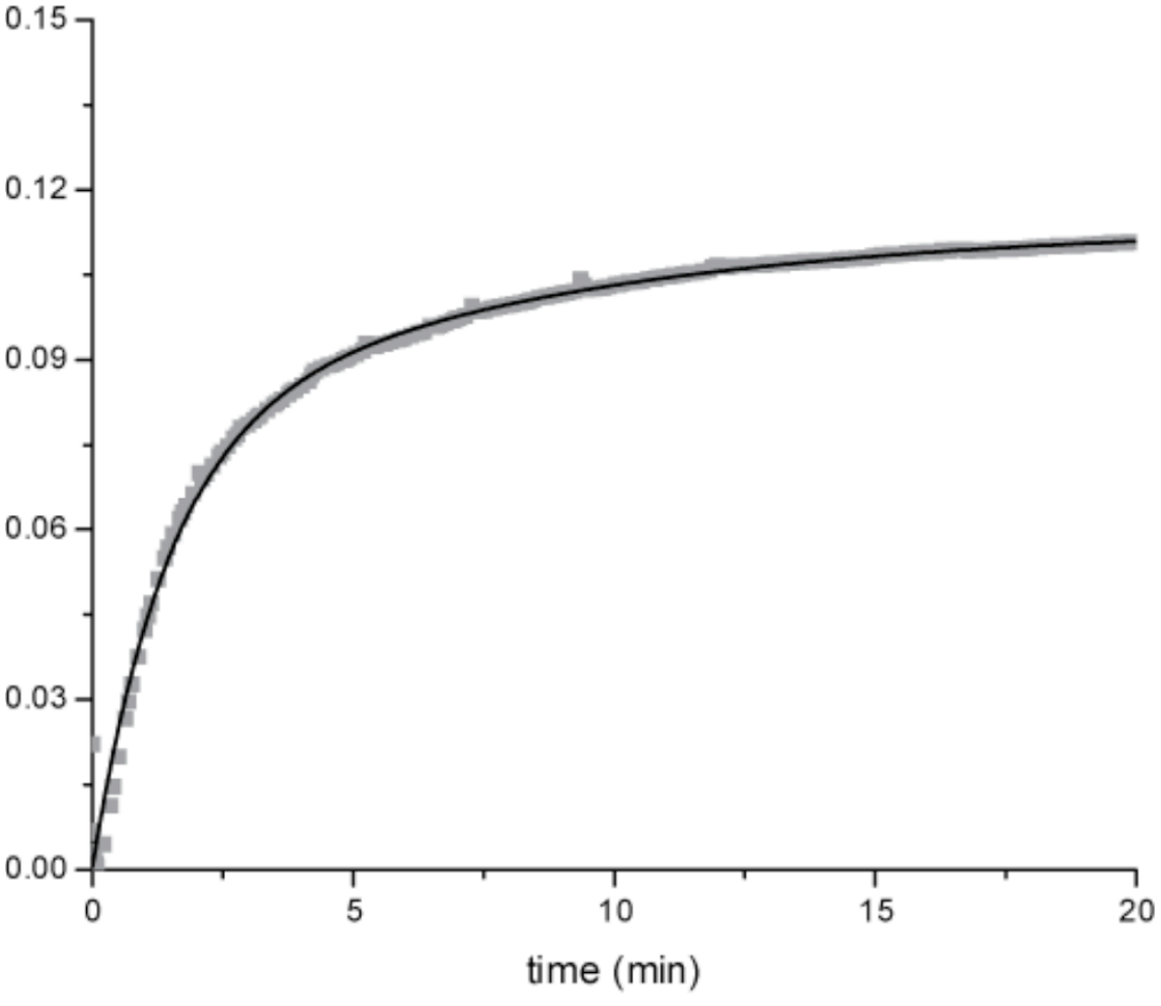

Figure 4: Release of *para*-nitrophenolate over time after exposure of cutinase (1.0 equivalent) to *rac*-**1** (0.5 equivalents, a) and *rac*-**2** (0.5 equivalents, b); the continuous black line represents the fit to the data (shown in grey) using the double exponential function.

As is shown in Table 1, the rate constant for the faster reacting enantiomer of NCN-pincer platinum inhibitor **1** is greater than that of the SCS-pincer palladium inhibitor **2**, whereas the rate constants are about equal for the slow reacting enantiomers of the two inhibitors. As a consequence, the enantioselectivity factor E (k_2/k_1) is much greater for inhibitor **1** (E*=24) than for inhibitor **2**.

It is interesting to note that crystallographic evidence points to the S_P NCN-pincer platinum phosphonate enantiomer being selectively bonded to Ser_{120} of cutinase. The difference in reactivity we observed for the two enantiomers provides further evidence that this configuration found in the crystal is the preferred one formed in the solution experiments – and not a sheer crystallization artefact. It is noteworthy that in most structures of cutinase with covalently bonded phosphonates derived from triglyceride substrates both binding pockets in cutinase are occupied.[13, 19, 22, 27, 29, 40, 41] For these compounds the R_P enantiomer is generally observed.

Interestingly, the subtle differences of these NCN- and SCS-pincer head groups, albeit relatively far away from the chiral phosphonate atom, apparently have a distinct influence on the reactivity in forming the cutinase hybrid compound. The NCN- and SCS-pincer metal inhibitors used in this study have both the possibility to become accommodated in either one of the two binding pockets. The dimethylamino groups of the NCN pincer platinum group in **1** are slightly more bulky than the thiomethoxy groups of SCS pincer palladium phosphonate **2**. Apparently this slightly larger NCN-pincer platinum inhibitor **1** prefers the larger of the two binding pockets in the enzyme. This shows that very subtle changes in the inhibitor molecules can give rise to a unique orientation in the enzyme, which may lead to a different protein environment for the bonded pincer and hence to different functional properties.
In contrast, the SCS-pincer palladium inhibitor **2** reacts slower than **1** and showed less stereopreference between enantiomers, E*=6 (Table 1). Thus, it cannot be unequivocally concluded that the faster reacting enantiomer of inhibitor **2** gives rise to the covalently bonded S_P-enantiomer of **cut-2**, as observed by the crystallization studies.[39] However, the results of our NMR studies point to the binding of one species only, and this, most likely being the faster reacting enantiomer. The structural and kinetic studies then demonstrate that the pincer molecules can be oriented differently in cutinase, depending on the equivalents of inhibitor used to prepare the covalently bonded species. It should be noted that at inhibitor concentrations above 1 equivalent for 2 mM cutinase, the reactions proceeded too fast to be completely followed by conventional spectrophotometric techniques. Although rapid mixing stopped-flow devices could solve this problem, their application was considered to be outside the scope of this work focusing on the kinetics of both rapid and slow reacting enantiomers.

Conclusions

The resolved crystal structures for cutinase inhibited by ECE pincer metal phosphonates **1** and **2,** *i.e.* **cut-1** and **cut-2**, respectively, showed that in the solid state the respective inhibited phosphorous centres have opposite stereochemistry, i.e *S* for the NCN and *R* for the SCS head grouping.[39] The present solution studies using ^{31}P NMR and the study of the inhibition kinetics of cutinase inhibited by varying amounts of **1** and **2** described show, that both enantiomers of the racemic phosphonates **1** and **2** react with the Ser^{120} residue in the cutinase active site, but with distinctly different rates. Furthermore, the use of 2.5 equivalents of the inhibitor showed that under these conditions only one diastereomer of **cut-1** and **cut-2**, respectively, is formed. The kinetic studies also reveal that as compared with **2**, phosphonate **1** is the faster inhibitor with **1** showing a more pronounced stereoselectivity (E*=24 for **1** *vs.* E*=6 for **2**). These differences in kinetic inhibition behaviour between **1** and **2** show that the nature of the head groups, *i.e.* the nature of the substituents, CH_2NMe_2/PtCl *vs.* CH_2SMe/PdBr have a profound effect on the selectivity of the inhibition process.
As cutinase is a relatively small lipase with an open and exposed active site, the influence of the protein backbone on the metal centre of the pincer complex can be expected to be relatively moderate. When lipases with a deeply embedded active site

(*e.g. chromobacterium viscosum* lipase) are inhibited by pincer phosphonates **1** or **2**, the steric and electronic influences of the protein backbone might be even more pronounced. These influences can considerably determine the pincer metal centre activity and selectivity, *e.g.* when the pincer protein hybrids are applied in catalytic or coordination studies involving various lipase protein backbones.

Experimental Section

General procedures: All reagents were used as supplied from Acros or Sigma-Aldrich, unless stated otherwise. MeCN was distilled over CaH_2. The enzyme inhibition studies and dialysis experiments were performed in air at 25 °C. Water for the preparation of the buffer solutions was filtered with the Milli-Q filtration system (Millipore, Quantum Ultrapure) prior to use. The dialysis cassettes (Slide-A-Lyzer™, 10,000 MWCO, 0.1-0.5 mL or 0.5-3 mL) for the purification of the enzyme-ECE pincer metal hybrids were purchased from Pierce. Cutinase mutant N172K was provided by Unilever. NMR measurements were performed on a Varian Inova 300 MHz or Varian Oxford 400 MHz spectrometer at 298 K. A sealed glass tube containing H_3PO_4 (22.71 mM) was used as internal standard and reference in all ^{31}P NMR experiments. UV-VIS spectra were recorded on a Varian Cary 50 Scan UV-visible spectrometer. The syntheses of **1**[35] and **2**[35] were carried out as reported.

Preparation of Tris/Triton buffer: To Triton X-100 (0.1 g) were added Tris (0.6057 g, 0.0050 mol) and MilliQ-H_2O (100 mL). The solution was acidified with aqueous HCl to pH 8.0 and used directly.

Tris buffer: Tris (250 mmol, 30.2838 g) was dissolved in MilliQ-H_2O (2.0 L), acidified with aqueous HBF_4 to pH 8.0 and used directly in the kinetic studies.

Inhibition of cutinase with 1 and 2 for ^{31}P NMR studies: The published inhibition protocol[35] was slightly modified: A solution of **1** or **2** in MeCN (50 mM; 1.0 eq: 0.70 μmol, 14.0 μL; 2.5 eq: 1.75 μmol, 35.0 μL) was added to a freshly prepared Tris/Triton buffer solution (pH 8.0) of cutinase mutant N172K (2.00 mM, 0.70 μmol, 350 μL, 1.0 eq.). The yellow solution was left at room temperature during 8 hours, incubated overnight at 7 °C and then dialysed two times with buffer (2 x 400 mL, 125 mM Tris, pH 8.0) at RT during 24 hours. The contents of the Slide-A-Lyzer™ dialysis cassettes were transferred into a NMR tube and used directly for the NMR analysis during 60h.
1.0 eq. of **1**: ^{31}P $\{^1H\}$ NMR (D_2O, 161.90 MHz, 298.1 K): δ 41.8, 35.8.
2.5 eq. of **1**: ^{31}P $\{^1H\}$ NMR (D_2O, 161.90 MHz, 298.1 K): δ 41.9.
1.0 eq of **2**: ^{31}P $\{^1H\}$ NMR (D_2O, 161.90 MHz, 298.1 K): δ 41.4, 35.5.
2.5 eq. of **2**: ^{31}P $\{^1H\}$ NMR (D_2O, 161.90 MHz, 298.1 K): δ 41.3.

Kinetic measurements: To solutions of freshly prepared Tris/Triton buffer in UV-vis cuvettes were added 2.5 μL (0.0125 μmol, 5mM in MeCN, 0.5 eq.) of solutions of racemic inhibitor **1**[35] or **2**,[35] the total final volume was kept constant at 987.5 μL. To

these solutions were added solutions of cutinase N172K mutant (12.5 μL, 2 mM, 0.0250 μmol) in Tris/Triton buffer, after which the release of *para*-nitrophenolate was followed spectrophotometrically at 400 nm during 30 min. The data were fitted to a double exponential function of the following form:

$AbsI = a0 - a1*exp[-k_1*t] - a2*exp[-k_2*t]$

In which k_1 and k_2 are the rate constants of the corresponding enantiomers.

References

1. Schmid, R. D.; Verger, R., *Angew. Chem. Int. Ed.* **1998,** 37, 1608-1633.
2. Bornscheuer, U. T.; Kazlauskas, R. J., *Hydrolases in Organic Synthesis, Regio- and Stereoselective Biotransformations* Wiley-VCH: Weinheim, 1999; p 1-368.
3. Drauz, K.; Waldmann, H., *Enzyme Catalysis in Organic Synthesis: A Comprehensive Handbook*. edn. 2 ed.; Wiley-VCH: Weinheim, 2002; p 1-1500.
4. Faber, K., *Biotransformations in Organic Chemistry*. 5th ed. ed.; Springer: Berlin, 2004; p 1-454.
5. Gotor-Fernandez, V.; Busto, E. G.; Gotor, V., *Adv. Synth. Catal.* **2006,** 348, 797-812.
6. Gotor-Fernandez, V.; Brieva, R.; Gotor, V., *J. Mol. Catal. B* **2006,** 40, 111-120.
7. Huerta, F. F.; Minidis, A. B. E.; Bäckvall, J.-E., *Chem. Soc. Rev.* **2001,** 30, 321-331.
8. Martin-Matute, B.; Bäckvall, J.-E., *Curr. Opin. Chem. Biol.* **2007,** 11, 226-232.
9. van Buijtenen, J.; van As, B. A. C.; Verbruggen, M.; Roumen, L.; Vekemans, J. A. M.; Pieterse, K.; Hilbers, P. A. J.; Hulshof, L. U.; Palmans, A. R. A.; Meijer, E. W., *J. Am. Chem. Soc.* **2007,** 129, 7393-7398.
10. Hunsen, M.; Abul, A.; Xie, W.; Gross, R., *Biomacromolecules* **2008,** 9, 518-522.
11. Kirk, O.; Wurtz Christensen, M., *Org. Process Res. Dev.* **2002,** 6, 446-451.
12. Olsson, A.; Linstrom, M.; Iversen, T., *Biomacromolecules* **2007,** 8, 757-760.
13. Egmond, M. R., *Action of Lipases*. Kluwer Academic Publishers: Dordrecht, 1996; p 183-191 an references mentioned therein.
14. Thalen, L. K.; Zhao, D.; Sortais, J.-B.; Paetzold, J.; Hoben, C.; Bäckvall, J.-E., *Chem. Eur. J.* **2009,** 15, 3403-3410.
15. Bogar, K.; Bäckvall, J.-E., *Tetrahedron Lett.* **2007,** 48, 5471-5474.
16. Haak, R. M.; F., B.; Jerphagnon, T.; Gayet, A. J. A.; Tarabiono, C.; Postema, C. P.; Ritleng, V.; Pfeffer, M.; Janssen, D. B.; Minnaard, A. J.; Feringa, B. L.; de Vries, J. G., *J. Am. Chem. Soc.* **2008,** 130, 13508-13509.
17. Brzozowski, A. M.; Derewenda, U.; Derewenda, Z. S.; Dodson, G. G.; Lawson, D. M.; Turkenburg, J. P.; Bjorkling, F.; Huge-Jensen, B.; Patkar, S. A.; Thim, L., *Nature* **1991,** 351, 491-494.
18. Mannesse, M. L. M.; Boots, J.-W. P.; Dijkman, R.; Slotboom, A. J.; van der Hijden, H. T. W. M.; Egmond, M. R.; Verheij, H. M.; de Haas, G. H., *Biochim. Biophys. Acta* **1995,** 1259, 56-64.
19. Cavalier, J.-F.; Buono, G.; Verger, R., *Acc. Chem. Res.* **2000,** 33, 579-589.
20. Sieber, S. A.; Cravatt, B. F., *Chem. Commun.* **2006**, 2311-2319.
21. Kasrayan, A.; Bocola, M.; Sandström, A. G.; Laven, G.; Bäckvall, J.-E., *ChemBioChem* **2008,** 8, 1409-1415.
22. Longhi, S.; Mannesse, M. L. M.; Verheij, H. M.; de Haas, G. H.; Egmond, M.; Knoops-Mouthuy, E.; Cambillau, C., *Protein Science* **1997,** 6, 275-286.
23. Dröge, M.; Boersma, Y. L.; van Pouderoyen, G.; Vrenken, T. E.; Ruggeberg, C. J.; Reetz, M. T.; Dijkstra, B. W.; Quax, W. J., *ChemBioChem* **2006,** 7, 149-157.
24. Kasrayan, A.; Bocola, M.; Sandstrom, A. G.; Laven, G.; Backvall, J.-E., *ChemBioChem* **8,** 8, 1409-1415.
25. Deussen, H. J.; Danielsen, S.; Breinholt, J.; Borchert, T. V., *Bioorg. Med. Chem. Lett.* **2000,** 10, 2027-2034.
26. Lang, D. A.; Mannesse, M. L. M.; de Haas, G. H.; Verheij, H. M.; Dijkstra, B. W., *Eur. J. Biochem.* **1998,** 254, 333-340.
27. Cambillau, C.; Longhi, S.; Nicolas, A.; Martinez, C., *Curr. Opin. Struct. Biol.* **1996,** 6, 449-455 and references metioned therein.
28. Grochulski, P.; Bouthillier, F.; Kazlauskas, R. J.; Serreqi, A. N.; Schrag, J. D.; Ziomek, E.; Cygler, M., *Biochemistry* **1994,** 33, 3494-3500.
29. Jelsch, C.; Longhi, S.; Cambillau, C., *Proteins: Structure, Function and Genetics* **1998,** 31, 320-333 and refences mentioned therein.
30. Lui, M.; Stefanic, Z.; Ceilinger, I.; Hodoscek, M.; Janezic, D.; Lenac, T.; Asler, I. L.; Sepac, D.; Tomic, S., *J. Phys. Chem. B* **2008,** 112, 4876-4883.
31. Mezzetti, A.; Schrag, J. D.; Cheong, C. S.; Kazlauskas, R. J., *Chemistry & Biology* **2005,** 12, 427-437.
32. Miled, N.; Roussel, A.; Bussetta, C.; Berti-Dupuis, L.; Riviere, M.; Buono, G.; Verger, R.; Cambillau, C.; Canaan, S., *Biochemistry* **2003,** 42, 11587-11593.
33. Roussel, A.; Miled, N.; Berti-Dupuis, L.; Riviere, M.; Spinelli, S.; Berna, P.; Gruber, V.; Verger, R.; Cambillau, C., *J. Biol. Chem.* **2002,** 277, 2266-2274.
34. Uppenberg, J.; Oehmer, N.; Norin, M.; Hult, K.; Kleywegt, G. J.; Patkar, S.; Waagen, V.; Anthonsen, T.; Jones, T. A., *Biochemistry* **1995,** 34, 16838-16851.

35. Kruithof, C. A.; Egmond, M. R.; Klein Gebbink, R. J. M.; van Koten, G., *Chem. Eur. J.* **2005,** 11, 6869-6877.
36. Albrecht, M.; van Koten, G., *Angew. Chem. Int. Ed.* **2001,** 40, 3750-3781.
37. Wieczorek, B.; Klimeck, T.; Dijkstra, H. P.; Egmond, M. R.; van Koten, G.; Klein Gebbink, R. J. M., to be submitted (Chapter 5 of this thesis).
38. Wieczorek, B.; Snelders, D. J. M.; Dijkstra, H. P.; Versluis, K.; Heck, A. J. R.; Lutz, M.; Spek, A. L.; Egmond, M. R.; Klein Gebbink, R. J. M.; van Koten, G., **2009**, to be submitted (Chapter 4 of this thesis).
39. Rutten, L.; Wieczorek, B.; Mannie, J.-P. B. A.; Kruithof, C. A.; Dijkstra, H. P.; Egmond, M. R.; Lutz, M.; Klein Gebbink, R. J. M.; Gros, P.; van Koten, G., *Chem. Eur. J.* **2009,** 15, 4270-4280 (Chapter 2 of this thesis).
40. Longhi, S.; Cambillau, C., *Biochim. Biophys. Acta* **1999,** 1441, 185-196.
41. Ransac, S.; Carriere, F.; Rogalska, E.; Verger, R.; Marguet, F.; Buono, G.; Pinho Melo, E.; Cabral, J. M. S.; Egloff, M.-P. E.; van Tilbeurgh, H.; Cambillau, C., *The Kinetics, Specificities and Structural Features of Lipases*. Kluwer Academic Publishers: Dordrecht, 1996; p 143-182 and references mentioned therein.

CHAPTER 4

Coordination Chemistry in Water of a Free and a Lipase-Embedded NCN-Pincer Platinum Centre with Neutral and Ionic Triaryl Phosphines

The coordination of various anionic, neutral and cationic phosphines with different steric bulk to the platinum metal centre of low-molecular weight cationic NCN-pincer platinum complexes as well as to the platinum metal centre of a NCN-pincer platinum cation embedded in cutinase (**cut-1**; mol.wt. 20619.3) was studied in aqueous media. A ^{31}P NMR study investigating the coordination of a phosphine to the cationic NCN-pincer platinum centre in **[2-OH$_2$][OTf]** in both D_2O and Tris buffer showed that the coordination mode of the phosphine to the metal centre is strongly affected by buffer molecules. Two crystal structures of a pincer-phosphine and a pincer-buffer molecule coordination complex with hydrogen bridges provoking a dimeric supramolecular structure confirmed that the coordination observed in solution occurred in the solid state as well. A ^{31}P NMR and ESI-MS study of **cut-1** showed that the coordination of various phosphines to the enzyme-embedded platinum centre is affected by the protein backbone, which discriminates between phosphines based on their size. By using ^{31}P NMR spectroscopy and ESI-MS spectrometry, the straightforward study of the coordination of phosphines to **cut-1** was possible, thereby avoiding the need of the application of laborious biochemical procedures. To the best of our knowledge, this is the first example of a systematic study involving the selective binding of organic ligands to the metal centre of a semisynthetic metalloprotein, unequivocally demonstrating that the well-established coordination chemistry for small-molecular complexes can be transferred to biological molecules. This initial study allows future explorations in the field of selective protein targeting and identification, like in protein profiling or screening studies.

Introduction

The coordination chemistry of metal ions embedded in proteins plays a crucial role in living systems; *e.g.* the typical 3D structures and catalytic activities of metalloproteins are determined by the coordination of the protein backbone to one or more transition metal ions.[1-4] By modifying specific amino acid fragments in existing metalloproteins, the exact positioning of the metal centre in the protein backbone and its reactivity can be elucidated. These studies showed that the nature of both the metal ions (*e.g.* Cu(I), Zn(II), Ni(II)) and the amino acids involved can dramatically influence the tertiary and quaternary structures and the functionalities of the metalloprotein.[5-14]

By combining proteinengineering techniques with metal coordination chemistry, different artificial metalloproteins have been developed. Pioneering work was reported by Whitesides in 1978[15] and later by Ward et al.[5, 8, 16-18] using the biotin-(strept)avidin system. Different metal (*e.g.* rhodium) coordination complexes were non-covalently embedded into (strept)avidin thus creating an enantioselective hybrid catalyst, *i.e.* the stereochemical properties of the protein backbone are transferred to the embedded metal centre. Besides the biotin-(streptavidin) system, also other proteins, like *apo*-myoglobin and heme-oxygenase,[6-10, 19, 20] papain[21] and carbonic anhydrases, were used as scaffolds to construct artificial metalloenzymes.[22] By strategically embedding a transition metal catalyst into a chiral protein, the influence of the protein backbone can be optimally exploited to tune the activity of the metal centre, as *e.g.* in catalytic applications. Besides in catalysis, protein-embedded metal centres have mainly been used in anticarcinogenic and biomedical studies[23-26] and have been applied as redox systems,[27, 28] illustrating the great potential of these protein-metal hybrid systems.

Recently, our group reported on the covalent anchoring of a ECE-pincer platinum moiety to a lipase,[29] where E is a neutral, two-electron heteroatom donor, like NMe_2 or SMe. In these ECE-pincer metal complexes, the bis-*ortho*-chelation of the metal ion by the two E-donating groups provides further stability to the central M—C bond, making the ECE-pincer metal complexes compatible with aqueous solvent media and biological molecules, like proteins.

Recently, we were able to obtain X-ray crystal structures of a number of these pincer-cutinase hybrids, which allowed us to obtain a detailed picture of the orientation of the pincer groups in the protein pocket.[29] It appeared that in the case of a NCN-pincer platinum complex embedded in cutinase, depending on the type of buffer used (either chloride-rich or chloride-poor), either a monomeric NCN-pincer platinum chloride-lipase hybrid **[cut-1-Cl]** or a dimeric hybrid **[cut-1-Cl-cut-1]$^+$** in which two cationic NCN-pincer platinum-lipase hybrids are bridged through a single chloride ion, was formed (Figure 1b).[29] From the structural features of the two hybrids it was obvious that, in the case of the dimer, the two protein-embedded NCN-pincer platinum cations apparently are exposed enough to allow bridge

formation by a small halide atom and thus the assembly of two NCN-pincer platinum chloride-lipase hybrids to one cationic dimer. This shows that the metal centre is available for further reaction, *e.g.* coordination chemistry and catalysis.
As a follow-up of this work, it was decided to explore the coordination properties of the protein-embedded NCN-pincer platinum centre with a series of cationic, neutral and anionic phosphine ligands (Figure 2, *vide infra*). It was anticipated that classical coordination chemistry could be expanded towards artificial biological hybrid systems, thereby adding novel, largely unexploited properties to biological molecules. The various phosphines that have been used in this model study had been selected for their solubility properties in water and for their differences in bulkiness. Furthermore, we hoped to develop analysis protocols that allowed us to monitor the coordination reactions in a straightforward manner, *e.g.* by ^{31}P NMR and ESI-MS methods, thereby avoiding laborious biochemical analysis protocols. To evaluate the influence of the protein backbone on the binding of these phosphines to the platinum centre, we also performed the same coordination chemistry on the parent NCN-pincer platinum complexes lacking the protein *para*-substituent.

a)

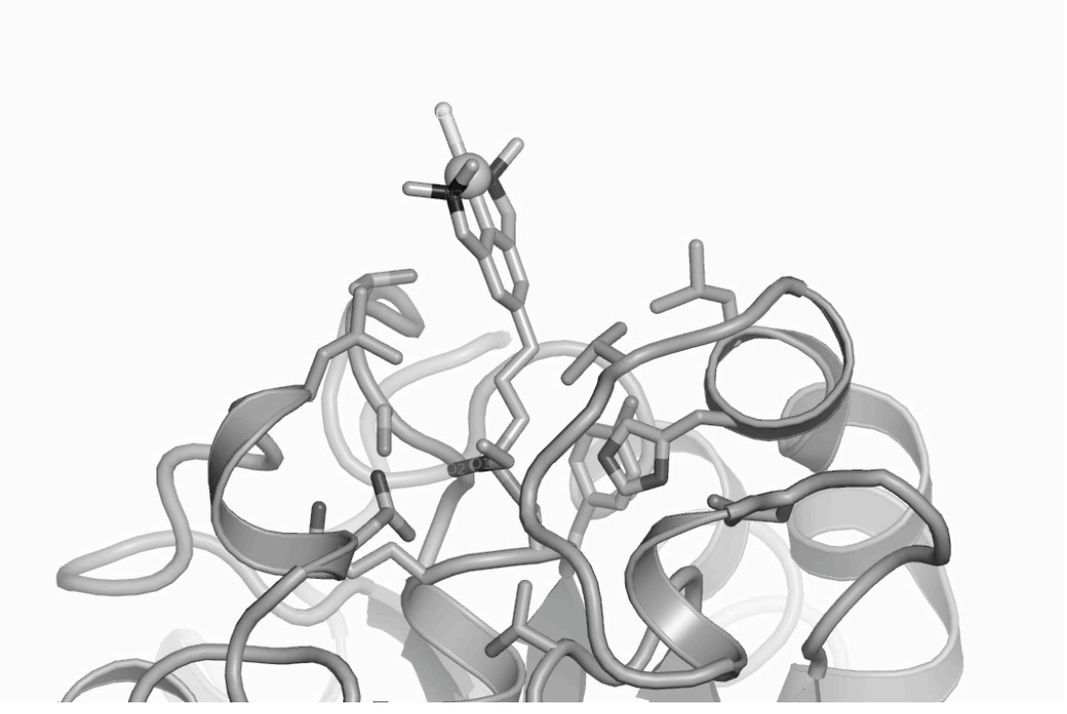

b)

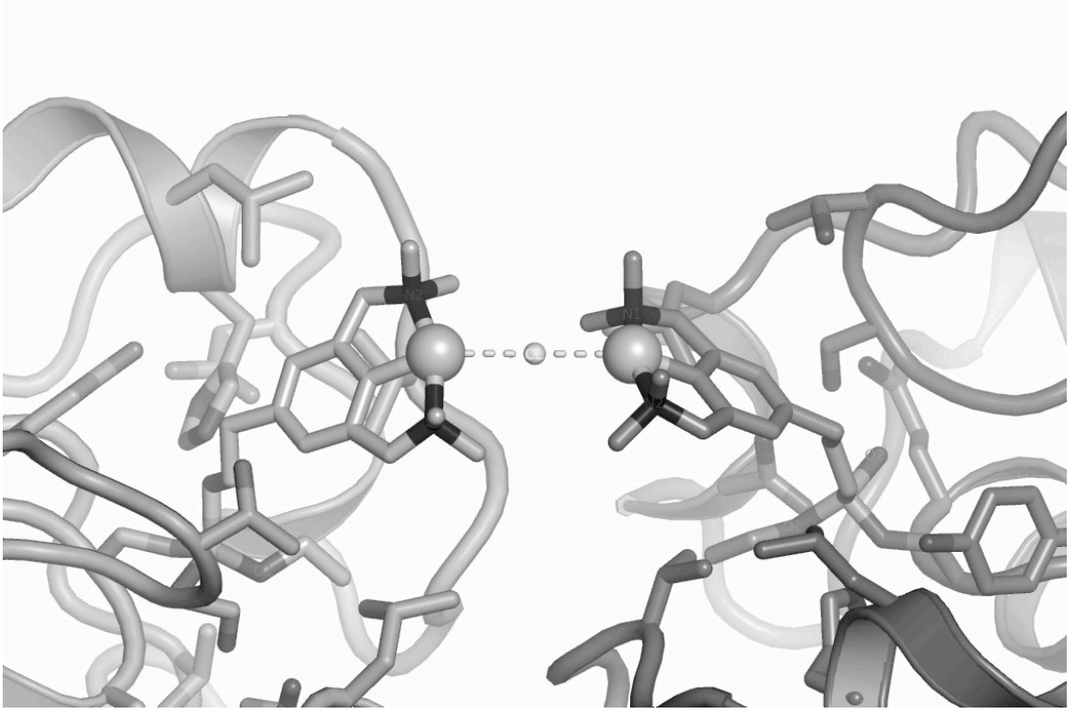

Figure 1: a) Part of the molecular structure of **[cut-1-Cl]** in the solid state showing the covalent attachment of the NCN-pincer platinum moiety, b) the dimeric structure with the chloride ion bridging the two platinum(II) cations to form **[cut-1-Cl-cut-1]**$^{+}$ as obtained from crystallization in chloride-poor buffer.[29, 30]

Results

Previous studies have shown, that cationic ECE pincer metal complexes possessing non-coordinating anions, like triflate or tetrafluoroborate, are ideal building blocks in supramolecular coordination chemistry studies.[31-40] Therefore, it was decided to synthesize the cationic NCN-pincer platinum complexes **[1-OH$_2$][OTf]** and **[2-OH$_2$][OTf]**[39, 41] from their corresponding halide analogues (**1-Cl**[30] and **2-Cl**,[39, 41] respectively, Scheme 1a) with AgOTf and subsequent filtration of the resulting reaction mixture over Celite (removal of AgCl). **[1-OH$_2$][OTf]** was characterized by elemental analysis, ^{1}H, ^{13}C, ^{19}F and ^{31}P NMR spectroscopy and MALDI-TOF MS.

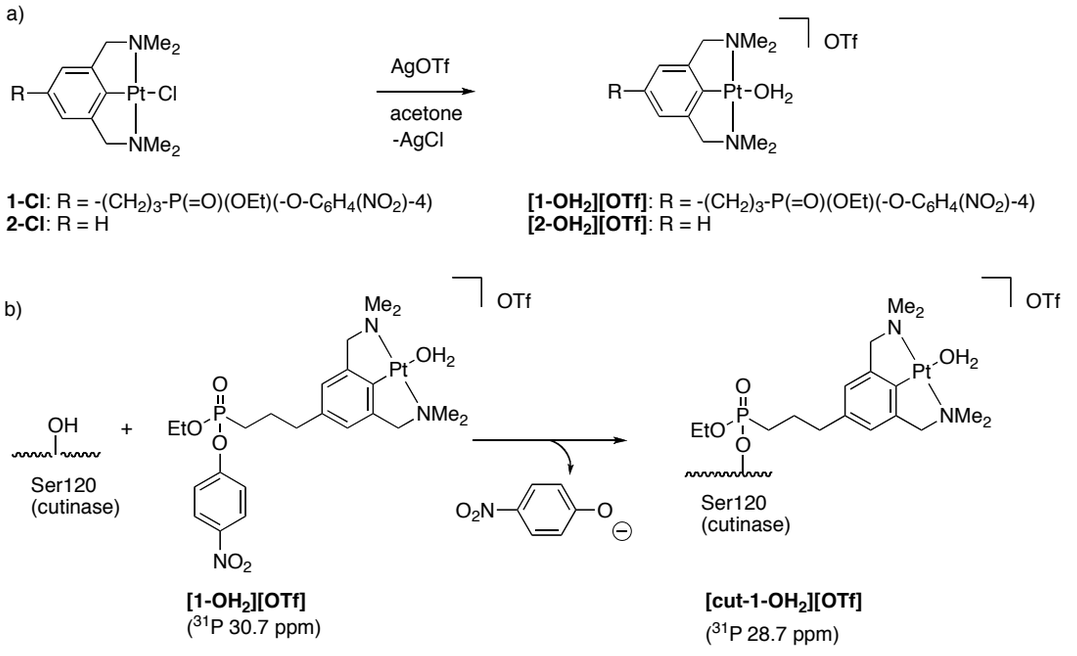

Scheme 1: a) Synthesis of the cationic NCN-pincer platinum complexes **[1-OH_2][OTf]** and **[2-OH_2][OTf]**; b) Covalent anchoring of **[1-OH_2][OTf]** to cutinase (the ^{31}P NMR values are given in brackets).

The cutinase-pincer hybrid molecule **[cut-1-OH_2][OTf]** was obtained by inhibition of cutinase (125 mM Tris, pH 8, acidified with HBF_4*, i.e.* in the absence of chloride anions) with a solution of **[1-OH_2][OTf]** (4 eq. in MeCN); the *para*-nitrophenolate leaving group of **[1-OH_2][OTf]** was replaced by the nucleophilic oxygen atom of the Ser_{120} residue in the active side of cutinase. After inhibition, excess inhibitor **[1-OH_2][OTf]** and *para*-nitrophenolate were removed by dialysis (Scheme 1b). Subsequent analysis of **[cut-1-OH_2][OTf]** by ESI-MS (*m/z* 21134.8, corresponding to **[cut-1]$^+$** (calc. 21137.5)**;** note *m/z* of **[cut-1-Cl]** is 21173.0) and ^{31}P NMR (phosphonate-P δ 28.7 ppm, Scheme 1) showed that complete and irreversible inhibition of cutinase had occurred.

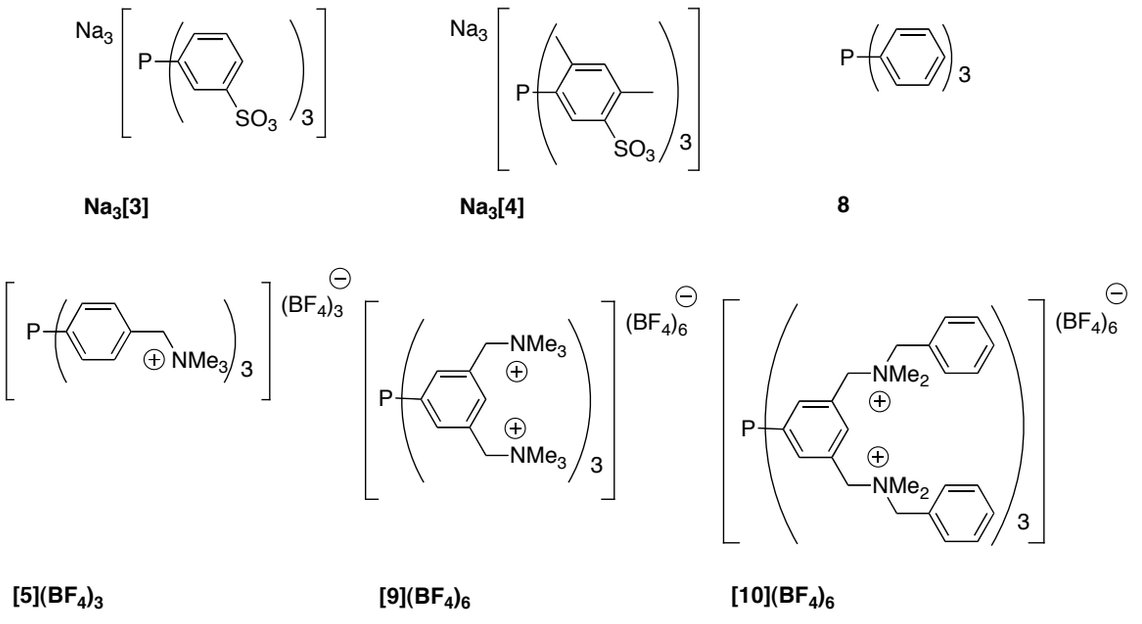

Na_3[3] **Na_3[4]** **8**

[5]$(BF_4)_3$ **[9]$(BF_4)_6$** **[10]$(BF_4)_6$**

Figure 2: The various anionic, neutral and cationic phosphines used in the coordination studies with cationic NCN-pincer platinum triflate complexes **[1-OH_2][OTf]** and **[cut-1-OH_2][OTf],** respectively.

*Coordination studies of **[2-OH_2][OTf]** with phosphine ligands in aqueous media monitored by ^{31}P NMR spectroscopy.*

To explore the coordination chemistry of cationic NCN-pincer platinum complexes to the various phosphines (Figure 2) by ^{31}P NMR in aqueous media, a model study was carried out first with pincer complex **[2-OH_2][OTf]** and phosphine **Na_3[3]**[42] ($P(C_6H_4(SO_3Na)\text{-}3)_3$, TPPTS), whereby both **[2-OH_2][OTf]** and **Na_3[3]** were soluble under the aqueous conditions described. Two aqueous solvent systems were selected for our studies: 1) neat D_2O, and 2) a halide-ion free Tris buffer (Tris = tris(hydroxylmethyl)aminomethane, pH 8.0) as it is a standard buffer for many enzyme studies. The solvent system with Tris allowed us to study the influence of Tris on the coordination chemistry of the phosphines.

For the study in D_2O, various equivalents (0.1-5.0 eq.) of a solution of **Na_3[3]** (δ^{31}P -5.7 ppm) in D_2O were added to a solution of **[2-OH_2][OTf]**[39, 41] in D_2O. The resulting solutions were analysed by ^{31}P NMR spectroscopy 5 minutes after mixing as well as after 2 days (Table 1, Scheme 2). Upon addition of 0.1-1.0 eq. of **Na_3[3]** the only signal observed in the ^{31}P NMR spectra was a sharp resonance at 30.6 ppm with $^1J(^{31}P\text{-}^{195}Pt)$ 2100 Hz (Table 1, Scheme 2). No resonance pointing to the presence of free phosphine was observed, indicating that all phosphine molecules had coordinated to platinum. The spectrum revealed no change after 2 days, clearly indicating the formation of a stable coordination product. The $^1J(^{31}P\text{-}^{195}Pt)$ value (2100 Hz) is indicative of a coordination of the phosphine *trans* with respect to C_{ipso}

(the carbon atom directly bound to platinum),[43-45] *i.e.* of the presence of a complex with a phosphine coordination mode as depicted for complex **Na_2[2-3]** (Scheme 2).

Table 1: ^{31}P NMR data of solutions from addition of 0.1-5.0 equivalents of phosphine **Na_3[3]** to **[2-OH_2][OTf]** in D_2O and the (proposed) species **Na_2[2-3]**, ***cis*-Na_5[2-(3)$_2$(D_2O)]**, ***trans*-Na_5[2-(3)$_2$(D_2O)]**, formed (a 22.71 mM H_3PO_4 solution was used as internal standard and reference).

δ^{31}P NMR Resonance signals in D_2O[a, b]		
Eq. of **Na_3[3]** (*after 5 minutes*)		
0.1	30.59 (2110.3)	**Na_2[2-3]**
0.5	30.63 (2108.7)	**Na_2[2-3]**
1.0	30.65 (2117.8)	**Na_2[2-3]**
1.5	30.65 (2110.3) *51%*	**Na_2[2-3]**
	22.84 (1604.3; 14.9) *28%*	***cis*-Na_5[2-(3)$_2$(D_2O)]**
	10.67 (3913.7; 13.3) *21%*	***cis*-Na_5[2-(3)$_2$(D_2O)]**
2.0	30.65 (2141.4) *16%*	**Na_2[2-3]**
	22.87 (1611.7; 14.9) *45%*	***cis*-Na_5[2-(3)$_2$(D_2O)]**
	10.70 (3928.6; 13.3) *36%*	***cis*-Na_5[2-(3)$_2$(D_2O)]**
	-5.55 *3%*	**Na_3[3]**
5.0	22.88 (1614.9; 14.9) *31%*	***cis*-Na_5[2-(3)$_2$(D_2O)]**
	10.72 (3929.6; 13.3) *24%*	***cis*-Na_5[2-(3)$_2$(D_2O)]**
	-5.67 *45%*	**Na_3[3]**
Eq. of **Na_3[3]** (*after 2 days*)		
0.1	30.60 (2141.4)	**Na_2[2-3]**
0.5	30.67 (2101.1)	**Na_2[2-3]**
1.0	30.65 (2112.9)	**Na_2[2-3]**
1.5	30.65 (2117.6) *47%*	**Na_2[2-3]**
	23.80 (3173.2) *19%*	***trans*-Na_5[2-(3)$_2$(D_2O)]**
	22.74 (1617.5; 13.8) *21%*	***cis*-Na_5[2-(3)$_2$(D_2O)]**
	10.58 (3887.8) *13%*	***cis*-Na_5[2-(3)$_2$(D_2O)]**

2.0	30.65 (2090.9) 16%	**Na_2[2-3]**
	23.85 (3159.6) *18%*	***trans*-Na_5[2-$(3)_2(D_2O)$]**
	22.80 (1613.8; 14.2) *36%*	***cis*-Na_5[2-$(3)_2(D_2O)$]**
	10.68 (3918.6) *29%*	***cis*-Na_5[2-$(3)_2(D_2O)$]**
5.0	23.94 *1%*	***trans*-Na_5[2-$(3)_2(D_2O)$]**
	22.84 (1611.7; 14.9) *28%*	***cis*-Na_5[2-$(3)_2(D_2O)$]**
	10.69 (3946.6; 13.1) *22%*	***cis*-Na_5[2-$(3)_2(D_2O)$]**
	-5.54 *49%*	**Na_3[3]**

[a] 298.1 K; numbers in brackets are $^1J(^{31}P\text{-}^{195}Pt)$ or $^2J(^{31}P\text{-}^{31}P)$ values; numbers in italics give the relative abundance of the compound based on ^{31}P NMR integration; [b] The signal of the phosphine oxide and its relative abundance are not shown.

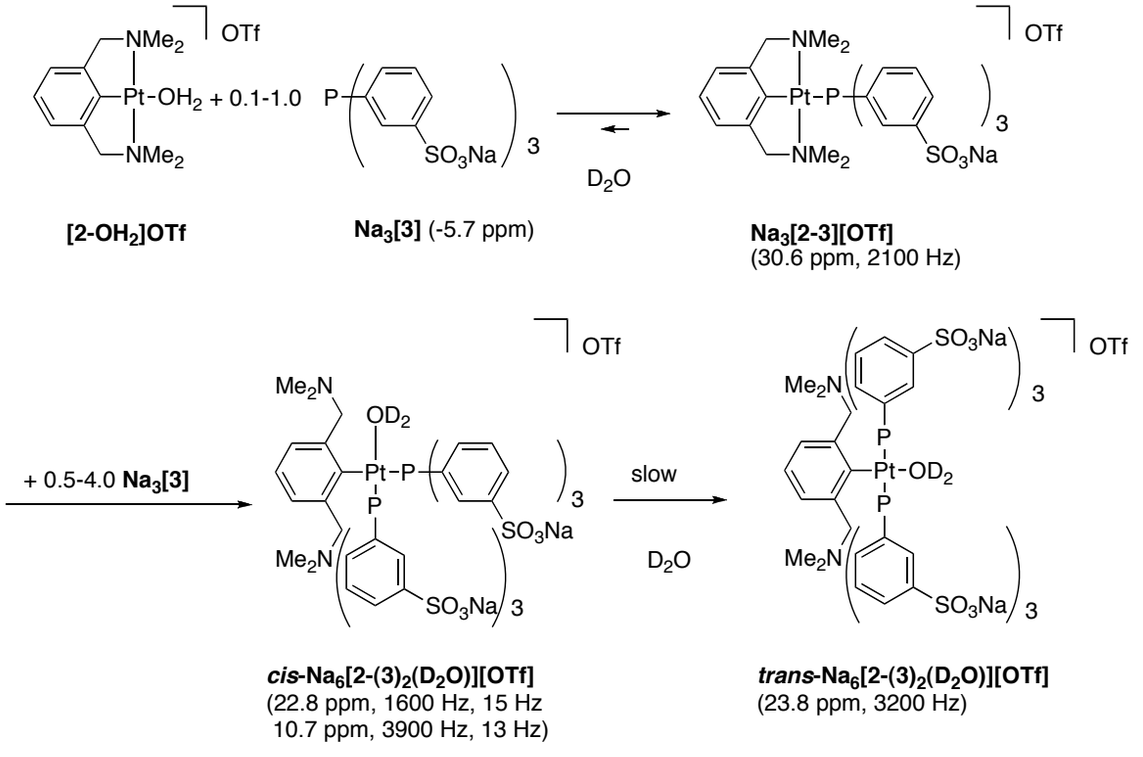

Scheme 2: Observed resonances in ^{31}P NMR upon the addition of 0.1-5.0 equivalents of **Na_3[3]** to **[2-OH_2][OTf]** in D_2O and the proposed species, **Na_2[2-3]**, ***cis*-Na_5[2-$(3)_2(D_2O)$]** and ***trans*-Na_5[2-$(3)_2(D_2O)$]** formed. The ^{31}P NMR resonances and the $^1J(^{31}P\text{-}^{195}Pt)$ and $^2J(^{31}P\text{-}^{31}P)$ (for ***cis*-Na_5[2-$(3)_2(D_2O)$]**), respectively, are given in brackets.

When more than 1.0 equivalent of phosphine **Na_3[3]** was added to a solution of **[2-OH_2][OTf]**, the coordination of a second phosphine to platinum was observed. At

22.9 and 10.7 ppm, doublet resonances ($^{2}J(^{31}P\text{-}^{31}P)$ 13-15 Hz) appeared with $^{1}J(^{31}P\text{-}^{195}Pt)$ of 1600 and 3900 kHz, respectively (Table 1). These signals are attributed to a species in which two phosphines are coordinated to the platinum centre and where the two phosphines hold a mutual *cis*-position (***cis*-Na$_5$[2-(3)$_2$(D$_2$O)]**, Scheme 2). The $^{1}J(^{31}P\text{-}^{195}Pt)$ 1600 Hz and 3900 Hz coupling constants of ***cis*-Na$_5$[2-(3)$_2$(D$_2$O)]** are attributed to the phosphine bound *trans*[43,44,45] and *cis*[43,46-48] to C_{ipso}, respectively, which is in good agreement with literature values for related complexes (*e.g.* 3100-4400 Hz for *cis*-coordination and 1600-2000 Hz for *trans*-coordination).
When these solutions were left standing for two more days, a singlet signal was growing into the spectrum at 23.8 ppm ($^{1}J(^{31}P\text{-}^{195}Pt)$ 3200 Hz, pointing to the co-presence of a Pt-complex with two chemically and magnetically identical phosphines. These resonances suggested that on standing an isomerization of ***cis*-Na$_5$[2-(3)$_2$(D$_2$O)]** to ***trans*-Na$_5$[2-(3)$_2$(D$_2$O)]** had occurred (Scheme 2). The formation of ***trans*-Na$_5$[2-(3)$_2$(D$_2$O)]** is supported by $^{1}J(^{31}P\text{-}^{195}Pt)$ values from literature ranging from 2980-3060 Hz[49-52] and a crystal structure of a PCP pincer platinum complex.[49] When one equivalent of phosphine **Na$_3$[3]** was added to a solution of independently prepared **Na$_2$[2-3]** (*vide infra*), the same isomerization behaviour was observed, with the initial formation of coordination complex ***cis*-Na$_5$[2-(3)$_2$(D$_2$O)]** which ultimately converted into ***trans*-Na$_5$[2-(3)$_2$(D$_2$O)]**. Also here, no free **Na$_3$[3]** was detected after one and two days, respectively, indicating once more that all the phosphine present coordinated quantitatively to the NCN-pincer platinum complex.

Isolation and crystallographic studies.
To confirm the formation of one of the *in situ* observed coordination complexes, we decided to isolate and fully analyse coordination complex **Na$_2$[2-3]**. Mixing of **[2-OH$_2$][OTf]** and **Na$_3$[3]** (1:1) in H_2O and subsequent work-up yielded a white powder. Elemental analysis and mass spectrometry of this powder clearly showed that a 1:1 phosphine-NCN-pincer platinum complex was formed. The ^{31}P NMR resonance (30.6 ppm) and coupling data ($J(^{31}P\text{-}^{195}Pt)$ 2100 Hz) were identical to those observed during the titration experiment (*vide supra* and Scheme 2). The ^{1}H NMR resonances, especially the aromatic and aliphatic signals of the pincer moiety, indicated a symmetric molecule with *trans*-coordination of the phosphine with respect to C_{ipso} (triplet and doublet for the aromatic pincer proton signals with $^{3}J_{H\text{-}H}$ = 7.2 Hz, two singlets for $-CH_2$ and $-NMe_2$ proton signals at 4.12 and 2.37 ppm, respectively).
To confirm the proposed structure of **Na$_2$[2-3]**, we tried to obtain single crystals suitable for an X-ray crystal structure determination. As initial attempts to crystallize **Na$_2$[2-3]** from pure water failed, we added several droplets of CH_2Cl_2, after which some crystals were formed at the CH_2Cl_2/H_2O interface. The X-ray crystal structure determination of these crystals revealed the unexpected formation of an ionic coordination complex with an interesting molecular structure (Figure 3, relevant bond distances and angles are given in Table 2). In the asymmetric unit, three pincer platinum(II) cations are present, of which one is coordinated to the trianionic phosphine thus forming a dianionic NCN-pincer phosphine complex **[2-3]$^{2-}$** (residue

1). The remaining two NCN-pincer cations are coordinated to water **[2-OH$_2$]$^+$** (residues 2 and 3) and act as counter-cations to yield a charge neutral unit cell. The sodium and triflate ions present in the original aqueous solution of **Na$_2$[2-3]** apparently did not turn up in the crystallized material. The phosphine in residue 1 (Figure 3) binds to the NCN-pincer cation *trans* with respect to C_{ipso} (Pt1-P1 = 2.3627(12) Å). The orientation of the phosphine and the Pt-P bond distance (Table 2) are comparable to the crystal structure data of other ECE-pincer-phosphine complexes, which contain a monodentate phosphine that is coordinated *trans* to C_{ipso}.[44, 45] Selected bond lengths and angles of **[2-OH$_2$]$_2$[2-3]** are given in Table 2.
The reason for this surprising crystallization behaviour might originate from the use of CH_2Cl_2 as co-solvent during crystallization. As phosphine **Na$_3$[3]** is insoluble in CH_2Cl_2 and the crystals were formed at the H_2O/CH_2Cl_2 interface, the different solubility of coordination complex **Na$_2$[2-3]** in the H_2O and CH_2Cl_2 phase might have provoked the observed crystallization.

a)

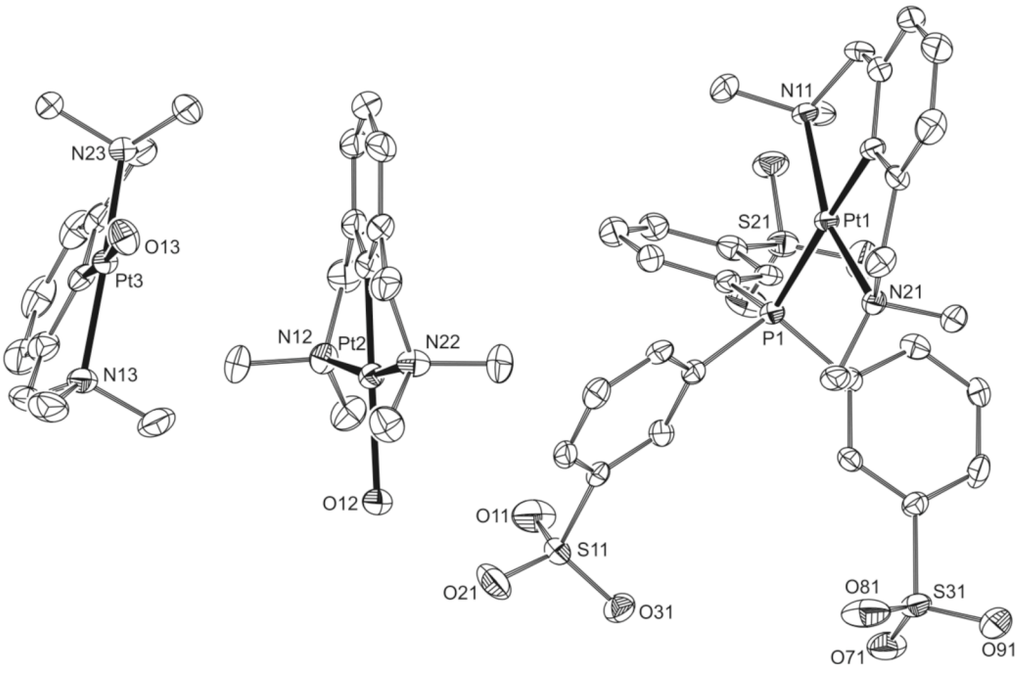

b)

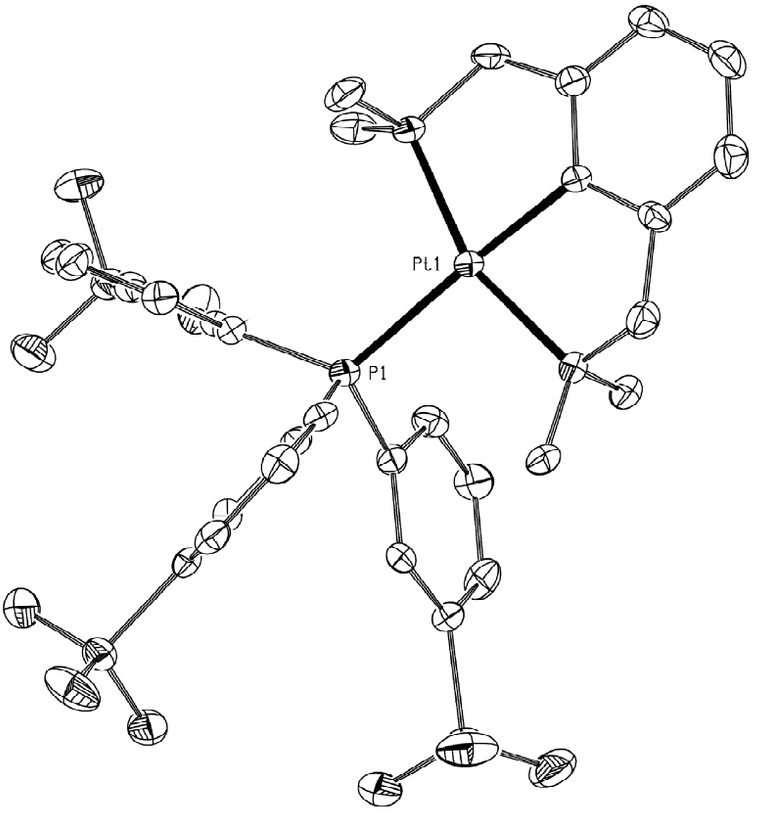

Figure 3: a) Packing of **[2-OH$_2$]$_2$[2-3]** (residues 1-3) in the asymmetric unit (three co-crystallized water molecules are omitted for clarity) and b) molecular structure of the NCN pincer platinum-phosphine **[2-3]$^{2-}$** dianionic moiety (residue 1). Hydrogen atoms are omitted for clarity and displacement ellipsoids are drawn at the 50% probability level.

Table 2: Selected bond lengths (Å) and angles (°) for **[2-OH$_2$]$_2$[2-3]**.

bond lengths (Å)			
Pt1-P1	2.3627(12)	Pt1-N21	2.131(4)
Pt1-N11	2.130(4)	Pt1-C11	1.970(5)
P1-C131	1.823(5)	P1-C251	1.835(5)
P1-C191	1.833(5)	Pt2-N12	2.071(4)
Pt2-N22	2.073(4)	Pt2-C12	1.917(5)
Pt2-O12	2.176(3)	Pt3-N13	2.080(4)
Pt3-N23	2.061(4)	Pt3-C13	1.902(5)
Pt3-O13	2.159(4)		

bond angles (deg)			
C11-Pt1-P1	176.87(14)	C11-Pt1-N11	80.48(17)
C11-Pt1-N21	79.95(17)	N21-Pt1-N11	159.84(15)
C191-P1-C131	99.0(2)	C131-P1-C251	107.1(2)
C251-P1-C191	104.8(2)	C12-Pt2-O12	177.53(19)
C12-Pt2-N12	82.7(2)	C12-Pt2-N22	82.8(2)
C13-Pt2-O13	175.41(17)	C13-Pt3-N13	82.48(19)
C13-Pt3-N23	82.13(19)		
torsion angles (deg)			
N21-Pt1-P1-C251	-54.7(2)	N21-Pt1-P1-C131	65.6(2)
N21-Pt1-P1-C251	-174.7(2)	N11-Pt1-P1-C251	120.7(2)
N11-Pt1-P1-C131	-119.1(2)	N11-Pt1-P1-C191	0.6(2)
C21-C11-Pt1-N11	172.2(4)	C61-C11-Pt1-N21	168.0(4)
P1-Pt1-C11-C61	-179(2)	C62-C12-Pt2-N22	-9.3(4)
C22-C12-Pt2-N12	-13.6(4)	C63-C13-Pt3-N23	10.0(4)
C23-C13-Pt3-N13	15.7(4)		

*NMR studies with **[2-OH$_2$]OTf** and phosphine **Na$_3$[3]** in Tris buffer.*

A slightly different coordination behaviour was observed when instead of D_2O Tris buffer was used as a solvent for the study of the coordination behaviour of phosphine **Na$_3$[3]** to the cationic pincer-platinum complex **[2-OH$_2$][OTf]**. Again for this study, various equivalents of **Na$_3$[3]** (0.1-5.0 eq.) dissolved in D_2O were added to **[2-OH$_2$][OTf]** dissolved in Tris buffer (125 mM, pH 8.0, acidified with HBF_4; final concentration of **[2-OH$_2$][OTf]** in Tris was 19 mM). Subsequently, the different solutions were analysed by ^{31}P NMR spectroscopy after 5 minutes and 1, 2 and 19 days.

Upon the addition of up to one equivalent of phosphine **Na$_3$[3]**, initially the appearance of a ^{31}P resonance peak at 30.6 ppm ($^1J(^{31}P\text{-}^{195}Pt)$ 2100 Hz) was observed (Table 3), which is the same signal as was observed in the coordination study in D_2O, *i.e.* assigned to the phosphine bound *trans* with respect to C_{ipso} (complex **Na$_2$[2-3]**, Scheme 2 and 3). However, when the same mixture was analysed after 1 day, a second signal at 8.6 ppm ($^1J(^{31}P\text{-}^{195}Pt)$ 4010 Hz) had appeared (Table 3), which gradually became more intense over time and ultimately after 19 days was the only resonance present in the spectrum. Its $^1J(^{31}P\text{-}^{195}Pt)$ value of 4010 Hz is indicative of a phosphine coordination *cis* with respect to C_{ipso},[44, 46-48] which in this case would imply an isomerization of the coordinated phosphine from

trans to *cis*. As the occurrence of the resonance at 8.6 ppm with $^{1}J(^{31}P\text{-}^{195}Pt)$ = 4010 Hz was only observed in the presence of Tris-buffer, the formation of the *cis*-coordination complex (*i.e.* ***cis*-Na$_2$[2-(3)(Tris)$_2$]**) from the *trans*-coordination complex is most probably assisted by the presence of Tris-molecules.
In a control experiment, where independently synthesized **Na$_2$[2-3]** (*vide infra*) was dissolved in d_{11}-Tris-buffer and subsequently analysed by ^{1}H NMR and ^{31}P NMR spectroscopy the exact same *trans*- to *cis*-transition of the coordinated phosphine was observed, as described above. This observation supports the formation of coordination complex ***cis*-Na$_2$[2-(3)(Tris)$_2$]** from complex **Na$_2$[2-3]**, as depicted in Scheme 3.

When more than one equivalent of phosphine **Na$_3$[3]** was added, two additional signals were observed, besides the signals of the monocoordinated *cis*- and *trans*-species in ^{31}P NMR. These two signals at 22.1 ppm ($^{1}J(^{31}P\text{-}^{195}Pt)$ 1640 Hz, $^{1}J(^{31}P\text{-}^{31}P)$ 14 Hz) and 10.1 ppm ($^{1}J(^{31}P\text{-}^{195}Pt)$ 3850 Hz, $^{1}J(^{31}P\text{-}^{31}P)$ 13 Hz) were both doublets (Table 3), indicating the coordination of two different phosphines to the same platinum centre in a *cis*-orientation (complex ***cis*-Na$_5$[2-(3)$_2$(Tris)]**, Scheme 3). An isomerisation of the biscoordinated product, as observed for the study in D_2O (***cis*-Na$_5$[2-(3)$_2$(D$_2$O)]** → ***trans*-Na$_5$[2-(3)$_2$(D$_2$O)]**, Scheme 2) did not occur when Tris buffer was used as a solvent.

Interestingly, even with an excess of 5.0 eq. of phosphine **Na$_3$[3]** present, we could still observe a small amount of the monocoordinated product, besides the biscoordinated product. Furthermore, the ratio between mono- and biscoordinated product did not change over time. This observation, which is different from the observations in D_2O, is most probably due to the competitive coordination of Tris to the cationic NCN pincer metal centre. Apparently, the huge excess of Tris (125 mM Tris to 19 mM **[2-OH$_2$][OTf]**) and its competitive coordination to platinum could only allow partial formation of the biscoordinated complex ***cis*-Na$_5$[2-(3)$_2$(Tris)]**.

Table 3: Resonance values observed in ^{31}P NMR upon the addition of 0.1-5.0 equivalents of **Na_3[3]** to **[2-OH_2][OTf]** in Tris-buffer and the (proposed) species formed.

Eq. of **Na_3[3]**	Tris	
	(*after 5 minutes*)	
0.1	30.62 (2090.8)	**Na_2[2-3]**
0.5	30.63 (2106.1)	**Na_2[2-3]**
1.0	30.61 (2105.0) *73%*	**Na_2[2-3]**
	22.13 *13%*	***cis*-Na_5[2-$(3)_2$(Tris)]**
	10.09 *10%*	***cis*-Na_5[2-$(3)_2$(Tris)]**
	8.54 *3%*	***cis*-Na_2[2-(3)$(Tris)_2$]**
1.5	30.64 (2105.5) *19%*	**Na_2[2-3]**
	22.13 (14.2; 1641.3) *38%*	***cis*-Na_5[2-$(3)_2$(Tris)]**
	10.09 (7.4; 3845.4) *30%*	***cis*-Na_5[2-$(3)_2$(Tris)]**
	8.57 (4149.0) *13%*	***cis*-Na_2[2-(3)$(Tris)_2$]**
2.0	30.64 (2078.8) *3%*	**Na_2[2-3]**
	22.13 (14.2; 1635.7) *37%*	***cis*-Na_5[2-$(3)_2$(Tris)]**
	10.15 (3863.6) *28%*	***cis*-Na_5[2-$(3)_2$(Tris)]**
	8.56 (4005.5) *18%*	***cis*-Na_2[2-(3)$(Tris)_2$]**
	-5.66 *13%*	**Na_3[3]**
5.0	22.09 (1637.8) *11%*	***cis*-Na_5[2-$(3)_2$(Tris)]**
	10.09 (3825.0) *7%*	***cis*-Na_5[2-$(3)_2$(Tris)]**
	8.50 (4020.3) *12%*	***cis*-Na_2[2-(3)$(Tris)_2$]**
	-5.70 *69%*	**Na_3[3]**
	(*after 1 day*)	
0.1	30.63 (2067.0) *59%*	**Na_2[2-3]**
	8.56 (4010.2) *41%*	***cis*-Na_2[2-(3)$(Tris)_2$]**
0.5	30.64 (2107.6) *66%*	**Na_2[2-3]**
	8.56 (4007.0) *34%*	***cis*-Na_2[2-(3)$(Tris)_2$]**
1.0	30.61 (2099.8) *53%*	**Na_2[2-3]**
	22.03 *12%*	***cis*-Na_5[2-$(3)_2$(Tris)]**
	10.01 *7%*	***cis*-Na_5[2-$(3)_2$(Tris)]**
	8.54 (4012.8) *28%*	***cis*-Na_2[2-(3)$(Tris)_2$]**
1.5	30.64 (2103.4) *25%*	**Na_2[2-3]**
	22.12 (12.9; 1641.8) *27%*	***cis*-Na_5[2-$(3)_2$(Tris)]**
	10.09 (8.1; 3830.5) *22%*	***cis*-Na_5[2-$(3)_2$(Tris)]**
	8.57 (4010.2) *26%*	***cis*-Na_2[2-(3)$(Tris)_2$]**
2.0	30.64 *0%*	**Na_2[2-3]**
	22.14 (14.2; 1634.0) *40%*	***cis*-Na_5[2-$(3)_2$(Tris)]**
	10.14 (3861.3) *30%*	***cis*-Na_5[2-$(3)_2$(Tris)]**

	8.56 (4009.1) *29%*	***cis*-Na_2[2-(3)$(Tris)_2$]**
5.0	22.09 (14.9; 1623.4) *10%*	***cis*-Na_5[2-$(3)_2$(Tris)]**
	10.16 (3878.1) *8%*	***cis*-Na_5[2-$(3)_2$(Tris)]**
	8.53 (3999.2) *12%*	***cis*-Na_2[2-(3)$(Tris)_2$]**
	-5.68 *70%*	**Na_3[3]**
	(*after 2 days*)	
0.1	30.62 (2084.3) *30%*	**Na_2[2-3]**
	8.55 (4014.6) *70%*	***cis*-Na_2[2-(3)$(Tris)_2$]**
0.5	30.63 (2097.6) *47%*	**Na_2[2-3]**
	8.56 (4014.9) *53%*	***cis*-Na_2[2-(3)$(Tris)_2$]**
1.0	30.61 (2118.1) *38%*	**Na_2[2-3]**
	22.12 *7%*	***cis*-Na_5[2-$(3)_2$(Tris)]**
	9.99 *7%*	***cis*-Na_5[2-$(3)_2$(Tris)]**
	8.54 (4005.5) *47%*	***cis*-Na_2[2-(3)$(Tris)_2$]**
1.5	30.64 (2095.9) *23%*	**Na_2[2-3]**
	22.12 (14.2; 1640.2) *24%*	***cis*-Na_5[2-$(3)_2$(Tris)]**
	10.07 (3871.0) *18%*	***cis*-Na_5[2-$(3)_2$(Tris)]**
	8.57 (4006.5) *36%*	***cis*-Na_2[2-(3)$(Tris)_2$]**
2.0	30.64 *0%*	**Na_2[2-3]**
	22.14 (14.4; 1642.9) *41%*	***cis*-Na_5[2-$(3)_2$(Tris)]**
	10.11 (9.8; 3872.9) *31%*	***cis*-Na_5[2-$(3)_2$(Tris)]**
	8.57 (4010.9) *28%*	***cis*-Na_2[2-(3)$(Tris)_2$]**
5.0	22.09 (14.2; 1650.4) *11%*	***cis*-Na_5[2-$(3)_2$(Tris)]**
	10.16 (3809.2) *6%*	***cis*-Na_5[2-$(3)_2$(Tris)]**
	8.53 (4010.9) *13%*	***cis*-Na_2[2-(3)$(Tris)_2$]**
	-5.68 *70%*	**Na_3[3]**
	(*after 19 days*)	
0.1	8.56 (4015.6)	***cis*-Na_2[2-(3)$(Tris)_2$]**
0.5	8.57 (4004.4)	***cis*-Na_2[2-(3)$(Tris)_2$]**
1.0	8.55 (4009.3)	***cis*-Na_2[2-(3)$(Tris)_2$]**
1.5	22.10 (15.4; 1628.1) *19%*	***cis*-Na_5[2-$(3)_2$(Tris)]**
	10.12 (13.0; 3814.3) *11%*	***cis*-Na_5[2-$(3)_2$(Tris)]**
	8.57 (4007.0) *70%*	***cis*-Na_2[2-(3)$(Tris)_2$]**
2.0	22.10 (14.7; 1636.0) *39%*	***cis*-Na_5[2-$(3)_2$(Tris)]**
	10.12 (13.1; 3864.5) *27%*	***cis*-Na_5[2-$(3)_2$(Tris)]**
	8.57 (4010.9) *34%*	***cis*-Na_2[2-(3)$(Tris)_2$]**
5.0	22.04 (14.4; 1643.6) *11%*	***cis*-Na_5[2-$(3)_2$(Tris)]**
	10.17 (3802.0) *7%*	***cis*-Na_5[2-$(3)_2$(Tris)]**
	8.53 (4000.0) *14%*	***cis*-Na_2[2-(3)$(Tris)_2$]**
	-5.80 *68%*	**Na_3[3]**

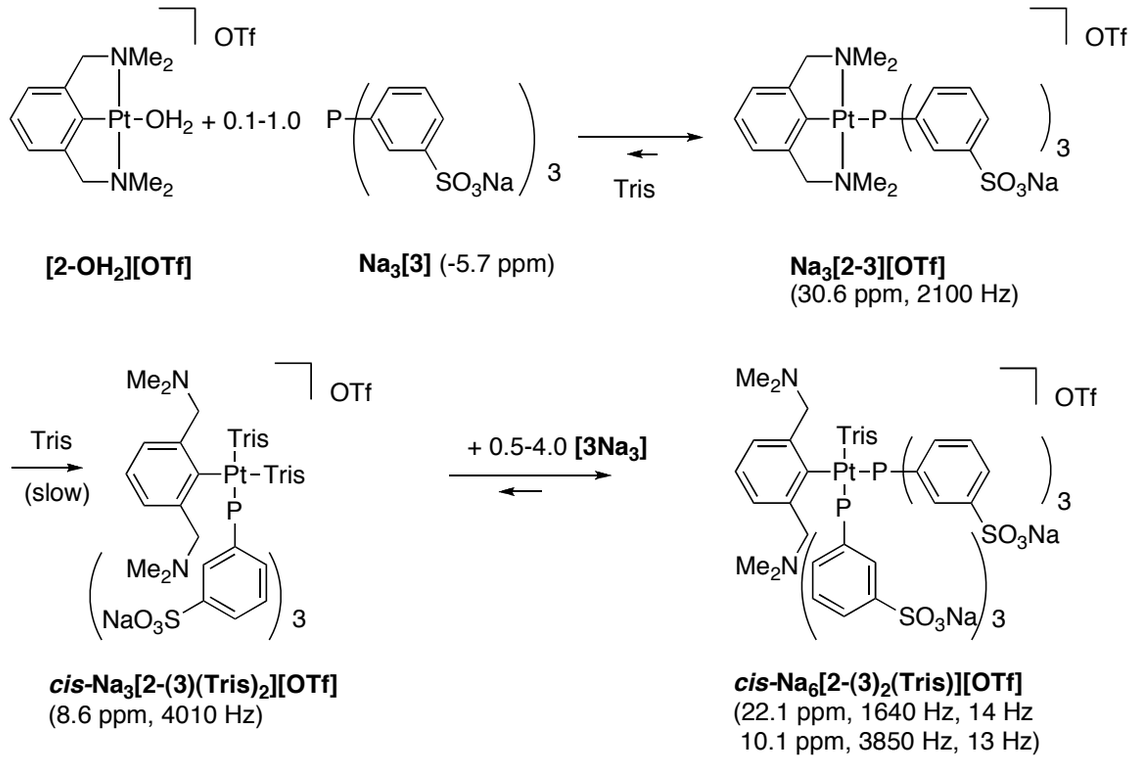

Tris: 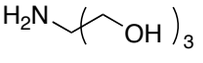

Scheme 3: Observed resonances in ^{31}P NMR upon the addition of 0.1-5.0 equivalents of **Na_3[3]** to **[2-OH_2][OTf]** in Tris-buffer (125 mM, pH 8.0) and the different species formed. The ^{31}P NMR resonances and the $^{1}J(^{31}P\text{-}^{195}Pt)$ and $^{2}J(^{31}P\text{-}^{31}P)$ (for ***cis*-Na_5[2-($(3)_2$(Tris)]**) values are given in brackets. Tris is also shown.

*Coordination of Tris to **[2-OH_2][OTf]***

Tris (pKa = 8.3) is a potentially tetradentate ligand having one $-NH_2$ and three –OH groups (Scheme 3). As the coordination products formed between **[2-OH_2][OTf]** and phosphine **Na_3[3]** were different in D_2O and Tris-buffer (Schemes 2 and 3), the coordination of Tris to **[2-OH_2][OTf]** was investigated separately. To this purpose a solution of Tris was mixed with a solution of **[2-OH_2][OTf]** (in D_2O, molar ratio Tris/**[2-OH_2][OTf]** = 1/1) and at time intervals ^{1}H NMR spectra were recorded. In Figure 4 the spectra for after 5 minutes, 1 day and 19 days, respectively are shown.

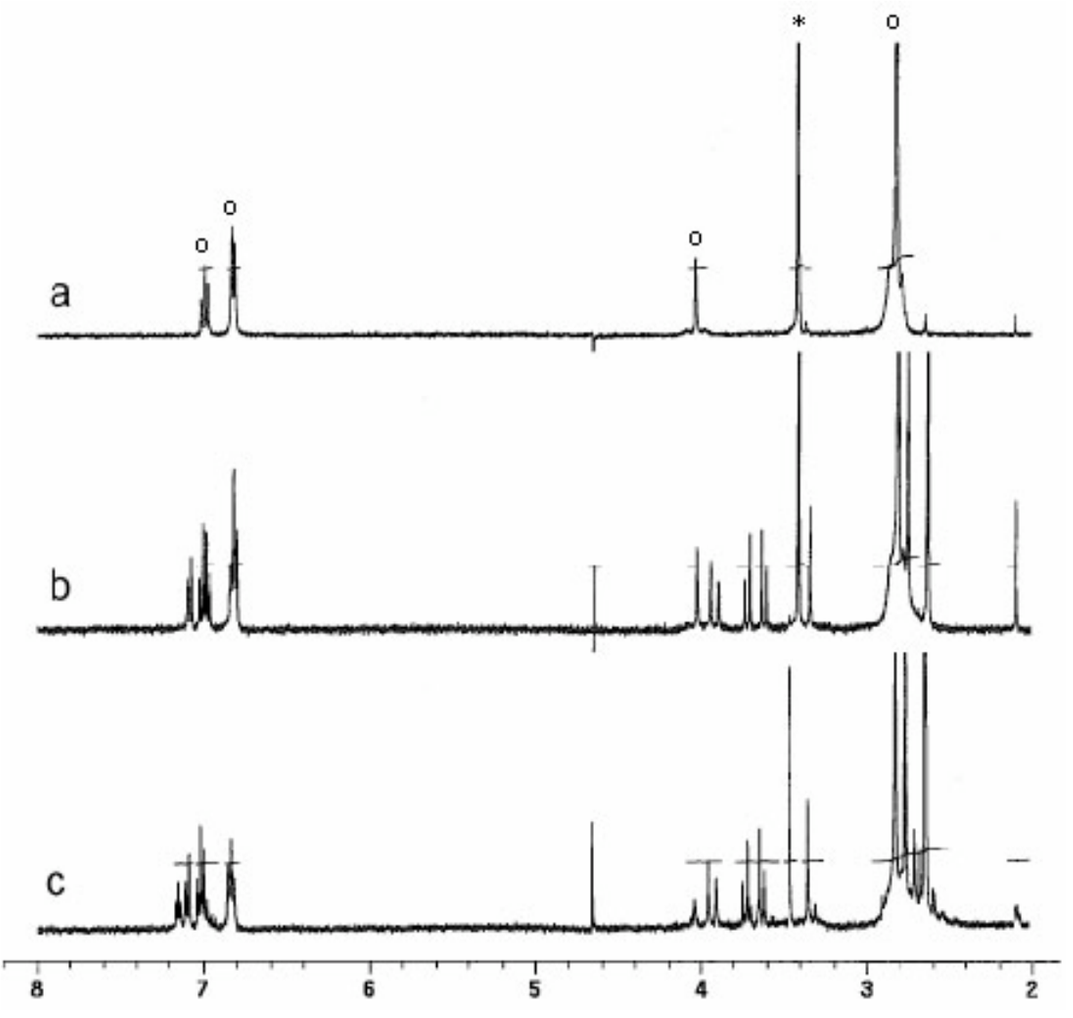

Figure 4: ^{1}H NMR spectra of a Tris : **[2-OH$_2$][OTf]** mixture (1:1 molar ratio) in D_2O; a) 5 minutes after mixing, b) after 1 day and c) after 18 days and 16 hours heating to 90°C. (Note that all spectra were recorded at room temperature, the resonances for **[2-OH$_2$][OTf]** are depicted with o; the resonance for uncoordinated Tris is depicted as *).

In the NMR spectra some significant changes are visible. Whereas at 5 minutes after mixing well-resolved signals for both the cationic NCN-pincer platinum complex **[2-OH$_2$][OTf]** and for uncoordinated Tris at 3.41 ppm were still visible, after 1 and 19 days, respectively, a more complex pattern was observed. The doublet and triplet pattern in the aromatic region of the pincer aromatic ring had changed into several multiplets, indicating an asymmetric substitution on the pincer arene ring. In the aliphatic region additional signals had appeared, indicating the decoordination of one of the two or even both –NMe_2 groups from the NCN-pincer platinum grouping. The AB pattern of the –CH_2 protons, visible at 3.67 ppm, is in concert with an asymmetric structure. From Figure 4 it is obvious that Tris can coordinate to the metal centre of cationic **[2-OH$_2$][OTf]** in several ways, although the exact nature of these structures

could not unambiguously be determined by NMR. The coordination of Tris in a *trans*- and *cis*-fashion with respect to C_{ipso} could explain the observed asymmetric pattern of the aromatic region and the multiple signals observed in the aliphatic region. On the other hand, it is also possible that Tris coordinates in a chelating manner, which could also explain the asymmetry of the NMR spectrum.

As it was difficult to deduce the actual coordination mode of Tris to the cationic NCN-pincer platinum moiety, we studied the coordination of ethanolamine (2-hydroxyethylamine) (pKa = 9.3) to **[2-OH$_2$][OTf]** in D_2O at pH 7. As ethanolamine possesses only one hydroxyl group as compared to three for Tris, ethanolamine was considered to be a suitable, though less complex model for Tris.

When a 1:1 mixture of ethanolamine and **[2-OH$_2$][OTf]** in D_2O was analysed by ^{1}H NMR, it was observed that the original two multiplet signals of uncoordinated ethanolamine (3.47 and 2.59 ppm) shifted to 3.73 and 2.98 ppm. The aliphatic pincer signals shifted equally from 4.02 and 2.82 ppm to 4.00 and 2.88 ppm, respectively (all values in D_2O). These data suggest the formation of a coordination complex between ethanolamine and **[2-OH$_2$][OTf]**.

When a 1:1 mixture of **[2-OH$_2$][OTf]** and ethanolamine was crystallized from H_2O, single crystals were obtained. An X-ray crystal structure determination of these crystals revealed the molecular structure of coordination complex **[2-(NH$_2$(CH$_2$)$_2$OH)][OTf]** in the solid state (Figure 5, relevant bond distances are given in Table 4). The ORTEP plot of **[2-(NH$_2$(CH$_2$)$_2$OH)][OTf]** shows that the NH_2-group of ethanolamine coordinates to the platinum ion of the pincer-moiety *trans* to C_{ipso}, while the hydroxyl group is non-coordinated. However, these hydroxyl groups do play a prominent role in the formation of the observed dimer structure involving hydrogen bonding between the OTf anions and the hydroxyl groups.

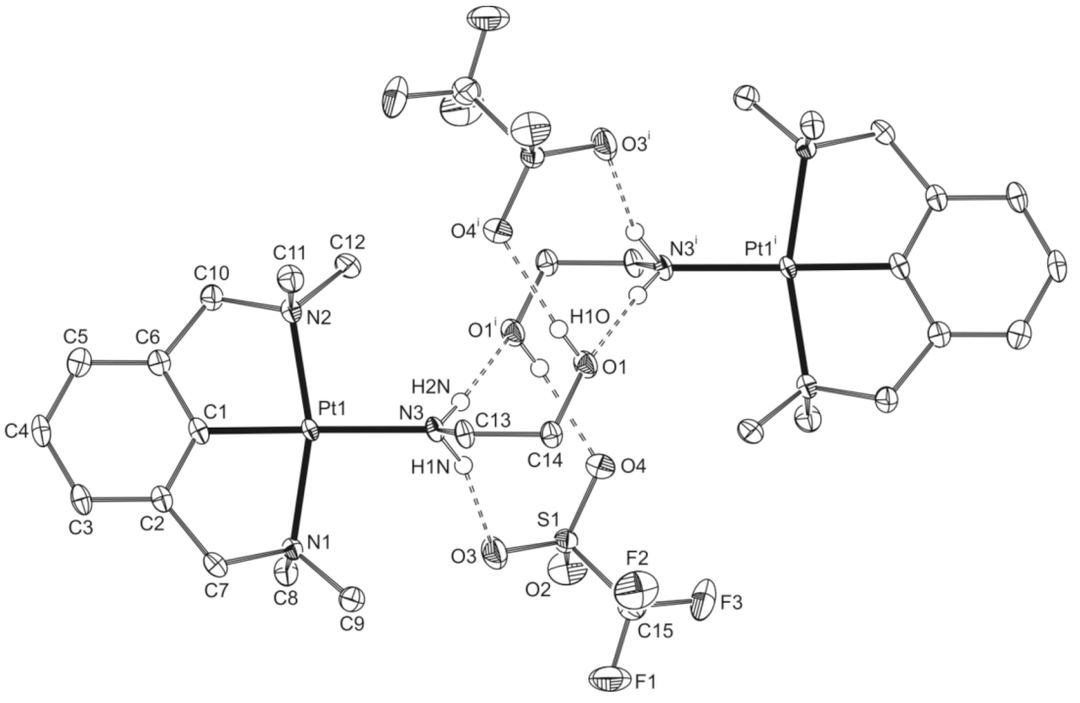

Figure 5: Displacement ellipsoid plot (50% probability level) of coordination complex **[2-(NH_2-(CH_2)$_2$-OH)][OTf]**. C-H hydrogen atoms are omitted for clarity. Symmetry operation i: 2-x, -y, 1-z.

Table 4: Selected bond lengths (Å) and angles (°) for **[2-(NH_2-(CH_2)$_2$-OH)][OTf]**.

Bond lengths		Bond angles	
Pt1-C1	1.935(4)	N1-Pt1-N2	162.20(14)
Pt1-N1	2.095(3)	N3-Pt1-C1	176.54(13)
Pt1-N2	2.088(3)	N2-Pt1-C1	81.59(16)
Pt1-N3	2.170(3)	N1-Pt1-C1	80.85(16)
N3-C13	1.498(5)		

*Coordination of phosphines **Na_3[4]** and **[5](BF_4)$_3$** to **[2-OH_2][OTf]** in D_2O*

To investigate the influence of the steric requirements of the selected neutral, cationic and anionic phosphines on their coordination to the NCN-pincer platinum cation, the reactions of anionic phosphine **Na_3[4]** and cationic phosphine **[5](BF_4)$_3$** to **[2-OH_2][OTf]** were studied. To a solution of **[2-OH_2][OTf]** were added various equivalents of a solution of either **Na_3[4]** or **[5](BF_4)$_3$** and the resulting solutions were analysed by ^{31}P NMR spectroscopy (Scheme 4).

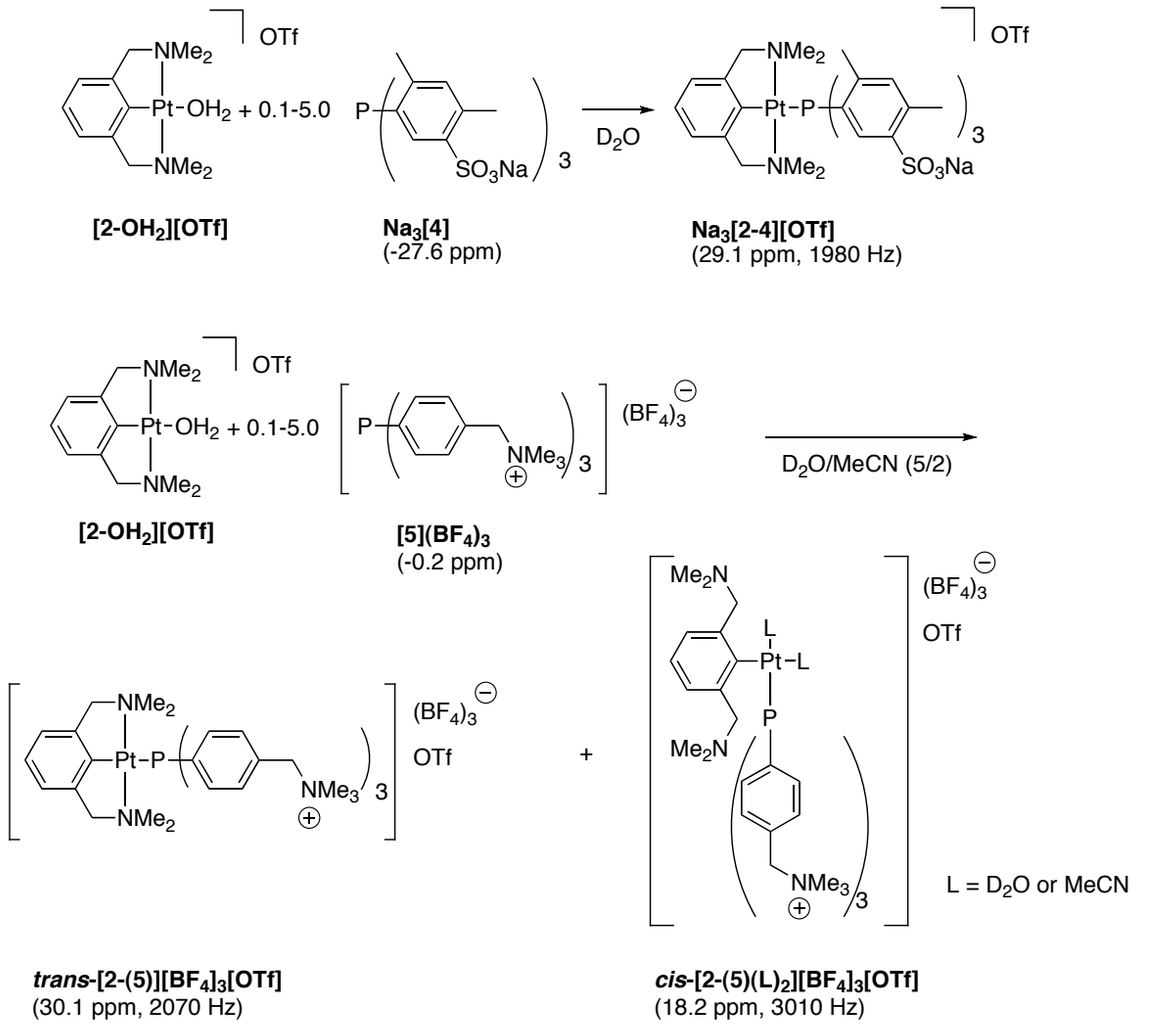

Scheme 4: Coordination of phosphines **Na_3[4]** and **[5](BF_4)$_3$**, respectively to **[2-OH_2][OTf]**.

For anionic phosphine **Na_3[4]**, the coordination of only one phosphine to the NCN-pincer platinum cation was observed in D_2O, even when up to five equivalents were added. The titration study and the preparative synthesis of **Na_2[2-4]** in D_2O gave in the ^{31}P NMR spectra a chemical shift of 29.1 ppm with $^1J(^{31}P\text{-}^{195}Pt)$ = 1940 Hz, which pointed to a structure with a phosphine group coordinating *trans* to C_{ipso} (Scheme 4).

When various equivalents of cationic **[5](BF_4)$_3$** were added to **[2-OH_2][OTf]** dissolved in a water/acetonitrile mixture (5/2 v/v), again the coordination of only one phosphine to one metal centre was observed. However, in this case the coordination of the phosphine *cis* with respect to C_{ipso} was observed as well, with 20% *trans* ($^1J(^{31}P\text{-}^{195}Pt)$ 2070 Hz) and 80% *cis* ($^1J(^{31}P\text{-}^{195}Pt)$ 3010 Hz) coordination complex (***trans*-[2-(5)][BF_4]$_3$[OTf]** and ***cis*-[2-(5)(L)$_2$][BF_4]$_3$[OTf],** Scheme 4). Also here, the coordination of a second phosphine was not observed upon addition of

more than one equivalent of **[5](BF$_4$)$_3$**. Complexes **Na$_3$[2-4][OTf]** and **[2-(5)][BF$_4$]$_3$[OTf]** were synthesized and the pure white coloured products were fully analyzed by NMR spectroscopy and high-resolution ES mass spectrometry (see experimental section for details).

Besides steric bulk, also the σ-bond donating properties of the phosphorous atoms are a determining factor for the coordination power of phosphine ligands (like PR_3). It is known that the σ-bond donating properties of the phosphorous atom are influenced by the charge of the different R-groups.[53, 54] These σ-bond donating properties can be measured after converting the phosphines to the corresponding $Se{=}PR_3$ derivatives with selenium and subsequent measurement of their $^1J(^{31}P\text{-}^{77}Se)$ coupling constant.[53, 54]

The $^1J(^{31}P\text{-}^{77}Se)$ coupling values of the phosphorous selenides sodium 3-phosphoroselenoylbenzene sulfonate **Na$_3$[6]** and *N*,*N*,*N*-trimethyl-1-(4-phosphoroselenoylphenyl)methanaminium **[7](BF$_4$)$_3$** (Table 5), are nearly identical, indicating similar σ-bond donating properties of **Na$_3$[3]** and **[5](BF$_4$)$_3$**.

Table 5: ^{31}P NMR properties of selenium oxides **Na$_3$[6]** and **[7](BF$_4$)$_3$** in D_2O.

$Se{=}PR_3$	δ (ppm) for ^{31}P nucleus	$^1J(^{31}P\text{-}^{77}Se)$
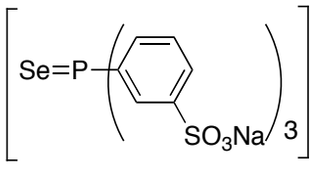 **Na$_3$[6]**	35.9	707
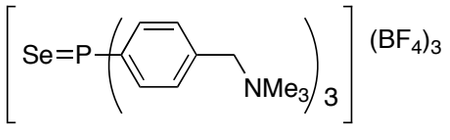 **[7](BF$_4$)$_3$**	35.0	701

*^{31}P NMR study with the semisynthetic metalloprotein **[cut-1-OH$_2$][OTf]** and phosphine **Na$_3$[3]**.*

From the crystal structures it became apparent that the cutinase-embedded pincer-metal centre was exposed to the solvent.[29] Therefore, it was anticipated that the pincer head group should be available for the coordination to various phosphines. The coordination of phosphine **Na$_3$[3]** to the cationic pincer-cutinase hybrid **[cut-1-OH$_2$][OTf]** was studied by adding different equivalents of **Na$_3$[3]** (0.5, 1.0 and 1.5 eq. in D_2O) to a solution of **[cut-1-OH$_2$][OTf]** (2 mM) in Tris buffer (125 mM, pH 8.0, acidified with HBF_4, 10% D_2O). The resulting solution was analyzed by ^{31}P NMR spectroscopy. Interestingly, we observed only one resonance around 8.8 ppm ($^1J(^{31}P$-

^{195}Pt) 3970 Hz) for a coordinated phosphine **Na_3[3]**, regardless of the amount of **Na_3[3]** added. As an illustrative example, the spectrum of **[cut-1-OH_2][OTf]** in the presence of **Na_3[3]** (1.5 eq) is shown in Figure 6b.

a)

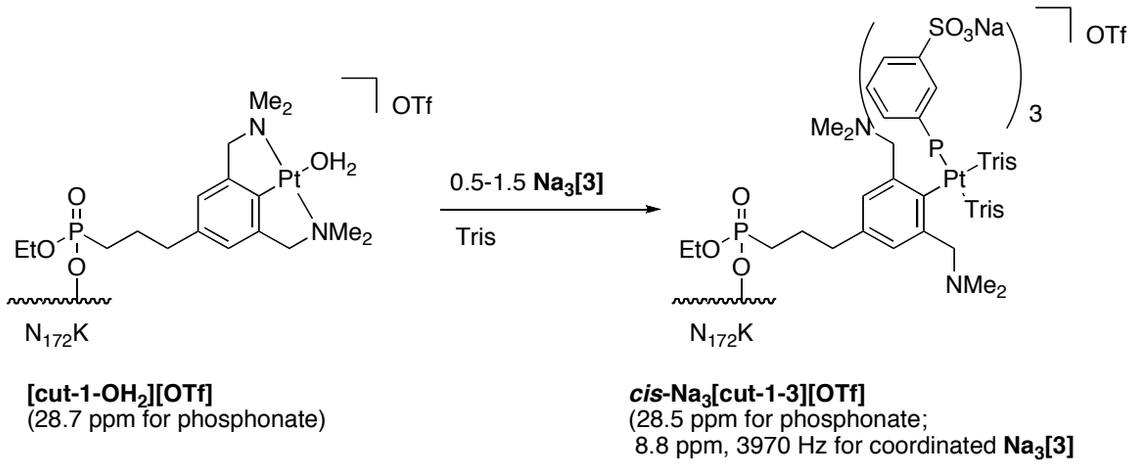

[cut-1-OH_2][OTf]
(28.7 ppm for phosphonate)

***cis*-Na_3[cut-1-3][OTf]**
(28.5 ppm for phosphonate;
8.8 ppm, 3970 Hz for coordinated **Na_3[3]**

b)

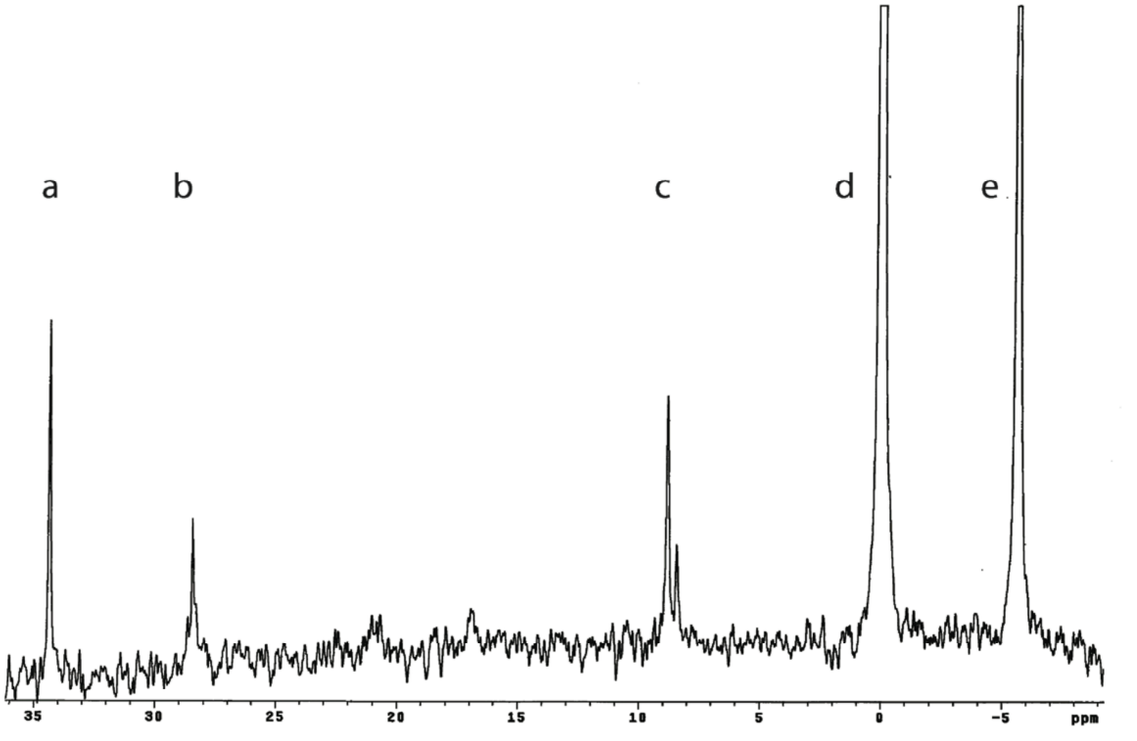

Figure 6: a) Proposed molecular structure of pincer-phosphine coordination complex ***cis*-Na_2[cut-1-3]** formed upon addition of 0.5-1.5 eq. of **Na_3[3]** to **[cut-1-OH_2][OTf]**. b) ^{31}P NMR spectrum of a 1.5/1 mixture of **Na_3[3]** and **[cut-1-OH_2][OTf]** (assignment of the signals: a: phosphine oxide, b: phosphonate, c: **Na_3[3]** coordinated to platinum, d: internal standard, e: free **Na_3[3]**). Measurements were performed in Tris buffer.

The position of the peak and its (^{1}J(^{31}P-^{195}Pt) 3970 Hz) coupling constant indicate that the phosphine is coordinated *cis* to C_{ipso} of the pincer platinum moiety.[43, 47-49, 52, 55] In contrast to the formation of the biscoordination product ***trans*-Na$_5$[2-(3)$_2$(D$_2$O)]** (Scheme 2), the addition of an excess of **Na$_3$[3]** (1.5 eq.) did not lead to the formation of biscoordinated cutinase-pincer hybrid species. Most likely the steric bulk of the protein backbone prevents the coordination of a second phosphine to the metal centre.

*ESI-MS studies: Titration of **[cut-1-OH$_2$][OTf]** with various equivalents of phosphine **Na$_3$[3]**.*

To investigate and quantify the coordination of phosphines to **[cut-1-OH$_2$][OTf]** further, we decided to study the coordination of **Na$_3$[3]** to **[cut-1-OH$_2$][OTf]** by ESI-MS. For this purpose we added different portions of a solution of **Na$_3$[3]** (1.0-5.0 eq.) to a solution of **[cut-1-OH$_2$][OTf]**. In order to obtain high–resolution mass spectra we had to perform these experiments in NH_4Ac instead of Tris buffer. Importantly, a separate coordination study in NH_4Ac buffer showed similar results as those obtained in Tris, which justified the buffer switch required for this ESI-MS study.

After addition of 1.0 eq. of **Na$_3$[3]**, mostly the monocoordinated complex **Na$_3$[cut-1-3]$^+$** was observed (Figure 7), along with traces of **[cut-1]$^+$** and traces of bisphosphine coordinated **H$_6$[cut-1-(3)$_2$]$^+$**. The latter was surprising as no proof of the protein-hybrid with two coordinating phosphines was observed with ^{31}P NMR (*vide supra*). However, after further dilution of this solution (5 x and 10 x) and analysis, these biscoordination peaks disappeared and thus turned out to be aspecific. A control experiment showed that aspecific phosphine coordination to free **cut**, thus without pincer platinum moiety, occurred under concentrated conditions as well, but disappeared when diluted further. The mass spectrum in Figure 7 showed a characteristic pattern of three shoulder peaks, with the peak with the highest intensity corresponding to the coordinated phosphine where all the three Na^+ ions were replaced by H^+ (**H$_3$[cut-1-3]$^+$**, Table 6), displaying a +1 charged phosphine-metallopincer cutinase coordination complex. The shoulder peaks correspond to the replacement of two or one Na^+ ions by H^+, respectively **H$_2$Na[cut-1-3]$^+$** and **HNa$_2$[cut-1-3]$^+$**.

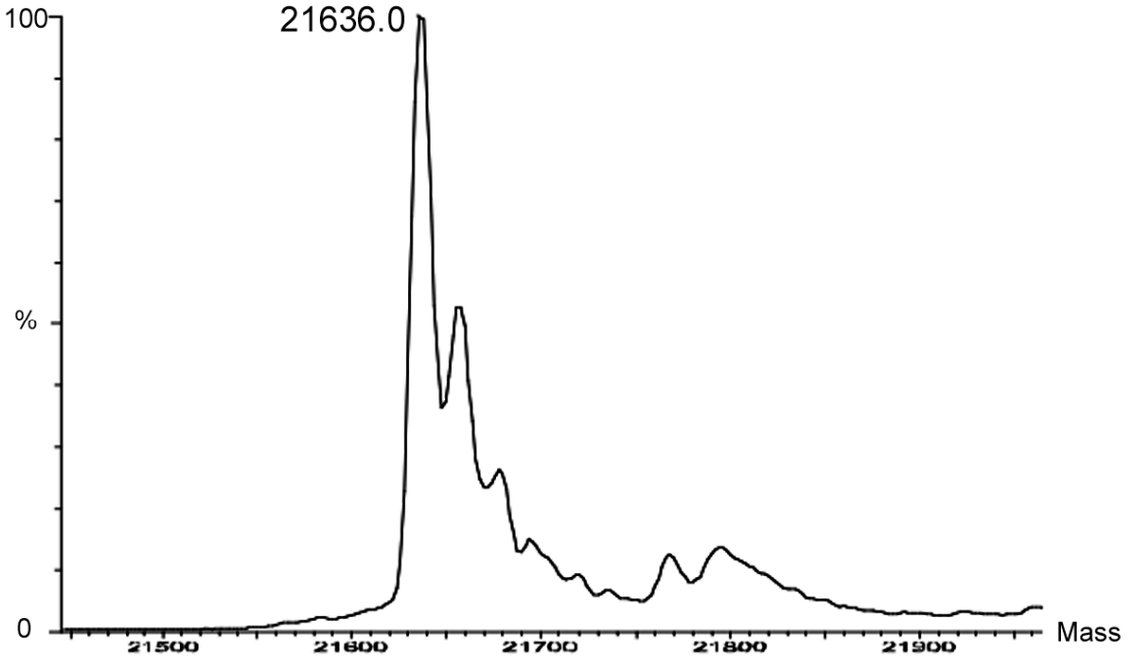

Figure 7: Deconvoluted ESI-MS spectrum of a 1:1 mix of **[cut-1-OH$_2$][OTf]** and phosphine **Na$_3$[3]**; the highest peak corresponds to (**H$_3$[cut-1-3]$^+$**), the shoulder peaks at higher masses correspond to the association of one or two sodium ions (**H$_2$Na[cut-1-3]$^+$** and **HNa$_2$[cut-1-3]$^+$**, respectively).

*ESI-MS studies with **[cut-1-OH$_2$][OTf]** and other phosphines.*

Encouraged by these results, we also studied the coordination behaviour of the bulkier and differently charged phosphines with **[cut-1-OH$_2$][OTf]** as this potentially could be a straightforward manner to probe the availability of metal centres in semisynthetic metalloenzymes. Therefore, to **[cut-1-OH$_2$][OTf]** (1 eq.) were added different phosphines (1 eq.) and these samples were subsequently analyzed by ESI-MS. In Table 6, the results for different water-soluble cationic and anionic (**Na$_3$[4], [5](BF$_4$)$_3$**, **[9](BF$_4$)$_6$**, **[10](BF$_4$)$_6$**) and water-insoluble, neutral phosphines (**8**) are given.

Table 6: Coordination of different phosphines to **[cut-1-OH$_2$][OTf]** analysed by ESI-MS.

Phosphine added	Mass calculated	Mass detected
None (**[cut-1-OH$_2$][OTf]**)	21137.4609	21136.15±0.43 **[cut-1]$^+$**
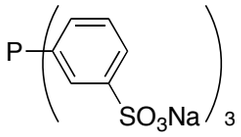 **Na$_3$[3]**[a]	21636.9121 21659.39	21639.00 **H$_3$[cut-1-3]$^+$** 21660.50 **H$_2$Na[cut-1-3]$^+$**
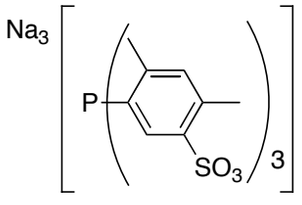 **Na$_3$[4]**[a, c]	21721.0716	21136.15±0.43 **[cut-1]$^+$** (50%) 21722.77±0.18[c] **[cut-1-4H$_3$]$^+$** (50%)
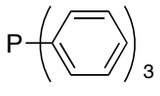 **8**[b]	21399.55	21136.85±0.02 **[cut-1]$^+$** 21399.74±0.00 **[cut-1-8]$^+$**
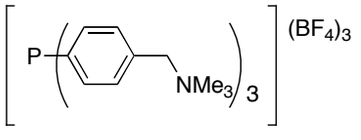 **[5](BF$_4$)$_3$**[a]	21615.80	21136.15±0.43 **[cut-1]$^+$** *Not observed*
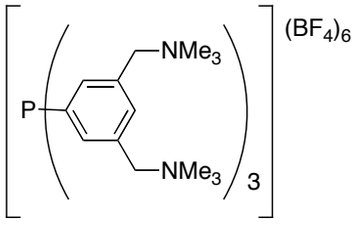 **[9](BF$_4$)$_6$**[a]	22354.05	21136.15±0.43 **[cut-1]$^+$** *Not observed*
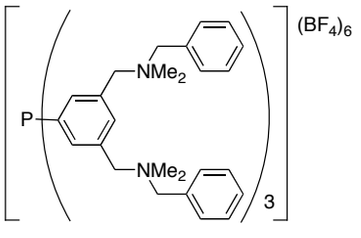 **[10](BF$_4$)$_6$**[a]	22809.92	21136.15±0.43 **[cut-1]$^+$** *Not observed*

[a] 1.0 eq. of phosphine added; [b] **8** was added as solid, insoluble powder (504 eq.); [c] **Na$_3$[cut-1-4]$^+$**, **HNa$_2$[cut-1-4]$^+$** and **H$_2$Na[cut-1-4]$^+$** and **H$_3$[cut-1-4]$^+$** were all observed, for clarity only the **H$_3$[cut-1-4]$^+$** signal is given here.

With compound **Na_3[4]** we only observed partial coordination of the phosphine to **[cut-1-OH_2][OTf]** when 1.0 eq. of **Na_3[4]** was added. In this case around 50% of free **[cut-1]$^+$** was still observed according to mass spectrometry.
Triphenylphosphine **8** lacks charged groups and is insoluble in the aqueous buffer used. When **8** was added to **[cut-1-OH_2][OTf]**, partial formation of **[cut-1-8]$^+$** was observed, *i.e.* a buffer soluble complex was formed. In order to test whether the coordination of **8** to **[cut-1-OH_2][OTf]** might be aspecific, a dilution experiment with ESI-MS analysis of the solution was carried out. These experiments indicated that the coordination was selective indeed. Thus, even though **8** itself is water-insoluble, selective coordination to the embedded platinum to give water-soluble **[cut-1-8]$^+$** does occur.
After having observed coordination of anionic and neutral phosphines to **[cut-1-OH_2][OTf]**, we investigated the coordination of water-soluble, cationic phosphines **[5]$(BF_4)_3$**, **[9]$(BF_4)_6$** and **[10]$(BF_4)_6$.**[56] However, after addition of 1.0 eq. of either **[5]$(BF_4)_3$, [9]$(BF_4)_6$** or **[10]$(BF_4)_6$**, we did not see any evidence for the presence of **cut-1-phosphine** coordination complexes in the ESI-mass spectra, showing that no detectable coordination of these phosphines to the protein-embedded metal centre had occurred.

Discussion

As a proof of principle study to expand the use of metalloproteins in classical coordination chemistry, we tried to assess the reactivity and availability of a synthetic organometallic moiety that was introduced in a protein scaffold, such as those that recently were developed by our group.[29, 30] Previous structural analysis of one of these semisynthetic metalloproteins in the solid state[29] had shown that the formation of a dimeric metalloprotein induced by coordination of the embedded metal centres was possible (see Figure 1b). This result suggested that classical coordination chemistry occurs with these bio-organometallic materials, at least in the solid state. We were interested to see whether this coordination chemistry with embedded metal sites would be possible in solution as well, as that would greatly enhance the applicability of this type of semisynthetic metalloproteins. Consequently, the coordination properties of the metal centre of the cationic NCN-pincer platinum moiety embedded in cutinase (**[cut-1-OH_2][OTf]**, Scheme 1) were investigated by screening the metal centre for its binding properties to several phosphines. Notably, as we are currently also studying the catalytic properties of similar pincer metal protein hybrids[57] as well as the use of luminescent NCN-pincer platinum complexes as site-selective protein labels,[58] this study can serve as a starting point in assaying the accessibility and the chemical properties of protein-embedded ECE-pincer metal centres.

The model study with **[2-OH_2][OTf]** showed that all the phosphines that are of interest for this study do coordinate to the small molecular NCN-pincer metal centre.

In the case of the anionic model phosphine **Na_3[3]**, with sulfonate substituents in the *meta*-position of the aromatic ring, even two phosphines can coordinate to one metal centre, when an excess of the phosphine is present (Scheme 2). Both in Tris buffer and in D_2O, the coordination of two molecules of **Na_3[3]** to one cationic metal centre was observed when an excess of ligand was used. When up to 1 equivalent of **Na_3[3]** was added, only monocoordinated species were observed. However, the monodentate coordination mode of **Na_3[3]** (*cis* or *trans* with respect to C_{ipso}) to the pincer metal centre was different in both solvents. In D_2O only the product in which the phosphine is coordinated *trans* to C_{ipso} was observed, even after standing for 2 days. This *trans*-coordination of **Na_3[3]** to **[2-OH_2][OTf]** was initially also observed in Tris as well, but after several days a shift of the phosphine towards a *cis*-coordination mode was observed, which is most probably due to the competing coordination of Tris to the cationic NCN pincer platinum centre. Due to the different possible coordination modes of Tris (Tris can potentially coordinate to platinum via its NH_2 or OH groups) and the big excess of Tris present in solution (*e.g.* 125 mM Tris to 19 mM **Na_3[3]**), the exact coordination mode of Tris is difficult to derive from the NMR data obtained. Therefore, we also performed a model study with ethanolamine, as a simplified model of Tris. The crystal structure of ethanolamine coordinated to the NCN pincer platinum moiety (Figure 5) showed a coordination of the NH_2-group *trans* to C_{ipso} in the solid state. NMR studies on the other hand suggested the presence of species with different coordination geometries for Tris (*cis* or *trans*) in solution. The coordination mode of the ethanolamine to the cationic NCN pincer platinum centre in the solid state indicates a relatively strong interaction between the platinum centre and the amine-nitrogen. Also in the case of Tris in solution it is likely that this occurs first (rapid) followed by transformation into other coordination modes, *e.g. cis* with respect to C_{ipso}, as was evidenced from NMR.

Contrary to **Na_3[3]**, only one molecule of the anionic phosphine **Na_3[4]** and of the cationic phosphine **[5](BF_4)$_3$** coordinate to **[2-OH_2][OTf]**. As the overall charges of phosphines **Na_3[3]** and **Na_3[4]** are the same, the coordination of only one molecule of **Na_3[4]** is most likely caused by the additional steric bulk of the two methyl groups in the 4- and 6-position of the aromatic ring when compared to **Na_3[3]**. For the cationic phosphine **[5](BF_4)$_3$**, on the other hand, this is less obvious as the additional steric bulk is located at the 4-position of the aromatic ring, thus away from the coordinating phosphorous atom. Moreover, the results of ^{31}P NMR studies with the selenium oxides **Na_3[6]** and **[7](BF_4)$_3$** showed that the σ-donating properties of **[5](BF_4)$_3$** and **Na_3[3]** are very similar, which indicates that a difference in σ donation can not be a reason for the different coordination behaviour of **[5](BF_4)$_3$** to **[2-OH_2][OTf].** It seems likely that a third reason, *i.e.* the occurrence of intramolecular, inter-ligand Coulombic repulsion can explain the coordination of just one phosphine molecule to the platinum centre. It must be noted that phosphines **Na_3[3]** and **Na_3[4],** and **[5](BF_4)$_3$** carry opposite charges (anionic *versus* cationic) which affects their coordination behaviour in a different manner.[56] The anionic

moieties in phosphines **Na_3[3]** and **Na_3[4]** can affect the coordination properties of these phosphines more profoundly as compared with the cationic grouping in **[5]$(BF_4)_3$**. Besides the effects of Coulombic repulsion, the anionic groups can be involved in the formation of a hydratation shell of tightly bonded water-molecules around the charged groups (including eventually also the counter cations, *e.g.* Na^+) which can affect the properties of the phosphine such as its steric bulk and cone-angle.

The ^{31}P NMR and ESI-MS coordination studies showed that significant differences exist between the coordination properties of small-molecular cationic pincer **[2-OH_2][OTf]** and the NCN-pincer platinum group in **[cut-1-OH_2][OTf]** in the presence of Tris. Firstly, only one molecule of phosphine **Na_3[3]** does coordinate to **[cut-1-OH_2][OTf]** (even when an excess of **Na_3[3]** was present). Moreover, in contrast to the initial *trans*-coordination to **[2-OH_2]$^+$** the phosphine coordinated in a *cis*-fashion (typical chemical shift and coupling constant) to **[cut-1-OH_2]$^+$**. This can either be caused by the competitive coordination of the Tris buffer molecules to the metal centre or induced by the steric bulk of the protein backbone surrounding the embedded Pt centre. For the small molecular pincer complex **[2-OH_2][OTf]** in Tris, the *cis*-coordination of the phosphine to the metal centre appeared slowly and only after 19 days was the *cis*-coordination product the only signal observed in ^{31}P NMR. The ^{31}P NMR spectra with **[cut-1-OH_2][OTf]** in Tris were collected over the weekend and the only signal observed was the one for the *cis*-coordination (*cis* to C_{ipso}) product, strongly suggesting that in the case of **[cut-1-OH_2][OTf]** the protein backbone strongly affected the kinetics of the *trans*- to *cis*-isomerization process. Ample evidence[59, 60] is available that an important prerequisite for the *trans*- to *cis*-isomerization to occur is the dissociation of at least one Pt-N bond. As *cis*-coordination of an external ligand causes severe steric interference with the de-coordinated *ortho*-CH_2NMe_2 grouping this process will also induce de-coordination of the second *ortho*-CH_2NMe_2 grouping and concomitant rotation of the aryl ring out of the Pt-coordination plane, thereby releasing steric strain in coordination plane of the complex.
Moreover, the steric bulk of the protein backbone[29] also affects the stability of the eventually formed phosphine coordination product as is indicated by the results of the ESI-MS study. This showed that the bulkier phosphine **Na_3[4]** coordinated only partially to **[cut-1-OH_2][OTf]**, whereas the cationic phosphines **[5]$(BF_4)_3$** and **[9]$(BF_4)_6$** did not coordinate at all. Interestingly, the water-insoluble phosphine **8** did also coordinate to **[cut-1-OH_2][OTf]** forming a soluble adduct.

Conclusions

This study has shown that the coordination of various phosphines to an artificial metal centre in a semisynthetic metalloenzyme is feasible. We demonstrated that the well-established coordination chemistry for small-molecular complexes can be

transferred to novel semisynthetic metalloprotein systems. The principles of classical coordination chemistry can be expanded to ECE pincer-metal lipase hybrids in which the semisynthetic metalloprotein systems exerts its own, unique coordination behaviour dictated by the specific influence of the protein backbone on the cationic pincer metal centre. The results suggest that these effects are both of kinetic (*cf.* effect on the Pt-N dissociation-association process of the NCN-pincer platinum moiety) and thermodynamic nature (*cf.* influence of the size of the phosphine in its complex with the embedded Pt centre on its stability). An intriguing question arises when the volume and shape of the starting NCN-pincer platinum moiety, which is rather two-dimensional, is compared with those of the *cis*-phosphine coordination product that is clearly three-dimensional with the de-coordinated *ortho*-CH_2NMe_2 groupings orientated perpendicular to the Pt-'s coordination plane and the bulky, negatively charged phosphine. It is obvious that sterics play a role because coordination of two of these phosphines to the protein embedded platinum centre seems impossible (in contrast with the bis-phosphine complexes obtained with the small molecule platinum compound). It is obvious that on the basis of the different shapes, volumes and polarity of starting and coordination products and taking into account the structure of neutral **[cut-1-Cl]** in the solid state showing the constraints in the embedded site, further study is needed.
Finally, the coordination studies described here were all performed in a strongly polar medium, in water or in aqueous Tris, respectively. Due to the fact that all phosphines except **8** are charged, polar effects influencing the interaction of the coordinated phosphines with the hydrophilic and hydrophobic areas of the protein backbone surrounding the embedded Pt centre and the complexed, charged phosphines have to be considered.

Notably, we demonstrated for the first time that the coordination properties of complex metal-protein hybrid systems can be studied using standard chemical analysis techniques (^{31}P NMR spectroscopy and ESI-MS spectrometry), thereby creating straightforward analysis protocols without a need for laborious biochemical analysis procedures. This proof of principle study has opened the door to various potential new applications in which the unique properties of synthetic metal complexes and biomolecules are combined. For example, selective targeting and identification of (semisynthetic) metalloenzymes in biological media, *e.g.* in protein profiling or screening studies or in assaying the anticancer activities or spectroscopic properties of metal complexes in biological media, comes within reach.

Experimental Procedures

General comments: Tris(hydroxylmethyl)aminomethane (Tris), MeCN and triphenylphosphine **8** were purchased from Acros Organics. Aqueous HBF_4 (50%, special), NH_4Ac (99.99%), $P(C_6H_4(SO_3Na)\text{-}3)_3$ (**Na_3[3]**) and Sephadex™ LH-20 (pre-swollen in MilliQ-H_2O) were purchased from Sigma-Aldrich. D_2O (Cambridge Isotope

Laboratories Inc.) was degassed prior to use. MeCN and CH_2Cl_2 were distilled over CaH_2. Water for the preparation of the buffer solutions was filtered with the Milli-Q filtration system (Millipore, Quantum Ultrapure) prior to use. The dialysis cassettes (Slide-A-Lyzer™, 10,000 MWCO, 0.1-0.5 mL or 0.5-3.0 mL) for the purification of NCN-pincer platinum chloride/enzyme-hybrid **[cut-1-OH$_2$][OTf]** were purchased from Pierce. Cutinase mutant N172K was provided by Unilever. A sealed glass tube containing H_3PO_4 (22.71 mM) was used as internal standard and reference in all ^{31}P NMR experiments. Electrospray ionization mass spectra were recorded on a Micromass LCT spectrometer. All samples were introduced using a nanoflow electrospray source (Protana, Odense, Denmark) and all spectra were calibrated with a CsI solution (50 mg/mL in MQ-H_2O). Matrix-assisted laser desorption ionization mass spectrometry experiments were performed with a Voyager-DE Pro (Applied Biosystems) instrument in the reflector mode with 2,5-dihydroxybenzoic acid as matrix. Microanalyses were performed by Dornis und Kolbe, Mikroanalytisches Laboratorium (Mülheim a/d Ruhr, Germany). NMR measurements were performed on a Varian Inova 300 MHz or Varian Oxford 400 MHz spectrometer. The syntheses of **1-Cl**[30] and **[2-OH$_2$][OTf]** [39, 41] were carried out as reported.

Tris buffer: Tris (250 mmol, 30.2838 g) was dissolved in MilliQ-H_2O (2.0 L) and acidified with aqueous HBF_4 to pH 8.0.

NH$_4$OAc buffer: NH_4OAc (300 mmol, 23.1240 g) was dissolved in MilliQ-H_2O (2.0 L). The final solution had pH 7.0.

Synthesis of [1-OH$_2$][OTf]: To a solution of **1-Cl**[30] (0.0383 g, 0.0553 mmol, 1.0 eq.) in wet acetone (50 mL) was added AgOTf (0.0170 g, 0.0663 mmol, 1.2 eq.). The mixture was stirred for 1.5 h, after which the mixture was filtered over Celite (3 x). All volatiles were removed *in vacuo*, after which the crude off-white oil was used directly for inhibition without further purification (0.0311 g, 0.0377 mmol, 68 %). ^{1}H NMR (C_6D_6, 399.942 MHz, 298.1 K): δ 7.79 (d, 2H, Ar*H*, $^3J_{H\text{-}H}$ = 8.8 Hz), 7.04 (d, 2H, Ar*H*, $^3J_{H\text{-}H}$ = 8.8 Hz), 6.33 (s, 2H, Ar*H*), 4.10-3.80 (m, 2H, CH_2O), 3.30 (s, 4H, -CH_2N), 2.55 (s, 12H, -N(CH_3)$_2$), 2.46 (t, 2H, ArCH_2, $^3J_{H\text{-}H}$ = 7.0 Hz), 1.97-1.89 (m, 2H, PCH$_2$CH_2), 1.82-1.74 (m, 2H, PCH_2), 0.96 (t, 3H, -CH_3, $^3J_{H\text{-}H}$ = 7.0 Hz). ^{31}P {^{1}H} NMR (C_6D_6, 161.90 MHz, 298.1 K): δ 30.67. ^{13}C {^{1}H} NMR (C_6D_6, 100.576 MHz, 298.1 K): δ 155.76 (d, $^2J_{C\text{-}P}$ = 7.9 Hz, Ar*C*), 144.65 (Ar*C*), 144.46 (Ar*C*), 136.9 (Ar*C*), 125.50 (Ar*C*), 123.19 (Ar*C*), 120.75 (d, $^3J_{C\text{-}P}$ = 4.5 Hz, 2Ar*C*), 119.53 (Ar*C*), OTf not resolved due to overlap with C_6D_6, 75.52 (2 x -*C*H$_2$-NMe$_2$), 62.55 (d, $^2J_{C\text{-}P}$ = 7.0 Hz, PO*C*H$_2$), 53.55 (2 x –N*Me$_2$*), 36.70 (d, $^2J_{C\text{-}P}$ = 16.1 Hz, PCH$_2$*C*H$_2$), 25.65 (d, $^1J_{C\text{-}P}$ = 141.0 Hz, P*C*H$_2$), 24.70 (d, $^3J_{C\text{-}P}$ = 4.9 Hz, PCH$_2$CH$_2$*C*H$_2$), 16.20 (d, $^3J_{C\text{-}P}$ = 5.4 Hz, *C*H$_3$). ^{19}F {^{1}H} NMR (C_6D_6, 376.270 MHz, 298.1 K): δ -77.79 (OTf$^-$). MS (MALDI) for $C_{24}H_{35}F_3N_3O_9PPtS$ (M, 824.1431): *m/z* 657.1041 **[1]$^+$** (calc. 657.1805), 642.1120 **[1-Me]$^+$** (calc. 642.1571). Anal. calcd. for $C_{24}H_{35}F_3N_3O_9PPtS$: C 34.95, H 4.28, N 5.10, P 3.76. Found: C 34.90, H 4.26, N 5.18, P 3.67.

Inhibition of cutinase with [1-OH$_2$][OTf] for ^{31}P NMR studies: The published inhibition protocol[30] was slightly modified: A solution of **[1-OH$_2$][OTf]** in MeCN (53.0 μL, 100 mM, 5.2960 μmol, 4 eq.) was added to a buffer solution (125 mM Tris, pH 8.0) of cutinase mutant N172K (2.0369 mM, 1.3240 μmol, 650 μL, 1 eq.). The yellow solution was left at room temperature during 4 hours and then stored in the fridge overnight. The solution was dialysed three times with buffer (3 x 400 mL, 125 mM Tris, pH 8.0) at RT during 24 hours. The contents of the Slide-A-Lyzer™ dialysis cassettes were transferred into a NMR tube and used directly for the NMR titration. ^{31}P {^{1}H} NMR (D_2O, 161.90 MHz, 298.1 K): δ 28.72 (EtO-P(O)-O-).

Inhibition of cutinase with [1-OH$_2$][OTf] for ESI-MS studies: The published inhibition protocol[30] was slightly modified: A solution of **[1-OH$_2$][OTf]** in MeCN (41.54 μL, 50 mM, 2.0733 μmol, 2.5 eq.) was added to a buffer solution (125 mM Tris, pH 8.0, acidified with HBF_4) of cutinase mutant N172K (0.25 mM, 0.8293 μmol, 3.3173 mL, 1.0 eq.). The yellow solution was left at room temperature during 1.5 hours and then dialysed twice with buffer (2 x 400 mL, 150 mM NH_4Ac) at RT during 24 hours. MS (ES+; H_2O): *m/z* 21134.76 **[cut-1]$^+$** (calc. 21137.46).

Titration of [2-OH$_2$][OTf] with Na$_3$[3] in D$_2$O: These experiments were performed in NMR tubes. To solutions of pincer complex **[2-OH$_2$][OTf]** (0.0204 M, 350 μL, 7.14 μmol) in D_2O were added different equivalents of a freshly prepared solution of **Na$_3$[3]** (0.3350 M) in D_2O (0.1 eq.: 2.1 μL, 0.5 eq.: 10.7 μL, 1.0 eq.: 21.3 μL, 1.5 eq.: 32.0 μL, 2.0 eq.: 42.6 μL, 5.0 eq.: 107.0 μL). After equilibration (5 minutes), the solutions were analysed by ^{31}P NMR spectroscopy. ^{31}P {^{1}H} NMR (D_2O, 161.90 MHz, 298.1 K): 0.1 eq of **Na$_3$[3]**: δ 30.59 ($^1J_{P\text{-}Pt}$ = 2110.3 Hz). 0.5 eq of **Na$_3$[3]**: δ 34.51 (P=O), 30.63 ($^1J_{P\text{-}Pt}$ = 2108.7 Hz). 1.0 eq of **Na$_3$[3]**: δ 34.51 (P=O), 30.65 ($^1J_{P\text{-}Pt}$ = 2117.8 Hz). 1.5 eq of **Na$_3$[3]**: δ 34.57 (P=O), 30.65 ($^1J_{P\text{-}Pt}$ = 2110.3 Hz), 22.84 (d, $^2J_{P\text{-}P}$ = 14.9 Hz, $^1J_{P\text{-}Pt}$ = 1604.3 Hz), 10.67 (d, $^2J_{P\text{-}P}$ = 13.3 Hz, $^1J_{P\text{-}Pt}$ = 3913.7 Hz); product ratio based on integrals: 30.65 (51%), 22.84 (28%), 10.67 (21%). 2.0 eq of **Na$_3$[3]**: 34.59 (P=O), 30.65 ($^1J_{P\text{-}Pt}$ = 2141.4 Hz), 22.87 (d, $^2J_{P\text{-}P}$ = 14.9 Hz, $^1J_{P\text{-}Pt}$ = 1611.7 Hz), 10.70 (d, $^2J_{P\text{-}P}$ = 13.3 Hz, $^1J_{P\text{-}Pt}$ = 3928.6 Hz), -5.55 (free phosphine); product ratio based on integrals: 30.65 (16%), 22.87 (45%), 10.70 (36%), -5.55 (3%). 5.0 eq of **Na$_3$[3]**: 34.56 (P=O), 22.88 (d, $^2J_{P\text{-}P}$ = 14.9 Hz, $^1J_{P\text{-}Pt}$ = 1614.9 Hz), 10.72 (d, $^2J_{P\text{-}P}$ = 13.3 Hz, $^1J_{P\text{-}Pt}$ = 3929.6 Hz), -5.67 (free phosphine); product ratio based on integrals: 22.88 (31%), 10.72 (24%), -5.67 (45%).
After 48 h, the solutions were analysed again. ^{31}P {^{1}H} NMR (D_2O, 161.90 MHz, 298.1 K): 0.1 eq of **Na$_3$[3]**: 30.60 ($^1J_{P\text{-}Pt}$ = 2141.4 Hz). 0.5 eq of **Na$_3$[3]**: 34.54 (P=O), 30.67 ($^1J_{P\text{-}Pt}$ = 2101.1 Hz). 1.0 eq of **Na$_3$[3]**: 34.51 (P=O), 30.65 ($^1J_{P\text{-}Pt}$ = 2112.9 Hz). 1.5 eq of **Na$_3$[3]**: 34.56 (P=O), 30.65 ($^1J_{P\text{-}Pt}$ = 2117.6 Hz), 23.80 ($^1J_{P\text{-}Pt}$ = 3173.2 Hz), 22.74 (d, $^2J_{P\text{-}P}$ = 13.8 Hz, $^1J_{P\text{-}Pt}$ = 1617.5 Hz), 10.58 (br s, $^1J_{P\text{-}Pt}$ = 3887.8 Hz); product ratio based on integrals: 30.65 (47%), 23.80 (19%), 22.74 (21%), 10.58 (13%). 2.0 eq of **Na$_3$[3]**: 34.59 (P=O), 30.65 ($^1J_{P\text{-}Pt}$ = 2090.9 Hz),

23.85 ($^1J_{P\text{-}Pt}$ = 3159.6 Hz), 22.80 (d, $^2J_{P\text{-}P}$ = 14.2 Hz, $^1J_{P\text{-}Pt}$ = 1613.8 Hz), 10.68 (br s, $^1J_{P\text{-}Pt}$ = 3918.6 Hz); product ratio based on integrals: 30.65 (16%), 23.85 (18%), 22.80 (36%), 10.68 (29%). 5.0 eq of **Na_3[3]**: 34.53 (P=O), 23.94 ($^1J_{P\text{-}Pt}$ not resolved), 22.84 (d, $^2J_{P\text{-}P}$ = 14.9 Hz, $^1J_{P\text{-}Pt}$ = 1611.7 Hz), 10.69 (d, $^2J_{P\text{-}P}$ = 13.1 Hz, $^1J_{P\text{-}Pt}$ = 3946.6 Hz), -5.54 (free phosphine); product ratio based on integrals: 23.94 (0%), 22.84 (28%), 10.69 (22%), -5.54 (50%).

Titration of [cut-1-OH_2][OTf] with Na_3[3] in Tris: These experiments were performed in a NMR tube. To a solution of cutinase-pincer hybrid **[cut-1-OH_2][OTf]** (2.0369 mM, 350 μL, 0.7129 μmol) in Tris buffer (125 mM, pH 8.0, acidified with HBF_4) were added D_2O (35 μL) and different aliquots of a freshly prepared solution of **Na_3[3]** (0.0361 M) in D_2O (3 portions of 9.9 μL, 0.3565 μmol, 0.5 eq. each). After equilibration (5 minutes), the solutions were analysed by ^{31}P NMR spectroscopy. $^{31}P\{^1H\}$ NMR (D_2O, 161.90 MHz, 298.1 K): δ 0.5 eq of **Na_3[3]**: 34.20 (P=O), 30.76, 28.72 (EtO-P(O)-O-), 8.83 ($^1J_{P\text{-}Pt}$ not resolved). 1.0 eq of **Na_3[3]**: 34.34 (P=O), 28.45 (EtO-P(O)-O-), 8.82 ($^1J_{P\text{-}Pt}$ = 3977.9 Hz), -5.65 (free phosphine). 1.5 eq of **Na_3[3]**: 34.37 (P=O), 28.46 (EtO-P(O)-O-), 8.82 ($^1J_{P\text{-}Pt}$ = 3962.0 Hz), -5.66 (free phosphine).

Titration of [cut-1-OH_2][OTf] with Na_3[3] for ESI-MS studies: To solutions of **[cut-1-OH_2][OTf]** (0.2500 mM, 25 μL, 0.0063 μmol) in NH_4Ac (150 mM) were added different equivalents of a freshly prepared solution of **Na_3[3]** (2.5685 mM) in MQ-H_2O (0.5 eq.: 1.2 μL, 1.0 eq.: 2.4 μL, 1.5 eq.: 3.6 μL, 2.0 eq.: 4.9 μL). After dilution (10x or 100x), the solutions were injected into the ESI mass spectrometer.
0.5 eq of **Na_3[3]** (10x diluted): MS (ES+; H_2O): *m/z* 21680.00 **HNa_2[cut-1-3]$^+$** (calc. 21682.38), 21658.00 **H_2Na[cut-1-3]$^+$** (calc. 21659.39), 21636.00 **H_3[cut-1-3]$^+$** (calc. 21636.40), 21134.76 **[cut-1]$^+$** (calc. 21137.46).
1.0 eq of **Na_3[3]** (10x diluted): *m/z* 21637.37 **H_3[cut-1-3]$^+$** (calc. 21636.40), 22158.00 **H_2Na[cut-1-3]$^+$** (calc. 22158.33).
1.0 eq of **Na_3[3]** (100x diluted): *m/z* 21637.37 **H_3[cut-1-3]$^+$** (calc. 21636.40).
1.5 eq of **Na_3[3]** (10x diluted): *m/z* 21637.37 **H_3[cut-1-3]$^+$** (calc. 21636.40), 22158.00 **H_2Na[cut-1-3]$^+$** (calc. 22158.33).
2.0 eq of **Na_3[3]** (10x diluted): *m/z* 21637.37 **H_3[cut-1-3]$^+$** (calc. 21636.40), 22158.00 **H_2Na[cut-1-3]$^+$** (calc. 22158.33).

Control experiment with free cutinase and Na_3[3] for ESI-MS: To a solution of cutinase mutant N172K (0.2500 mM, 25 μL, 0.0063 μL) in NH_4Ac (150 mM) was added a solution of **Na_3[3]** (2.5685 mM) in MQ-H_2O. After dilution (10x or 100x), the solutions were injected into the ESI mass spectrometer. 10x diluted: *m/z* 20617.72 **[cut]$^+$** (calc. 20619.30), 21128.05 **H_3[cut-3]$^+$** (calc. 21118.24). 100x diluted: *m/z* 20617.72 **[cut]$^+$** (calc. 20619.30).

Preparative synthesis of Na_3[2-3][OTf]: To a solution of **[2-OH_2][OTf]** [39, 41] (200 mL, 0.5031 g, 0.9090 mmol, 1.0 eq.) in MQ-H_2O was added **Na_3[3]** (0.5167 g, 0.9090 mmol, 1.0 eq.). The colourless solution was stirred for 5 minutes, after which all volatiles were removed *in vacuo*, yielding a white solid (1.1107 g, 0.8865 mmol, 98 %). The ^{1}H NMR signals were assigned with the aid of ^{1}H COSY and ^{1}H NMR spectra; the ^{13}C NMR signals were assigned with the aid of APT spectra. ^{1}H NMR (D_2O, 399.942 MHz, 298.1 K): δ 8.43 (d, 3H, 3 x ArC*H*(2), $^3J_{P-H}$ = 12.0 Hz), 7.92 (d, 3H, 3 x ArC*H*(6), $^3J_{H-H}$ = 7.6 Hz), 7.87 (dd, 3H, 3 x ArC*H*(4), $^3J_{P-H}$ = 9.6 Hz, $^3J_{H-H}$ = 7.6 Hz), 7.63 (dd, 3H, 3 x ArC*H*(5), $^3J_{H-H}$ = 7.6 Hz, $^3J_{H-H}$ = 7.6 Hz), 7.12 (t, 1H, PtArC*H*(4), $^3J_{H-H}$ = 7.2 Hz), 7.01 (d, 2H, 2 x PtArC*H*(3,5), $^3J_{H-H}$ = 7.2 Hz), 4.12 (br s, 4H, 2 x –CH_2, $^3J_{Pt-H}$ not resolved), 2.37 (br s, 12H, 2 x –N(CH_3)$_2$, $^3J_{Pt-H}$ not resolved). ^{31}P {^{1}H} NMR (D_2O, 161.90 MHz, 298.1 K): δ 34.39 (P=O), 30.63 ($^1J_{P-Pt}$ = 2103.4 Hz); product ratio based on integrals: 34.39 (1%), 30.63 (99%). ^{13}C {^{1}H} NMR (D_2O, 100.577 MHz, 298.1 K): δ 144.9 (3 x Ar*C*(1)), 144.1 (d, 3 x Ar*C*(2), $^2J_{P-C}$ = 11.3 Hz), 136.9 (d, 3 x Ar*C*(4), $^2J_{P-C}$ = 9.8 Hz), 131.8 (d, 3 x Ar*C*(3), $^1J_{P-C}$ = 18.0 Hz), 131.5 (PtAr*C*(1)), 131.1 (PtAr*C*(2,6)), 130.8 (d, 3 x Ar*C*(5) or Ar*C*(6), J_{P-C} = 8.6 Hz), 128.9 (PtAr*C*(3,5)), 127.1 (PtAr*C*(4)), 120.0 (d, 3 x Ar*C*(5) or Ar*C*(6), J_{P-C} = 4.5 Hz), 119.8 (q, OTf, $^1J_{C-F}$ = 317.2 Hz), 79.71 (2 x *C*H_2), 54.69 (2 x N(*C*H_3)$_2$). ^{19}F {^{1}H} NMR (D_2O, 376.27 MHz, 298.1 K): δ -79.26 (OTf^-). MS (ES+; H_2O): *m/z* 954.10 **Na_3[2-3]$^+$** (calc. 954.03), 932.12 **Na_2H[2-3]$^+$** (calc. 932.04), 910.13 **NaH_2[2-3]$^+$** (calc. 910.06), 888.16 **H_3[2-3]$^+$** (calc. 888.08). Anal. calcd. for $C_{31}H_{31}F_3N_2Na_3O_{12}PPtS_4$: C 33.73, H 2.83, N 2.54, P 2.81. Found: C 33.62, H 2.80, N 2.56, P 2.76.

Crystallization of Na_3[2-3][OTf] from CH_2Cl_2/H_2O and X-ray Crystal Structure Determination: A concentrated solution of **Na_3[2-3][OTf]** in MQ-H_2O was left standing in air (RT). After 5 days droplets of CH_2Cl_2 were carefully added and the mixture was left standing for 10 more days (RT), after which colourless crystals had been formed, which were floating at the CH_2Cl_2/H_2O interface. $[C_{12}H_{21}N_2OPt]_2^+$ $[C_{30}H_{31}N_2O_9PtS_3]^{2-}$ · $3H_2O$, Fw = 1748.65, colourless plate, 0.27 x 0.15 x 0.06 mm^3, triclinic, $P\bar{1}$ (no. 2), a = 11.1503(1), b = 12.3898(1), c = 23.9191(3) Å, α = 92.8724(4), β = 90.6454(4), γ = 113.0244(6)°, V = 3035.65(5) Å^3, Z = 2, D_x = 1.913 g/cm^3, μ = 7.09 mm^{-1}. 48549 Reflections were measured on a Nonius KappaCCD diffractometer with rotating anode (graphite monochromator, λ = 0.71073 Å) up to a resolution of $(\sin\theta/\lambda)_{max}$ = 0.65 Å^{-1} at a temperature of 150(2) K. Intensity integration was performed with HKL2000.[61] The SADABS[62] program was used for absorption correction and scaling based on multiple measured reflections (0.18-0.65 correction range). 13868 Reflections were unique (R_{int} = 0.048), of which 10908 were observed [I>2σ(I)]. The structure was solved with Direct Methods using the program SHELXS-97[63] and refined with SHELXL-97[63] against F^2 of all reflections. Non hydrogen atoms were refined with anisotropic displacement parameters. Hydrogen atoms were introduced in calculated positions and refined with a riding model. 742 Parameters were refined with no restraints. R1/wR2 [I > 2σ(I)]: 0.0339 /

0.0640. R1/wR2 [all refl.]: 0.0548 / 0.0701. S = 1.034. Residual electron density between -1.09 and 1.78 e/Å^3. Geometry calculations and checking for higher symmetry was performed with the PLATON program.[64]

Size exclusion chromatography with Na$_3$[2-3][OTf]: A solution (1 mL) of **Na$_3$[2-3][OTf]** (0.0615 g, 0.0557 mmol) was chromatographed over a column of pre-swollen Sephadex™ LH-20 beads (eluent: MQ-H_2O, column length: 18 cm, Ø: 1 cm, 21 fractions collected). The fractions with UV active compound were combined (fractions 2-6) and evaporated *in vacuo* (0.0558 g, 0.0505 mmol, 91%). ^{1}H NMR (D_2O, 399.942 MHz, 298.1 K): δ 8.42 (d, 3H, 3 x ArC*H*(2), $^3J_{P-H}$ = 11.6 Hz), 7.93 (d, 3H, 3 x ArC*H*(6), $^3J_{H-H}$ = 8.0 Hz), 7.87 (dd, 3H, 3 x ArC*H*(4), $^3J_{P-H}$ = 10.2 Hz, $^3J_{H-H}$ = 7.4 Hz), 7.63 (dd, 3H, 3 x ArC*H*(5), $^3J_{H-H}$ = 7.4 Hz, $^3J_{H-H}$ = 8.0 Hz), 7.11 (t, 1H, PtArC*H*(4), $^3J_{H-H}$ = 7.2 Hz), 7.01 (d, 2H, 2 x PtArC*H*(3,5), $^3J_{H-H}$ = 7.2 Hz), 4.11 (br s, 4H, 2 x –CH_2, $^3J_{Pt-H}$ not resolved), 2.37 (br s, 12H, 2 x –N(CH_3)$_2$, $^3J_{Pt-H}$ not resolved). ^{31}P {^{1}H} NMR (D_2O, 161.90 MHz, 298.1 K): δ 34.25 (P=O), 30.59 ($^1J_{P-Pt}$ = 2106.5 Hz); product ratio based on integrals: 34.25 (3%), 30.59 (97%). ^{19}F {^{1}H} NMR (D_2O, 376.27 MHz, 298.1 K): δ -79.21 (OTf^-).

VT NMR study with preparatively synthesized Na$_3$[2-3][OTf] in D_2O: This experiment was performed in a NMR tube. To compound **Na$_3$[2-3][OTf]** (0.0048 g, 4.3484 μmol) was added D_2O (350 μL). After equilibration (5 minutes), the solution was analysed by ^{31}P NMR spectroscopy. ^{31}P {^{1}H} NMR (D_2O, 121.48 MHz, 298.1 K): δ 34.53 (P=O), 30.67 ($^1J_{P-Pt}$ = 2097.6 Hz). Directly after, the mixture was heated to 80°C during 55 minutes. After equilibration (5 minutes at 80°C), the solution was analysed again: ^{31}P {^{1}H} NMR (D_2O, 121.48 MHz, 353.1 K): δ 33.61 (P=O), 31.30 ($^1J_{P-Pt}$ = 2097.1 Hz). After 2h, the solution was analysed again: ^{31}P {^{1}H} NMR (D_2O, 121.48 MHz, 353.1 K): δ 33.55 (P=O), 31.27 ($^1J_{P-Pt}$ = 2093.8 Hz). Finally, the tube was stored at RT for 19 days, after which the mixture was analyzed again: ^{31}P {^{1}H} NMR (D_2O, 161.90 MHz, 298.1 K): δ 34.53 (P=O), 30.66 ($^1J_{P-Pt}$ = 2102.4 Hz).

Addition of 0.5 equivalents of Na$_3$[3] to preparatively synthesized Na$_3$[2-3][OTf]: This experiment was performed in a NMR tube. To a solution of **Na$_3$[2-3][OTf]** (5.0278 μmol, 0.0144 M, 350 μL) in D_2O was added a solution of **Na$_3$[3]** (2.5139 μmol, 0.1120 M, 22.4 μL) in D_2O. After equilibration (5 minutes), the solution was analysed by ^{31}P NMR spectroscopy. ^{31}P {^{1}H} NMR (D_2O, 121.48 MHz, 298.1 K): δ 34.58 (P=O), 30.66 ($^1J_{P-Pt}$ = 2112.0 Hz), 23.81 ($^1J_{P-Pt}$ not resolved), 22.72 (br s, $^1J_{P-Pt}$ = 1600.7 Hz), 10.58 (br s, $^1J_{P-Pt}$ = 3955.5 Hz), -5.66 (free phosphine). product ratio based on integrals: 34.58 (2%), 30.66 (55%), 23.81 (3%), 22.72 (21%), 10.58 (15%), -5.66 (5%). After 20h, the solution was analysed again: ^{31}P {^{1}H} NMR (D_2O, 121.48 MHz, 298.1 K): δ 34.58 (P=O), 30.66 ($^1J_{P-Pt}$ = 2113.9 Hz), 23.79 ($^1J_{P-Pt}$ not resolved), 22.73 (d, $^2J_{P-P}$ = 14.9 Hz, $^1J_{P-Pt}$ = 1636.0 Hz), 10.64 (br s, $^1J_{P-Pt}$ = 3878.4 Hz); product ratio based on integrals: 34.58 (4%), 30.66

(57%), 23.79 (7%), 22.73 (19%), 10.64 (13%). After 1 more day, the solution was analysed again: ^{31}P {^{1}H} NMR (D_2O, 121.48 MHz, 298.1 K): δ 34.58 (P=O), 30.66 ($^{1}J_{P\text{-}Pt}$ = 2105.5 Hz), 23.77 ($^{1}J_{P\text{-}Pt}$ not resolved), 22.70 (d, $^{2}J_{P\text{-}P}$ = 15.4 Hz, $^{1}J_{P\text{-}Pt}$ = 1620.3 Hz), 10.61 (br s, $^{1}J_{P\text{-}Pt}$ = 3904.7 Hz); product ratio based on integrals: 34.58 (9%), 30.66 (57%), 23.77 (6%), 22.70 (19%), 10.61 (9%).

Titration of [2-OH$_2$][OTf] with Na$_3$[3] in Tris: These experiments were performed in NMR tubes. To solutions of pincer complex **[2-OH$_2$][OTf]** (0.0190 M, 350 μL, 6.66 μmol) in Tris buffer (125 mM, pH 8.0, acidified with HBF_4) were added D_2O (35 μL) and different equivalents of a freshly prepared solution of **Na$_3$[3]** (0.3549 M) in D_2O (0.1 eq.: 1.9 μL, 0.5 eq.: 9.4 μL, 1.0 eq.: 18.8 μL, 1.5 eq.: 28.2 μL, 2.0 eq.: 37.5 μL, 5.0 eq.: 93.9 μL). After equilibration (5 minutes), the solutions were analysed by ^{31}P NMR spectroscopy. ^{31}P {^{1}H} NMR (D_2O, 161.90 MHz, 298.1 K): 0.1 eq of **Na$_3$[3]**: 30.62 ($^{1}J_{P\text{-}Pt}$ = 2090.8 Hz). 0.5 eq of **Na$_3$[3]**: 34.23 (P=O), 30.63 ($^{1}J_{P\text{-}Pt}$ = 2106.1 Hz). 1.0 eq of **Na$_3$[3]**: 34.31 (P=O), 30.61 ($^{1}J_{P\text{-}Pt}$ = 2105.0 Hz), 22.13 (br s, $^{1}J_{P\text{-}Pt}$ not resolved), 10.09 (br s, $^{1}J_{P\text{-}Pt}$ not resolved), 8.54 ($^{1}J_{P\text{-}Pt}$ not resolved); product ratio based on integrals: 30.61 (73%), 22.13 (13%), 10.09 (10%), 8.54 (3%). 1.5 eq of **Na$_3$[3]**: 34.39 (P=O), 30.64 ($^{1}J_{P\text{-}Pt}$ = 2105.5 Hz), 22.13 (d, $^{2}J_{P\text{-}P}$ = 14.2 Hz, $^{1}J_{P\text{-}Pt}$ = 1641.3 Hz), 10.08 (br s, $^{1}J_{P\text{-}Pt}$ = 3845.4 Hz), 8.57 ($^{1}J_{P\text{-}Pt}$ = 4149.0 Hz); product ratio based on integrals: 30.64 (19%), 22.13 (38%), 10.09 (30%), 8.54 (13%). 2.0 eq of **Na$_3$[3]**: 34.42 (P=O), 30.64 ($^{1}J_{P\text{-}Pt}$ = 2078.8 Hz), 22.13 (d, $^{2}J_{P\text{-}P}$ = 14.2 Hz, $^{1}J_{P\text{-}Pt}$ = 1635.7 Hz), 10.15 (br s, $^{1}J_{P\text{-}Pt}$ = 3863.6 Hz), 8.56 ($^{1}J_{P\text{-}Pt}$ = 4005.5 Hz), -5.66 (free phosphine); product ratio based on integrals: 30.64 (3%), 22.13 (37%), 10.15 (28%), 8.56 (18%), -5.66 (13%). 5.0 eq of **Na$_3$[3]**: 34.40 (P=O), 22.09 (br s, $^{1}J_{P\text{-}Pt}$ = 1637.8 Hz), 10.09 (br s, $^{1}J_{P\text{-}Pt}$ = 3825.0 Hz), 8.50 ($^{1}J_{P\text{-}Pt}$ = 4020.3 Hz), -5.70 (free phosphine); product ratio based on integrals: 22.09 (11%), 10.09 (7%), 8.50 (12%), -5.70 (69%).
After 24 h, the solutions were analysed again. ^{31}P {^{1}H} NMR (D_2O, 161.90 MHz, 298.1 K): 0.1 eq of **Na$_3$[3]**: 30.63 ($^{1}J_{P\text{-}Pt}$ = 2067.0 Hz), 8.56 ($^{1}J_{P\text{-}Pt}$ = 4010.2 Hz); product ratio based on integrals: 30.63 (59%), 8.56 (41%). 0.5 eq of **Na$_3$[3]**: 34.25 (P=O), 30.64 ($^{1}J_{P\text{-}Pt}$ = 2107.6 Hz), 8.56 ($^{1}J_{P\text{-}Pt}$ = 4007.0 Hz); product ratio based on integrals: 30.63 (66%), 8.56 (34%). 1.0 eq of **Na$_3$[3]**: 34.31 (P=O), 30.61 ($^{1}J_{P\text{-}Pt}$ = 2099.8 Hz), 22.03 (br s, $^{1}J_{P\text{-}Pt}$ not resolved), 10.01 (br s, $^{1}J_{P\text{-}Pt}$ not resolved), 8.54 ($^{1}J_{P\text{-}Pt}$ = 4012.8 Hz); product ratio based on integrals: 30.61 (53%), 22.03 (12%), 10.01 (7%), 8.54 (28%). 1.5 eq of **Na$_3$[3]**: 34.41 (P=O), 30.64 ($^{1}J_{P\text{-}Pt}$ = 2103.4 Hz), 22.13 (d, $^{2}J_{P\text{-}P}$ = 12.9 Hz, $^{1}J_{P\text{-}Pt}$ = 1641.8 Hz), 10.06 (br s, $^{1}J_{P\text{-}Pt}$ = 3830.5 Hz), 8.57 ($^{1}J_{P\text{-}Pt}$ = 4010.2 Hz); product ratio based on integrals: 30.64 (25%), 22.12 (27%), 10.09 (22%), 8.57 (26%). 2.0 eq of **Na$_3$[3]**: 34.45 (P=O), 30.64 ($^{1}J_{P\text{-}Pt}$ not resolved), 22.14 (d, $^{2}J_{P\text{-}P}$ = 14.2 Hz, $^{1}J_{P\text{-}Pt}$ = 1634.0 Hz), 10.14 (br s, $^{1}J_{P\text{-}Pt}$ = 3861.3 Hz), 8.56 ($^{1}J_{P\text{-}Pt}$ = 4009.1 Hz); product ratio based on integrals: 30.64 (0%), 22.14 (40%), 10.14 (30%), 8.56 (29%). 5.0 eq of **Na$_3$[3]**: 34.40 (P=O), 22.09 (d, $^{2}J_{P\text{-}P}$ = 14.9 Hz, $^{1}J_{P\text{-}Pt}$ = 1623.4 Hz), 10.16 (br s, $^{1}J_{P\text{-}Pt}$ = 3878.1 Hz), 8.50 ($^{1}J_{P\text{-}Pt}$ = 3999.2

Hz), -5.68 (free phosphine); product ratio based on integrals: 22.09 (10%), 10.16 (8%), 8.53 (12%), -5.68 (70%).
After another 24h, the solutions were analysed again. ^{31}P {^{1}H} NMR (D_2O, 161.90 MHz, 298.1 K): 0.1 eq of **Na_3[3]**: 30.62 ($^{1}J_{P\text{-}Pt}$ = 2084.3 Hz), 8.55 ($^{1}J_{P\text{-}Pt}$ = 4014.6 Hz); product ratio based on integrals: 30.62 (30%), 8.55 (70%). 0.5 eq of **Na_3[3]**: 34.25 (P=O), 30.63 ($^{1}J_{P\text{-}Pt}$ = 2097.6 Hz), 8.56 ($^{1}J_{P\text{-}Pt}$ = 4014.9 Hz); product ratio based on integrals: 30.63 (47%), 8.56 (53%). 1.0 eq of **Na_3[3]**: 34.32 (P=O), 30.61 ($^{1}J_{P\text{-}Pt}$ = 2118.1 Hz), 22.12 (br s, $^{1}J_{P\text{-}Pt}$ not resolved), 9.99 (br s, $^{1}J_{P\text{-}Pt}$ not resolved), 8.54 ($^{1}J_{P\text{-}Pt}$ = 4005.5 Hz); product ratio based on integrals: 30.61 (38%), 22.12 (7%), 9.99 (7%), 8.54 (47%). 1.5 eq of **Na_3[3]**: 34.42 (P=O), 30.64 ($^{1}J_{P\text{-}Pt}$ = 2095.9 Hz), 22.12 (d, $^{2}J_{P\text{-}P}$ = 14.2 Hz, $^{1}J_{P\text{-}Pt}$ = 1640.2 Hz), 10.07 (br s, $^{1}J_{P\text{-}Pt}$ = 3871.0 Hz), 8.57 ($^{1}J_{P\text{-}Pt}$ = 4006.5 Hz); product ratio based on integrals: 30.64 (23%), 22.12 (24%), 10.07 (18%), 8.57 (36%). 2.0 eq of **Na_3[3]**: 34.46 (P=O), 30. 64 ($^{1}J_{P\text{-}Pt}$ not resolved), 22.14 (d, $^{2}J_{P\text{-}P}$ = 14.4 Hz, $^{1}J_{P\text{-}Pt}$ = 1642.9 Hz), 10.13 (br s, $^{1}J_{P\text{-}Pt}$ = 3872.9 Hz), 8.57 ($^{1}J_{P\text{-}Pt}$ = 4010.9 Hz); product ratio based on integrals: 30.65 (2%), 22.14 (40%), 10.13 (30%), 8.57 (28%). 5.0 eq of **Na_3[3]**: 34.40 (P=O), 22.09 (d, $^{2}J_{P\text{-}P}$ = 14.2 Hz, $^{1}J_{P\text{-}Pt}$ = 1650.4 Hz), 10.16 (br s, $^{1}J_{P\text{-}Pt}$ = 3877.2 Hz), 8.53 ($^{1}J_{P\text{-}Pt}$ = 4010.9 Hz), -5.68 (free phosphine); product ratio based on integrals: 22.09 (11%), 10.16 (6%), 8.53 (13%), -5.68 (70%).
After 17 more days the solutions were analysed again. ^{31}P {^{1}H} NMR (D_2O, 161.90 MHz, 298.1 K): 0.1 eq of **Na_3[3]**: 8.56 ($^{1}J_{P\text{-}Pt}$ = 4015.6 Hz). 0.5 eq of **Na_3[3]**: 34.33 (P=O), 8.57 ($^{1}J_{P\text{-}Pt}$ = 4004.4 Hz). 1.0 eq of **Na_3[3]**: 34.40 (P=O), 8.55 ($^{1}J_{P\text{-}Pt}$ = 4009.3 Hz). 1.5 eq of **Na_3[3]**: 34.49 (P=O), 22.10 (d, $^{2}J_{P\text{-}P}$ = 15.4 Hz, $^{1}J_{P\text{-}Pt}$ = 1628.1 Hz), 10.12 (d, $^{2}J_{P\text{-}P}$ = 13.0 Hz, $^{1}J_{P\text{-}Pt}$ = 3814.3 Hz), 8.57 ($^{1}J_{P\text{-}Pt}$ = 4007.0 Hz); product ratio based on integrals: 22.10 (19%), 10.12 (11%), 8.57 (70%). 2.0 eq of **Na_3[3]**: 34.50 (P=O), 22.10 (d, $^{2}J_{P\text{-}P}$ = 14.7 Hz, $^{1}J_{P\text{-}Pt}$ = 1636.0 Hz), 10.12 (d, $^{2}J_{P\text{-}P}$ = 13.1 Hz, $^{1}J_{P\text{-}Pt}$ = 3864.5 Hz), 8.57 ($^{1}J_{P\text{-}Pt}$ = 4010.9 Hz); product ratio based on integrals: 22.10 (39%), 10.12 (27%), 8.57 (34%). 5.0 eq of **Na_3[3]**: 34.45 (P=O), 22.04 (d, $^{2}J_{P\text{-}P}$ = 14.4 Hz, $^{1}J_{P\text{-}Pt}$ = 1643.6 Hz), 10.17 (br s, $^{1}J_{P\text{-}Pt}$ = 3802.0 Hz), 8.53 ($^{1}J_{P\text{-}Pt}$ = 4000.0 Hz), -5.80 (free phosphine); product ratio based on integrals: 22.04 (11%), 10.17 (7%), 8.53 (14%), -5.80 (68%).

Coordination of ethanolamine to [2-OH_2][OTf] and crystallization of complex [2-NH_2-$(CH_2)_2$-OH][OTf]: This experiment was performed in a NMR tube. To **[2-OH_2][OTf]** (0.0116 g, 0.2096 mmol, 1.0 eq.) in D_2O (1.0 mL) was added ethanolamine (1.3 μL, 0.2096 mmol, 1.0 eq.). After 5 minutes a ^{1}H NMR spectrum was recorded. ^{1}H NMR (D_2O, 399.942 MHz, 298.1 K): 6.95 (t, 1H, ArC*H*(4), $^{3}J_{H\text{-}H}$ = 7.6 Hz), 6.81 (d, 2H, ArC*H*(3,5), $^{3}J_{H\text{-}H}$ = 7.6 Hz), 3.98 (s, 4H, 2 x –CH_2), 3.93 (br s), 3.65 (t, coord. HO-$(CH_2)_2$-NH_2, $^{3}J_{H\text{-}H}$ = 4.6 Hz), 3.45 (t, coord. HO-$(CH_2)_2$-NH_2, $^{3}J_{H\text{-}H}$ = 4.8 Hz), 2.93 (br s, coord. HO-$(CH_2)_2$-NH_2), 2.78 (s, 12H, 2 x NMe_2), 2.75 (br s), 2.62 (t, coord. HO-$(CH_2)_2$-NH_2, $^{3}J_{H\text{-}H}$ = 5.4 Hz). Slow evaporation of the solvent in air yielded crystals suitable for X-ray diffraction studies.

X-ray crystal structure determination of [2-NH_2-$(CH_2)_2$-OH][OTf]: $[C_{14}H_{26}N_3OPt]^+$ $(CF_3O_3S)^-$, Fw = 596.54, colourless block, 0.50 x 0.25 x 0.13 mm^3, triclinic, $P\overline{1}$ (no. 2), a = 9.1740(1), b = 10.3943(1), c = 11.6317(1) Å, α = 64.7206(6), β = 87.9559(5), γ = 83.6656(6)°, V = 996.746(17) $Å^3$, Z = 2, D_x = 1.988 g/cm^3, μ = 7.20 mm^{-1}. 18881 Reflections were measured on a Nonius KappaCCD diffractometer with rotating anode (graphite monochromator, λ = 0.71073 Å) up to a resolution of $(\sin\theta/\lambda)_{max}$ = 0.65 $Å^{-1}$ at a temperature of 150(2) K. Intensity integration was performed with HKL2000.[61] The SADABS[62] program was used for absorption correction and scaling based on multiple measured reflections (0.04-0.39 correction range). 4528 Reflections were unique (R_{int} = 0.038), of which 4465 were observed [$I>2\sigma(I)$]. The structure was solved with Direct Methods using the program SHELXS-97[63] and refined with SHELXL-97[63] against F^2 of all reflections. Non hydrogen atoms were refined with anisotropic displacement parameters. Hydrogen atoms were introduced in calculated positions and refined with a riding model. An extinction coefficient was included in the refinement resulting in a value of 0.0088(8). 249 Parameters were refined with no restraints. R1/wR2 [$I > 2\sigma(I)$]: 0.0304 / 0.0810. R1/wR2 [all refl.]: 0.0308 / 0.0812. S = 1.111. Residual electron density between -2.83 and 3.02 e/$Å^3$. Geometry calculations and checking for higher symmetry was performed with the PLATON program.[64]

NMR analysis of Na_3[3]: $^{31}P\{^1H\}$ NMR (D_2O, 161.90 MHz, 298.1 K): δ -5.66 $^{13}C\{^1H\}$ NMR (D_2O, 100.577 MHz, 298.1 K): δ 143.2 (d, 3 x Ar*C*(3), $^1J_{P\text{-}C}$ = 7.4 Hz), 136.8 (3 x Ar*C*(1)), 136.6 (d, 3 x Ar*C*(4) or Ar*C*(2), $^2J_{P\text{-}C}$ = 17.0 Hz), 130.4 (d, 3 x Ar*C*(2) or Ar*C*(4), $^1J_{P\text{-}C}$ = 23.2 Hz), 129.9 (d, 3 x Ar*C*(5), $J_{P\text{-}C}$ = 6.2 Hz), 120.0 (3 x Ar*C*(6)).

NMR analysis of [2-OH_2][OTf]: ^1H NMR (D_2O, 399.942 MHz, 298.1 K): δ 7.12 (t, 1H, PtArC*H*(4), $^3J_{H\text{-}H}$ = 7.2 Hz), 7.01 (d, 2H, 2 x PtArC*H*(3,5), $^3J_{H\text{-}H}$ = 7.2 Hz), 4.02 (br s, 4H, 2 x –CH_2, $^3J_{Pt\text{-}H}$ not resolved), 2.82 (br s, 12H, 2 x –N(CH_3)$_2$, $^3J_{Pt\text{-}H}$ not resolved). $^{13}C\{^1H\}$ NMR (D_2O, 100.58 MHz, 298.1 K): δ 144.8 (Ar*C*(4)), 134.1 (Ar*C*(1)), 125.1 (PtAr*C*(2.6)), 120.0 (Ar*C*(3,6)), 75.73 (2 x *C*H_2), 53.10 (2 x N(*C*H_3)$_2$).

Preparative synthesis of (O)P(C_6H_4(SO_3Na)-3)$_3$: To a solution of **Na_3[3]** (0.8810g, 1.5499 mmol, 1.0 eq.) in MQ-H_2O was added a H_2O_2 solution (35 wt%, 265.5 µL, 3.0998 mmol, 2.0 eq.). after stirring for 2h all volatiles were removed *in vacuo*, yielding a white solid (0.8877 g, 1.5189 mmol, 98 %). $^{31}P\{^1H\}$ NMR (D_2O, 161.90 MHz, 298.1 K): δ 34.64 (P=O).

Coordination test of (O)P(C_6H_4(SO_3Na)-3)$_3$ with [2-OH_2][OTf]: To a solution of **[2-OH_2][OTf]** (0.0801 g, 0.1447 mmol, 1.0 eq.) in MQ-H_2O was added solid (O)P(C_6H_4(SO_3Na)-3)$_3$ after stirring for 30 minutes all volatiles were removed *in*

vacuo yielding a white powder (0.1630 g). ^{31}P {^{1}H} NMR (D_2O, 161.90 MHz, 298.1 K): δ 34.21 (P=O).

Model study to investigate the coordination of Tris to [2-OH$_2$][OTf]: This experiment was performed in a NMR tube. To a solution of **[2-OH$_2$][OTf]** in D_2O (0.0108 M, 3.7943 μmol, 350 μL, 1.0 eq.) was added a solution of Tris (0.1329 M, 3.7943 μmol, 28.5 μL, 1.0 eq.). After mixing ^{1}H NMR spectra were recorded after 5 minutes and 1 day. After 18 days the mixture was heated to 90°C overnight, after which another ^{1}H NMR spectrum was taken.

Titration of [2-OH$_2$][OTf] with Na$_3$[4] in D$_2$O: These experiments were performed in NMR tubes. To solutions of pincer complex **[2-OH$_2$][OTf]** (0.0108 M, 350 μL, 3.78 μmol) in D_2O were added different equivalents of a freshly prepared solution of **Na$_3$[4]** (0.2628 M) in D_2O (0.1 eq.: 1.4 μL, 0.5 eq.: 7.2 μL, 1.0 eq.: 14.4 μL, 1.5 eq.: 21.7 μL, 2.0 eq.: 28.9 μL, 5.0 eq.: 72.2 μL). After equilibration (5 minutes), the solutions were analysed by ^{31}P NMR spectroscopy. ^{31}P {^{1}H} NMR (D_2O, 161.90 MHz, 298.1 K): 0.1 eq of **Na$_3$[4]**: δ 29.09 ($^{1}J_{P\text{-}Pt}$ not resolved). 0.5 eq of **Na$_3$[4]**: δ 29.10 ($^{1}J_{P\text{-}Pt}$ = 1994.8 Hz). 1.0 eq of **Na$_3$[4]**: δ 29.10 ($^{1}J_{P\text{-}Pt}$ = 1975.1 Hz). 1.5 eq of **Na$_3$[4]**: δ 29.09 ($^{1}J_{P\text{-}Pt}$ = 1985.7 Hz), -27.38 (free phosphine). 2.0 eq of **Na$_3$[4]**: 29.09 ($^{1}J_{P\text{-}Pt}$ = 1981.0 Hz), -27.47 (free phosphine). 5.0 eq of **Na$_3$[4]**: 40.69 (P=O), 29.09 ($^{1}J_{P\text{-}Pt}$ = 1979.9 Hz), -27.91 (free phosphine).
After 5 days, the solutions were analysed again. ^{31}P {^{1}H} NMR (D_2O, 161.90 MHz, 298.1 K): δ 0.1 eq of **Na$_3$[4]**: δ 29.09 ($^{1}J_{P\text{-}Pt}$ not resolved). 0.5 eq of **Na$_3$[4]**: δ 29.08 ($^{1}J_{P\text{-}Pt}$ = 1994.8 Hz). 1.0 eq of **Na$_3$[4]**: δ 29.09 ($^{1}J_{P\text{-}Pt}$ = 1978.9 Hz). 1.5 eq of **Na$_3$[4]**: δ 29.09 ($^{1}J_{P\text{-}Pt}$ = 1985.7 Hz), -27.38 (free phosphine). 2.0 eq of **Na$_3$[4]**: 29.09 ($^{1}J_{P\text{-}Pt}$ = 1986.4 Hz), -27.47 (free phosphine). 5.0 eq of **Na$_3$[4]**: 40.69 (P=O), 29.09 ($^{1}J_{P\text{-}Pt}$ = 1987.3 Hz), -27.91 (free phosphine).

Preparative synthesis of coordination complex Na$_3$[2-4][OTf]: A solution of **Na$_3$[4]** (62.4 mg, 0.0952 mmol) in degassed demiwater (5 mL) was added to a solution of **[2-OH$_2$][OTf]** (51.4 mg, 0.0929 mmol) in degassed demiwater (5 mL). The mixture was stirred at room temperature for 2 h and subsequently dried *in vacuo*, yielding the product as an off-white powder (0.1120 g, >99%). ^{1}H NMR (D_2O, 399.94 MHz, 298.1 K): δ 9.88 (d, 1H, PAr, $J_{H\text{-}P}$ = 18.0 Hz), 7.91 (d, 1H, PAr, $J_{H\text{-}P}$ = 4.4 Hz), 7.89 (d, 1H, PAr, $J_{H\text{-}P}$ = 3.6 Hz), 7.65 (d, 1H, PAr, $J_{H\text{-}P}$ = 4.4 Hz), 7.42 (d, 1H, PAr, $J_{H\text{-}P}$ = 2.0 Hz), 7.24 (d, 1H, PAr, $J_{H\text{-}P}$ = 4.4 Hz), 7.18 (d, 1H, NCN-ArC*H*(4), $^{3}J_{H\text{-}H}$ = 7.2 Hz), 7.12 (d, 2H, NCN-ArC*H*(3,5), $^{3}J_{H\text{-}H}$ = 7.2 Hz), 4.72 (d, 1H, -CH_2, $^{2}J_{H\text{-}H}$ = 14.0 Hz), 4.47 (d, 1H, -CH_2, $^{2}J_{H\text{-}H}$ = 14.0 Hz), 3.86 (d, 1H, -CH_2, $^{2}J_{H\text{-}H}$ = 14.4 Hz), 3.74 (d, 1H, -CH_2, $^{2}J_{H\text{-}H}$ = 14.0 Hz), 3.31 (s, 3H, PArCH_3), 2.99 (s, 3H, PArCH_3), 2.71 (s, 6H, -N(CH_3)$_2$), 2.59 (s, 3H, PArCH_3), 2.48 (s, 3H, PArCH_3), 2.40 (s, 3H, PArCH_3), 1.94 (s, 6H, -N(CH_3)$_2$), 1.70 (s, 3H, PArCH_3). Due to the complicated pattern in the ^{13}C {^{1}H} NMR spectrum, the peaks were not assigned. ^{31}P {^{1}H} NMR (D_2O, 161.90

MHz, 298.1 K): δ 29.08 (s, $^{1}J_{P\text{-}Pt}$ = 1942.0 Hz). MS (ES+; H_2O): *m/z* 1038.14 **Na_3[2-4]$^+$** (calc. 1038.12).

Titration of [2-OH_2][OTf] with [5](BF_4)$_3$ in D_2O: This experiment was performed in a NMR tube. To a solution of pincer complex **[2-OH_2][OTf]** (0.0177 M, 200 μL, 3.54 μmol) in D_2O were added different equivalents of a freshly prepared solution of **[5](BF_4)$_3$** (0.0101 M) in D_2O/MeCN (5/2) (0.5 eq.: 174.3 μL, 1.0 eq.: 348.7 μL, 2.0 eq.: 697.4 μL) After equilibration (5 minutes), the solutions were analysed by ^{31}P NMR spectroscopy. ^{31}P {^{1}H} NMR (D_2O, 161.90 MHz, 298.1 K): 0.5 eq of **[5](BF_4)$_3$**: δ 29.66 ($^{1}J_{P\text{-}Pt}$ not resolved). 1.0 eq of **[5](BF_4)$_3$**: δ 29.66 (s, $^{1}J_{P\text{-}Pt}$ not resolved), 18.15 (s, $^{1}J_{P\text{-}Pt}$ not resolved). 2.0 eq of **[5](BF_4)$_3$**: δ 29.67 (s, $^{1}J_{P\text{-}Pt}$ not resolved), 18.15 (s, $^{1}J_{P\text{-}Pt}$ not resolved), -0.2 (free phosphine).

Synthesis of coordination complex ([2]—[5])(BF_4)$_3$[OTf]: A solution of **[5](BF_4)$_3$** (66.1 mg, 0.0894 mmol) in degassed demiwater/MeCN (7 mL, 5/2 v/v) was added to a solution of **[2-OH_2][OTf]** (48.7 mg, 0.0880 mmol) in degassed demiwater (5 mL). The mixture was stirred at room temperature for 2 h and subsequently dried *in vacuo*, yielding the product as an off-white powder (0.1200 g, >99%). ^{1}H NMR (D_2O/CD_3CN (5/2 v/v), 299.95 MHz, 298.1 K): δ 8.42 (m, Ar), 8.2 (br. m, Ar), 8.08 (d, $^{3}J_{H,H}$ = 7.8 Hz, Ar), 7.49 (d, $^{3}J_{H,H}$ = 7.2 Hz, Ar), 7.37 (m, Ar), 7.19 (d, $^{3}J_{H,H}$ = 7.2 Hz, Ar), 6.85 (d, $^{3}J_{H,H}$ = 7.8 Hz, Ar), 4.85 (s, PArCH_2), 4.52 (s, NCN-ArCH_2), 4.42 (s, NCN-ArCH_2), 3.72 (s, NCN-ArCH_2), 3.40 (s, N(CH_3)$_3$), 3.29 (s, N(CH_3)$_2$), 2.79 (s, N(CH_3)$_2$). Due to the complicated pattern in the ^{13}C {^{1}H} NMR spectrum, the peaks were not assigned. ^{31}P {^{1}H} NMR (D_2O/CD_3CN (5/2 v/v), 121.42 MHz, 298.1 K): δ 39.78 (s, $^{1}J_{P\text{-}Pt}$ = 2068 Hz), 18.15 (s, $^{1}J_{P\text{-}Pt}$ = 3008 Hz). MS (ES+; MeCN): *m/z* 519.228 **[([2]—[5])(BF_4)$_2$]$^{2+}$** (calc. 519.230), 550.194 **[([2]—[5])(BF_4)[OTf]]$^{2+}$** (calc. 550.194).

References:

1. Banci, L.; Bertini, I.; Ciofi-Baffoni, S.; Katsari, E.; Katsaros, N.; Kubicek, K.; Mangani, S., *Proc. Nat. Acad. Sci.* **2005,** 102, 3994.
2. Banci, L.; Bertini, I.; Calderone, V.; Ciofi-Baffoni, S.; Mangani, S.; Martinelli, M.; Palumaa, P.; Wang, S., *Proc. Nat. Acad. Sci.* **2006,** 103, 8595.
3. Bertini, I.; Sigel, A.; Sigel, H., *Handbook on Metalloproteins*. Marcel Dekker: New York, 2001; p 1-1800.
4. Forzi, L.; Sawers, R. G., *Biometals* **2007,** 20, 565-578.
5. Creus, M.; Pordea, A.; Rossel, T.; Sardo, A.; Letondor, C.; Ivanova, A.; LeTrong, I.; Stenkamp, R. E.; Ward, T. R., *Angew. Chem. Int. Ed.* **2008,** 47, 1400-1404.
6. Yokoi, N.; Ueno, T.; Unno, M.; Matsui, T.; Ikeda-Sato, M.; Watanabe, Y., *Chem. Commun.* **2008**, 229-231.
7. Ueno, T.; Abe, S.; Yokoi, N.; Watanabe, Y., *Coord. Chem. Rev.* **2007,** 251, 2717-2731.
8. Ueno, T.; Koshiyama, T.; Abe, S.; Yokoi, N.; Ohashi, M.; Nakajima, H.; Watanabe, Y., *J. Organomet. Chem.* **2007,** 692, 142-147.
9. Ueno, T.; Norihiko, Y.; Abe, S.; Watanabe, Y., *J. Inorg. Biochem.* **2007,** 101, 1667-1675.
10. Satake, Y.; Abe, S.; Okazaki, S.; Ban, N.; Hikage, T.; Ueno, T.; Nakajima, H.; Suzuki, A.; Yamane, T.; Nishiyama, H.; Watanabe, Y., *Organometallics* **2007,** 26, 4904-4908.
11. Oshovsky, G. V.; Reinhoudt, D. N.; Verboom, W., *Angew. Chem. Int. Ed.* **2007,** 46, 2366.
12. Slim, M.; Sleiman, H. F., *Bioconjugate Chem.* **2004,** 15, 949-953.
13. Kam-Wing Lo, K.; Hui, W.-K.; Chun-Ming Ng, D., *J. Am. Chem. Soc.* **2002,** 124, 9344-9345.
14. Chen, P. R.; He, C., *Curr. Opin. Chem. Biol.* **2008,** 12, 214-221.
15. Wilson, M. E.; Whitesides, G. M., *J. Am. Chem. Soc.* **1978,** 100, 306-307.
16. Steinreiber, J.; Ward, T. R., *Coord. Chem. Rev.* **2008,** 252, 751.
17. Pierron, J.; Malan, C.; Creus, M.; Gradinaru, J.; Hafner, I.; Ivanova, A.; Sardo, A.; Ward, T. R., *Angew. Chem. Int. Ed.* **2008,** 47, 701-705.
18. Collot, J.; Gradinaru, J.; Humbert, N.; Skander, M.; Zocchi, A.; Ward, T. R., *J. Am. Chem. Soc.* **2003,** 125, 9030-9031.
19. Ohashi, M.; Koshiyama, T.; Ueno, T.; Yanase, M.; Fujii, H.; Watanabe, Y., *Angew. Chem. Int. Ed.* **2003,** 42, 1005-1008.
20. Carey, J. R.; Ma, S. K.; Pfister, T. D.; Garner, D. K.; Kim, H. K.; Abramite, J. A.; Wang, Z.; Guo, Z.; Lu, Y., *J. Am. Chem. Soc.* **2004,** 126, 10812-10813.
21. Panella, L.; Broos, J.; Jin, J.; Fraaije, M. W.; Janssen, D. B.; Jeronimus-Stratingh, M.; Feringa, B. L.; Minnaard, A. J.; De Vries, J. G., *Chem. Commun.* **2005,** 45, 5656-5658.
22. Gallagher, J.; Zelenko, O.; Walts, A. D.; Sigman, D. S., *Biochemistry* **1998,** 37, 2096-2104.
23. McNae, I. W.; Fishburne, K.; Habtemariam, A.; Hunter, T. M.; Melchart, M.; Wang, F.; Walkinshaw, M. D.; Sadler, P. J., *Chem. Commun.* **2004**, 1786-1787.
24. Chen, H.; Parkinson, J. A.; Morris, R. E.; Sadler, P. J., *J. Am. Chem. Soc.* **2003,** 125, 173-186.
25. Alberto, R., *Bioorganometallics*. Wiley-VCH: Weinheim, 2006; p 97-124.
26. Jaouen, G., *Bioorganometallics: Biomolecules, Labelling, Medicine*. Wiley-VCH: Weinheim, 2006; p 1-472.
27. Peterson, J. R.; Smith, T. A.; Thordarson, P., *Chem. Commun.* **2007**, 1899-1901.
28. Meggers, E., *Chem. Commun.* **2009**, 1001-1010.
29. Rutten, L.; Wieczorek, B.; Mannie, J.-P. B. A.; Kruithof, C. A.; Dijkstra, H. P.; Egmond, M. R.; Lutz, M.; Spek, A. L.; Gros, P.; Klein Gebbink, R. J. M.; van Koten, G., *Chem. Eur. J.* **2009,** 15, 4270-4280 (Chapter 2 of this thesis).
30. Kruithof, C. A.; Casado, M. A.; Guillena, G.; Egmond, M. R.; van der Kerk-van Hoof, A.; Heck, A. J. R.; Klein Gebbink, R. J. M.; van Koten, G., *Chem. Eur. J.* **2005,** 11, 6869-6877.
31. Albrecht, M.; van Koten, G., *Angew. Chem. Int. Ed.* **2001,** 40, 3750-3781.
32. Suijkerbuijk, B. M. J. M.; Aerts, B. N. H.; Dijkstra, H. P.; Lutz, M.; Spek, A. L.; van Koten, G.; Klein Gebbink, R. J. M., *Dalton Trans.* **2007**, 1273-1276.
33. Huck, W. T. S.; Prins, L. J.; Fokkens, R. H.; Nibbering, N. M. M.; van Veggel, F. C. J. M.; Reinhoudt, D. N., *J. Am. Chem. Soc.* **1998,** 120, 6240-6246.

34. Hall, J. R.; Loeb, S. J.; Shimizu, G. K. H.; Yap, G. P. A., *Angew. Chem. Int. Ed.* **1998,** 37, 121-123.
35. Gerhardt, W. W.; Weck, M., *J. Org. Chem.* **2006,** 71, 6333-6341.
36. Yount, W. C.; Loveless, D. M.; Craig, S. L., *J. Am. Chem. Soc.* **2005,** 127, 14488-14500.
37. Terheijden, J.; Van Koten, G.; Grove, D. M.; Vrieze, K., *J. Chem. Soc. Dalton Trans.* **1987**, 1359-1366.
38. South, C. R.; Higley, M. N.; Leung, K. C.-F.; Lanari, D.; Nelson, A.; Grubbs, R. H.; Stoddart, J. F.; Weck, M., *Chem. Eur. J.* **2006,** 12, 3789-3797.
39. Schmülling, M.; Grove, D. M.; van Koten, G.; van Eldik, R.; Veldman, N.; Spek, A. L., *Organometallics* **1996,** 15, 1384-91.
40. Jude, H.; Krause Bauer, J. A.; Connick, W. B., *Inorg. Chem.* **2004,** 43, 725-733.
41. Terheijden, J.; van Koten, G.; Vinke, I. C.; Spek, A. L., *J. Am. Chem. Soc.* **1985,** 107, 2891-2895.
42. *In the following text the phosphine is depicted as a close contact ion pair Na3[3]. It can be anticipated that in aqueous solution this phosphine is present as a solvent separated ion pair Na3[3]. Actually elemental analysis pointed to the isolation of Na3[2-3][OTf]*.
43. Otto, S.; Samuleev, P. V.; Polyakov, V., A.; Ryabov, A. D.; Elding, L. I., *Dalton Trans.* **2004**, 3662-3668.
44. Maassarani, F.; Davidson, M. F.; Wehman-Ooyevaar, I. C. M.; Grove, D. M.; van Koten, M. A.; Smeets, W. J. J.; Spek, A. L.; van Koten, G., *Inorg. Chim. Acta* **1995,** 235, 327-338.
45. Hanan, G. S.; Kickham, J. E.; Loeb, S. J., *Organometallics* **1992,** 11, 3063-3068.
46. Kleij, A. W.; Klein Gebbink, R. J. M.; Lutz, M.; Spek, A. L.; van Koten, G., *J. Organomet. Chem.* **2001,** 621, 190-196.
47. Meijer, M. D.; de Wolf, E.; Lutz, M.; Spek, A. L.; van Klink, G. P. M.; van Koten, G., *Organometallics* **2001,** 20, 4198-4206.
48. Poverenov, E.; Gandelman, M.; Shimon, L. J. W.; Rozenberg, H.; Ben-David, Y.; Milstein, D., *Organometallics* **2005,** 24, 1082-1090.
49. Albrecht, M.; Dani, P.; Lutz, M.; Spek, A. L.; van Koten, G., *J. Am. Chem. Soc.* **2000,** 122, 11822-11833.
50. Manna, J.; Whiteford, J. A.; Stang, P. J.; Muddiman, D. C.; Smith, R. D., *J. Am. Chem. Soc.* **1996,** 118, 8731-8732.
51. Bennett, Martin A.; Jin, H.; Willis, A. C., *J. Organomet. Chem.* **1993,** 451, 249-256.
52. Gorla, F.; Venanzi, L. M.; Albinati, A., *Organometallics* **1994,** 13, 43-54.
53. Allen, D. W.; Nowell, I. W.; Taylor, B. F., *J. Chem. Soc., Dalton Trans.* **1985**, 2505-2508.
54. Allen, D. W.; Taylor, B. F., *J. Chem. Soc., Dalton Trans.* **1982**, 51-54.
55. Meijer, M. D.; Kleij, A. W.; Lutz, M.; Spek, A. L.; van Koten, G., *J. Organomet. Chem.* **2001,** 640, 166-169.
56. Snelders, D. J. M.; Van Koten, G.; Klein Gebbink, R. J. M., *J. Am. Chem. Soc.* **2009,** 131, 11407-11416.
57. Wieczorek, B.; Klimeck, T.; Dijkstra, H. P.; Egmond, M. R.; Van Koten, G.; Klein Gebbink, R. J. M., to be submitted (Chapter 5 of this thesis).
58. Wieczorek, B.; Lemcke, B.; Dijkstra, H. P.; Egmond, M. R.; Klein Gebbink, R. J. M.; Van Koten, G., to be submitted (Chapter 6 of this thesis).
59. van der Zeijden, A. A. H.; Van Koten, G.; Luijk, R.; Nordemann, R. A.; Spek, A. L., *Organometallics* **1988,** 7, 1549-1556.
60. Sutter, J.-P.; James, S. L.; Steenwinkel, P.; Karlen, T.; Grove, D. M.; Veldman, N.; Smith, R. D.; Spek, A. L.; Van Koten, G., *Organometallics* **1996,** 15, 941-948.
61. Otwinowski, Z.; Minor, W., *Methods in Enzymology*. Academic Press: 1997; Vol. 276, p 307-326.
62. Sheldrick, G. M. *SADABS: Area-Detector Absorption Correction*, 2.10; Universitaet Goettingen: Goettingen, 1999.
63. Sheldrick, G. M., *Acta Cryst.* **2008,** A64, 112-122.
64. Spek, A. L., *Acta Cryst.* **2009,** D65, 148-155.

CHAPTER 5

An Abiotic C-C Coupling Reaction Catalyzed by Semisynthetic Pincer-Metalloenzymes

Various transition metal complexes, including small molecular water-soluble (**4**) and water-insoluble (**5**) SCS pincer-palladium complexes and an SCS pincer-palladium cutinase hybrid catalyst (**cut-1**), were used as catalysts in an aqueous abiotic C-C coupling reaction in air. The selectivities (linear versus branched product) and activities of the different catalysts were influenced by the nature of their *para*-subsituent, *i.e.* proton, triethyleneglycol or cutinase. The order of selectivity towards the linear product was found to be **cut-1** (4.3) > **5** (2.4) > **4** (0.4). Surprisingly, **cut-1** was found to produce more product than small molecular water-soluble catalyst **4**, showing an activating influence of the protein-backbone on the catalytic pincer moiety. By changing the properties of the *para*-substituent, the electronic and solubility properties of the pincer complexes can be changed, thereby influencing their catalytic activity and selectivity.

Introduction

The introduction of non-natural transition metal complexes into proteins has become an important tool to expand the applications of bioinorganic chemistry;[1-5] the metal centre can be embedded into a biological environment, thereby expanding the functional and structural properties of naturally occurring proteins towards the rich chemistry of transition metal ions and coordination complexes. Transition metal complexes incorporated into proteins have, among others, been used for the luminescent labelling of proteins,[6-18] in electrochemical[19] and biomimetic studies,[20] as structural and crystallographic probes,[21-23] in the directed evolution of novel proteins,[24, 25] and as artificial metalloenzymes in catalytic studies.[20, 26-48] The use of proteins as chiral scaffolds in enantioselective catalytic reactions is currently attracting a lot of attention, thereby aiming at optimum use of the steric bulk and chiral induction of the protein backbone on the metal centre. Various reactions catalyzed by these semisynthetic metalloenzymes have been studied, *e.g.* oxidation,[21, 27, 33, 34, 37, 44-46, 48] reduction,[41] ester[38, 42] and amide[43] bond hydrolysis, and several hydrogenation[22, 24, 26, 29-32, 35, 39, 40] reactions. Only very few examples of C-C coupling reactions, like asymmetric allylic alkylations[28, 36] and Diels-Alder reactions[47, 49] have been reported in this respect so far.

Different artificial metalloprotein systems based on various proteins and transition metal complexes are known, with the most prominent examples being the non-covalent biotin/(strept)avidin system, for which the biotin moiety is modified with different transition metal complexes,[1, 3] and *apo*-myo- or *apo*-haemoglobin, where the porphyrin moiety has been replaced by other covalently attached prosthetic groups, *e.g.* salen-complexes.[20, 21, 27, 34, 37]

At our laboratory, various semisynthetic pincer-metalloenzymes have been developed recently[23, 50, 51] by covalent anchoring of an organometallic phosphonate to the lipase cutinase (Figure 1). Phosphonates are known to irreversibly inhibit serine hydrolases (lipases belong to the superfamily of serine hydrolases) by binding covalently to the activated serine in the active site of the enzyme, thereby blocking the enzymatic activity.[52-56] We synthesized phosphonate inhibitors substituted with various organometallic ECE pincer complexes (Figure 1a shows an example of an SCS-pincer palladium complex),[50] and attached them covalently to the active site of cutinase. These semisynthetic pincer-metalloenzymes have been proven to be very stable and could be crystallized, resulting in the elucidation of several crystal structures.[23] For example, the crystal structure of the cutinase-based semisynthetic enzyme containing SCS-pincer palladium complex **1** (**cut-1**, Figure 1b) shows unequivocally that the SCS-pincer palladium moiety is located at the surface of the protein, being accessible for solvent or substrate molecules.

a)

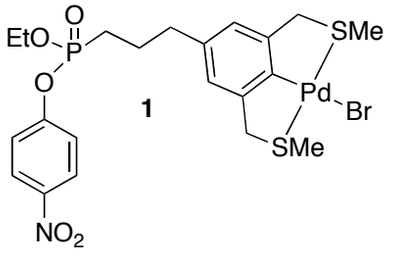

b)

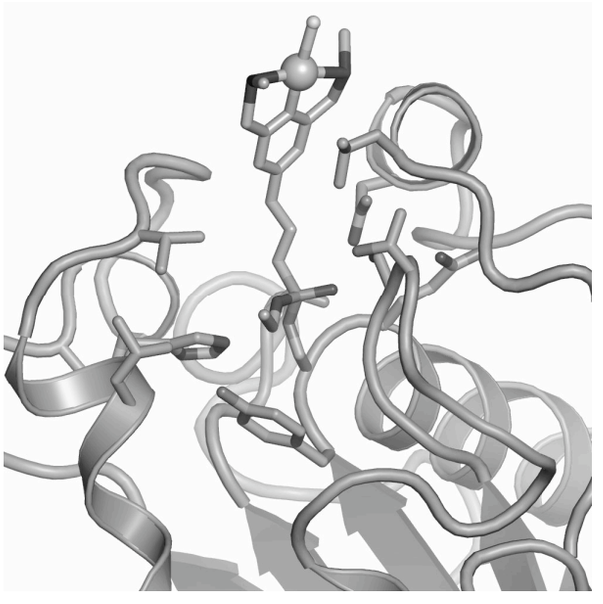

Figure 1: a) Organometallic SCS-pincer palladium inhibitor **1** used in this catalytic study;[50] b) crystal structure of the cutinase embedded SCS-pincer palladium complex **cut-1**.[23]

ECE-pincer metal complexes are a class of very well-studied organometallic compounds, which have been applied to synthesize organometallic polymers and dendrimers, silica, carbohydrates, peptides, and proteins.[50, 57-64] Besides their excellent properties as sensoring materials and building blocks in supramolecular chemistry,[58, 63-66] they have also proven to be versatile catalysts in different catalytic reactions,[62, 67-69] including their use in tandem catalytic studies.[70]

Recently, pincer palladium complexes were reported to be excellent catalysts for the C-C coupling reaction between a boronic acid and vinyloxirane (Scheme 1). This reaction was performed in a semi-aqueous THF/H_2O (10:1 v/v) mixture under very mild reaction conditions.[67] The reported linear/branched ratios were found to depend on the type of ECE-palladium pincer catalyst used (Scheme 1). For our pincer-palladium cutinase systems we were searching for new C-C coupling reactions that could potentially be used in combination with semisynthetic metalloenzymes. We anticipated that the C-C coupling reaction between a boronic acid and vinyloxirane would be a suitable probe for this study. Furthermore, this reaction could be an interesting tool to study whether the protein backbone has any special influence by monitoring the linear/branched ratio of the product.

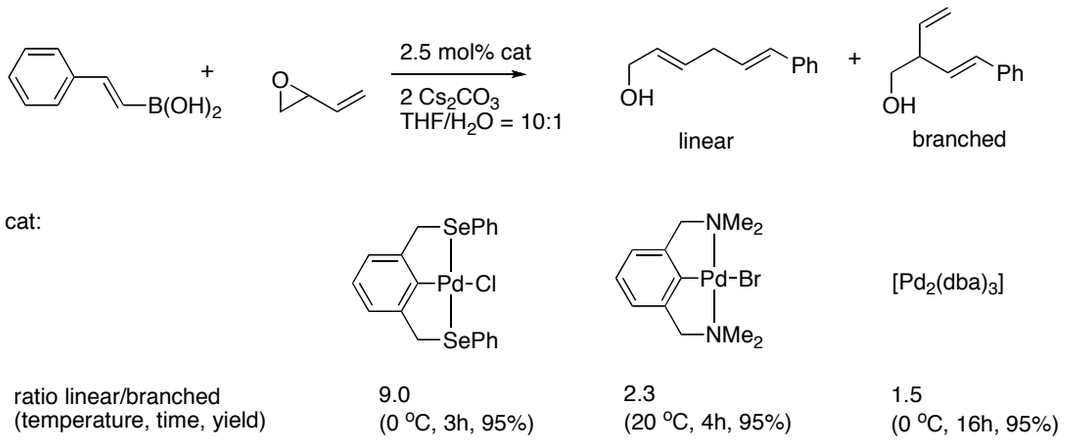

Scheme 1: C-C coupling reaction by Szabo et. al[67] which had been studied with different semisynthetic pincer-metalloenzymes in a THF/H_2O mixture; the linear/branched ratios for different parent catalysts reported from literature are given.

Here, we report the use of a cutinase-pincer palladium semisynthetic metalloenzyme in a C-C coupling reaction between a boronic acid and vinyloxirane in aqueous media and a comparison of the performance of this catalyst with respect to the selectivities and activities of small molecular pincer catalysts.

Results and Discussion

*Synthesis of the water-soluble reference catalyst **4***

In order to be able to compare the catalytic results of the semisynthetic enzyme **cut-1** to non-enzymatic SCS-pincer palladium complexes, it was decided to first prepare a water-soluble SCS-pincer palladium complex as a reference catalyst. The previous work of Bergbreiter[62] and Reinhoudt[71] was used as an inspiration for the synthesis of the low-molecular weight hydrophilic reference catalyst **4** (Scheme 2).

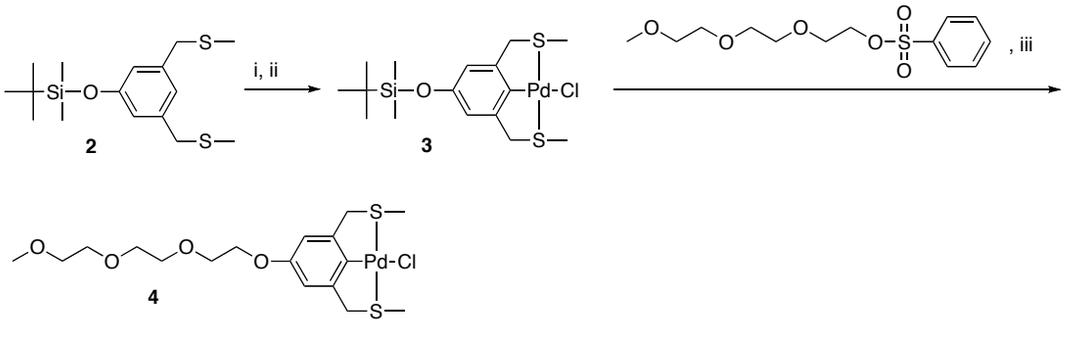

Scheme 2: Synthesis of the water-soluble catalyst **4**. Conditions: i: $[Pd(MeCN)_4](BF_4)_2$, Hunig's base; MeCN, 50 °C, 2 days; ii: NaCl, acetone; iii: K_2CO_3, 18-crown-6, acetone, Bu_4NF.

For the synthesis of starting material **2**, the published procedures for ^{R}SCS (R = Ph, naphthyl, *t*-butyl, ethyl)[62, 71] were slightly adapted (see experimental section for details). The metalation to obtain **3** was performed with $[Pd(MeCN)_4](BF_4)_2$ as Pd(II) precursor in MeCN in the presence of Hünig's base at slightly elevated temperatures for 2 days, followed by treatment with NaCl to afford the halide complex **3**. The water-soluble target complex **4** was obtained after *in situ* removal of the TBDMS protecting group with Bu_4NF, followed by an ether coupling with a short oligo-ethylene glycol tosylate precursor in the presence of base. Due to the amphiphilic nature of **4** (high solubility in both CH_2Cl_2 and H_2O), repetitive washings with CH_2Cl_2/H_2O were needed to obtain the pure product, which also explains the somewhat low isolated yield (15%). Complex **4** was fully characterized by ^{1}H, ^{13}C NMR, MALDI-TOF and high resolution ES-MS.[72]

*Crystal structure of **3** and fluxional behaviour of **3** and **4** in solution*

When a solution of **3** in CH_2Cl_2/MeCN was slowly evaporated in air, crystals suitable for X-ray diffraction studies were obtained. The molecular structure of the analyzed crystals is shown in Figure 2. Selected distances and angles are given in Table 1.

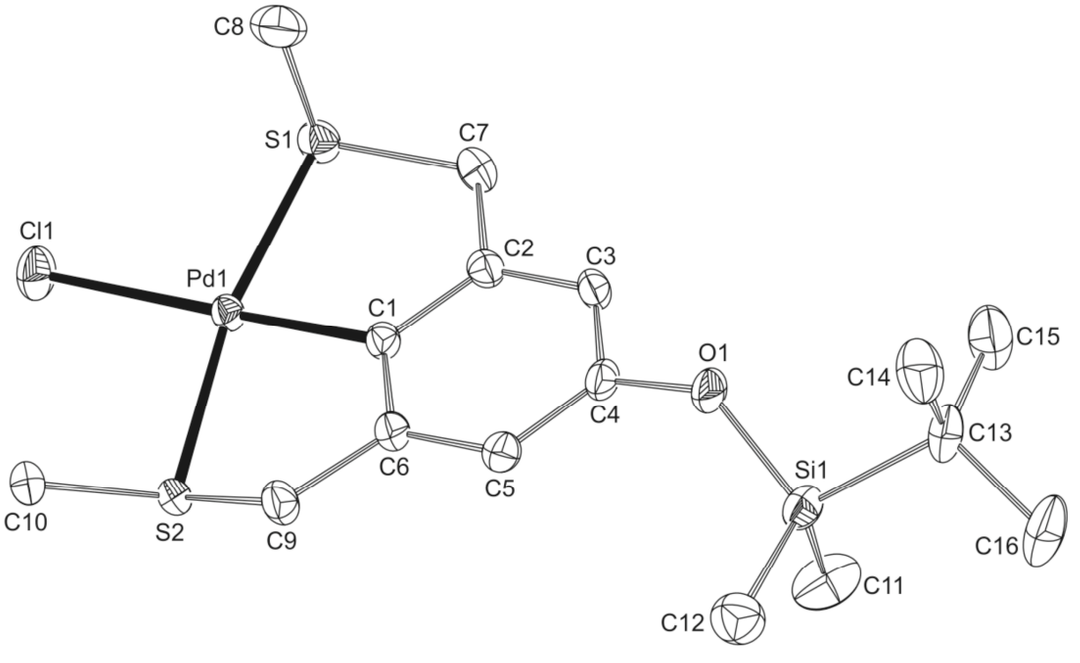

Figure 2: ORTEP plot (50% probability level) of the molecular structure of complex **3** (the hydrogen atoms have been omitted for clarity).

Table 1: Selected distances (Å), angles and torsion angles (°) for the crystal structure of complex **3**.

Distances			
Pd1-C1	1.9729(13)	Pd1-S1	2.2927(4)
Pd1-Cl1	2.3881(3)	Pd1-S2	2.2807(3)
C4-O1	1.3768(16)	O1-Si1	1.6538(10)
Angles			
C1-Pd1-Cl1	176.79(4)	C4-O1-Si1	130.98(9)
C1-Pd1-S1	85.66(4)	C1-Pd1-S2	84.14(4)
Torsion Angles			
C1-C6-C9-S2	23.94(16)	Pd1-S1-C7-C2	-15.70(10)
C1-C2-C7-S1	12.10(16)	Pd1-S2-C9-C6	-29.32(10)
C4-O1-Si1-C13	163.37(13)		

^{Me}SCS-pincer palladium complex **3** crystallized in a single conformational structure with a local approximate mirror plane through the Cl1-Pd1-C1 bond. The two methyl groups point in the same direction, perpendicular to the plane of the aromatic ring (Figure 2). This conformation has been observed before for pincer complex [PdBr(^{Me}SCS)] (**5**).[51] The palladium-carbon, palladium-sulfur and palladium-chlorine bond distances are comparable to other SCS-pincer palladium crystal structures (Pd-C = 1.952-2.035 Å, Pd-S = 2.2832-2.299 Å, Pd-Cl = 2.391-2.410 Å, Table 1).[51, 58, 61, 73, 74] The bond and torsion angles are similar to the *meso*-structure of **5**.[51]

The NMR analysis of complexes **3** and **4** in deuterated chloroform revealed an intermediate exchange behaviour (doublet, $^{2}J_{H\text{-}H}$ = 99.0 Hz, see experimental section for details) for the benzylic protons of the pincer arms, pointing towards dynamic processes between *rac*, *meso* and *asymm*-isomers in solution. A careful analysis of the exchange phenomena of such ^{Me}SCS pincer metal complexes has been recently reported by us.[51]

Preparation of the SCS pincer palladium lipase hybrid catalyst

The synthesis of the semisynthetic enzyme **cut-1** was carried out using an earlier published procedure (Scheme 3).[50, 75] For the anchoring of **1** to cutinase (**cut**), a cutinase solution (250 μM) in Tris buffer (pH 8.0) was incubated with an excess of **1** (3 equiv., 50 mM solution in MeCN) overnight, after which the solution was dialysed with Tris buffer (125 mM, pH 8.0, 2 x 400 mL during 24h) to remove excess inhibitor **1**. The subsequent activity test showed no residual hydrolytic activity of the native enzyme, indicating quantitative inhibition by SCS-pincer palladium phosphonate **1**.

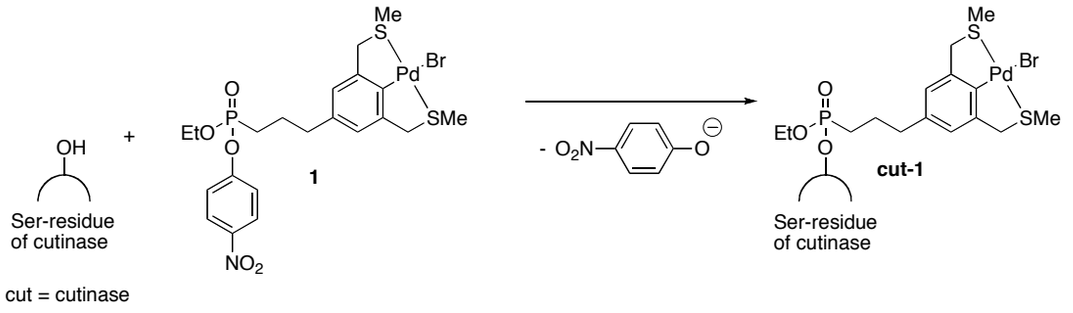

Scheme 3: Anchoring of SCS-pincer palladium phosphonate inhibitor **1** to the lipase cutinase.

Catalytic studies

Before studying the catalytic behaviour of **cut-1** in an abiotic C-C coupling reaction between *trans*-2-phenylvinylboronic acid and vinyloxirane, we first determined the optimal reaction conditions with the non-enzyme containing catalysts **4** and **5** (Table 2). In initial studies we confirmed that the water-soluble (**4**) and the water-insoluble (**5**)[51] SCS-pincer palladium catalysts were both active under the published reaction conditions and concentrations (12 mM [Pd], 2.5 mol%, THF/H_2O=10/1, Scheme 1).[67] As such high catalyst concentrations and the presence of large amounts of organic co-solvents are not compatible with the lipase hybrid catalysts, the catalytic studies had to be performed and optimized under more diluted, fully aqueous conditions using buffer. Due to the anticipated incompatibility of the protein scaffold with high temperatures (>40 °C) and the relatively low boiling point and the volatile nature of vinyloxirane (65 °C), it was decided to perform the catalytic studies at room temperature. Previous studies by our group with cutinases modified with phosphonates showed that the highest workable concentrations for homogeneous cutinase solutions were in the range of 150-250 μM.[50, 60, 75] Therefore, we decided to start the catalytic tests with catalyst concentrations ranging from 50-250 μM. A first catalytic run with catalysts **4** and **5** in Tris buffer (0.5-2.5 mol% catalyst, catalyst conc. 50-250 μM, 2.0 equiv. base, 1.0 equiv. boronic acid, 10.0 equiv. epoxide, ambient temperature) gave rise to product formation and consequently these conditions were used as a starting point for the determination of the optimum catalyst loading for **cut-1**. To test whether the conditions determined for **4** and **5** were appropriate for the cutinase hybrid catalyst, the catalyst loadings for **cut-1** were varied between 0.5-2.5 mol% (50-250 μM), while the total reaction volume (211.6 μL) was kept constant. After 6 days (140 hours) the different reaction mixtures were analysed by HPLC, and the highest conversion (17% product) observed was obtained with 2 mol% of **cut-1** (200 μM). Several control reactions without any catalyst showed that no blank reaction had occurred.

These optimized conditions (0.02 equiv. catalyst, 10 equiv. epoxide, 2.0 equiv. Cs_2CO_3, 1.0 equiv. boronic acid in Tris buffer) were used to compare the reference catalysts **4** and **5** to the semisynthetic enzyme **cut-1** in the catalytic abiotic C-C

coupling reaction (Table 2). For all catalytic runs, the catalyst loading (2 mol%) and the total reaction volume (211.6 μM) were kept constant and the reaction was monitored at room temperature.

Table 2: Catalytic studies with SCS-pincer palladium complexes and lipase hybrids in buffer.[a]

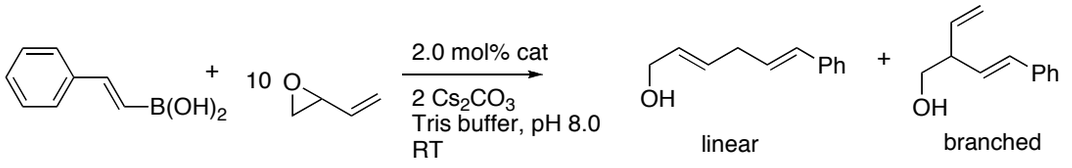

Catalyst	Time (h)	Product formation[b]	Ratio lin/bran
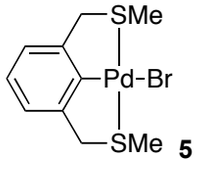 **5**	90	18%	2.4
5	140	49%	2.4
5	375	64%	2.4
4	20	8%	0.4
4	140	12%	0.4
4	375[c]	12%	0.4
$Pd(dba)_2$•$CHCl_3$	20	23%	0.4
$Pd(dba)_2$•$CHCl_3$	140	23%	0.4
$Pd(dba)_2$•$CHCl_3$	375[c]	23%	0.4
cut-1	90	10%	4.3
cut-1	140	17%	4.3
cut-1	375[c]	31%	4.3
cut	375	0%	-
blank	375	0%	-

[a] 125 mM Tris buffer, pH 8.0; [b] based on boronic acid, determined by HPLC; [c] after complete consumption of boronic acid.

Of the non-enzyme substituted catalysts, the water-insoluble catalyst **5** showed the highest product yield of all with 64% product formation after 375 h. The water-soluble pincer catalyst **4** and $Pd(dba)_2$•$CHCl_3$ were less active,[72] with a stagnation of product formation after 140 h and <20 h, respectively. Catalyst **5** had the highest preference for the linear product (ratio: 2.4) in comparison to **4** and $Pd(dba)_2$•$CHCl_3$ (ratio: 0.4). All catalysts displayed constant linear/branched product ratios during the different runs, indicating a consistent catalytically active species. The product formation for catalyst **4** and $Pd(dba)_2$•$CHCl_3$ stopped after 140h and <20h, respectively, indicating that the catalytically active species might have decomposed.

Apparently, the (in)solubility of the different SCS pincer palladium complexes in the aqueous buffer system is not the determining factor for their catalytic activities, with catalyst **5**, which possesses the lowest water-solubility, giving the highest product formation.
For the SCS pincer palladium lipase hybrid **cut-1**, 31% conversion was obtained after 375 hours. Interestingly, **cut-1** also displayed the highest selectivity for the linear product (linear/branched = 4.3), which is significantly higher than for the small molecular catalysts. Also for **cut-1** the linear/branched ratio remained constant during the complete catalytic run. After 375 hours, no boronic acid was present anymore, indicating that the boronic acid had either reacted towards the product or had hydrolysed. Cutinase itself, without any palladium source present, was not catalytically active.
The differences in selectivity and activity between catalysts **4** and **5** (linear/branched = 0.4 and 2.4; 12% and 64% product yield after 375h, respectively) are rather unexpected and could be explained by the different nature of the *para*-substituent for **4** and **5** (oligoethylene glycol *vs.* hydrogen) or the differences in solubility of the two catalysts. With the oxygen atom being a mesomeric electron donating substituent on the pincer ring in comparison to hydrogen,[76] the electron density at the SCS-pincer palladium centre might be slightly higher for **4** than for **5**. This might enhance the susceptibility of the palladium metal centre in **4** towards reductive elimination, possibly explaining the low catalytic activity (12% yield) and the apparent stop of product formation after 140 hours.
The insolubility of catalyst **5** in the aqueous media applied could also play a role in explaining its higher catalytic activity and different selectivity. Due to its insolubility, complex **5** could possibly cluster together and therefore give rise to an enhanced formation of the linear product (linear/branched ratio 2.4), as observed. The steric hindrance of neighbouring pincer molecules in the cluster could thereby impose the preferential formation of the linear product. The insolubility of **5** could also explain its enhanced catalytic activity in comparison to **4**, as the decomposition of **5** might be slower.
The steric bulk of the protein backbone of **cut-1** also influenced the product selectivity of the catalyst, thereby giving rise to an enhanced formation of the linear product.

This study was inspired by the catalytic results obtained by Szabo et al.,[67] who proved that ECE pincer palladium complexes were excellent catalysts in C-C coupling reactions in organic media. In comparison to their results,[67] the reactions described here are performed in pure aqueous media, are 60 times more diluted and a slightly lower catalyst loading is used (2.0 mol% instead of 2.5 mol%), causing the considerable increase in reaction time from several hours to several days. Interestingly, the linear/branched selectivity for the SCS-pincer palladium catalyst **5** (ratio: 2.4) is comparable to the selectivity of the [PdBr(^{Me}NCN)] pincer catalyst

(ratio: 2.3, Scheme 1), whereas the linear/branched selectivity was highest for the [PdCl(^{Ph}SeCSe)] catalyst (ratio: 9.0).

Conclusions

Here, we described the successful synthesis of water-soluble SCS-pincer palladium complexes, *i.e.* a triethylene glycol substituted SCS-pincer complex (**4**) and a protein-embedded SCS-pincer palladium complex. These materials were applied in an abiotic C-C coupling reaction between a boronic acid and an epoxide in aqueous media and compared to a water-insoluble reference catalyst (**5**) and $Pd(dba)_2$•$CHCl_3$.
All complexes were catalytically active with the activities and selectivities of the catalysts being influenced by the *para*-substituents. The linear/branched ratio was highest with the cutinase-embedded catalyst and lowest with the water-soluble SCS pincer palladium catalyst. The highest activities were achieved with the water-insoluble SCS pincer palladium catalyst **5**, whereas the small molecular water-soluble pincer palladium catalyst **4** exhibited low activities. The differences between catalysts **4** and **5** are most probably caused by the nature of the *para*-substituent (electronic influence of oligoethylene glycol *versus* hydrogen) combined with the steric bulk imposed by clustering of the water-insoluble catalyst **4**.
This study shows that abiotic reactions in water catalyzed by semisynthetic pincer-metalloenzymes are possible with different selectivities in comparison to the small-molecular parent-complexes. These selectivities are greatly influenced by the nature of the *para*-substituent, *e.g.* the protein backbone.

Experimental Section

General comments: All synthetic experiments were conducted at room temperature (unless stated otherwise) under a dry nitrogen atmosphere using standard Schlenk techniques. All glassware was dried carefully before use. Solvents were dried over appropriate materials and distilled prior to use (pentane, toluene, THF and Et_2O were distilled from sodium/benzophenone and CH_2Cl_2 and MeCN from CaH_2 to obtain dry and pure solvents). Reagents were obtained from commercial sources, used without further purification and stored under nitrogen atmosphere. $Pd(dba)_2$•$CHCl_3$ was synthesized according to literature procedures.[77] The syntheses of palladium pincer complexes **1**,[50] and **5**[51] and (5-(tert-butyldimethylsilyloxy)-1,3-phenylene dimethanol)[71, 78] were carried out as reported. ^1H (300 or 400 MHz) and $^{13}C\{^1H\}$ (75 or 100 MHz) NMR spectra were recorded on either Varian Inova 300 or Varian AS400 spectrometers at 25°C, chemical shifts are in ppm referenced to residual solvent resonances. The MALDI-TOF mass spectra were acquired using a Voyager-DE Bio-Spectrometry Workstation mass spectrometer. The matrix α-cyano-4-hydroxycinnamic acid and the sample (~30mg/ml) were dissolved in acetonitrile/H_2O (1:1, v/v) and 0.2 µl of both solutions were mixed and placed on a titanium MALDI target and analyzed after evaporation of the solvent. Elemental microanalyses were

obtained from H. Kolbe Mikroanalytisches Laboratorium, Mülheim an der Ruhr, Germany. Water for the preparation of the buffer solutions was filtered with the Milli-Q filtration system (Millipore, Quantum Ultrapure) prior to use. The dialysis cassettes (Slide-A-Lyzer™, 10,000 MWCO, 0.1-0.5 mL or 0.5-3 mL) for the purification of pincer palladium hybrid were purchased from Pierce. Cutinase mutant N172K was provided by Unilever. Prior to inhibition cutinase was analyzed by gel-electrophorese to assess its purity.

HPLC analyses: HPLC analyses were performed on a Thermo Separation products HPLC machine with a GraceSmart RP18 5u column (ID 4.6 mm, length 250 mm, PN 5138810) and a Finnigan MAT Spectra SYSTEM UV6000LP detector (detection wavelengths 254 and 280 nm). A SpectraSeries P2000 HPLC pump with an Alltech Elite™ Degassing System and a Chromquest Workstation was used. For the elution of the products a linear gradient of NH_4OAc buffer (50 mM in H_2O) and MeCN was used, starting from 35% MeCN/65% buffer at t=0 min to 26% MeCN/74% buffer after t=64 min, with a flow rate of 1.0 mL/min.

Preparation of the Tris buffer solution: Tris (250 mmol, 30.2838 g) was dissolved in MilliQ-H_2O (2.0 L) and acidified with aqueous HBF_4 to pH 8.0.

Preparation of the Tris/Triton buffer solution: Triton X-100 (1.0000 g, 1.6000 mmol) and Tris (6.0568 g, 50 mmol) were dissolved in MQ-H_2O (1.0 L) and acidified with 30% aqueous HCl to pH 8.0.

2-(2-(2-methoxyethoxy)ethoxy)ethyl 4-methylbenzene-sulfonate:[79] The published procedure was slightly modified: To a solution of p-toluenesulfonyl chloride (10.50 g, 55.10 mmol, 1.1 equiv.) in CH_2Cl_2 (30 mL), at -5 °C was added triethylene glycol monomethyl ether (8.21 g, 50.00 mmol, 1.0 equiv.). The temperature was maintained at -5°C, while KOH (11.28 g, 201.30 mmol, 4.0 equiv.) was added in small amounts under vigorous stirring, after which the mixture was stirred overnight. CH_2Cl_2 (40 mL) and ice water (60 mL) were added, the aqueous layer was separated and extracted with CH_2Cl_2 (3 x 50 mL). The combined organic phases were washed with water (2 x 50mL), separated and dried with $MgSO_4$, subsequently filtered and concentrated *in vacuo*. The product was isolated as a clear colorless oil (15.62 g, 49.60 mmol, 98%). ^{1}H NMR (300 MHz, $CDCl_3$): δ = 7.78 (2H, *o*-C_6H_4, $^3J_{H,H}$ = 8.4 Hz, d), 7.32 (2H, *m*-C_6H_4, $^3J_{H,H}$ = 8.4 Hz, d), 4.14 (2H, CH_2, $^3J_{H,H}$ = 4.8 Hz, t), 3.66 (2H, CH_2, $^3J_{H,H}$ = 5.0, t), 3.60-3.49 (8H, CH_2, m), 3.35 (3H, O-CH_3, s), 2.43 (3H, CH_3-Ar, s).

(3,5-bis(chloromethyl)phenoxy)(tert-butyl)dimethylsilane:[71] The published procedure was slightly modified: Et_3N (2.09 mL, 15.00 mmol, 2.5 equiv.) was added to a solution of (5-(tert-butyldimethylsilyloxy)-1,3-phenylene dimethanol)[71, 78](1.0 eq, 1.61 g, 6.00 mmol, 1.0 equiv.) in CH_2Cl_2 (80 mL) and the resulting solution was

cooled to 0 °C with a ice bath. Mesyl chloride (1.16 mL, 15.00 mmol, 2.5 equiv.) was added dropwise, after which the reaction mixture was heated to 50 °C for 40 h. The reaction mixture was washed with H_2O (3 x 25 mL) and the combined organic layers were dried over $MgSO_4$. Evaporation of the filtrate *in vacuo* afforded a light-brown transparent oil (1.47 g, 4.83 mmol, 80%). The oil was dissolved in THF (40 mL) and KCl (0.52g, 6.97 mmol, 1.5 eq) and 18-crown-6 (0.06 g, 0.23 mmol) were added. The resulting solution was heated to reflux for 4 days, after which the clear-transparent reaction mixture was allowed to cool to RT and all volatiles were evaporated *in vacuo*. Next, the mixture was dissolved in CH_2Cl_2 and washed with water (3 x 20 mL), the combined organic layers were dried over $MgSO_4$, filtered and concentrated *in vacuo* to yield a clear-transparent oil with crystal streaks. Subsequently, a flame distillation was carried out to obtain the product (0.93 g, 3.04 mmol, 50%). ^{1}H NMR (300 MHz, $CDCl_3$): δ = 7.02 (1H, Ar*H*, s), 6.87 (2H, Ar*H*, s), 4.53 (4H, Ar-CH_2, s), 1.04 (9H, CCH_3, s), 0.26 (6H, SiCH_3, s).

(3,5-bis(methylthiomethyl)phenoxy)(tert-butyl) dimethyl-silane:[71] The published procedure was slightly modified: To a solution of (3,5-bis(chloromethyl)phenoxy)(tert-butyl)dimethylsilane (4.16 g, 13.65 mmol, 1.0 equiv.) in THF (200 mL) was added NaSMe (2.76 g, 39.38 mmol, 2.9 equiv.) and 15-crown-5 (0.2 mL, 0.98 mmol, 0.1 equiv.). This mixture was stirred for 5 days at 50 °C. After cooling down to room temperature all volatiles were removed *in vacuo*, Et_2O (30 mL) was added and the solution was washed with H_2O (30 mL), after which the water layer was extracted with Et_2O (3 x 30 mL). The organic layers were combined and all volatiles were removed *in vacuo*. The obtained oil was purified by column chromatography using alumina neutral gel and hexane/ethyl acetate (9:1, v/v) as eluent. After flame distillation of the product and removal of volatiles *in vacuo* using high vacuum ($4 \cdot 10^{-7}$ mbar, 10h, 80 °C) a light-yellow oil was obtained (1.85 g, 5.63 mmol, 41%). ^{1}H NMR (400 MHz, $CDCl_3$): δ = 6.84 (1H, Ar*H*, s), 6.69 (2H, *o*-Ar*H*, s), 3.60 (4H, *m*-Ar-CH_2, s), 1.98 (6H, S-CH_3, s), 0.98 (9H, CCH_3, s), 0.20 (6H, SiCH_3, s). ^{13}C{^{1}H} NMR (100 MHz, $CDCl_3$): δ = 155.8 (O*C*Ar), 139.8 (Ar*C*-CH_2), 122.6 (Ar*C*H), 119.3 (*o*-Ar*C*H), 38.14 (*C*H_2S), 25.75 (C(*C*H_3)$_3$), 18.25 (*C*(CH_3)$_3$), 14.90 (S*C*H_3), -4.33 (Si*C*H_3). Elem. anal. calc. for $C_{16}H_{28}OS_2Si$ (328.61): C, 58.48; H, 8.59; S, 19.52; found: C, 58.58; H, 8.65; S, 19.37.

[PdCl{$C_6H_2(CH_2SCH_3)_2$-2,6-(TBDMS-O)-4}] 3: To a solution of (3,5-bis(methylthiomethyl)phenoxy)(tert-butyl) dimethyl-silane (1.0 eq, 0.98 g, 2.98 mmol) in MeCN (40 mL) was added Hünig base (0.8 eq, 0.42 mL, 2.40 mmol) and $[Pd(MeCN)_4](BF_4)_2$ (1.06 g, 2.38 mmol, 0.8 eq) in MeCN (50 mL). The resulting yellow-orange mixture was stirred at 50 °C for 2 days to yield a brownish mixture. The mixture was allowed to cool to RT and filtered over Celite. Subsequently, all volatiles were evaporated to yield a yellow-orange oil. This oil was dissolved in acetone (120 mL) and NaCl (1.05 eq, 0.17 g, 2.91 mmol) was added in one portion and stirred at RT. Subsequently, all volatiles were evaporated, CH_2Cl_2 (30 mL) was

added and the organic layer was washed with H_2O (2 x 30 mL). The organic layer was dried over $MgSO_4$, filtered and concentrated *in vacuo.* The yellow residue was dissolved in a minimum of CH_2Cl_2 and the product was precipitated by addition of hexane. After filtration and evaporation of all volatiles *in vacuo* complex **3** was isolated as a yellow crystalline solid (0.16 g, 0.35 mmol, 15%). After slow evaporation of a solution of **3** in CH_2Cl_2/MeCN in air crystals suitable for X-ray diffraction studies were grown. ^{1}H NMR (300 MHz, $CDCl_3$): δ = 6.47 (2H, Ar*H*, s), 4.19 (4H, C*H*$_2$, $^2J_{H,H}$ = 99.0 Hz, d), 2.77 (6H, SC*H*$_3$, s), 0.95 (9H, CC*H*$_3$, s), 0.15 (6H, SiC*H*$_3$, s). ^{13}C{^{1}H} NMR (100 MHz, $CDCl_3$): δ = 153.5 (O*C*Ar), 151.1 (Pd*C*), 149.3 (Ar*C*), 114.6 (Ar*C*H$_2$), 49.13 (*C*H$_2$S), 25.75 (C(*C*H$_3$)$_3$), 23.19 (SCH$_3$), 18.25 (*C*(CH$_3$)$_3$), -4.29 (Si*C*H$_3$). MS (MALDI-TOF): *m/z* 433.27 ([M-Cl]$^+$) (calc. 433.03), 903.19 ([2xM-Cl]$^+$) (calc. 903.04). Elemen. anal. calc. for $C_{16}H_{27}ClOPdS_2Si$ (469.47): C, 40.93; H, 5.80; Pd, 22.67; S, 13.66; found: C, 40.89; H, 5.87; Pd, 22.62; S, 13.57.

X-ray crystal structure determination of 3:
$C_{16}H_{27}ClOPdS_2Si$, Fw = 469.44, yellow plate, 0.36 x 0.33 x 0.09 mm^3, monoclinic, $P2_1/c$ (no. 14), a = 20.7396(4), b = 6.3856(3), c = 15.4324(2) Å, β = 96.949(1)°, V = 2028.77(12) Å^3, Z = 4, D_x = 1.537 g/cm^3, μ = 1.31 mm^{-1}. 61225 Reflections were measured on a Nonius KappaCCD diffractometer with rotating anode (graphite monochromator, λ = 0.71073 Å) up to a resolution of $(\sin\theta/\lambda)_{max}$ = 0.65 Å^{-1} at a temperature of 150(2) K. Intensity integration was performed with EvalCCD.[80] The SADABS[81] program was used for absorption correction and scaling based on multiple measured reflections (0.53-0.89 correction range). 4667 Reflections were unique (R_{int} = 0.023), of which 4333 were observed [I>2σ(I)]. The structure was solved with Direct Methods using the program SHELXS-97[82] and refined with SHELXL-97[82] against F^2 of all reflections. Non hydrogen atoms were refined with anisotropic displacement parameters. All hydrogen atoms were located in difference Fourier maps and refined with a riding model. 206 Parameters were refined with no restraints. R1/wR2 [I > 2σ(I)]: 0.0155 / 0.0391. R1/wR2 [all refl.]: 0.0180 / 0.0402. S = 1.053. Residual electron density between -0.37 and 0.32 e/Å^3. Geometry calculations and checking for higher symmetry was performed with the PLATON program.[83]

Complex 4: To a solution of **3** (0.32 g, 0.68 mmol, 1.0 equiv.) in acetone (15 mL) were added K_2CO_3 (0.47 g, 3.42 mmol, 5.0 eq), 18-crown-6 (0.01 g, 0.03 mmol, 0.05 equiv.) and a solution of 2-(2-(2-methoxyethoxy)ethoxy)ethyl 4-methylbenzene-sulfonate (0.17 g, 0.55 mmol, 0.8 equiv.) in acetone (5 mL). The resulting orange solution was treated dropwise with Bu_4NF (0.68 mL, 0.68 mmol, 1.0 equiv.), after which the colour of the solution changed to red immediately. The reaction mixture was allowed to reflux for 36 h. After evaporation of all volatiles *in vacuo*, CH_2Cl_2 (5 mL) was added and the mixture was filtered over Celite. The filtrate was washed with H_2O (7 x 5 mL), and the water layers were extracted with CH_2Cl_2 (2 x 5 mL) after every washing step. The combined organic layers were dried with

$MgSO_4$, filtered and dried *in vacuo*. The crude product was purified by column chromatography (l: 20.0 cm, d: 0.7 cm) using Sephadex LH20 as the stationary phase and CH_2Cl_2 as eluent. The first fraction was purified by high vacuum ($9 \cdot 10^{-7}$ mbar, 10 h, 80 °C), after which the column filtration was repeated. The obtained product was dissolved in CH_2Cl_2 (0.5 mL) and washed with MQ-H_2O (3 x 5 mL). After evaporation of all volatiles *in vacuo*, **4** was isolated as a yellow oil (0.04 g, 0.08 mmol, 15%). ^{1}H NMR (300 MHz, $CDCl_3$): δ = 6.57 (2H, Ar*H*, s), 4.21 (4H, CH_2, $^2J_{H,H}$ = 99.9 Hz, d), 4.04-3.52 (12H, OCH_2, m), 3.37 (3H, OCH_3, s), 2.77 (6H, SCH_3, s). ^{13}C{^{1}H} NMR (100 MHz, $CDCl_3$): δ = 156.9 (Ar*C*S), 150.4 (Pd*C*), 149.3 (Ar*C*O), 109.5 (Ar*C*H_2), 72.00-67.73 (OEG-*C*), 59.13 (O*C*H_3), 49.18 (S*C*H_2), 23.16 (S*C*H_3). MS (MALDI-TOF): *m/z* 465.34 ([M-Cl]$^+$) (calc. 465.04), 967.29 ([2xM-Cl]$^+$) (calc. 967.35). HR ES MS (501.3969): *m/z* 501.0152 ([M]$^+$) (calc. 501.0098), 465.0386 ([M-Cl]$^+$) (calc. 465.0510), 523.9972 ([M+Na]$^+$) (calc. 523.9996). Elemen. anal. calc. for $C_{17}H_{27}ClO_4PdS_2$ (501.3969): C, 40.72; H, 5.43; found: C, 39.92; H, 5.51.

SCS-pincer palladium cutinase hybrid cut-1: The published inhibition protocol[50] was slightly modified: To a freshly prepared solution of cutinase mutant N172K (0.25 µmol, 250 µM, 1 mL, 1.0 equiv.) in Tris buffer (125 mM, pH 8.0, acid. with HBF_4) was added a solution of pincer palladium complex **1** (15.0 µL, 50 mM, 0.75 µmol, 3.0 equiv.) in MeCN. The mixture was left standing overnight, after which the mixture was dialysed with Tris buffer (2 x 400 mL) during 24 h. The contents of the dialysis membrane were transferred into an Eppendorf cuvette and diluted further with Tris buffer to the desired concentration for the catalysis experiments.

Activity tests with cut and cut-1: To a solution of Tris/Triton buffer (1.493 mL) was added a solution of *para*-nitrophenylbutyrate (7 µL, 0.35 µmol, 50 mM) in MeCN. To this mixture was added the respective enzyme (1 µL), after which the release of *para*-nitrophenolate was measured at 400 nm during 5 min. By doing so, the activities of the inhibited and free enzyme were compared.

Determination of the optimum catalyst loading: To different solutions of **cut-1** (A: 250 µM, 0.05 µmol, 0.025 equiv.; B: 200 µM, 0.04 µmol, 0.020 equiv.; C: 150 µM, 0.03 µmol, 0.015 equiv.; D: 100 µM, 0.02 µmol, 0.010 equiv.; E: 50 µM, 0.01 µmol, 0.005 equiv.) in Tris (200 µL) were added boronic acid (7.4 µL, 2.0 µmol, 40 mg/mL solution in DMSO, 1.0 equiv.), Cs_2CO_3 (2.6 µL, 4.0 µmol, 500 mg/mL solution in MQ-H_2O, 2.0 equiv.) and racemic vinyloxirane (1.6 µL, 20.0 µmol, 10.0 equiv.). The mixture was shaken at 25 °C (600 rpm) and after different time intervals samples were taken from the reaction mixture (30.0 µL). These samples were acidified with an aqueous HCl-solution (2.0 µL, 1M). After addition of the internal standard (2.0 µL, 12.0 mg/mL solution of anisole in MeCN), 5 µL of this solution was injected and analysed by HPLC.

Catalysis experiments: A typical catalysis run was performed as follows: To a solution of **cut-1** (200 μM, 0.04 μmol) in Tris buffer (210 μL) was added boronic acid (7.4 μL, 2.0 μmol, 40 mg/mL solution in DMSO, 1.0 equiv.), Cs_2CO_3 (2.6 μL, 4.0 μmol, 500 mg/mL solution in MQ-H_2O, 2.0 equiv.) and racemic vinyloxirane (1.6 μL, 20.0 μmol, 10.0 equiv.). The mixture was shaken at 25 °C (600 rpm) and after different time intervals samples were taken from the reaction mixture (30.0 μL). These samples were acidified with an aqueous HCl-solution (2.0 μL, 1M). After addition of the internal standard (12.0 mg/mL solution of anisole in MeCN), 5 μL of this solution was injected and analysed by HPLC.

Catalysis experiments with small molecular catalysts 4, 5 or $Pd(dba)_2$•$CHCl_3$: A typical catalysis run was performed as follows: To Tris buffer (200 μL) was added a solution of **4**, **5** or $Pd(dba)_2$•$CHCl_3$ (10 μL, 4 mM, 0.04 μmol) in MeCN, boronic acid (7.4 μL, 2.0 μmol, 40 mg/mL solution in DMSO, 1.0 equiv.), Cs_2CO_3 (2.6 μL, 4.0 μmol, 500 mg/mL solution in MQ-H_2O, 2.0 equiv.) and racemic vinyloxirane (1.6 μL, 20.0 μmol, 10.0 equiv.). The mixture was shaken at 25 °C (600 rpm) and after different time intervals samples were taken from the reaction mixture (30.0 μL). These samples were acidified with an aqueous HCl solution (2.0 μL, 1M). After addition of the internal standard (12.0 mg/mL solution of anisole in MeCN), 5 μL of this solution was injected and analysed by HPLC.

References

1. Creus, M.; Ward, T. R., *Org. Biomol. Chem.* **2007,** 5, 1835-1844.
2. Ward, T. R., *Chem. Eur. J.* **2005,** 11, 3798-3804.
3. Thomas, C. M.; Ward, T. R., *Chem. Soc. Rev.* **2005,** 34, 337-346.
4. Pordea, A.; Ward, T. R., *Chem. Commun.* **2008**, 4239-4249.
5. Ueno, T.; Abe, S.; Yokoi, N.; Watanabe, Y., *Coord. Chem. Rev.* **2007,** 251, 2717-2731.
6. Slim, M.; Sleiman, H. F., *Bioconjugate Chem.* **2004,** 15, 949-953.
7. Slim, M.; Durisic, N.; Grutter, P.; Sleiman, H. F., *ChemBioChem* **2007,** 8, 804-812.
8. Ma, D.-L.; Shum, T. Y.-T.; Zhang, F.; Che, C.-M.; Yang, M., *Chem. Commun.* **2005**, 4675-4677.
9. Youn, H. Y.; Terpetschnig, E.; Szmacinski, H.; Lakowicz, J. R., *Analytical Biochemistry* **1995,** 232, 24-30.
10. Lau, J. S.-Y.; Lee, P.-K.; Tsang, K. H.-K.; Ng, C. H.-C.; Lam, Y.-W.; Cheng, S.-H.; Lo, K. K.-W., *Inorg. Chem.* **2009,** 48, 708-718.
11. Albano, G.; Belser, P.; De Cola, L.; Gandolfi, M. T., *Chem. Commun.* **1999**, 1171-1172.
12. Lo, K. K.-W., *Struct. Bond.* **2007,** 123, 205-245.
13. Lo, K. K.-W.; Hui, W.-K., *Inorg. Chem.* **2005,** 44, 1992-2002.
14. Lo, K. K.-W.; Hui, W.-K.; Chung, C.-K.; Tsang, K. H.-K.; Ng, C. H.-C.; Zhu, N.; Cheung, K.-K., *Coord. Chem. Rev.* **2005,** 249, 1434-1450.
15. Lo, K. K.-W.; Lee, P.-K.; Lau, J. S.-Y., *Organometallics* **2008,** 27, 2998-3005.
16. Lo, K. K.-W.; Lee, T. K.-M.; Lau, J. S.-Y.; Poon, W.-L.; Cheng, S.-H., *Inorg. Chem.* **2008,** 47, 200-208.
17. Yang, X.-J.; Drepper, F.; Wu, B.; Sun, W.-H.; Haehnel, W.; Janiak, C., *Dalton Trans.* **2005**, 256-267.
18. Sculimbrene, B.; Imperiali, B., *J. Am. Chem. Soc.* **2006,** 128, 7346-7352.
19. Ryabov, A. D.; Goral, V. N.; Gorton, L.; Csoregi, E., *Chem. Eur. J.* **1999,** 5, 961-967.
20. Ueno, T.; Yokoi, N.; Unno, M.; Matsui, T.; Tokita, Y.; Yamada, M.; Ikeda-Saito, M.; Nakajima, H.; Watanabe, Y., *Proc. Natl. Acad. Sci. USA* **2006,** 103, 9416-9421.
21. Ueno, T.; Koshiyama, T.; Abe, S.; Yokoi, N.; Ohashi, M.; Nakajima, H.; Watanabe, Y., *J. Organomet. Chem.* **2007,** 692, 142-147.
22. Creus, M.; Pordea, A.; Rossel, T.; Sardo, A.; Letondor, C.; Ivanova, A.; LeTrong, I.; Stenkamp, R. E.; Ward, T. R., *Angew. Chem. Int. Ed.* **2008,** 47, 1400-1404.
23. Rutten, L.; Wieczorek, B.; Mannie, J.-P. B. A.; Kruithof, C. A.; Dijkstra, H. P.; Egmond, M. R.; Lutz, M.; Klein Gebbink, R. J. M.; Gros, P.; van Koten, G., *Chem. Eur. J.* **2009,** 15, 4270-4280 (Chapter 2 of this thesis).
24. Reetz, M. T.; Peyralans, J. J.-P.; Maichele, A.; Fu, Y.; Maywald, M., *Chem. Commun.* **2006**, 4318-4320.
25. Reetz, M. T.; Rentzsch, M.; Pletsch, A.; Maywald, M., *Chimia* **2002,** 56, 721-723.
26. Panella, L.; Broos, J.; Jin, J.; Fraaije, M. W.; Janssen, D. B.; Jeronimus-Stratingh, M.; Feringa, B. L.; Minnaard, A. J.; De Vries, J. G., *Chem. Commun.* **2005,** 45, 5656-5658.
27. Carey, J. R.; Ma, S. K.; Pfister, T. D.; Garner, D. K.; Kim, H. K.; Abramite, J. A.; Wang, Z.; Guo, Z.; Lu, Y., *J. Am. Chem. Soc.* **2004,** 126, 10812-10813.
28. Christensen, C. A.; Meldal, M., *Chem. Eur. J.* **2005,** 11, 4121-4131.
29. Rusbandi, U. E.; Lo, C.; Skander, M.; Ivanova, A.; Creus, M.; Humbert, N.; Ward, T. R., *Adv. Synth. Catal.* **2007,** 349, 1923-1930.
30. Lin, C.-C.; Lin, C.-W.; Chan, A. S. C., *Tetrahedron: Asymmetry* **1999,** 10, 1887-1893.
31. Skander, M.; Malan, C.; Ivanova, A.; Ward, T. R., *Chem. Commun.* **2005**, 4815-4817.
32. Letondor, C.; Pordea, A.; Humbert, N.; Ivanova, A.; Mazurek, S.; Novic, M.; Ward, T. R., *J. Am. Chem. Soc.* **2006,** 128, 8320-8328.
33. Thomas, C. M.; Letondor, C.; Humbert, N.; Ward, T. R., *J. Organomet. Chem.* **2005,** 690, 4488-4491.
34. Ueno, T.; Koshiyama, T.; Ohashi, M.; Kondo, K.; Kono, M.; Suzuki, A.; Yamane, T.; Watanabe, Y., *J. Am. Chem. Soc.* **2005,** 127, 6556-6562.
35. Yamaguchi, H.; Hirano, T.; Kiminami, H.; Taura, D.; Harada, A., *Org. Biomol. Chem.* **2006,** 4, 3571-3573.
36. Pierron, J.; Malan, C.; Creus, M.; Gradinaru, J.; Hafner, I.; Ivanova, A.; Sardo, A.; Ward, T. R., *Angew. Chem. Int. Ed.* **2008,** 47, 701-705.

37. Ohashi, M.; Koshiyama, T.; Ueno, T.; Yanase, M.; Fujii, H.; Watanabe, Y., *Angew. Chem. Int. Ed.* **2003,** 42, 1005-1008.
38. Davies, R. R.; Kuang, H.; Qi, D.; A., M.; Mayaan, E.; Distefano, M. D., *Bioorg. Med. Chem. Lett.* **1999,** 9, 79-84.
39. Wilson, M. E.; Whitesides, G. M., *J. Am. Chem. Soc.* **1978,** 100, 306-307.
40. Skander, M.; Humbert, N.; Collot, J.; Gradinaru, J.; Klein, G.; Loosli, A.; Sauser, J.; Zocchi, A.; Gilardoni, F.; Ward, T. R., *J. Am. Chem. Soc.* **2004,** 126, 14411-14418.
41. Letondor, C.; Humbert, N.; Ward, T. R., *Proc. Natl. Acad. Sci. USA* **2005,** 102, 4683-4687.
42. Davies, R. R.; Distefano, M. D., *J. Am. Chem. Soc.* **1997,** 119, 11643-11652.
43. Gallagher, J.; Zelenko, O.; Walts, A. D.; Sigman, D. S., *Biochemistry* **1998,** 37, 2096-2104.
44. Hayashi, T.; Hisaeda, Y., *Acc. Chem. Res.* **2002,** 35, 35-43.
45. Sato, H.; Hayashi, T.; Ando, T.; Hisaeda, Y.; Ueno, T.; Watanabe, Y., *J. Am. Chem. Soc.* **2004,** 126, 436-437.
46. Matsuo, T.; Murata, D.; Hisaeda, Y.; Hori, H.; Hayashi, T., *J. Am. Chem. Soc.* **2007,** 129, 12906-12907.
47. Reetz, M. T.; Jiao, N., *Angew. Chem. Int. Ed.* **2006,** 45, 2416-2419.
48. Kokubo, T.; Sugimoto, T.; Uchida, T.; Tanimoto, S.; Okano, M., *J. Chem. Soc., Chem. Commun.* **1983**, 769-770.
49. Coquiere, D.; Bos, J.; Beld, J.; Roelfes, G., *Angew. Chem. Int. Ed.* **2009,** 48, 5159-5162.
50. Kruithof, C. A.; Casado, M. A.; Guillena, G.; Egmond, M. R.; van der Kerk-van Hoof, A.; Heck, A. J. R.; Klein Gebbink, R. J. M.; van Koten, G., *Chem. Eur. J.* **2005,** 11, 6869-6877.
51. Kruithof, C. A.; Dijkstra, H. P.; Lutz, M.; Spek, A. L.; Klein Gebbink, R. J. M.; van Koten, G., *Organometallics* **2008,** 27, 4928-4937.
52. Longhi, S.; Cambillau, C., *Biochim. Biophys. Acta* **1999,** 1441, 185-196.
53. Longhi, S.; Mannesse, M. L. M.; Verheij, H. M.; De Haas, G. H.; Egmond, M.; Knoops-Mouthuy, E.; Cambillau, C., *Protein Sci.* **1997,** 6, 275-286.
54. Longhi, S.; Nicolas, A.; Creveld, L.; Egmond, M.; Verrips, C. T.; de Vlieg, J.; Martinez, C.; Cambillau, C., *Proteins* **1996,** 26, 442-458.
55. Schmidinger, H.; Birner-Gruenberger, R.; Riesenhuber, G.; Saf, R.; Susani-Etzerodt, H.; Hermetter, A., *ChemBioChem* **2005,** 6, 1776-1781.
56. Schmidinger, H.; Susani-Etzerodt, H.; Birner-Gruenberger, R.; Hermetter, A., *ChemBioChem* **2006,** 7, 527-534.
57. Albrecht, M.; Lutz, M.; Spek, A. L.; van Koten, G., *Nature* **2000,** 406, 970-971.
58. Hall, J. R.; Loeb, S. J.; Shimizu, G. K. H.; Yap, G. P. A., *Angew. Chem. Int. Ed.* **1998,** 37, 121-123.
59. Albrecht, M.; van Koten, G., *Angew. Chem. Int. Ed.* **2001,** 40, 3750-3781.
60. Kruithof, C. A.; Dijkstra, H. P.; Lutz, M.; Spek, A. L.; Egmond, M. R.; Klein Gebbink, R. J. M.; van Koten, G., *Eur. J. Inorg. Chem.* **2008,** 28, 4425-4432.
61. van Manen, H.-J.; Nakashima, K.; Shinkai, S.; Kooijman, H.; Spek, A. L.; van Veggel, F. C. J. M.; Reinhoudt, D. N., *Eur. J. Inorg. Chem.* **2000**, 2533-2540.
62. Bergbreiter, D. E.; Osburn, P. L.; Liu, Y.-S., *J. Am. Chem. Soc.* **1999,** 121, 9531-9538.
63. Yount, W. C.; Loveless, D. M.; Craig, S. L., *Angew. Chem. Int. Ed.* **2005,** 44, 2746-2748.
64. Huck, W. T. S.; Prins, L. J.; Fokkens, R. H.; Nibbering, N. M. M.; van Veggel, F. C. J. M.; Reinhoudt, D. N., *J. Am. Chem. Soc.* **1998,** 120, 6240-6246.
65. Huck, D. M.; Nguyen, H. L.; Coles, S. J.; Hursthouse, M. B.; Donnio, B.; Bruce, D. W., *J. Mater. Chem.* **2002,** 12, 2879-2886.
66. Huck, D. M.; Nguyen, H. L.; Horton, P. N.; Hursthouse, M. B.; Guillon, D.; Donnio, B.; Bruce, D. W., *Polyhedron* **2006,** 25, 307-324.
67. Kjellgren, J.; Aydin, J.; Wallner, O. A.; Saltanova, I. V.; Szabó, K. J., *Chem. Eur. J.* **2005,** 11, 5260-5268.
68. *The Chemistry of Pincer Compounds*. Elsevier: Amsterdam, 2007; p 1-466.
69. Singleton, J. T., *Tetrahedron* **2003,** 59, 1837-1857.
70. Gagliardo, M.; Selander, N.; Mehendale, N. C.; van Koten, G.; Klein Gebbink, R. J. M.; Szabó, K. J., *Chem. Eur. J.* **2008,** 14, 4800-4809.
71. Huck, W. T. S.; van Veggel, F. C. J. M.; Reinhoudt, D. N., *J. Mater. Chem.* **1997,** 7, 1213-1219.
72. *The elemental analysis of complex 4 indicated that this complex was not totally pure. The similar catalytic activity in comparison to Pd(dba)2•CHCl3 could indicate that the same*

catalytic species is active in the C-C coupling reaction. During the printing of this thesis experiments investigating the nature of the catalytic species were ongoing.
73. Lucena, N.; Casabo, J.; Escriche, L.; Sanchez-Castello, G.; Teixidor, F.; Kivekas, R.; Sillanpaa, R., *Polyhedron* **1996,** 15, 3009-3018.
74. Kickham, J. E.; Loeb, S. J., *Organometallics* **1995,** 14, 3584-3587.
75. Dijkstra, H. P.; Sprong, H.; Aerts, B. N. H.; Kruithof, C. A.; Egmond, M. R.; Klein Gebbink, R. J. M., *Org. Biomol. Chem.* **2008,** 6, 523-531.
76. Slagt, M. Q.; Rodriguez, G.; Grutters, M. M. P.; Klein Gebbink, R. J. M.; Klopper, W.; Jenneskens, L. W.; Lutz, M.; Spek, A. L.; van Koten, G., *Chem Eur. J.* **2004,** 10, 1331-1344.
77. Komiya, S., *Synthesis of Organometallic Compounds*. Wiley: Chichester, UK, 1997.
78. Davies, P. J.; Grove, D. M.; van Koten, G., *Organometallics* **1997,** 16, 800-802.
79. Keegstra, E. M. D.; Zwikker, J. W.; Roest, M. R.; Jenneskens, L. W., *J. Org. Chem.* **1992,** 57, 6678-6680.
80. Duisenberg, A. J. M.; Kroon-Batenburg, L. M. J.; Schreurs, A. M. M., *J. Appl. Cryst.* **2003,** 36, 220-229.
81. Sheldrick, G. M. *SADABS: Area-Detector Absorption Correction*, 2.10; Universitaet Goettingen: Goettingen, 1999.
82. Sheldrick, G. M., *Acta Cryst.* **2008,** A64, 112-122.
83. Spek, A. L., *Acta Cryst.* **2009,** D65, 148-155.

CHAPTER 6

Site-Selective Ser-Hydrolase Labelling with a Luminescent Organometallic NCN-Platinum Complex

The synthesis, spectroscopic properties and protein binding studies of a novel luminescent organometallic NCN-platinum complex are described. The luminescent organometallic complex was linked to a serine hydrolase-reactive phosphonate group via click chemistry, and was exploited in serine hydrolase specific binding studies using gel-electrophoresis.

The NCN-platinum protein label was found to be a robust dye with absorbance and emission maxima between 374-380 nm and 482-493 nm, respectively, and quantum yields between 0.04-0.15.

Introduction

Luminescence probes are playing an important role in the study and understanding of biomolecular processes, such as protein functioning within cells,[1] membrane dynamics[2] and tumor cell surface targeting.[3] Various luminescence techniques, *e.g.* Förster Resonance Energy Transfer (FRET)[4, 5] and Single Molecule Spectroscopy[5, 6] have become increasingly important tools in the study of these phenomena. The design and development of novel luminescent probes is crucial for the advancement of this field.

Excellent examples illustrating the power of luminescence in biology are the use of the Green,[7] Yellow or Cyan Fluorescent Proteins (GFP, YFP, CFP) in the labelling of reporter molecules in cells to study intracellular dynamics.[8-13] Also various commercially available synthetic luminescent small-molecule organic dyes,[14, 15] with different emission wavelengths and various protein reactive groups (*e.g.* maleimide functional groups for cysteine labelling) are increasingly used in proteomics in order to screen for different types of proteins and monitor their activity profiles.[16, 17] These dyes are generally smaller in size and possess a lower molecular weight than the protein-based luminescent labels, which enables chemists to more easily alter their spectroscopic and protein binding properties through chemical synthesis.[16, 17]

In the emerging field of activity-based protein profiling, novel small molecular probes are highly desirable, *e.g.* for the targeting of cancer-inducing mutated proteins.[18] When luminescent dyes with different emission wavelengths are combined with various protein-reactive functional groups, a wide spectrum of the proteome can potentially be addressed and studied with these luminescent probes. For instance, Cravatt and co-workers have probed several different enzyme classes like aspartyl proteases, deubiquitinating enzymes, glycosidases and serine hydrolases through the design of a variety of enzyme targeted probes based on their active site reactivity and substrate selectivity.[19-21]

Currently, our group is working on the development of protein reactive probes as well, with the aim of modifying serine hydrolases and lipases for protein diagnosis purposes and/or for the construction of novel semisynthetic enzymes.[22-27] By doing so, various phosphonate inhibitors substituted by different organic[25, 26] and organometallic moieties[22-24, 27] have been used to target different lipases (Figure 1). Phosphonates have long been known to be substrate analogues for serine hydrolases and even phosphonates with various organic luminescent reporter tags have been studied by different groups.[20, 25, 28-30] So far, phosphonates substituted by organic dyes, *e.g.* luminescent dansyl (Figure 1),[25] rhodamine[18] and *para*-nitrobenzofurazan[31] groups have been used in luminescence labelling studies.

With the organometallic ECE-pincer metal phosphonate inhibitors[22-24] developed by our group, we have been exploiting the special properties of the heavy metal atom probe, *e.g.* as coordination target for phosphines and as phasing tool for the elucidation of protein crystal structures.[24, 32]

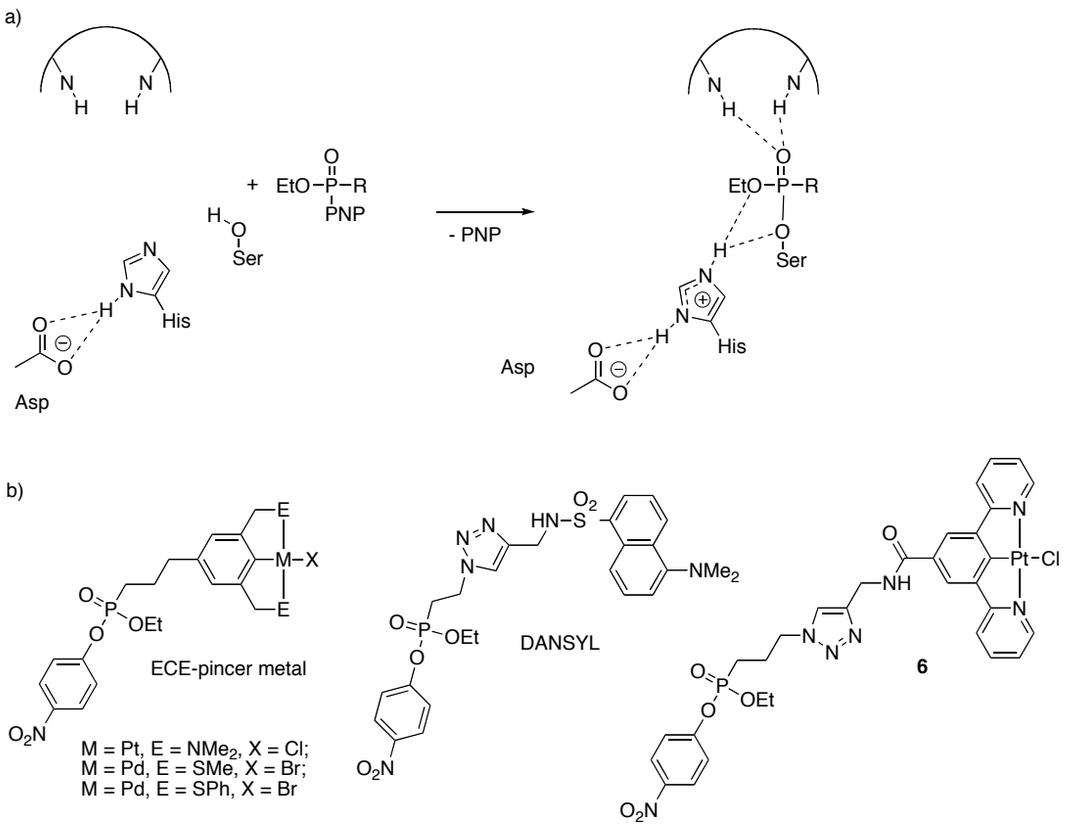

Figure 1: a) General inhibition reaction of serine hydrolases with phosphonates (PNP = *para*-nitrophenolate anion). b) Structures of organometallic ECE-pincer metal phosphonates (left),[23, 24] of an organic luminescent dansyl phosphonate inhibitor (middle),[25] and of the organometallic luminescent target inhibitor **6** (right).

Interestingly, many different coordination complexes with exciting luminescent properties are known from the literature,[33-35] but only very few of them have been used in the labelling of biomolecules,[36-53] which is mainly caused by the instability (*e.g.* water- or redox-sensitivity) of these complexes under biological conditions. Inspired by the high quantum yields of various organoplatinum complexes, as demonstrated by the Williams group[54-57] and by our own results on the design and applications of novel organometallic phosphonate inhibitors, we embarked on the modification of one of these highly luminescent NCN-platinum complexes[55] (complex **1**, Scheme 1), in order to develop a novel luminescent organometallic NCN-platinum phosphonate inhibitor (**6**, Figure 1, Scheme 1). Organometallic pincer complexes possess a covalent metal-carbon bond, which is completed by two *ortho*-chelated metal-hetero atom interactions.[22-24, 55, 58-60] This combination of metal-ligand interactions leads to a high stability in aqueous and biological media, which in turn let us to expect that these complexes would be stable luminescence labels for protein profiling.

Contrary to common organic luminescent probes, which generally emit from a singlet excited state, these complexes emit from a low lying triplet excited state, due to the influence of the heavy metal.[35, 56] In general, the absorbance and the emission maxima display a large Stokes shift, which is different from common organic luminescent dyes.[36, 41] These special features of organometallic luminescent complexes can potentially be used in novel spectroscopic techniques, *e.g.* luminescence resonance energy transfer (LRET) or anisotropy studies on dynamic protein interactions.[36, 51] Additionally, a rich and diverse chemistry is known for similar NCN transition metal complexes, including chemical sensing, supramolecular coordination chemistry and catalysis.[59]

Here, we report on the synthesis of the novel luminescent NCN pincer platinum probe **6** and its photophysical properties in both organic and biological media. We, furthermore, illustrate how this probe can be used for the efficient, diagnostic labelling of several proteins.

Results and Discussion

Synthesis of the luminescent pincer platinum phosphonate complex.
The synthesis of the luminescent NCN-platinum inhibitor **6** was pursued *via* two different routes a) and b), both by means of a Cu(I) catalysed click reaction as a crucial step to introduce the reactive PNP phosphonate group (PNP = *para*-nitrophenolate anion) using a propyl azido phosphonate reagent (**4**) similar to the ethyl azido phosphonate reagent[25] developed earlier by us (Scheme 1). The Cu(I) catalyzed click reaction[61, 62] between an azide and an alkyne has been widely studied and is known to be very selective, tolerant to functional groups and can be performed under very mild conditions, even with unactivated alkynes.[63, 64] Due to the anticipated sensitive nature of the PNP-phosphonate group (PNP is a very good leaving group), it was initially decided to perform the click reaction as the last step in the synthesis of **6** (pathway a, Scheme 1).

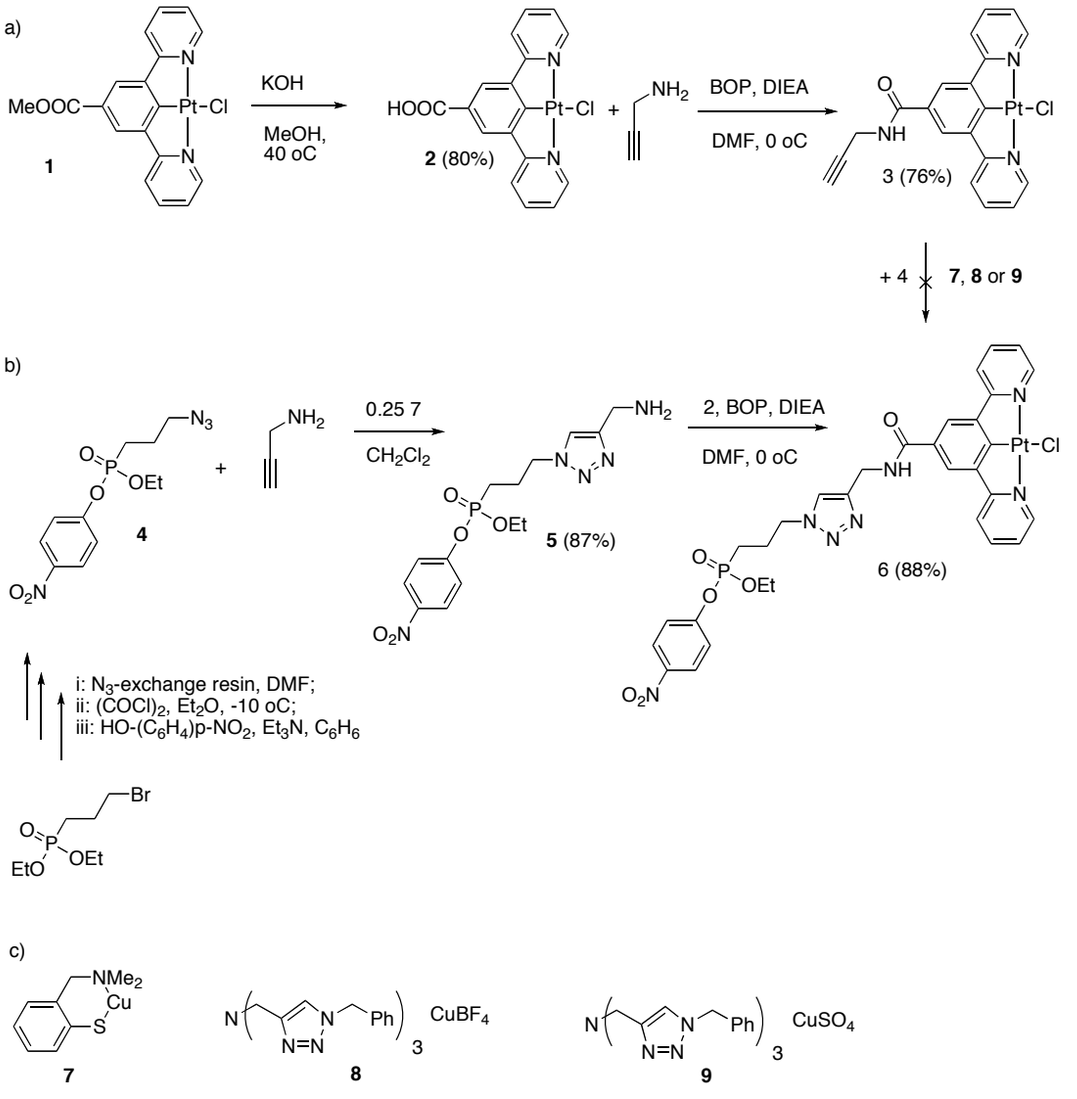

Scheme 1: Explored routes (a and b) towards the synthesis of the luminescent pincer platinum phosphonate inhibitor **6**; the different tested click catalysts are shown under c.

Route a started with the hydrolysis of ester **1**[65] to the corresponding acid **2**, after which an amide coupling was performed with propargylamine to obtain complex **3**. Contrary to the general ease with which click reactions are performed,[61, 62] initial attempts to realize the subsequent Cu(I) catalyzed click reaction under standard reaction conditions (acetylene:azide = 1:1, 10-20 mol% **9** in MeCN or DMF/THF = 1:1) did not work. Therefore, it was decided to screen for optimum reaction conditions by varying the solvents, Cu(I) catalysts (**7**[66], **8** and **9**[63]), catalyst loadings (10-23 mol%), concentrations, reaction temperatures (RT-40 ^{o}C) and times (12h-5 days). Based on ^{31}P and ^{1}H NMR analysis, none of these screens gave rise to any formation of the desired product. This was rather surprising, since other NCN-

platinum type complexes containing acetylene moieties were successfully applied under standard click reaction conditions in our laboratory before.[67] Therefore it was decided to attempt an alternative synthesis route to **6**.

In the alternative route b, the click reaction between phosphonate **4** and propargyl amine was performed in the first step, with aminoarenethiolate catalyst **7** giving the highest activity when compared to the commonly used click catalysts **8** or **9**.[61, 63] The subsequent amide coupling reaction of **5** with **2** in the presence of BOP gave rise to the formation of target molecule **6**, which was isolated in 77% overall yield starting from **4**. Complex **6** was characterized by ^{1}H, ^{31}P, ^{13}C NMR and IR spectroscopy, high-resolution mass spectrometry and by photophysical methods (*vide infra*). Notably, both the organometallic complex **2** and phosphonate **5** did not show any signs of decomposition under the applied reaction conditions. The resulting inhibitor **6** possesses only limited solubility in common organic solvents; it was only found to be sufficiently soluble in DMSO, DMF and in a DMF/buffer mixture for the inhibition studies, and therefore these solvents were used in the subsequent enzyme inhibitions and in the spectroscopic studies.

Spectroscopic characterization of the various NCN pincer platinum complexes.
The various NCN-platinum complexes (**1**-**3**, **6**, Scheme 1) were characterized by UV-vis absorption (Figure 2) and emission spectroscopy (Figure 3). The photophysical data for **1**-**3** and the phosphonate inhibitor **6** are collected in Table 1. Due to both the limited solubility of each of these complexes in common organic solvents and their complete insolubility in water or buffer solutions, solvents commonly used for spectroscopic analyses (*e.g.* CH_2Cl_2, hexane or THF) could not be used. As a result, the solvent used by the Williams group (dichloromethane),[55] was not suitable for the spectroscopic studies of **1**-**3** and **6**. DMF appeared to be the only solvent in which all complexes dissolved readily. Since DMF is a strongly coordinating solvent, it is not the ideal solvent for performing the spectroscopic studies; coordinating solvents are very likely to decrease the photophysical properties of the luminescent platinum complexes (*i.e.* lowering the quantum yield). However, it is the only solvent that allows comparison of all complexes (**1**-**3**, **6**). Note, that in cases where a complex is soluble in another solvent besides DMF, the spectroscopic data in this solvent are reported as well (Table 1).

Table 1: Photophysical data of the pincer platinum complexes **1**-**3** and inhibitor **6**.

Complex	Solvent[a]	Absorbance λ_{max} (nm)[b]	ε ($M^{-1}cm^{-1}$)	Luminescence λ_{max} (nm)[b]	Quantum yield[b, c]
1	DMF	380	14940	481[d]	0.08
	MeCN	376	10980	480[d]	0.31
	CH_2Cl_2	380	9840	482[e]	0.38
2	DMF	380	9270	481[e]	0.21
	MeCN	377	3120	480[d]	0.08
3[f]	DMF	380	8770	485[e]	0.17
6	DMF	380	12320	493[d]	0.05
	MeCN	377	3650	487[d]	0.04
	CH_2Cl_2	380	8220	490[d]	0.15
	DMF[g]	374	9470	482[d]	0.04

[a] Sample dissolved in the indicated solvent; the solubility of all complexes in H_2O, 125 mM Tris (pH 8.0), Tris (50 mM), 0.1% (m/m) Triton (pH 8.0) or 150 mM NH_4OAc buffer was too low to allow for appropriate measurements; [b] measured in deaerated solutions; [c] uncertainty ±20%; [d] value was obtained from measurements using $[Ru(bpy)_3]Cl_2$ in H_2O (ϕ = 0.028) as internal standard; [e] value was obtained from measurements using $[Ru(bpy)_3](PF_6)_2$ in MeCN (ϕ = 0.062) as internal standard; [f] the solubility of complex **3** in MeCN and CH_2Cl_2 was too low to allow for measurements; [g] a 150 mM NH_4OAc buffer/DMF mix (1/1 v/v) was used.

The UV-vis absorption spectra of **1**-**3** and **6** in DMF display very similar features with a strong absorbance region between 350-440 nm (Figure 2). All complexes have an absorbance maximum between 374-380 nm, seeming to be almost independent of the nature of the solvent used (Table 1, *vide infra*). The strong features in the absorbance region from 350-440 nm are assigned to $^1\pi$-π* transitions of the ligands and to charge transfer transitions.[55]

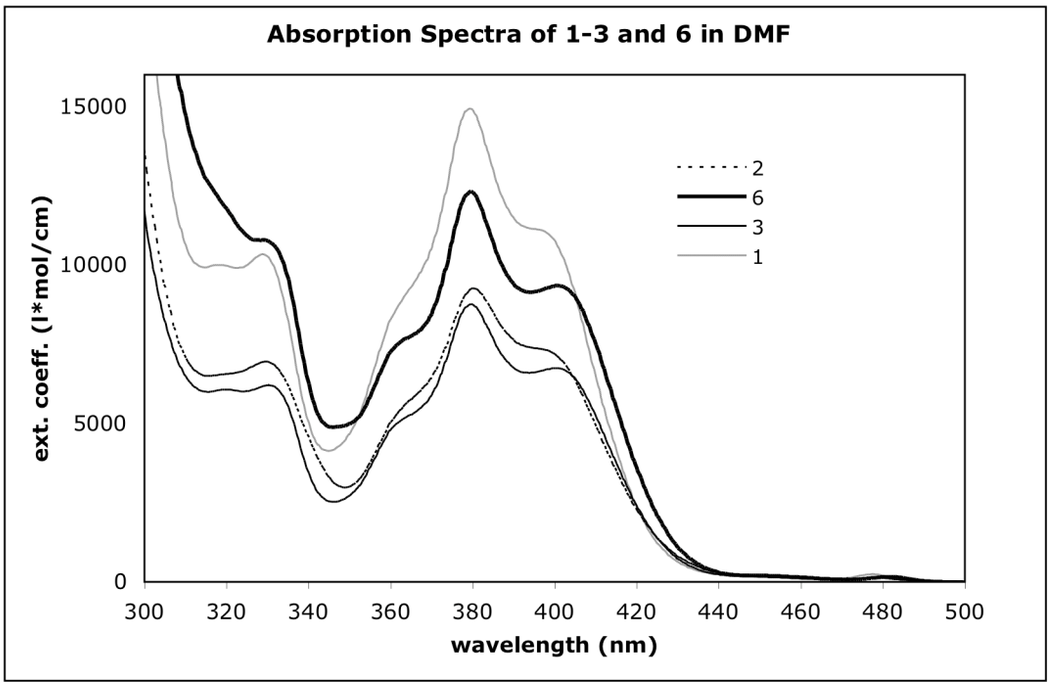

Figure 2: Absorption spectra of NCN-platinum complexes **1**-**3** and inhibitor **6** in DMF

All complexes are luminescent in solution and the emission spectra display very similar features with maxima between 480-493 nm (Figure 3). The quantum yields in different solvents vary from 0.04-0.38, with the highest quantum yield for the parent ester complex **1** in dichloromethane and lower quantum yields for inhibitor **6** (Table 1).

The emission maxima are slightly red-shifted with a small Stokes shift increasing in the order **1**=**2**<**3**<**6**. Similar to the red shift of the lower energy absorption features (Figure 2), the emission energy is also red shifted when changing the *para*-substituent of the NCN-platinum complex from –C(O)OMe (complex **1**) to –C(O)N(H)-R (**3** and inhibitor **6**), which is probably due to the electronic nature of the different substituents.[68] The quantum yield for **6** in DMF is slightly decreased in comparison to **1**-**3**.

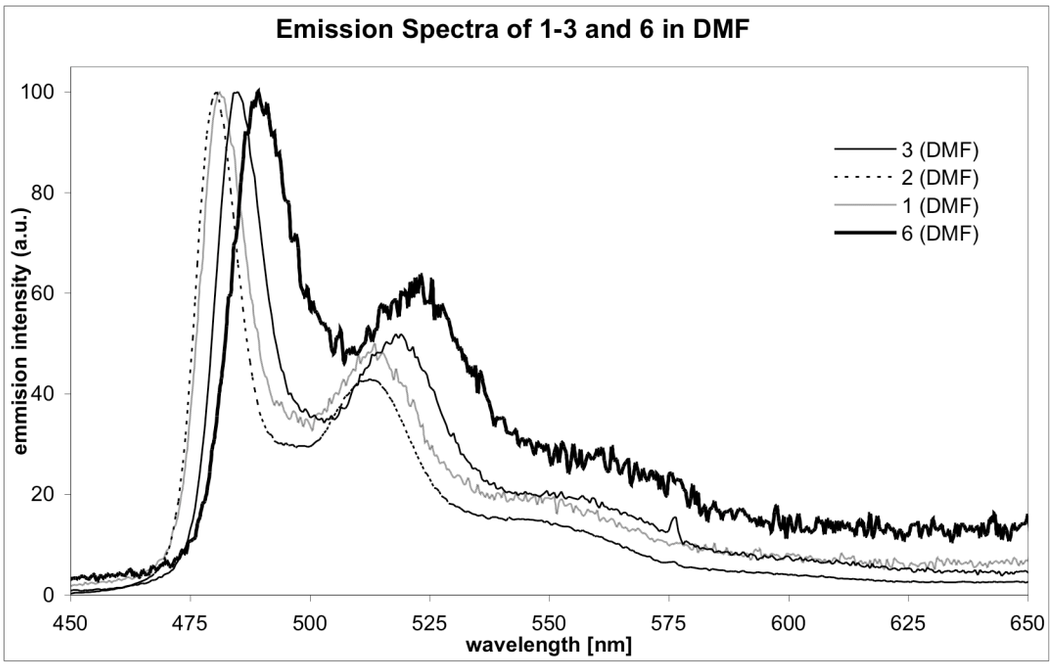

Figure 3: Normalized Emission spectra of NCN-platinum complexes **1**-**3** and inhibitor **6** in DMF.

*Lipase labelling studies with inhibitor **6.***

The pincer platinum phosphonate inhibitor **6** was applied as a site-selective inhibitor in labelling studies of different serine hydrolases. Due to the poor solubility of **6**, previous protocols to study artificial enzymes[22-26] were adapted for protein labelling studies with luminescent probe **6**. As a model protein for the labelling studies cutinase from *Fusarium solani pisi* (21 kDa) was chosen. Cutinase is a lipase with high esterase activity which is also known to be very reactive towards phosphonate inhibitors.[22, 23, 25] Therefore, to a solution of cutinase in buffer (200 μM, pH 8.0) was added a solution of phosphonate **6** (6 equivalents, 10 mM) in DMF. After incubation overnight, the excess of inhibitor was removed by dialysis with buffer (see experimental section for details) and an activity test of the resulting solution was performed. This test showed no residual ester-hydrolysis activity for cutinase, indicating complete inhibition of cutinase by **6** as a result of the formation of **cut-6**.[22-24] Illumination of the inhibited cutinase batches at 257 nm showed that the enzyme solutions were luminescent after inhibition and dialysis (Figure 4), indicating successful protein labelling (**cut-6**) and a high stability of the organometallic label **6** under the described conditions. After exposure of the **cut-6** solution to UV-light during 5 minutes the solution was still luminescent. Storage of the **cut-6** protein solution in the fridge during 6 weeks also did not affect its emission properties.

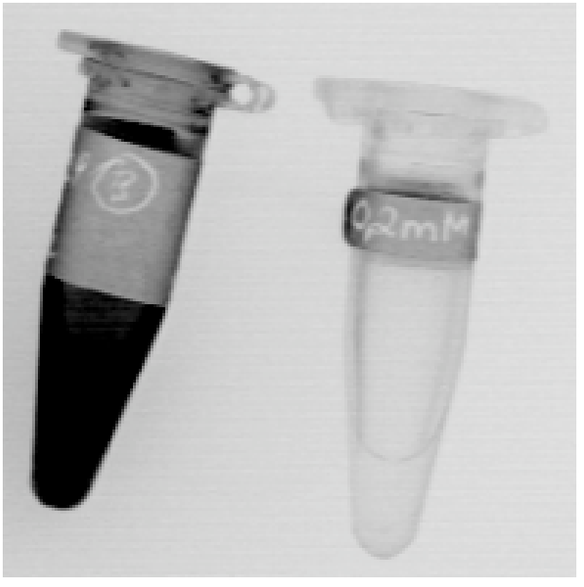

Figure 4: Photograph of cutinase solutions (200 μM) under UV-light (excitation wavelength 257 nm); left: After incubation with inhibitor **6** and subsequent dialysis (**cut-6**); right: Cutinase solution without inhibitor.

Encouraged by these results, it was decided to investigate the labelling properties of **6** towards other proteins[25, 26] and to assay the formation and stability of the covalent **protein-6** adducts by performing gel-electrophoresis. For this study, the serine hydrolases *Bacillus subtilis* lipase A (BSLA)[69] (19 kDa), commercially available *Candida antarctica* lipase B (33 kDa), and cutinase as reference protein were chosen.

The solutions of the respective enzymes in buffer (pH 8.0) were incubated with a solution of luminescent inhibitor **6** (in DMF) overnight. Also, a control experiment without **6** was performed simultaneously. These solutions were used (*i.e.* without any further treatment) in gel-electrophoresis using a SDS-PAGE gel. The luminescence and Coomassie stained photograph of the gel are shown in Figure 5.

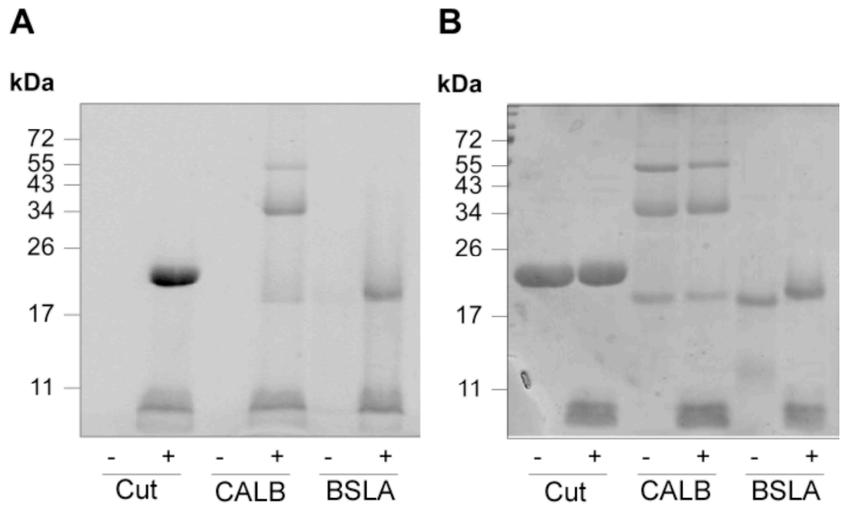

Figure 5: Luminescence (A) and Coomassie (B) stained gel of cutinase (Cut), *Candida antarctica* lipase B (CALB) and *Bacillus subtilis* lipase A (BSLA) without (-) and after (+) exposure to **6** overnight. As the samples were not dialysed prior to gel-electrophoresis, the excess of unreacted **6** at the lower end of the gels (below the 11 kDa line) is visible.

The luminescent gel photograph shows that luminescent labelling of cutinase, CALB and BSLA did occur indeed (Figure 5A). The Coomassie stained photograph of the same gel shows that also in the samples without **6** protein was present (Figure 5B). Since SDS-PAGE is run under denatured protein conditions, these experiments clearly prove the covalent labelling of the different proteins by **6**. The different **protein-6** molecules were still luminescent after gel-electrophoresis conditions, showing again the stability of inhibitor **6**.

*Spectroscopy with **cut-6** at different pH values and under denatured conditions.*
Different, commonly used organic dyes, like *e.g.* fluorescein, are not very photostable and their luminescence emission properties often depend on the polarity and pH value of their environment.[16, 17] Furthermore, the active site His^{188} residue in cutinase (Figure 1, pKa(His) ~ 6.5) could be (de)protonated, thereby potentially exerting an influence on the spectroscopic properties of the luminescent metal dye in **cut-6**. To investigate the chemical robustness and the influence of the environment polarity and of the pH value on the spectroscopic properties of protein label **6**, it was decided to analyse a **cut-6** solution at different pH values in Tris/Triton buffer and under denatured conditions. The emission spectrum of **cut-6** at pH 5, 7 and 9 in Tris/Triton buffer is shown in Figure 6. For all measurements the quantum yield remained constant within the experimental error (0.20-0.12, uncertainty ±20%).

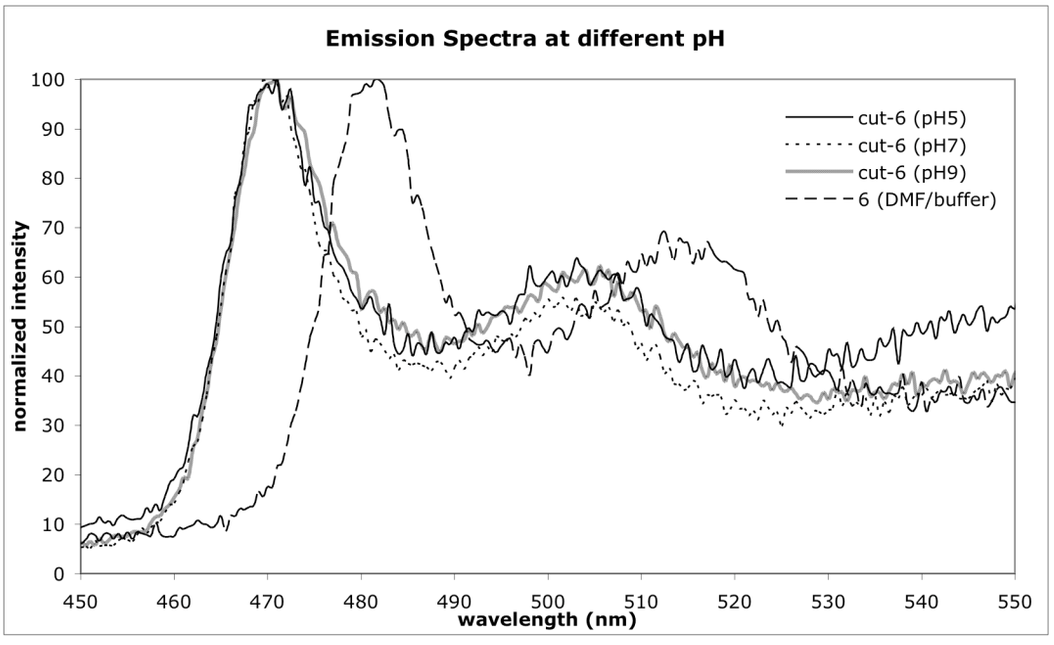

Figure 6: Normalized luminescence spectra of **cut-6** at pH 5, 7 and 9 in Tris/Triton buffer; for comparison, the spectrum of inhibitor **6** in DMF/buffer (1/1 v/v, buffer: Tris/Triton, pH 8.0) has been included.

Table 2: The absorbance λ_{max}, luminescence λ_{max} and quantum yield values for **cut-6** at pH 5, 7 and 9 in Tris/Triton buffer.

Compound	pH[a]	Absorbance λ_{max} (nm)	Luminescence λ_{max} (nm)	Quantum yield[b]
cut-6	5	376	471	0.20
cut-6	7	378	470	0.13
cut-6	9	377	471	0.12
6	8 (DMF/buffer)	374	482	0.04

[a] Measurements were performed in 0.1% (m/m) Triton, 50 mM Tris buffer at the indicated pH value; [b] uncertainty ±20%.

The luminescence spectra of **cut-6** at pH 5, 7 and 9 all display very similar features with nearly identical absorbance (376-378 nm) and emission (470-471 nm) maxima (Figure 6, Table 2). The absorbance and emission maxima of **cut-6** in Tris/Triton buffer are blue shifted in comparison to inhibitor **6** in DMF or in a DMF/buffer mixture (Table 1), indicating solvatochromism. The quantum yield of **cut-6** at pH 5, 7 and 9 is also higher than for **6** in DMF or DMF/buffer (Table 1), which was attributed to the

hydrophobic environment of the cutinase active site[24, 70-72] into which the metal moiety is embedded in **cut-6**.

The study of **cut-6** at different pH values showed that the dye is remarkably stable in the pH range 5-9, making it widely applicable.[24, 70-72] The protonated (< pH 6.5) or deprotonated (> pH 6.5) state of the ^{188}His residue in cutinase did not significantly affect the spectroscopic properties of the dye. This spectroscopic behaviour differs from commonly used luminescent organic dyes like fluorescein and rhodamine,[14, 41] being pH dependent, and from some other biological transition metal labels like redox-active probes (*e.g.* ferrocene derivatives),[36] which have been reported to be very sensitive for changes in pH.

Conclusions

The design, syntheses and spectroscopic analyses of luminescent inhibitor **6** and its use in protein labelling studies are demonstrated. It turns out that inhibitor **6** is a very stable, luminescent organometallic complex, which can be selectively used for the labelling of various lipases. Complexes **1**-**3** and **6** display the expected photophysical properties with the emission energy and quantum yield decreasing after introduction of the amide functionality (for **3** and **6**), but maintaining a clearly luminescent complex. The luminescent properties of **6** can potentially be used in novel spectroscopic applications, *e.g.* Luminescence Resonance Energy Transfer (LRET)[51] with an organic dye and subsequent phosphorescence emission by this dye, thereby expanding the spectroscopic toolbox for studying biomolecules.

Previous studies by our group[25] have shown that phosphonate inhibitors are selective for serine hydrolases and do not react with other proteins lacking the reactive active-site residue. Furthermore, we illustrated that such inhibitors can even be used to selectively label proteins in living cells and as such have been used for protein isolation and identification. This opens up the possibility to use **6** as a luminescent lipase-specific label in cell-lysates and for future proteomic applications. Currently, we are investigating how the properties of organometallic pincer complexes can be used in this area, *e.g.* by exploiting the unique coordination properties of the platinum metal centre.[32]

In conclusion, this study shows that organometallic pincer-platinum complexes[73] can be used for diagnostic targeting of proteins, which in combination with a serine hydrolase reactive phosphonate inhibitor opens up new activity-based protein profiling possibilities. The proof-of-principle methodology demonstrated here is by no means limited to serine hydrolases; the chemical versatility of pincer complexes also allows attachment to other biochemical probes like, *e.g.*, carbohydrates or oligopeptides.[58, 59, 74, 75]

Experimental Section

General comments: All reagents were used as supplied from Acros or Sigma-Aldrich, unless stated otherwise. MeCN and CH_2Cl_2 were distilled over CaH_2. All synthetic procedures were performed under an inert atmosphere using Schlenk techniques and distilled solvents, unless stated otherwise. The enzyme inhibition studies and dialysis experiments were performed in air. Water for the preparation of the buffer solutions was filtered with the Milli-Q filtration system (Millipore, Quantum Ultrapure) prior to use. The dialysis cassettes (Slide-A-Lyzer™, 10,000 MWCO, 0.1-0.5 mL or 0.5-3 mL) for the purification of enzyme NCN-platinum hybrids were purchased from Pierce. cutinase mutant N172K was provided by Unilever. BSLA was provided by Prof. Wim J. Quax and co-workers.[69] CALB (batch PPW 4534) was purchased from Novo Nordisk A/S, Copenhagen, Denmark. Electrospray ionization mass spectra and high resolution electrospray ionization mass spectra were recorded on a Micromass LCT spectrometer. All samples were introduced using a nanoflow electrospray source (Protana, Odense, Denmark) and all spectra were calibrated with a CsI solution (50 mg/mL in MQ-H_2O). Matrix-assisted laser desorption ionization mass spectrometry experiments were performed with a Voyager-DE Pro (Applied Biosystems) instrument in the reflector mode with trihydroxy anthracene in MeCN as matrix. Photographs of SDS-PAGE gels were taken in a BioRad GelDoc 2000 workstation (exciation wavelength 257 nm). Elemental microanalyses were performed by Dornis and Kolbe, Mikroanalytisches Laboratorium (Mülheim a/d Ruhr, Germany). NMR measurements were performed on a Varian Inova 300 MHz or Varian Oxford 400 MHz spectrometer at 298 K. The syntheses of **1**[65] and **7**[66] were carried out as reported.

Electronic spectroscopic measurements: UV-vis spectra were recorded on a Varian Cary 50 Scan UV-visible spectrometer. Luminescence spectra were obtained on a SPEX fluorolog spectrometer with $[Ru(bpy)_3](PF_6)_2$ in degassed MeCN as standard (φ_r = 0.062). Emission quantum yields were measured by the method of Crosby and Demas[76] in degassed solvents and calculated by $\varphi_S = \varphi_r(B_r/B_s)(n_s/n_r)^2(D_s/D_r)$, where n is the refractive index of the solvents and D is the integrated intensity. The quantity B is calculated by $B = 1\text{-}10^{-AL}$, where A is the absorbance and L is the optical path length.

Diethyl 3-azidopropylphosphonate: To a solution of diethyl 3-bromopropylphosphonate (4.42 g, 0.017 mol, 1 eq.) in DMF (250 mL) was added azide exchange resin (44.88 g, surface loading 3.8 mmol/g, 0.17 mol, 10 eq.), after which the suspension was stirred at 40 °C during 3 days. The beads were filtered off and washed with Et_2O (2 x 200 mL), and the solution was filtered over Celite (2x), after which all volatiles were removed *in vacuo*. The crude product was distilled with the 2nd fraction containing the product (5.7 mbar, 105 °C, 2.79 g, 0.013 mol, 74%). The ^1H NMR signals were assigned with the aid of COSY spectra. ^1H NMR ($CDCl_3$,

298K, 400 MHz) δ: 1.30 (t, 6H, $^3J_{H-H}$ = 4.4 Hz, 2 x P-O-CH_2CH_3), 1.73-1.89 (m, 4H, 2 x –CH_2), 3.35 (t, 2H, $^3J_{H-H}$ = 6.6 Hz, -CH_2), 4.02-4.12 (m, 4H, 2 x –CH_2CH_3). ^{31}P NMR ($CDCl_3$, 298K, 162 MHz) δ: 31.84. ^{13}C NMR ($CDCl_3$, 298K, 101 MHz) δ: 16.60 (d, $^3J_{C-P}$ = 5.8 Hz, 2 x P-O-CH_2CH_3), 22.58 (d, $^3J_{C-P}$ = 4.5 Hz, $PCH_2CH_2CH_2N_3$) 23.02 (d, $^1J_{C-P}$ = 143.0 Hz, PCH_2), 51.61 (d, $^2J_{C-P}$ = 16.6 Hz, PCH_2CH_2), 61.80 (d, $^2J_{C-P}$ = 6.2 Hz, 2 x P-O-CH_2CH_3). MS (ES+, MeCN) for $C_7H_{16}N_3O_3P$ (M, 221.0929): *m/z* 222.1007 $[M+H]^+$ (calcd. 222.1002), 244.0827 $[M+Na]^+$ (calcd. 244.0821). Anal. calcd. for $C_7H_{16}N_3O_3P$: C 38.01, H 7.29, N 19.00, P 14.00. Found: C 37.91, H 7.21, N 18.85, P 13.91. IR (liquid) ν = 2094.7, 1445.2, 1392.3, 1368.5, 1349.2, 1237.7, 1019.0, 952.3, 781.5, 704.0.

Ethyl 3-azidopropylphosphonochloridate: To a solution of diethyl 3-azidopropylphosphonate (2.60 g, 0.012 mol, 1 eq.) in Et_2O (100 mL), which had been cooled to -10 °C, was added freshly distilled oxalyl chloride (9.9 mL, 14.90 g, 0.12 mol, 10 eq.), after which the solution was stirred at RT. The progress of the reaction was monitored by ^{31}P NMR. After 3 days, fresh oxalyl chloride (9.9 mL) was added. After 11 additional days all volatiles were evaporated *in vacuo*, yielding a slightly yellowish oil (2.25 g, 0.011 mol, 91 %). The ^{1}H NMR signals were assigned with the aid of COSY spectra. ^{1}H NMR ($CDCl_3$, 298K, 400 MHz) δ: 1.38 (t, 3H, $^3J_{H-H}$ = 4.6 Hz, P-O-CH_2CH_3), 1.90-2.02 (m, 2H, $PCH_2CH_2CH_2N_3$), 2.17-2.25 (m, 2H, $PCH_2CH_2CH_2N_3$ or $PCH_2CH_2CH_2N_3$), 3.42 (t, 2H, $^3J_{H-H}$ = 6.4 Hz, $PCH_2CH_2CH_2N_3$ or $PCH_2CH_2CH_2N_3$), 4.15-4.35 (m, 2H, –CH_2CH_3). ^{31}P NMR ($CDCl_3$, 298K, 162 MHz) δ: 43.82. ^{13}C NMR ($CDCl_3$, 298K, 101 MHz) δ: 16.12 (d, $^3J_{C-P}$ = 7.0 Hz, P-O-CH_2CH_3), 22.59 (d, $^3J_{C-P}$ = 5.0 Hz, $PCH_2CH_2CH_2N_3$), 31.00 (d, $^1J_{C-P}$ = 126.4 Hz, PCH_2), 51.08 (d, $^2J_{C-P}$ = 19.1 Hz, PCH_2CH_2), 63.62 (d, $^2J_{C-P}$ = 8.3 Hz, P-O-CH_2CH_3). IR (liquid) ν = 2985.6, 2941.4, 2096.2, 1445.1, 1394.9, 1368.9, 1349.3, 1256.2, 1018.4, 967.2, 848.5, 749.2, 711.2. Due to the hydrolysis sensitivity of 3-azidopropylphosphonochloridate, the crude product was used directly in the next synthesis step.

Ethyl 4-nitrophenyl 3-azidopropylphosphonate (4): A solution of paranitrophenol (0.7152 g, 5.1416 mmol, 1 eq.) and distilled triethylamine (2.6014 g, 3.57 mL, 0.0257 mol, 5 eq.) in dry benzene (50 mL) was added dropwise to a solution of 3-azidopropylphosphonochloridate (1.0879 g, 5.1416 mmol, 1 eq.) in dry benzene (20 mL), after which the mixture was stirred at RT for 2 hours. All volatiles were removed *in vacuo*, after which the residue was dissolved in Et_2O (150 mL) and washed with 1M K_2CO_3 (2 x 100 mL), brine (2 x 100 mL) and H_2O (3 x 100 mL). The organic layer was dried over Na_2SO_4 and after filtration and removal of all volatiles *in vacuo* a slightly orange oil was obtained (1.5998 g, 5.0911 mmol, 99%). The ^{1}H NMR signals were assigned with the aid of COSY spectra. ^{1}H NMR ($CDCl_3$, 298K, 400 MHz) δ: 1.31 (t, 3H, $^3J_{H-H}$ = 7.0 Hz, P-O-CH_2CH_3), 1.90-2.10 (m, 4H, $PCH_2CH_2CH_2N_3$, $PCH_2CH_2CH_2N_3$ or $PCH_2CH_2CH_2N_3$), 3.42 (t, 2H, $^3J_{H-H}$ = 6.4 Hz, $PCH_2CH_2CH_2N_3$ or $PCH_2CH_2CH_2N_3$), 4.10-4.31 (m, 2H, P-O–CH_2CH_3), 7.38 (d, 2H, $^3J_{H-H}$ = 9.6 Hz), 8.22

(d, 2H, $^{3}J_{H\text{-}H}$ = 9.6 Hz). ^{31}P NMR ($CDCl_3$, 298K, 162 MHz) δ: 29.78. ^{13}C NMR ($CDCl_3$, 298K, 101 MHz) δ: 16.53 (d, $^{3}J_{C\text{-}P}$ = 5.8 Hz, P-O-CH_2CH_3), 22.42 (d, $^{3}J_{C\text{-}P}$ = 5.0 Hz, $PCH_2CH_2CH_2N_3$), 23.40 (d, $^{1}J_{C\text{-}P}$ = 143.4 Hz, PCH_2), 51.38 (d, $^{2}J_{C\text{-}P}$ = 17.4 Hz, PCH_2CH_2), 63.42 (d, $^{2}J_{C\text{-}P}$ = 7.1 Hz, P-O-CH_2CH_3), 121.2 (d, $^{3}J_{C\text{-}P}$ = 4.6 Hz, Ar*C*2, Ar*C*6), 125.9 (Ar*C*3, Ar*C*5), 144.8 (Ar*C*4), 155.7 (d, $^{2}J_{C\text{-}P}$ = 8.2 Hz, P-O-Ar*C*1). MS (ES+, MeCN) for $C_{11}H_{15}N_4O_5P$ (M, 314.0780): *m/z* 315.0858 $[M+H]^+$ (calcd. 315.0853), 337.0678 $[M+Na]^+$ (calcd. 337.0672). Anal. calcd. for $C_{11}H_{15}N_4O_5P$: C 42.04, H 4.81, N 17.83, P 9.86. Found: C 41.96, H 4.76, N 17.78, P 9.94. IR (liquid) ν = 3479.4, 3114.5, 3081.4, 2985.0, 2939.3, 2873.2, 2455.0, 2101.9, 1613.8, 1591.7, 1520.1, 1488.9, 1446.0, 1347.2, 1226.2, 1162.6, 1111.2, 1031.4, 914.8, 861.6, 752.8, 689.1, 636.9, 608.3.

Ethyl 4-nitrophenyl 3-(4-(aminomethyl)-1*H*-1,2,3-triazol-1-yl)propylphosphonate (5): To a solution of phosphonate **4** (0.4475 g, 0.0014 mol, 1.0 eq.) in degassed dichloromethane (1 mL) was added propargylamine (127.7μL, 0.0020 mol, 0.1098 g, 1.4 eq.), the copper amino arenethiolate catalyst (0.0082 g, 0.0356 mmol, 0.025 eq.) and more dichloromethane (1mL). The solution was stirred overnight, after which all volatiles were evaporated *in vacuo* and the residue was dissolved in CH_2Cl_2 (50 mL). The organic layer was washed with 1M K_2CO_3 (2 x 50 mL), brine (2 x 50 mL) and water (2 x 50 mL). After drying on Na_2SO_4 and filtration over celite, all volatiels were evaporated *in vacuo*. The oil was dissolved in a minimum of dichloromethane and precipitated with hexane. After drying *in vacuo* a yellow oil was obtained (0.4598 g, 1.2450 mmol, 87 %). The ^{1}H NMR signals were assigned with the aid of COSY spectra. ^{1}H NMR ($CDCl_3$, 298K, 400 MHz) δ: 1.28 (t, 3H, $^{3}J_{H\text{-}H}$ = 7.0 Hz, P-O-CH_2CH_3), 1.90-1.98 (m, 2H, $PCH_2CH_2CH_2N_3$), 2.24-2.35 (m, 2H, $PCH_2CH_2CH_2N_3$), 3.35 (d, 2H, $^{2}J_{H\text{-}H}$ = 511.1 Hz, -NH_2), 4.02-4.27 (m, 2H, P-O-CH_2CH_3), 4.46 (t, 3H, $^{3}J_{H\text{-}H}$ = 6.8 Hz, $PCH_2CH_2CH_2N_3$), 7.34 (d, 2H, $^{3}J_{H\text{-}H}$ = 9.2 Hz, Ar*H*), 7.54 (s, 1H, triazole*H*), 8.20 (d, 2H, $^{3}J_{H\text{-}H}$ = 9.2 Hz, Ar*H*). ^{31}P NMR ($CDCl_3$, 298K, 162 MHz) δ: 29.00. ^{13}C NMR ($CDCl_3$, 298K, 101 MHz) δ: 16.56 (d, $^{3}J_{C\text{-}P}$ = 6.2 Hz, P-O-CH_2CH_3), 23.26 (d, $^{1}J_{C\text{-}P}$ = 143.8 Hz, PCH_2), 23.66 (d, $^{3}J_{C\text{-}P}$ = 4.6 Hz, $PCH_2CH_2CH_2N_3$), 49.98 (d, $^{2}J_{C\text{-}P}$ = 17.0 Hz, PCH_2CH_2), 63.64 (d, $^{2}J_{C\text{-}P}$ = 7.0 Hz, P-O-CH_2CH_3), 115.9 (triazole *C*=CH), 121.7 (CH_2-NH_2), 126.4 (triazole C=*C*H), 121.2 (d, $^{3}J_{C\text{-}P}$ = 4.5 Hz, Ar*C*2, Ar*C*6), 126.0 (Ar*C*3, Ar*C*5), 144.9 (Ar*C*4), 155.5 (d, $^{2}J_{C\text{-}P}$ = 8.6 Hz, P-O-Ar*C*1). MS (ES+, MeCN) for $C_{14}H_{20}N_5O_5P$ (M, 369.3129): *m/z* 370.1280 $[M+H]^+$ (calcd. 370.1275), 392.1100 $[M+Na]^+$ (calcd. 392.1094). HR MS (ES+, MeCN) for $C_{14}H_{20}N_5O_5P$ (M, 369.3129): *m/z* 370.1233 $[M+H]^+$ (calcd. 370.1275). IR (solid) ν = 2937.8, 1612.4, 1590.2, 1519.6, 1490.0, 1345.4, 1218.6, 1161.5, 1105.8, 1029.4, 911.1, 853.2, 751.0, 688.3.

(4-(methoxycarbonyl)-2,6-di(pyridin-2-yl)phenyl)platinum(II) chloride (1): This complex was prepared according to the literature procedure.[65] ^{1}H NMR (400 MHz, $CDCl_3$): δ 9.38 (2H, dd, $^{3}J_{H\text{-}H}$ = 5.6 Hz, $^{4}J_{H\text{-}H}$ = 1.6 Hz, $^{2}J_{Pt\text{-}H}$ = 35.19, 46.79 Hz,

H^6-py), 8.14 (2H, s, $^4J_{Pt\text{-}H}$ = 4.0 Hz, H^4 and H^6), 8.00 (2H, dt, $^3J_{H\text{-}H}$ = 7.80 Hz, $^4J_{H\text{-}H}$ = 1.6 Hz, H^4-py) 7.81 (2H, d, $^4J_{H\text{-}H}$ = 5.6 Hz, 7.8 Hz, H^3-py), 7.36 (2H, ddd, $^4J_{H\text{-}H}$ = 5.6 Hz, 7.8 Hz, $^4J_{H\text{-}H}$ = 1.6 Hz, H^5-py), 3.94 (3H, s, CH_3).

(4-Carboxy-2,6-di(pyridin-2-yl)phenyl)platinum(II) chloride (2): KOH (1.08 g 19.24 mmol, 100 equivalents) was dissolved in MeOH (5 ml). (4-(Methoxycarbonyl)-2,6-di(pyridin-2-yl)phenyl)platinum(II) chloride (100 mg, 0.192 mmol, 1 equivalent) was suspended in this solution. The suspension was stirred at 40 °C for 24 h. A 4 M HCl (9.62 mL, 38.48 mmol, 200 equivalents) solution was added to the suspension. The yellow precipitate was washed with water (3 x 20 mL) and MeOH (2 x 20 mL) and evaporated to dryness. A yellow solid was obtained (78.3 mg 80%, 0.155 mmol) ^{1}H-NMR (400 MHz, $CDCl_3$): δ 13.00 (1H, s), 9.12 (2H, d, $^3J_{H\text{-}H}$ 5.8 Hz, $^3J_{H\text{-}Pt}$ 34.0 Hz, py-H^6), 8.28 (4H, m, H^2 and H^4 and py-H^3), 8.23 (2H, dt, $^3J_{H\text{-}H}$ 7.4 Hz, $^4J_{H\text{-}H}$ 1.6 Hz), 7.60 (2H, ddd. $^3J_{H\text{-}H}$ 5.8 Hz, 7.4 Hz, py-H^5). ^{13}C-NMR (75 MHz, DMSO): δ 168.4 (C=O), 167.8 (C^6-py), 166.3 (C^4-py), 156.1 (C^2), 152.0 (quat), 141.3 (quat), 141.3 (C^4 and C^6), 126.7 (C^4-py), 125.5 (quat), 121.52 (quat). MALDI-TOF MS: 469.8722 $(M\text{-}Cl)^+$; calculated mass for $C_{20}H_{14}N_3OPt$: 470.0468. HR MS (ES+, MeCN) for $C_{17}H_{11}ClN_2O_2Pt$ (M, 505.0157): *m/z* 488.0559 $[M\text{-}Cl+H_2O]^+$ (calcd. 488.0574).

(4-(Prop-2-ynylcarbamoyl)-2,6-di(pyridin-2-yl)phenyl)platinum(II) chloride (3): Compound **1** (73.3 mg, 0.145 mmol, 1 eq.), propargylamine (15.97 mg, 0.290 mmol, 2 equivalents) and DIEA (23.41 mg, 0.181 mmol, 1.25 equivalents) were dissolved in DMF (20 mL) and cooled during 10 minutes with ice to 0°C. Subsequently BOP (67.25 mg, 0.152 mmol, 1.05 equivalents) was added. After 24 h all volatiles were removed under reduced pressure. The resulting yellow powder was washed with $CHCl_3$ (3 x 20 ml) and Et_2O (2 x 20 ml) and dried under reduced pressure (60.0 mg, 76%, 0.12 mmol). ^{1}H-NMR (400 MHz, $CDCl_3$): δ 9.13 (2H, d, $^3J_{H\text{-}H}$ = 5.9 Hz, $^3J_{H\text{-}Pt}$ = 35.2 Hz, H^6-py), 8.88 (1H, t, $^3J_{H\text{-}H}$ = 5.4 Hz, N*H*), 8.26 (2H, t, $^3J_{H\text{-}H}$ = 8.0 Hz, H^4-py), 8.25 (2H, s, H^3 and H^6), 8.15, (2H, d, $^3J_{H\text{-}H}$ = 8.0 Hz, H^3-py), 7.60 (2H, t, $^3J_{H\text{-}H}$ = 5.9 Hz, H^5-py), 4.12 (2H, dd, $^3J_{H\text{-}H}$ = 5.4 Hz, $^4J_{H\text{-}H}$ = 2.4 Hz, NH-CH_2), 3.17 (1H, t, $^4J_{H\text{-}H}$ = 2.4 Hz, C≡C-*H*). ^{13}C-NMR (75 MHz, DMSO): δ 166.6, 152.2, 141.1, 129.8, 124.8, 121.0. MALDI-TOF MS: 507.1562 $(M\text{-}Cl)^+$; calculated mass for $C_{20}H_{14}N_3OPt$: 507.0785. Elemental analysis: Calculated ($C_{18}H_{13}ClN_2O_2Pt$): 44.25% C, 2.60% H, 7.74% N, 35.93% Pt. Found: 44.12% C, 2.48% H, 7.79% N, 36.10% Pt.

Complex 6: To phosphonate **5** (0.0607 g, 0.1643 mmol, 1.0 eq.) dissolved in dry DMF (1 mL) was added complex **2** (0.0831 g, 0.1643 mmol, 1.0 eq.) and more DMF (5 mL). The solution was cooled to 0 °C, after which DIEA (33.9 μL, 0.2054 mmol, 1.25 eq.) and BOP (0.0763 g, 0.1725 mmol, 1.05 eq.) were added. After stirring overnight all volatiles were evaporated *in vacuo*. The solid residue was dissolved in CH_2Cl_2 (50 mL) and washed with 1M K_2CO_3 (2 x 50 mL), brine (2 x 50 mL) and water (2 x 50 mL). After drying over Na_2SO_4 and filtration over Celite all volatiles were evaporated *in vacuo* to obtain a yellow solid (0.1239 g, 0.1446 mmol, 88 %). The ^{1}H

NMR signals were assigned with the aid of COSY and long range COSY spectra. ^{1}H NMR (DMSO-d_6, 298K, 400 MHz) δ: 1.20 (t, 3H, $^{3}J_{H\text{-}H}$ = 7.0 Hz, P-O-CH_2CH_3), 1.98-2.10 (m, 4H, $PCH_2CH_2CH_2N_3$), 4.09-4.15 (m, 2H, P-O-CH_2CH_3), 4.44 (t, 3H, $^{3}J_{H\text{-}H}$ = 6.8 Hz, $PCH_2CH_2CH_2N_3$), 4.57 (d, 2H, $^{4}J_{H\text{-}H}$ = 5.6 Hz, CH_2NH), 7.42 (d, 2H, $^{3}J_{H\text{-}H}$ = 9.2 Hz, PNPAr*H*), 7.59 (2H, t, $^{3}J_{H\text{-}H}$ = 5.9 Hz, H^{5}-py), 8.07 (s, 1H, triazole*H*), 8.12 (2H, d, $^{3}J_{H\text{-}H}$ = 7.2 Hz, H^{3}-py), 8.24 (d, 2H, $^{3}J_{H\text{-}H}$ = 9.2 Hz, PNPAr*H*), 8.24-8.27 (m, 4H, t, H^{4}-py, H^{3}, H^{6}), 8.97 (1H, t, $^{3}J_{H\text{-}H}$ = 7.0 Hz, N*H*), 9.12 (2H, d, $^{3}J_{H\text{-}H}$ = 5.9 Hz, H^{6}-py). ^{31}P NMR (DMSO-d_6, 298K, 162 MHz) δ: 30.19. ^{13}C NMR (d_6-DMSO, 298K, 101 MHz) δ: 16.81 (d, $^{3}J_{C\text{-}P}$ = 5.0 Hz, P-O-CH_2CH_3), 22.89 (d, $^{1}J_{C\text{-}P}$ = 140.8 Hz, PCH_2), 23.82 (d, $^{3}J_{C\text{-}P}$ = 4.6 Hz, $PCH_2CH_2CH_2$), 49.79 (d, $^{2}J_{C\text{-}P}$ = 19.0 Hz, PCH_2CH_2), 63.45 (d, $^{2}J_{C\text{-}P}$ = 7.2 Hz, P-O-CH_2CH_3), 116.5 (triazole *C*=CH), 121.3 (CH_2-NH_2), 122.1 (Ar*C*2, Ar*C*6), 123.9, 124.4, 124.6, 125.3, 126.5 (triazole C=*C*H), 126.9 (Ar*C*3, Ar*C*5), 130.1, 141.0, 141.4, 144.8, 145.7, 152.1, 156.1 (d, $^{2}J_{C\text{-}P}$ = 8.6 Hz, P-O-Ar*C*1), 166.2, 166.5. MS (ES+, MeCN) for $C_{31}H_{29}N_7O_6PPt$ (M, 856.1253): *m/z* 821.1586 [M-Cl]$^{+}$ (calcd. 821.1559), 880.1238 [M+Na]$^{+}$ (calcd. 880.1105). HR MS (ES+, MeCN) for $C_{31}H_{29}N_7O_6PPt$ (M, 856.1253): *m/z* 821.1575 [M-Cl]$^{+}$ (calcd. 821.1565). IR (solid) ν = 3071.5, 1644.3, 1609.0, 1591.1, 1519.4, 1475.7, 1344.3, 1219.0, 1159.1, 1110.7, 1027.3, 910.2, 860.0, 751.1, 687.7.

Inhibition of cutinase with complex 6: To a solution of cutinase (0.5 mL, 200 μM, 0.1 μmol, 1.0 eq.) in Tris (50 mM), 0.1% (m/m) Triton buffer (pH 8.0) was added a solution of complex **6** (30 μL, 10 mM, 0.3 μmol, 3.0 eq.) in DMF or MeCN. After 2h more inhibitor **6** was added (30 μL, 10 mM, 0.3 μmol, 3.0 eq.). After incubation overnight, the solution was dialysed during 24h with NH_4OAc buffer (150 mM, 2 x 400 mL) and an activity test was performed.

Activity tests: To different batches of Tris (50 mM), 0.1% (m/m) Triton buffer (1.493 mL, pH 8.0) was added a solution of *para*-nitrophenolbutyrate (7.0 μL, 50 mM) in MeCN. To these substrate solutions were added portions of inhibited and uninhibited cutinase (0.5 μL, 200 μM, 0.1 nmol) and the release of *para*-nitrophenolate was measured at 400 nm during 10 min.

Inhibitions for the gel-electrophoresis experiments: To solutions of cutinase (1.0 mg/mL), CALA (0.8 mg/mL) and CALB (2.0 mg/mL) in Tris (50 mM), 0.1% (m/m) Triton buffer (200 μL each) was added a solution of **6** (20.0 mM, 50.0 μL, 1.0 mmol) in DMF. The samples were incubated in the fridge overnight, after which the samples were analyzed with SDS-page. For this, the protein samples (20 μL) were loaded onto 12.5% SDS-PA gels and separated by gel electrophoresis.[77] Subsequently, the gel was analyzed under a UV lamp (257 nm, GelDoc), after which the gel was stained with Coomassie.

References

1. O'Hare, H. M.; Johnsson, K.; Gautier, A., *Curr. Opin. Struct. Biol.* **2007,** 17, 488-494.
2. Yamada, K.; Toyota, T.; Takakura, K.; Ishimaru, M.; Sugawara, T., *New J. Chem.* **2001,** 25, 667-669.
3. Frangioni, J. V., *Curr. Opin. Chem. Biol.* **2003,** 7, 626-634.
4. van Dongen, E. M. W. M.; Evers, T. H.; Dekkers, L. M.; Meijer, E. W.; Klomp, L. W. J.; Merkx, M., *J. Am. Chem. Soc.* **2007,** 129, 3494-3495.
5. Weiss, S., *Science* **1999,** 283, 1676-1683.
6. Nie, S.; Zare, R. N., *Annu. Rev. Biophys. Biomol. Struct.* **1997,** 26, 567-596.
7. Magliery, T. J.; Wilson, C. G. M.; Pan, W.; Mishler, D.; Ghosh, I.; Hamilton, A. D.; Regan, L., *J. Am. Chem. Soc.* **2005,** 127, 146-157.
8. Nienhaus, G. U., *Angew. Chem. Int. Ed.* **2008,** 47, 8992-8994.
9. Shaner, N. C.; Patterson, G. H.; Davidson, M. W., *J. Cell Sci.* **2007,** 120, 4247-4269.
10. Mitchell, F. L.; Frank, F.; Marks, G. E.; Suzuki, M.; Douglas, K. T.; Bryce, R. A., *Proteins* **2009,** 75, 28-39.
11. Chalfie, M., *Angew. Chem. Int. Ed.* **2009,** 48, 5603-5611.
12. Shimomura, O., *Angew. Chem. Int. Ed.* **2009,** 48, 5590-5602.
13. Tsien, R. Y., *Angew. Chem. Int. Ed.* **2009,** 48, 5612-5626.
14. Panchuk-Voloshina, N.; Haugland, R. P.; Bishop-Sterwart, J.; Bhalgat, M. K.; Millard, P. J.; Mao, F.; Leung, W.-Y.; Haugland, R. P., *J. Histochem. Cytochem.* **1999,** 47, 1179-1188.
15. Berlier, J. E.; Rothe, A.; Buller, G.; Bradford, J.; Gray, D. R.; Filanoski, B. J.; Telford, W. G.; Yue, S.; Liu, J.; Cheung, C.-Y.; Chang, W.; Hirsch, J. D.; Beechem, J. M.; Haugland, R. P.; Haugland, R. P., *J. Histochem. Cytochem.* **2003,** 51, 1699-1712.
16. Loudet, A.; Burgess, K., *Chem. Rev.* **2007,** 107, 4891-4932.
17. Ulrich, G.; Ziessel, R.; Harriman, A., *Angew. Chem. Int. Ed.* **2008,** 47, 1184-1201.
18. Nomura, D. K.; Durkin, K. A.; Chiang, K. P.; Quistad, G. B.; Cravatt, B. F.; Casida, J. E., *Chem. Res. Toxicol.* **2006,** 19, 1142-1150.
19. Drahl, C.; Cravatt, B. F.; Sorensen, E. J., *Angew. Chem. Int. Ed.* **2005,** 44, 5788-5809.
20. Barglow, K. T.; Cravatt, B. F., *Nature Methods* **2007,** 4, 822-827.
21. Salisbury, C. M.; Cravatt, B. F., *Proc. Natl. Acad. Sci. USA* **2007,** 104, 1171-1176.
22. Kruithof, C. A.; Casado, M. A.; Guillena, G.; Egmond, M. R.; van der Kerk-van Hoof, A.; Heck, A. J. R.; Klein Gebbink, R. J. M.; van Koten, G., *Chem. Eur. J.* **2005,** 11, 6869-6877.
23. Kruithof, C. A.; Dijkstra, H. P.; Lutz, M.; Spek, A. L.; Egmond, M. R.; Klein Gebbink, R. J. M.; van Koten, G., *Eur. J. Inorg. Chem.* **2008,** 28, 4425-4432.
24. Rutten, L.; Wieczorek, B.; Mannie, J.-P. B. A.; Kruithof, C. A.; Dijkstra, H. P.; Egmond, M. R.; Lutz, M.; Klein Gebbink, R. J. M.; Gros, P.; van Koten, G., *Chem. Eur. J.* **2009,** 15, 4270-4280 (Chapter 2 of this thesis).
25. Dijkstra, H. P.; Sprong, H.; Aerts, B. N. H.; Kruithof, C. A.; Egmond, M. R.; Klein Gebbink, R. J. M., *Org. Biomol. Chem.* **2008,** 6, 523-531.
26. Tsaytler, P.; Egmond, M. R.; Klein Gebbink, R. J. M.; Dijkstra, H. P., *Org. Biomol. Chem.*, manuscript in preparation.
27. Guillena, G.; Kruithof, C. A.; Casado, M. A.; Egmond, M. R.; van Koten, G., *J. Organomet. Chem.* **2003,** 668, 3-7.
28. Schmidinger, H.; Birner-Gruenberger, R.; Riesenhuber, G.; Saf, R.; Susani-Etzerodt, H.; Hermetter, A., *ChemBioChem* **2005,** 6, 1776-1781.
29. Schmidinger, H.; Susani-Etzerodt, H.; Birner-Gruenberger, R.; Hermetter, A., *ChemBioChem* **2006,** 7, 527-534.
30. Zandonella, G.; Stadler, P.; Haalck, L.; Spener, F.; Paltauf, F.; Hermetter, A., *Eur. J. Biochem.* **1999,** 262, 63.
31. Susani-Etzerodt, H.; Schmidinger, H.; Riesenhuber, G.; Birner-Gruenberger, R.; Hermetter, A., *Chem. Phys. Lip.* **2006,** 144, 60-68.
32. Wieczorek, B.; Snelders, D. J. M.; Dijkstra, H. P.; Versluis, K.; Heck, A. J. R.; Lutz, M.; Spek, A. L.; Egmond, M. R.; Klein Gebbink, R. J. M.; van Koten, G., manuscript in preparation (Chapter 4 of this thesis).
33. Chakraborty, S.; Wadas, T. J.; Hester, H.; Flaschenreim, C.; Schmehl, R.; Eisenberg, R., *Inorg. Chem.* **2005,** 44, 6284-6293.
34. Scaffidi-Domianello, Y. Y.; Nazarov, A. A.; Haukka, M.; Galanski, M.; Keppler, B. K.; Schneider, J.; Du, P.; Eisenberg, R.; Kukushkin, V. Y., *Inorg. Chem.* **2007,** 46, 4469-4482.

35. Balzani, V.; Bergamini, G.; Campagna, S.; Puntoriero, F., *Top. Curr. Chem.* **2007,** 280, 1-36.
36. Lo, K. K.-W., *Struct. Bond.* **2007,** 123, 205-245.
37. Albano, G.; Belser, P.; De Cola, L.; Gandolfi, M. T., *Chem. Commun.* **1999**, 1171-1172.
38. Lo, K. K.-W.; Lee, T. K.-M.; Lau, J. S.-Y.; Poon, W.-L.; Cheng, S.-H., *Inorg. Chem.* **2008,** 47, 200-208.
39. Lo, K. K.-W.; Hui, W.-K., *Inorg. Chem.* **2005,** 44, 1992-2002.
40. Lo, K. K.-W.; Hui, W.-K.; Chung, C.-K.; Tsang, K. H.-K.; Ng, C. H.-C.; Zhu, N.; Cheung, K.-K., *Coord. Chem. Rev.* **2005,** 249, 1434-1450.
41. Lo, K. K.-W.; Hui, W.-K.; Chung, C.-K.; Tsang, K. H.-K.; Ng, D. C.-M.; Zhu, N.; Cheung, K.-K., *Coord. Chem. Rev.* **2005,** 249, 1434-1450.
42. Lo, K. K.-W.; Lee, P.-K.; Lau, J. S.-Y., *Organometallics* **2008,** 27, 2998-3005.
43. Lo, K. K.-W.; Ng, D. C.-M.; Chung, C.-K., *Organometallics* **2001,** 20, 4999-5001.
44. Salmain, M.; Jaouen, G., *C. R. Chimie* **2003,** 6, 249-258.
45. Poupart, S.; Boudou, C.; Peixoto, P.; Massonneau, M.; Renard, P.-Y.; Romieu, A., *Org. Biomol. Chem.* **2006,** 4, 4165-4177.
46. Lau, J. S.-Y.; Lee, P.-K.; Tsang, K. H.-K.; Ng, C. H.-C.; Lam, Y.-W.; Cheng, S.-H.; Lo, K. K.-W., *Inorg. Chem.* **2009,** 48, 708-718.
47. Youn, H. Y.; Terpetschnig, E.; Szmacinski, H.; Lakowicz, J. R., *Analytical Biochemistry* **1995,** 232, 24-30.
48. Ma, D.-L.; Shum, T. Y.-T.; Zhang, F.; Che, C.-M.; Yang, M., *Chem. Commun.* **2005**, 4675-4677.
49. Slim, M.; Sleiman, H. F., *Bioconjugate Chem.* **2004,** 15, 949-953.
50. Yang, X.-J.; Drepper, F.; Wu, B.; Sun, W.-H.; Haehnel, W.; Janiak, C., *Dalton Trans.* **2005**, 256-267.
51. Sculimbrene, B.; Imperiali, B., *J. Am. Chem. Soc.* **2006,** 128, 7346-7352.
52. Slim, M.; Durisic, N.; Grutter, P.; Sleiman, H. F., *ChemBioChem* **2007,** 8, 804-812.
53. Wu, P.; Wong, E. L.-M.; Ma, D.-L.; Tong, G. S.-M.; Ng, K.-M.; Che, C.-M., *Chem. Eur. J.* **2009,** 15, 3652-3656.
54. Develay, S.; Gareth Williams, J. A., *Dalton Trans.* **2008**, 4562-4564.
55. Gareth Williams, J. A.; Beeby, A.; Davies, E. S.; Weinstein, J. A.; Wilson, C., *Inorg. Chem.* **2003,** 42, 8609-8611.
56. Gareth Williams, J. A., *Photochemistry and Photophysics of Coordination Compounds: Platinum*. 2007; Vol. 281, p 205-268.
57. Lu, W.; Chan, M. C. W.; Zhu, N.; Che, C.-M.; He, Z.; Wong, K.-Y., *Chem. Eur. J.* **2003,** 9, 6155-6166.
58. Wieczorek, B.; Dijkstra, H. P.; Egmond, M. R.; Klein Gebbink, R. J. M.; van Koten, G., *J. Organomet. Chem.* **2009,** 694, 812-822 (Chapter 1 of this thesis).
59. Albrecht, M.; van Koten, G., *Angew. Chem. Int. Ed.* **2001,** 40, 3750-3781.
60. Morales Morales, D.; Jensen, C., Elsevier: Amsterdam, 2007; p 1-450.
61. Rostovtsev, V. V.; Green, L. G.; Fokin, V. V.; Sharpless, K. B., *Angew. Chem. Int. Ed.* **2002,** 41, 2596-2599.
62. Tornoe, C. W.; Christensen, C.; Meldal, M., *J. Org. Chem.* **2002,** 67, 3057-3062.
63. Rodionov, V. O.; Presolski, S. I.; Gardinier, S.; Lim, Y.-H.; Finn, M. G., *J. Am. Chem. Soc.* **2007,** 129, 12696-12704.
64. Kolb, H. C.; Finn, M. G.; Sharpless, K. B., *Angew. Chem. Int. Ed.* **2001,** 40, 2004-2021.
65. Williams, J. A. G.; Beeby, A.; Davies, E. S.; Weinstein, J. A.; Wilson, C., *Inorg. Chem.* **2003,** 42, 8609-8611.
66. Knotter, D. M.; Grove, D. M.; Smeets, W. J. J.; Spek, A. L.; van Koten, G., *J. Am. Chem. Soc.* **1992,** 114, 3400-3410.
67. McDonald, A. R.; Dijkstra, H. P.; Suijkerbuijk, B. M. J. M.; Lutz, M.; Spek, A. L.; van Klink, G. P. M.; van Koten, G., *submitted*.
68. Slagt, M. Q.; van der Kuil, L.; Klein Gebbink, R. J. M.; van Koten, G., unpublished.
69. Boersma, Y. L.; Pijning, T.; Bosma, M. S.; van der Sllot, A. M.; Godinho, L. F.; Droege, M. J.; Winter, R. T.; van Pouderoyen, G.; Dijkstra, B. W.; Quax, W. J., *Chemistry & Biology* **2008,** 15, 782-789.
70. Longhi, S.; Cambillau, C., *Biochimica et Biophysica Acta* **1999,** 1441, 185-196.
71. Longhi, S.; Mannesse, M. L. M.; Verheij, H. M.; De Haas, G. H.; Egmond, M.; Knoops-Mouthuy, E.; Cambillau, C., *Protein Sci.* **1997,** 6, 275-286.

72. Longhi, S.; Nicolas, A.; Creveld, L.; Egmond, M.; Verrips, C. T.; de Vlieg, J.; Martinez, C.; Cambillau, C., *Proteins* **1996,** 26, 442-458.
73. *Complexes like inhibitor 6 can easily be converted into its cationic analogue, by abstraction of the halide ion (e.g. by using AgBF4 or AgOTf). By doing so, a vacant coordination site becomes available, which can be used for the coordination of various ligands, proteins or other potential probes. Consequently, the protein substituted organometallic moiety can be coordinated to other luminescent reporter molecules, or even solid supports, thereby enabling us to apply this system for microarrays. A similar pincer platinum complex covalently bound to cutinase already revealed that selective coordination of neutral phosphine ligands to the platinum centre is possible. This would make 6 a very versatile probe in studying proteins.*
74. Albrecht, M.; Rodriguez, G.; Schoenmaker, J.; van Koten, G., *Org. Lett.* **2000,** 2, 3461-3464.
75. Beccati, D.; Halkes, K. M.; Batema, G. D.; Guillena, G.; Carvalho de Souza, A.; van Koten, G.; Kamerling, J. P., *ChemBioChem* **2005,** 6, 1196-1203.
76. Crosby, G. A.; Demas, J. N., *J. Phys. Chem.* **1971,** 75, 991-1024.
77. Laemmli, U. K., *Nature* **1970,** 227, 680-685.

Chapter 7

Coordination of a Stilbazole to Cationic NCN-Pincer Platinum Complexes

The coordination of a stilbazole to a cationic NCN-pincer platinum complex investigated by NMR, UV-vis and luminescence spectroscopy, and X-ray crystallography is described and compared to the optical properties of an organometallic stilbazole complex. Due to the coordination of the stilbazole pyridine nitrogen atom to the metal centre, its push-pull properties are changed, resulting in a red-shift of the absorption and emission spectra and higher quantum yields of the coordination complex. Upon coordination to a cationic NCN-pincer metal centre, the spectral properties of a photoactive stilbazole dye can be changed, thereby allowing fine-tuning of the optical behaviour for its potential use in optical materials.

Introduction

Recently, the incorporation of transition metals in optical materials via coordination or covalent bonds has attracted a lot of interest as the special properties of the transition metal ion can uniquely alter the spectroscopic properties of organic molecules or ligands.[1] The great diversity of electronic properties upon incorporation of different metal centres into organic molecules can have a distinct effect on the non-linear optical properties of push-pull chromophores for novel optical materials, *e.g.* inorganic light-emitting diodes.[2] Coordination complexes involving transition metal ions have, among others, been used in electronic and luminescence studies,[1, 3-7] as functionalized polymers,[8-18] in the construction of self-assembled supramolecular structures,[19-27] as liquid crystals[28-31] and as sensing materials.[32-35]
By adjusting the organic framework of organometallic complexes, the spectroscopic properties of those complexes can often be fine-tuned for specific applications.[1, 7, 36, 37] For example, our group has recently developed several novel organometallic dyes derived from the *trans*-4-dimethylamino-4'-nitrostilbene family (DANS),[38-41] containing an organometallic pincer group (Figure 1a).

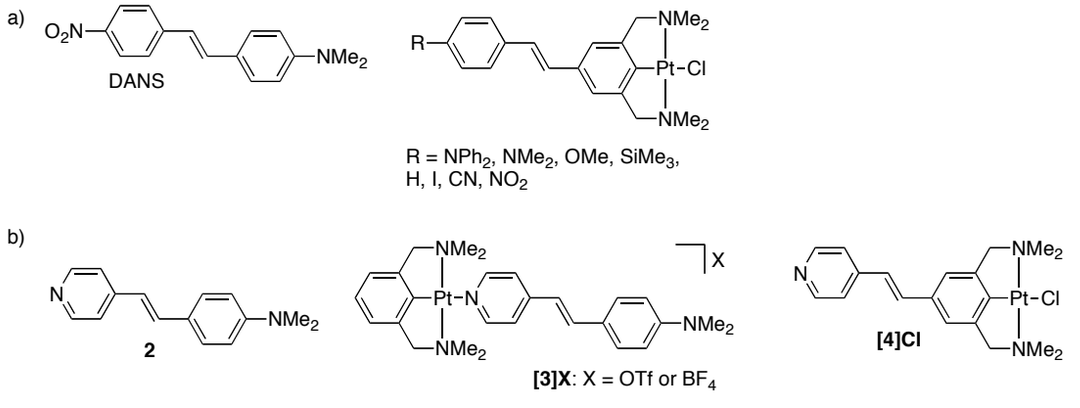

Figure 1: Examples of dyes with interesting photophysical properties: a) the organic DANS dye[38-41] and various organometallic stilbenoid NCN-pincer platinum complexes[42, 43] b) stilbazole **2** and the target molecules **[3]X** (X = OTf or BF_4) and **[4]Cl** described in this chapter.

DANS is a very well-studied, asymmetrically substituted *trans*-4,4'-stilbene (Figure 1a) with the NMe_2 group acting as a strong electron donor and the NO_2 being a strong electron acceptor, thereby forming at strong 'push-pull' system.[39-41] By introducing an organometallic pincer group, the polarizability of the π-electrons and the excited charge transfer state of the system can be influenced,[42, 43] resulting in new optical properties. For the organometallic stilbenoid NCN-pincer platinum complexes it has been established that the platinum pincer metal centre acts as a donor group, with the Hammett σ_P parameter value being similar to that of a NMe_2 group.[43, 44] The shifts in absorption maxima between the PtCl and the NMe_2

chromophores containing the NO_2 substituent as an acceptor group[43] show a significant influence of the pincer metal moiety on the spectroscopic properties of the dye, illustrating how the dye properties can be altered by incorporation of an organometallic complex. By changing the R group for the various organometallic stilbenoid NCN-pincer platinum complexes (Figure 1a), the donor-acceptor ('push-pull') properties of the different molecules could be further fine-tuned, which resulted in different spectroscopic and luminescent properties.[42, 43] Furthermore, it has been established that the optoelectronic properties of transition metal complexes can be fine-tuned very easily by changing the type of coordinating ligands.[1] It is clear that the application of metal complexes to dyes and electronic materials, widens the spectroscopic window, which is important for constructing new materials with unique spectroscopic features.

ECE-pincer metal complexes have been widely known for their rich chemistry.[45-47] They have, for example, been used in the development of novel optical materials,[42, 43] and as building blocks in supramolecular coordination chemistry.[3-6, 9, 10, 13-16, 26, 45, 48-51] Cationic ECE-pincer platinum and palladium complexes, for instance, can serve as anchoring points for the coordination of many different ligands (e.g. phosphorous-, sulfur- or nitrogen- containing ligands).[3-6, 9, 10, 13-16, 26, 51, 52] Due to these properties, we became interested in investigating the influence of pincer-coordination to pyridyl containing stilbene chromophores (**2**, Figure 1b). We envisaged, that the coordination of an NCN-pincer platinum complex to **2** would be a very easy way to influence its spectroscopic properties and enable us to alter the optical behaviour of the novel coordination complexes, as it had been shown for other pyridyl-pincer metal coordination complexes before.[3-6] Recently, Weck and co-workers have used stilbazole-derived dendritic building blocks in the design of polymeric supramolecular cruciforms involving ECE-pincer metal complexes,[17] to design novel functional polymers with interesting optical properties. However, monomeric 1:1 pincer-stilbazole complexes in relation to its spectroscopic properties have never been studied in detail.

Here, the coordination of a stilbazole to cationic NCN-pincer platinum centres is studied in different solvents and with different techniques (UV-vis, luminescence, NMR and X-ray crystallography) and compared to the spectroscopic properties of an organometallic pincer stilbazole complex and the non-coordinated stilbazole. Interestingly, the straightforward coordination of the organometallic pincer complex to the stilbazole has a significant influence on the spectroscopic properties of the stilbazole moiety, illustrating the ability of simple metal coordination chemistry to fine-tune the spectroscopic properties of dyes.

Results and Discussion

Synthesis of the NCN-Pincer platinum-stilbazole complexes

Coordination complexes **[3]X** were synthesized by mixing a solution of the cationic pincer platinum complex **[1]X** (X = OTf[53, 54] or BF_4[52]) with a stoichiometric solution of pyridyl stilbazole **2** in dichloromethane or acetone (Scheme 1).

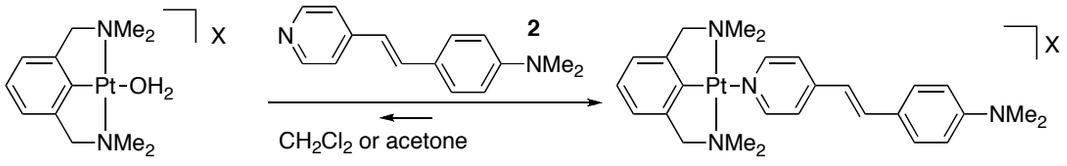

[1]X: X = OTf or BF_4 **[3]X**: X = OTf or BF_4

Scheme 1: Synthesis of the NCN-pincer platinum-stilbazole coordination complexes **[3]X** (X = OTf or BF_4).

All ^{1}H and ^{13}C NMR spectra showed complete conversion to **[3]X**, as no signals for free **[1]X** or **2** were observed (see experimental section for details). The *ortho*-H resonances of the stilbazole pyridine ring and the benzylic-H resonances of the pincer arms show a characteristic shift towards higher ppm values upon formation of **[3]X** (for example from 4.04 to 4.20 ppm for CH_2 and from 8.49 to 8.68 ppm for pyH_{ortho} in CD_2Cl_2 for **[3]OTf**). Since the largest shifts are observed for the pyridine protons (no shifts are observed for the dimethylaniline moiety), the data proof coordination of the pyridine nitrogen rather than the dimethylamino nitrogen. ^{195}Pt NMR showed a diagnostic shift from -3351 ppm for pincer complex **[1]OTf** to -3381 ppm for the coordination complex **[3]OTf** (both spectra recorded in CD_2Cl_2). Coordination complexes **[3]X** (X = OTf or BF_4) were fully characterized by MALDI-TOF mass spectrometry, elemental analysis, NMR, UV-VIS and luminescence spectroscopy (*vide infra*).

Interestingly, the coordination of **2** to **[1]X** could not be observed when the NMR study was performed in deuterated acetonitrile (room temperature, data not shown). Contrary to dichloromethane or acetone, acetonitrile is a strongly coordinating solvent competing with stilbazole **2** in coordinating to the cationic metal centre, which in this case prevents the coordination of **2** to **[1]X**.

The novel pincer stilbazole complex **[4]Cl** was synthesized *via* a Horner-Wadsworth-Emmons condensation reaction between aldehyde-functionalized pincer complex [PtCl(NCN-CHO-4)] **6** and phosphonate ester **5** in the presence of potassium *tert*-butoxide (Scheme 2).[43] Upon work-up, exclusively the *trans*-isomer precipitated out of the solution and was isolated by filtration as a greenish solid in 45% yield. **[4]Cl** was characterized by ^{1}H, ^{13}C NMR, IR spectroscopy, high-resolution ES-mass spectrometry and by different spectroscopic techniques (*vide infra*).

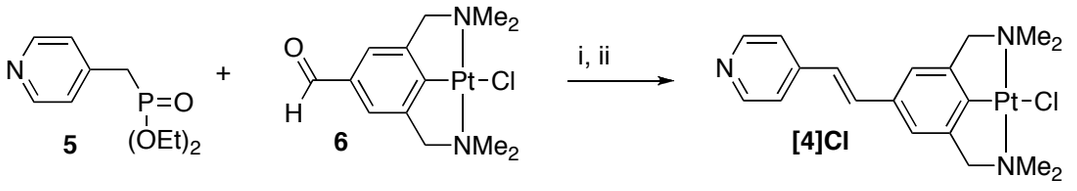

Scheme 2: Synthesis of the novel pincer stilbazole complex **[4]Cl**. i) *t*BuOK, THF, RT; ii) H_2O/NaCl.

*Crystal structure of coordination complex **[3]BF₄***

To gain insight into the structural arrangement of the **[3]X** coordination complexes in the solid state, different crystallization experiments were performed. When a solution of complex **[3]BF₄** in acetone was left standing in the dark, crystals suitable for single crystal X-ray structure determination were obtained. Complex **[3]BF₄** crystallizes with four molecules in the asymmetric unit, with an antiparallel arrangement of the coordination complex molecules (Figure 2), which had been observed for organometallic pincer-stilbene complexes (see Figure 1a) as well.[43] Selected bond lengths, angles and torsion angles are given in Table 1.

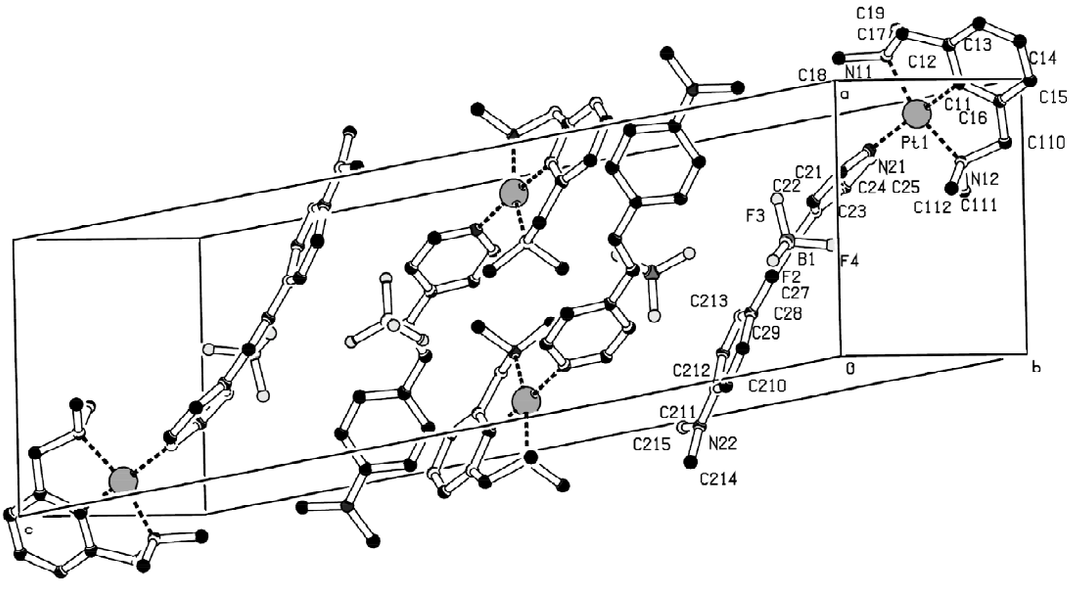

Figure 2: Plot of the unit cell with four molecules of **[3]BF₄**; the hydrogen atoms are omitted for clarity and the numbering scheme is shown.

Table 1: Selected bond lengths, distances (Å), angles and torsion angles (^{O}) for **[3]BF_4**.

Distances			
Pt1-C11	1.929(2)	C26-C27	1.336(3)
Pt1-N11	2.0818(17)	Pt1-B1	6.282(3)
Pt1-N12	2.0864(17)	B1-C26	5.365(4)
Pt1-N21	2.1446(17)	B1-C27	4.858(4)
Angles			
C11-Pt1-N11	81.66(7)	C211-N22-C215	120.4(2)
C11-Pt1-N12	81.73(8)	C211-N22-C214	120.5(2)
C11-Pt1-N21	176.47(7)	C23-C26-C27	124.8(2)
N11-Pt1-N12	163.38(7)	C28-C27-C26	126.9(2)
Torsion Angles			
C23-C26-C27-C28	-173.6(2)	C215-N22-C211-C212	-9.0(3)
C215-N22-C211-C210	169.7(2)	C214-N22-C211-C212	-176.4(2)

As was already observed with solution ^{1}H NMR spectroscopy, the crystal structure of **[3]BF_4** shows that the pyridine nitrogen atom (N21), rather than the NMe_2 nitrogen, coordinates to the NCN-pincer metal centre of **[3]BF_4** in the solid state.

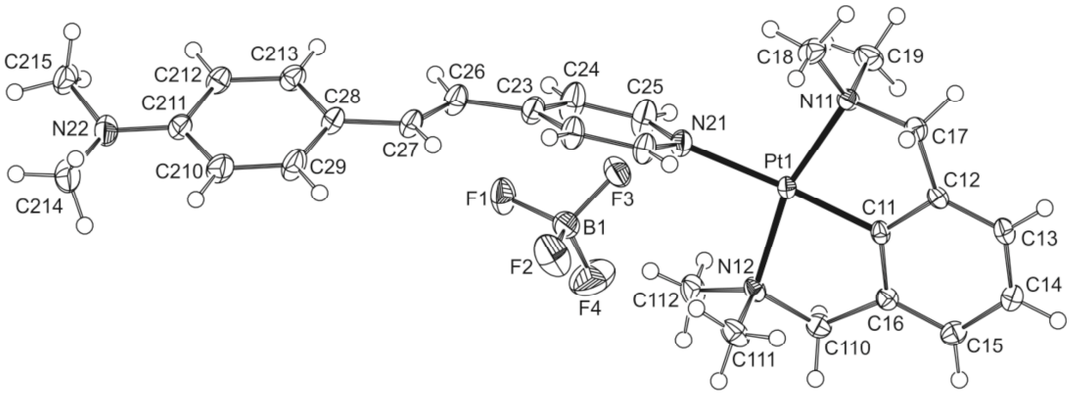

Figure 3: ORTEP plot (50% probability level) of **[3]BF_4** showing the bent overall shape.

The stilbazole ligand of **[3]BF_4** has an overall bent shape with the stilbazole pyridine nitrogen atom N21 and the aryl carbon atom C211 situated 0.4395(18) and 0.371(2) Å beneath the least-squares plane of the stilbazole double bond (C23-C26-C27-C28), which is commonly observed for stilbene- and stilbazole-type molecules (Figure 3).[42, 43]The platinum metal centre has a distorted square planar geometry surrounded by the NCN-pincer and the stilbazole pyridyl nitrogen ligands (Table 1). The bond length of the platinum-pyridyl nitrogen bond Pt1-N21 = 2.1446(17) Å is comparable to other

platinum-pyridyl coordination bond lengths (2.138(4)-2.159(3) Å).[3, 6, 55] The least-squares planes of the pincer aromatic ring and the stilbazole-pyridine ring form an angle of 74.54(10)° with each other. The dimethylamino group of the stilbazole moiety is nearly coplanar (torsion angles 169.6(2)°/-176.4(2)°) with the aryl rings (Table 1). The BF_4 anion is situated near the stilbazole double bond (B1-C27 = 4.858(4) Å), illustrating the ion separation of the coordination complex in the solid state.

Spectroscopic absorption studies

To study the influence of metal coordination on the spectroscopic properties of the stilbazole, the formed coordination complexes were studied by UV-vis and luminescence spectroscopy in different solvents. All spectroscopic data for **2**, **[1]OTf**, **[1]BF_4**, **[3]OTf**, **[3]BF_4** and **[4]Cl** are given in Table 2. The UV-vis spectra for **2**, **[1]BF_4** and **[3]BF_4** and the organometallic pincer-stilbazole **[4]Cl** in dichloromethane, acetone and methanol are shown in Figure 4 a-c, respectively. These three non- or weakly coordinating solvents were chosen to limit the competitive coordination with stilbazole **2** to the cationic NCN pincer metal centre.

Table 2: Spectroscopic data for **[1]OTf**, **2** and **[3]OTf** in different solvents at room temperature.

Compound	Solvent	λ_{max}[a]	ε[b]	λ_{emmax}[c]	Quantum yield
[1]OTf[d]	CH_2Cl_2	258.5	11920	320.5	0.02
	MeOH	258.0	10910	317.5	<0.01
[1]BF_4[d]	CH_2Cl_2	261.0	13030	310.0	0.03
	MeOH	258.0	9590	301.5	<0.01
2	CH_2Cl_2	373.0	52180	467.5	0.06
	MeOH	373.0	27050	503.0	0.07
	acetone	367.0	39300	485.0	0.06
[3]OTf	CH_2Cl_2	425.5	28430	526.0	0.45
	MeOH	397.0	20990	537.5	0.30
	acetone	406.5	33690	nd[e]	nd[e]
[3]BF_4	CH_2Cl_2	426.0	32540	528.0	0.47
	MeOH	400.0	26870	538.0	0.28
	acetone	405.0	32210	nd[e]	nd[e]
[4]Cl	CH_2Cl_2	364.0	30460	531.0	0.41
	MeOH	371.0	24600	461.0	0.10
	acetone	358.0	17690	458.5	0.08

[a] [nm]; [b] [$L \cdot cm^{-1} \cdot mol^{-1}$]; [c] excitation wavelength (nm) is λ_{max}; [d] λ_{max} of **[1]OTf** and **[1]BF_4** in acetone could not be determined, due to the strong absorbance of the solvent in this area of the UV-vis spectrum; [e] under the conditions applied (abs <0.1), no coordination complex was formed in this solvent (the absorbance maximum of the solution was equal to the absorbance maximum of **2** in acetone).

a)

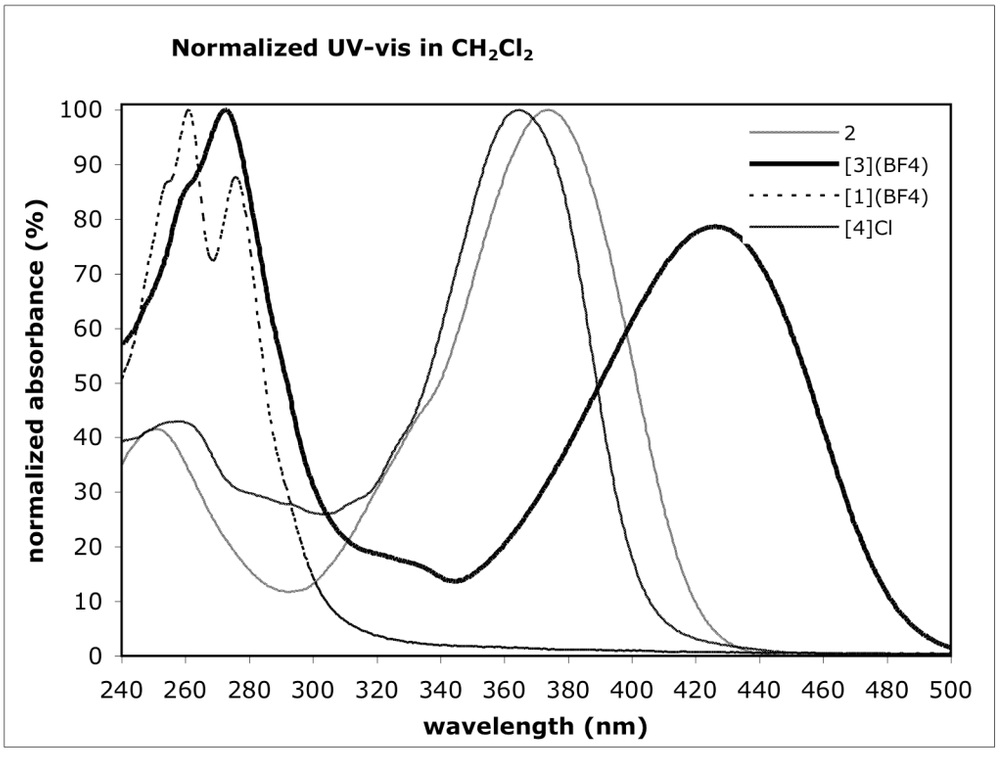
Normalized UV-vis in CH_2Cl_2
normalized absorbance (%)
wavelength (nm)
2
[3](BF4)
[1](BF4)
[4]Cl
0
10
20
30
40
50
60
70
80
90
100
240
260
280
300
320
340
360
380
400
420
440
460
480
500

b)

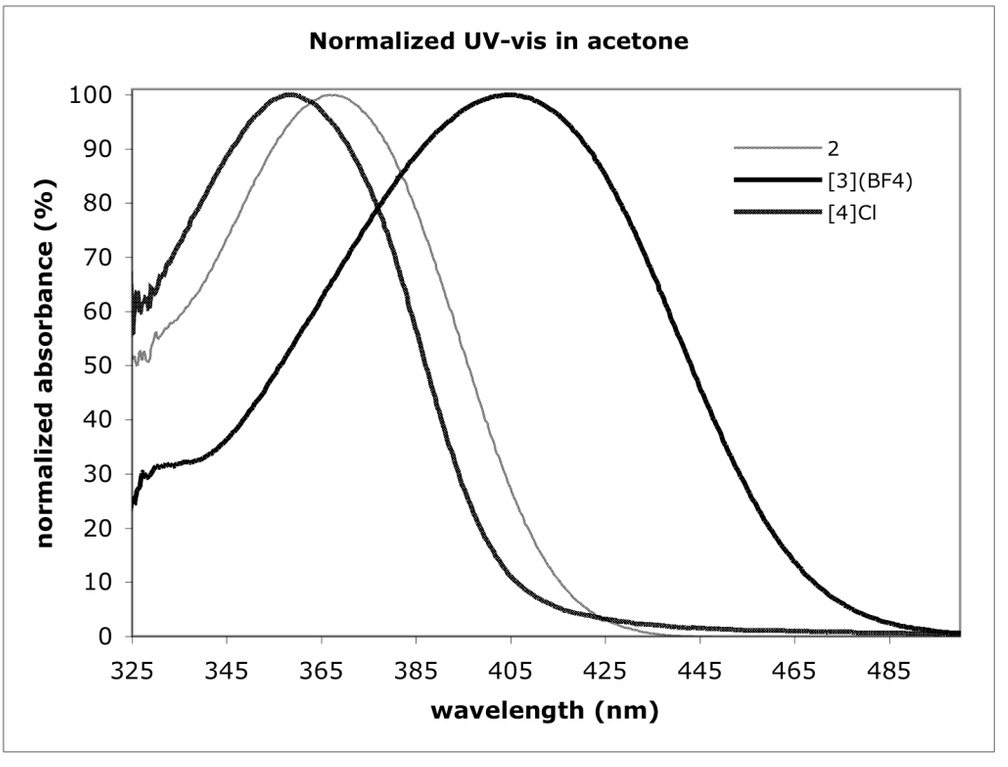
Normalized UV-vis in acetone
normalized absorbance (%)
wavelength (nm)
2
[3](BF4)
[4]Cl
0
10
20
30
40
50
60
70
80
90
100
325
345
365
385
405
425
445
465
485

c)

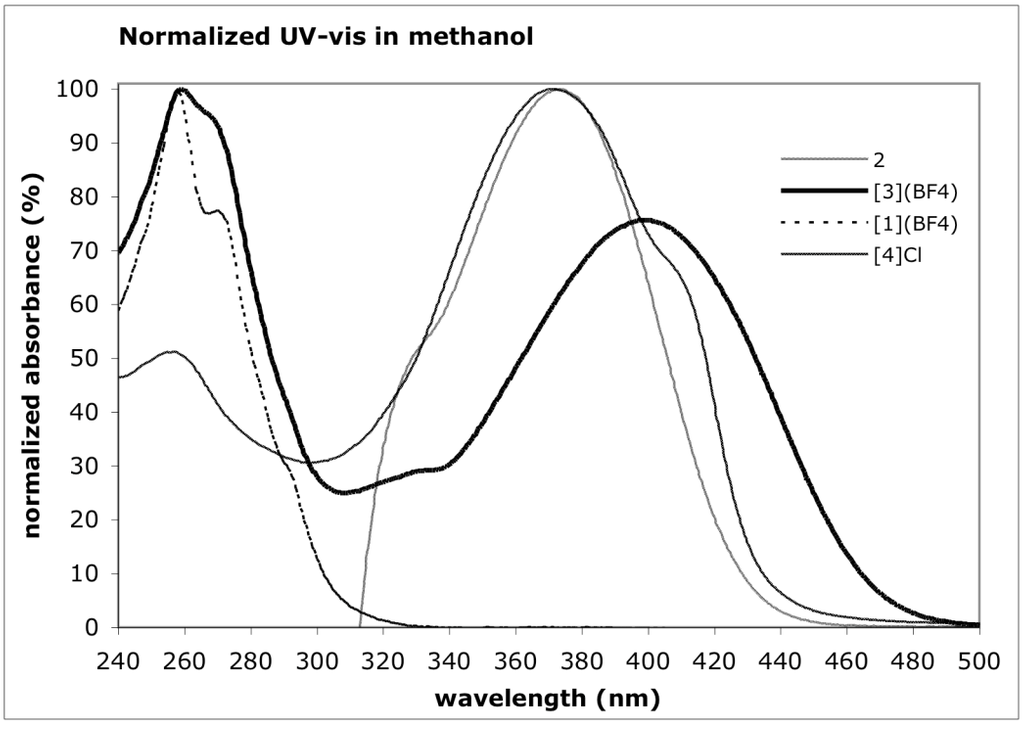

Figure 4: UV-vis spectra of **2**, **[1]OTf**, **[1]BF_4**, **[3]BF_4** and the organometallic pincer-stilbazole **[4]Cl** in CH_2Cl_2 (a), acetone (b) and methanol (c) at room temperature.

The absorption and emission spectra of **[3]BF_4**, **[3]OTf** and **[1]OTf**, **[1]BF_4**, analysed in different solvents, respectively, displayed nearly identical features (Table 2), therefore only the spectra of **[1]BF_4** and **[3]BF_4** are shown for clarity. The absorption maxima for the cationic NCN-pincer platinum complex **[1]BF_4** in dichloromethane and methanol lie between 258.0-261.0 nm and are assigned as metal-to-ligand charge transfer (MLCT) transitions.[5, 6, 56, 57] The absorption maxima in acetone could not be determined due to overlap with the solvent absorption. For stilbazole **2** the absorbance maxima lie between 367.0-373.0 nm, which are assigned to π-π* charge transfers,[8, 58] with a bathochromic shift increasing in the order acetone < CH_2Cl_2 = MeOH (Table 2). As no distinct solvent polarity dependence could be observed, a weakly polar ground state of the molecule is likely to exist.
For the coordination complex **[3]BF_4**, *i.e.* upon coordination of **2** to **[1]BF_4**, a red shift is observed with the biggest $\Delta\lambda_{max}$ in CH_2Cl_2, then acetone and the smallest observed shift in MeOH. The absorption maximum of **[3]BF_4** displays a bathochromic shift in the order MeOH < acetone < CH_2Cl_2, pointing to a polar ground state for **[3]BF_4**,[1] which is different from stilbazole **2**.
The absorption maxima for the organometallic pincer stilbazole complex **[4]Cl** in the different solvents lie between 358.0-371.0 nm (Table 2), being close but slightly

blue-shifted in comparison to stilbazole **2**. These results are in line with earlier studies, where it was shown that the PtCl(NCN) group in **[4]Cl** can be regarded as an electron donating group,[43] with the Hammett parameters σ_p of the PtCl substituent being similar to that of a NMe_2 group.[43, 44] The slight blue-shift of **[4]Cl** indicates that the PtCl group is a slightly weaker donor as compared to the NMe_2 group.

Luminescence studies

As stilbene and stilbazole molecules are known for their luminescent properties,[42, 43, 58] the coordination complexes **[3]BF_4**, pincer stilbazole complex **[4]Cl**, **[1]BF_4** and stilbazole **2** were studied by luminescence spectroscopy in different solvents (Table 2). The emission spectra for **[3]BF_4**, **[4]Cl** and **2** in dichloromethane are shown in Figure 5.

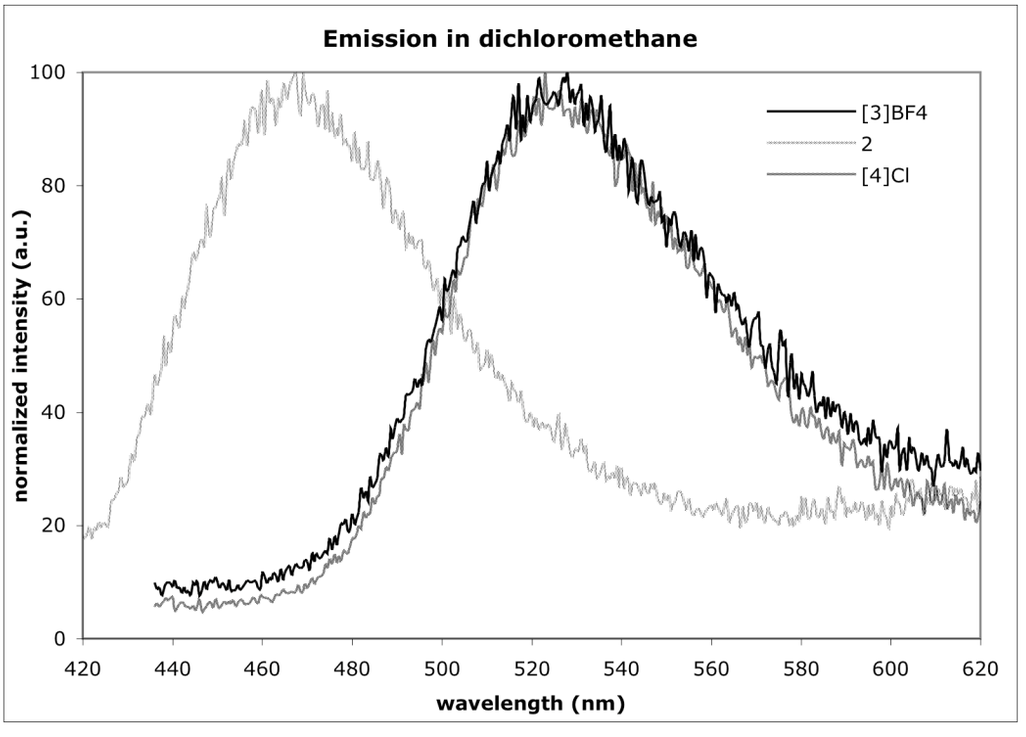

Figure 5: Emission spectra for **[3]BF_4**, **2** and **[4]Cl** in dichloromethane at room temperature.

For coordination complex **[3]BF_4** the emission maxima were strongly red shifted ($\Delta\lambda$ = 51-60.5 nm) in all solvents in comparison to stilbazole **2**, which is probably caused by the changes in the push-pull system as a result of the coordination. Due to the coordination of the stilbazole moiety to the platinum metal centre in **[3]BF_4**, the pyridine nitrogen electrons are dislocated onto the platinum ion, making the pyridine moiety a better acceptor group, resulting in a stronger push-pull system. The luminescence emission maxima for **2** (λ_{emmax} = 467.5-503.0 nm) displayed a

bathochromic shift upon increasing solvent polarity (Table 2), which is indicative for a dipole moment in the excited state.[1, 59] The emission maxima of coordination complex **[3]BF$_4$** displayed a bathochromic shift upon measurement in CH_2Cl_2 and MeOH, indicating the formation of a charge separated or dipolar excited state, like for **2**. The quantum yields for **[3]BF$_4$** were higher than for stilbazole **2**, which is most probably due to the stronger push-pull system in **[3]BF$_4$**. The emission maxima for **[4]Cl** lie between 436.0-531.0 nm with a bathochromic shift increasing in the order acetone < MeOH < CH_2Cl_2. The emission maxima for **[4]Cl** were blue-shifted in MeOH and acetone and red-shifted in CH_2Cl_2 when compared to the emission of stilbazole **2** in the same solvent. The absence of a bathochromic shift upon increase in solvent polarity points to a less polar excited state.

In comparison to the **[3]BF$_4$** coordination complex, the emission maximum for **[4]Cl** is slightly red-shifted in CH_2Cl_2 and blue-shifted in MeOH. The quantum yields for **[4]Cl** are higher than for **2**, but lower than the quantum yields of the **[3]BF$_4$** coordination complex (Table 2). These variations are probably caused by the differences in the push-pull systems for **2**, **[3]BF$_4$** and **[4]Cl**.

Conclusions

In conclusion, we have demonstrated that the straightforward, easy coordination of an organometallic moiety to a pyridyl stilbazole dye can significantly alter the luminescent properties of the dye. NMR, crystallographic and spectroscopic studies showed that the cationic NCN pincer platinum complex **[1]BF$_4$** is a suitable scaffold for the coordination to stilbazole **2** in the solid state and in solution. The crystal structure of **[3]BF$_4$** illustrated unambiguously the coordination of the pyridine nitrogen of **2** to the cationic NCN pincer platinum(II) centre of the pincer complex and the ion separation in the solid state, due to the non-coordinating BF_4 anion. The fact that **[3]BF$_4$** could be crystallized also showed the high stability of these novel materials. The facile synthesis of this type of molecules combined with their high stability makes this type of coordination complexes highly suitable for their application as optical materials, *e.g.* as laser dyes.
The formation of the **[3]BF$_4$** coordination complex in solution depended on the concentration and the coordinating nature of the solvent. In MeOH and CH_2Cl_2 the coordination complexes were readily formed (also under the diluted conditions required for the luminescence studies), whereas the formation of **[3]BF$_4$** in acetone was only observed under more concentrated conditions.
The different spectroscopic measurements illustrated that stilbazole **2** has a weakly polar ground state and a dipole moment in the excited state. Upon coordination of **2** to **[1]BF$_4$**, the ground and excited states of coordination complex **[3]BF$_4$** become both polar and the absorption and emission spectra are red-shifted when compared to **2**. The higher quantum yields of **[3]BF$_4$** in comparison to **2**, as well as the red-shift can be explained by a stronger donor-acceptor couple for **[3]BF$_4$**. By

coordinating to a NCN pincer platinum complex, the spectroscopic properties of the stilbazole dye are significantly changed, thus enabling fine-tuning of its spectroscopic properties and broadening its (potential) applicability as an optical material.
The absorption maxima for **2** are close to **[4]Cl**, indicating the similar donating nature of the NMe_2 and PtCl donor groups, which is also reflected by the similar Hammett parameters for both donor groups. By exchanging the halide anion of the pincer head group in **[4]Cl** (*e.g.* substitution of Cl^- by Br^-, I^-, OTf^- etc), the donating properties of the pincer metal centre can be altered, enabling the fine-tuning of the spectroscopic properties for **[4]Cl** as well.
This study has shown that the spectroscopic properties of a dye (**2**) can be changed in a very straightforward manner by coordination to a NCN pincer metal complex. By doing so, these stable materials can potentially be used in the development of novel optoelectronic materials, *e.g.* as organic/organometallic light-emitting diodes or liquid crystals. These results illustrate the power of metal-coordination to adjust the spectroscopic properties of dyes. Since metal-to-ligand coordination chemistry is very rich, this strategy offers many possibilities to fine-tune the spectroscopic properties of dyes for various applications. Due to the wide range of available ECE pincer metal building blocks and stilbazoles, the spectroscopic properties of the resulting coordination complexes can be fine-tuned and adapted according to the desired spectroscopic applications.

Experimental Section

General comments: Stilbazole **2** was purchased from Sigma-Aldrich. CH_2Cl_2 was distilled over CaH_2 prior to use. Matrix-assisted laser desorption ionization mass spectrometry experiments were performed with a Voyager-DE Pro (Applied Biosystems) instrument in the reflector mode with 2,5-dihydroxybenzoic acid as matrix. Microanalyses were performed by Kolbe, Mikroanalytisches Laboratorium (Mülheim a/d Ruhr, Germany). NMR measurements were performed on a Varian Inova 300 MHz or Varian Oxford 400 MHz spectrometer. $^{195}Pt\{^1H\}$ NMR spectra were recorded on a Varian Inova 300 MHz spectrometer (operating at 64.4 MHz) and referenced to Na_2PtCl_6 (1M in D_2O, δ = 0 ppm).[60] The syntheses of **[1]OTf**[53, 54] and **[1]BF_4**[52] were carried out as reported.

Electronic spectroscopic measurements: All spectroscopic measurements were performed in spectrophotometric grade solvents at room temperature. UV-VIS spectra were recorded on a Varian Cary 50 Scan UV-visible spectrometer. Luminescence spectra were obtained on a SPEX fluorolog instrument, equipped with a Spex 1680 double excitation monochromator, a Spex 1681 emission monochromator and a Spex 1911F detector. Luminescence spectra were corrected for the detector spectral response with the aid of a correction file provided by the manufacturer. Luminescence quantum yields were determined relative to 9,10-diphenylanthracene in degassed cyclohexane (φ_{fl} = 0.90, excitation wavelength 370

nm).[61] The emission quantum yield was measured by the method of Crosby and Demas[62] in degassed solvents and calculated by $\varphi_s = \varphi_r(B_r/B_s)(n_s/n_r)^2(D_s/D_r)$, where n is the refractive index of the solvents and D is the integrated intensity. The quantity B is calculated by $B = 1\text{-}10^{-AL}$, where A is the absorbance and L is the optical path length.

MALDI-TOF MS measurements: MALDI-TOF mass spectrometry measurements were acquired using a Voyager-DE Biospectrometry Workstation mass spectrometer. Sample solutions (1 mg/mL) were prepared in CH_2Cl_2 (**[3]OTf**, **[3]BF$_4$**). The matrix solution was 2,5-dihydroxybenzoic acid in CH_2Cl_2 (for **[3]OTf**, **[3]BF$_4$**). A 1.5 μL sample of the solution and 1.5 μL of the matrix were combined and placed on the titanium MALDI target plate and analyzed after evaporation of the solvents.

NMR analysis of [1]OTf:[53, 54] ^{1}H NMR (CD_2Cl_2, 298K, 300 MHz) δ: 3.03 (s, 12H, $^3J_{H\text{-}Pt}$ = 36.6 Hz, 2 x N(CH_3)$_2$), 4.04 (s, 4H, $^3J_{H\text{-}Pt}$ = 50.4 Hz, 2 x CH_2), 6.82 (d, 2H, $^3J_{H\text{-}H}$ = 7.4 Hz, Ar*H*), 7.02 (t, 1H, $^3J_{H\text{-}H}$ = 7.4 Hz, Ar*H*). ^{1}H NMR (acetone-d_6, 298K, 300 MHz) δ: 3.02 (s, 12H, $^3J_{H\text{-}Pt}$ = 37.5 Hz, 2 x N(CH_3)$_2$), 3.75 (s, 2H, coord. H_2O), 4.22 (s, 4H, $^3J_{H\text{-}Pt}$ = 49.5 Hz, 2 x CH_2), 6.86 (d, 2H, $^3J_{H\text{-}H}$ = 7.4 Hz, Ar*H*), 7.02 (t, 1H, $^3J_{H\text{-}H}$ = 7.4 Hz, Ar*H*). ^{195}Pt {^{1}H} NMR (CD_2Cl_2, 298 K, 64 MHz) δ: -3350.9. ^{13}C {^{1}H} NMR (CD_2Cl_2, 298K, 75 MHz) δ: 53.76 (2 x N(*C*H$_3$)$_2$, $^2J_{C\text{-}Pt}$ not resolved due to overlap with CD_2Cl_2 resonances), 76.06 (2 x –(*C*H$_2$)N, $^2J_{C\text{-}Pt}$ = 76.3 Hz), 119.7 (2 x Ar*C*H, $^3J_{C\text{-}Pt}$ = 43.3 Hz), 120.6 (q, OTf, $^1J_{C\text{-}F}$ = 321.5 Hz), 124.6 (2 x Ar*C*-(CH)$_2$-N), 132.4 (br s, ArC_{ipso}), 143.7 (1 x Ar*C*H).

NMR analysis of 2: The ^{1}H NMR signals were assigned with the aid of COSY spectra; the ^{13}C NMR signals were assigned with the aid of APT spectra. ^{1}H NMR (CD_2Cl_2, 298K, 400 MHz) δ: 3.01 (s, 6H, N(CH_3)$_2$), 6.73 (d, 2H, $^3J_{H\text{-}H}$ = 8.8 Hz, dma*H*meta), 6.84 (d, 1H, $^3J_{H\text{-}H}$ = 16.2 Hz, *H*Cdma), 7.27 (d, 1H, $^3J_{H\text{-}H}$ = 16.2 Hz, *H*Cpyr), 7.33 (d, 2H, $^3J_{H\text{-}H}$ = 5.6 Hz, py*H*meta), 7.45 (d, 2H, $^3J_{H\text{-}H}$ = 8.8 Hz, dma*H*ortho), 8.49 (d, 2H, $^3J_{H\text{-}H}$ = 5.6 Hz, py*H*ortho). ^{1}H NMR (acetone-d_6, 298K, 300 MHz) δ: 3.01 (s, 6H, N(CH_3)$_2$), 6.77 (d, 2H, $^3J_{H\text{-}H}$ = 9.3 Hz, dma*H*meta), 6.95 (d, 1H, $^3J_{H\text{-}H}$ = 16.2 Hz, *H*Cdma), 7.42 (d, 2H, $^3J_{H\text{-}H}$ = 16.2 Hz, *H*Cpyr), 7.43 (d, 2H, $^3J_{H\text{-}H}$ = 6.2 Hz, py*H*meta), 7.50 (d, 2H, $^3J_{H\text{-}H}$ = 9.3 Hz, dma*H*ortho), 8.47 (d, 2H, $^3J_{H\text{-}H}$ = 6.2 Hz, py*H*ortho). ^{13}C {^{1}H} NMR (CD_2Cl_2, 298K, 75 MHz) δ: 40.25 (NMe_2), 112.3 (2 x dma*C*meta), 120.4 (2 x py*C*meta), 121.1 (H*C*-dma), 124.3 (dma*C*para), 128.4 (2 x dma*C*ortho), 133.4 (H*C*-pyr), 145.6 (py*C*para), 150.2 (2 x py*C*ortho), 151.1 (dma*C*-NMe_2). ^{13}C {^{1}H} NMR (acetone-d_6, 298K, 100.6 MHz) δ: 39.65 (NMe_2), 112.4 (2 x dma*C*meta), 120.4 (2 x py*C*meta), 121.1 (H*C*-dma), 124.6 (dma*C*para), 128.5 (2 x dma*C*ortho), 133.5 (H*C*-pyr), 145.7 (py*C*para), 150.2 (2 x py*C*ortho), 151.3 (dma*C*-NMe_2).

[3]OTf: To a solution of complex **[1]OTf**[53, 54] (0.0401 g, 0.0725 mmol, 1.0 equiv.) in dichloromethane (2 mL) was added a solution of **2** (16.3605 mL, 4.4286 mM, 0.0725

mmol, 1.0 equiv.) in dichloromethane. After stirring in the dark for 30 minutes, all volatiles were removed *in vacuo* yielding a yellow solid (0.0539 g, 0.0709 mmol, 98 %). The ^{1}H NMR signals were assigned with the aid of COSY spectra; the ^{13}C NMR signals were assigned with the aid of APT spectra. ^{1}H NMR (CD_2Cl_2, 298K, 400 MHz) δ: 2.84 (s, 12H, $^{3}J_{H\text{-}Pt}$ = 29.6 Hz, 2 x N(CH_3)$_2$), 3.04 (s, 6H, N(CH_3)$_2$), 4.20 (s, 4H, $^{3}J_{H\text{-}Pt}$ = 45.6 Hz, 2 x CH_2), 6.75 (d, 2H, $^{3}J_{H\text{-}H}$ = 8.8 Hz, dma*H*meta), 6.91 (d, 1H, $^{3}J_{H\text{-}H}$ = 16.4 Hz, *H*Cdma), 6.94 (d, 2H, $^{3}J_{H\text{-}H}$ = 7.6 Hz, Ar*H*), 7.08 (t, 1H, $^{3}J_{H\text{-}H}$ = 7.6 Hz, Ar*H*), 7.50 (d, 1H, $^{3}J_{H\text{-}H}$ = 16.4 Hz, *H*Cpyr), 7.53 (d, 2H, $^{3}J_{H\text{-}H}$ = 8.8 Hz, dma*H*ortho), 7.69 (d, 2H, $^{3}J_{H\text{-}H}$ = 6.4 Hz, py*H*meta), 8.68 (d, 2H, $^{3}J_{H\text{-}H}$ = 6.4 Hz, py*H*ortho). ^{13}C {^{1}H} NMR (CD_2Cl_2, 298K, 100.6 MHz) δ: 40.17 (NMe_2), 54.06 (2 x N(*C*H_3)$_2$, $^{2}J_{C\text{-}Pt}$ not resolved due to overlap with CD_2Cl_2 resonances), 77.67 (2 x –(*C*H_2)N, $^{2}J_{C\text{-}Pt}$ not resolved), 112.2 (2 x dma*C*meta), 118.5 (H*C*dma), 119.8 (2 x Ar*C*H), 122.9 (OTf, $^{1}J_{C\text{-}F}$ not resolved), 123.3 (2 x Ar*C*-(CH_2)-N), 123.3 (2 x py*C*meta), 125.3 (H*C*py), 129.3 (2 x dma*C*ortho), 137.5 (1 x Ar*C*H), 143.5 (dma*C*para), 144.5 (ArC_{ipso}, $^{1}J_{C\text{-}Pt}$ = 62.8 Hz), 149.1 (py*C*para), 150.6 (2 x py*C*ortho), 151.8 (dma*C*-NMe_2). ^{195}Pt {^{1}H} NMR (CD_2Cl_2, 298 K, 64 MHz) δ: -3380.7. MS (MALDI) for $C_{28}H_{35}F_3N_4O_3PtS$ (M, 759.2030): *m/z* 610.4059 [M-OTf]$^{+}$ (calc. 610.2509), 764.4674 [M-OTf+DHB]$^{+}$ (calc. 764.2775). Anal. calcd. for $C_{28}H_{35}F_3N_4O_3PtS$: C 44.27, H 4.64, N 7.37, Pt 25.68. Found: C 44.20, H 4.63, N 7.42, Pt 25.55.

[3]BF_4: To a solution of complex **[1]BF_4**[52] (0.0376 g, 0.0765 mmol, 1.0 equiv.) in dichloromethane (2 mL) was added a solution of **2** (17.2852 mL, 4.4286 mM, 0.0765 mmol, 1.0 equiv.) in dichloromethane. After stirring in the dark for 30 minutes all volatiles were evaporated *in vacuo* and the solid was analysed by ^{1}H NMR (0.0528 g, 0.0757 mmol, 99 %). The solid was dissolved in acetone and was left standing in the dark on air. After several days crystals were formed, which were suitable for X–ray diffraction studies. ^{1}H NMR (acetone-d_6, 298K, 300 MHz) δ: 2.93 (s, 12H, $^{3}J_{H\text{-}Pt}$ = 21.0 Hz, 2 x N(CH_3)$_2$), 3.04 (s, 6H, N(CH_3)$_2$), 4.31 (s, 4H, $^{3}J_{Pt\text{-}H}$ = 25.1 Hz, 2 x CH_2), 6.80 (d, 2H, $^{3}J_{H\text{-}H}$ = 9.0 Hz, dma*H*meta), 6.94 (d, 2H, $^{3}J_{H\text{-}H}$ = 6.9 Hz, Ar*H*), 7.05 (t, 1H, $^{3}J_{H\text{-}H}$ = 6.9 Hz, Ar*H*), 7.10 (d, 1H, $^{3}J_{H\text{-}H}$ = 16.2 Hz, *H*Cdma), 7.57 (d, 2H, $^{3}J_{H\text{-}H}$ = 9.0 Hz, dma*H*ortho), 7.68 (d, 1H, $^{3}J_{H\text{-}H}$ = 16.2 Hz, *H*Cpyr), 7.87 (d, 2H, ^{3}J = 6.6 Hz, py*H*meta), 8.94 (d, 2H, $^{3}J_{H\text{-}H}$ = 6.6 Hz, py*H*ortho). ^{13}C {^{1}H} NMR (acetone-d_6, 298K, 100.6 MHz) δ: 39.56 (NMe_2), 53.43 (br s, 2 x N(*C*H_3)$_2$, $^{2}J_{C\text{-}Pt}$ not resolved), 77.38 (2 x –(*C*H_2)N, $^{2}J_{C\text{-}Pt}$ = 54.9 Hz), 112.3 (2 x dma*C*meta), 119.0 (H*C*dma), 119.5 (br s, 2 x Ar*C*H, $^{3}J_{C\text{-}Pt}$ not resolved), 123.1 (2 x py*C*meta), 123.8 (br s, 2 x Ar*C*-(CH_2)$_2$-N), 125.0 (H*C*py), 129.3 (2 x dma*C*ortho), 137.3 (1 x Ar*C*H), 144.2 (ArC_{ipso}), 145.0 (dma*C*para), 149.0 (py*C*para), 151.2 (2 x py*C*ortho), 152.1 (dma*C*-NMe_2). MS (MALDI) for $C_{27}H_{35}BF_4N_4Pt$ (M, 697.2539): *m/z* 610.3623 [M—BF_4]$^{+}$ (calc. 610.2509), 764.4735 [M-BF_4+DHB]$^{+}$ (calc. 764.2775). Anal. calcd. for $C_{28}H_{35}BF_4N_4Pt$: C 46.49, H 5.06, N 8.03. Found: C 46.23, H 5.03, N 7.98.

X-ray crystal structure determination of 3[BF_4]:
$[C_{27}H_{35}N_4Pt]BF_4$, Fw = 697.49, yellow plate, 0.30 x 0.27 x 0.04 mm^3, monoclinic, $P2_1/c$ (no. 14), a = 8.70596(15), b = 9.03191(9), c = 34.4977(3) Å, β = 97.110(1)°, V = 2691.75(6) $Å^3$, Z = 4, D_x = 1.721 g/cm^3, μ = 5.26 mm^{-1}. 46422 Reflections were measured on a Nonius KappaCCD diffractometer with rotating anode (graphite monochromator, λ = 0.71073 Å) up to a resolution of $(\sin\theta/\lambda)_{max}$ = 0.65 $Å^{-1}$ at a temperature of 150(2) K. Intensity integration was performed with EvalCCD.[63] The SADABS[64] program was used for absorption correction and scaling based on multiple measured reflections (0.27-0.81 correction range). 6171 Reflections were unique (R_{int} = 0.034), of which 5619 were observed [$I>2\sigma(I)$]. The structure was solved with automated Patterson methods using the program DIRDIF-99[65] and refined with SHELXL-97[66] against F^2 of all reflections. Non hydrogen atoms were refined with anisotropic displacement parameters. All hydrogen atoms were located in difference Fourier maps and refined with a riding model. 340 Parameters were refined with no restraints. R1/wR2 [$I > 2\sigma(I)$]: 0.0166 / 0.0334. R1/wR2 [all refl.]: 0.0215 / 0.0349. S = 1.098. Residual electron density between -0.70 and 0.50 e/$Å^3$. Geometry calculations and checking for higher symmetry was performed with the PLATON program.[67]

[4]Cl: The published procedure[43] for the synthesis of stilbenoid NCN-Pincer Pt(II) complexes was slightly adapted. In a dry Schlenk tube, *para*-aldehyde substituted pincer platinum derivative [PtCl(NCN-CHO-4)][43] **6** (50 mg, 0.11 mmol) and 4-[(diethylphosphono)methyl]pyridine[68] **5** (38 mg, 0.17 mmol) were dissolved in dry degassed THF (10-15 ml). Under a nitrogen outflow while stirring, *t*-BuOK (31 mg, 0.28 mmol) was added to the reaction mixture, directly causing a strong color change of the reaction mixture. After 2 hrs of stirring at RT the reaction mixture was quenched at 0 °C by the subsequent addition of ice and an aqueous NaCl solution. The emulsion was concentrated on the rotary evaporator. After addition of methanol the formed precipitate was isolated by filtration. The residue was washed with water and pentanes and dried on a filter by suction. The product was isolated as a yellow powder (26 mg, 0.05 mmol, 45% yield). The solubility of **[4]Cl** was generally low (highest solubility: 0.8 mM in dichloromethane), but high enough to perform the spectroscopic studies. The ^{1}H NMR signals were assigned with the aid of a COSY spectrum. ^{1}H NMR (CD_2Cl_2, 298K, 400 MHz) δ: 3.06 (s, 12H, $^3J_{H\text{-}Pt}$ = 34.8 Hz, 2 x N(CH_3)$_2$), 4.06 (s, 4H, $^3J_{H\text{-}Pt}$ = 23.6 Hz, 2 x CH_2), 6.98 (d, 1H, $^3J_{H\text{-}H}$ = 16.2 Hz, *H*Cpincer), 7.05 (s, 2H, Ar*H*), 7.24 (d, 1H, $^3J_{H\text{-}H}$ = 16.2 Hz, *H*Cpyr), 7.36 (d, 2H, $^3J_{H\text{-}H}$ = 5.2 Hz, py*H*meta), 8.50 (d, 2H, $^3J_{H\text{-}H}$ = 5.2 Hz, py*H*ortho). ^{1}H NMR (300 MHz, $CDCl_3$): δ = 8.53 (bs, 2H; ArH *ortho* to N), 7.36 (d, ^3J(H-H) = 5.7 Hz, 2H; ArH *meta* to N), 7.22 (d, ^3J(H-H) = 16.2 Hz, 1H; *trans* CH=CH), 7.02 (s, 2H; ArH), 6.94 (d, ^3J(H-H) = 16.2 Hz, 1H; *trans* CH=CH), 4.05 (s, ^3J(H-Pt) = 45.0 Hz, 4H; CH_2), 3.10 (s, ^3J(H-Pt) = 37.2 Hz, 12H; CH_3). ^{13}C {^{1}H} NMR (DMSO-d_6, 298K, 100.6 MHz) δ: 150.7, 149.0, 145.7, 144.9, 135.4, 131.8, 122.9, 121.1, 118.80, 77.12 (*C*H_2N),

54.51 (N(CH_3)$_2$). IR (ATR): $\tilde{\nu}$ = 3371, 2985, 2922, 1628, 1606, 1582, 1497, 1453, 1423, 1338, 1302, 1271, 1203, 1085, 1061, 1026, 966, 940, 863, 837, 739, 711, 668 cm^{-1}. HR MS (ES+, CH_2Cl_2) for $C_{19}H_{24}ClN_3Pt$ (M, 524.9525): *m/z* 524.1704 $[M]^+$ (calc. 524.1364).

References:

1. Cariati, E.; Pizzotti, M.; Roberto, D.; Tessore, F.; Ugo, R., *Coord. Chem. Rev.* **2006,** 250, 1210-1233 and references mentioned therein.
2. Friend, R. H.; Gymer, R. W.; Holmes, A. B.; Burroughes, J. H.; Marks, R. N.; Taliani, C.; Bradley, D. D. C.; Dos Santos, D. A.; Bredas, J. L.; Logdlund, M.; Salaneck, W. R., *Nature* **1999,** 397, 121-128.
3. Jude, H.; Krause Bauer, J. A.; Connick, W. B., *Inorg. Chem.* **2005,** 44, 1211-1220.
4. Jude, H.; Krause Bauer, J. A.; Connick, W. B., *J. Am. Chem. Soc.* **2003,** 125, 3446-3447.
5. Tastan, S.; Krause, J. A.; Connick, W. B., *Inorg. Chim. Acta* **2006,** 359, 1889-1898.
6. Jude, H.; Krause Bauer, J. A.; Connick, W. B., *Inorg. Chem.* **2004,** 43, 725-733.
7. Balzani, V.; Bergamini, G.; Campagna, S.; Puntoriero, F., *Top. Curr. Chem.* **2007,** 280, 1-36 and references mentioned therein.
8. Burdeniuk, J.; Milstein, D., *J. Organomet. Chem.* **1993,** 451, 213-220.
9. Pollino, J. M.; Weck, M., *Org. Lett.* **2002,** 4, 753-756.
10. South, C. R.; Burd, C.; Weck, M., *Acc. Chem. Res.* **2007,** 40, 63-74.
11. Hofmeier, H.; Hoogenboom, R.; Wouters, M. E. L.; Schubert, U. S., *J. Am. Chem. Soc.* **2005,** 127, 2913-2921.
12. Wang, X.-Y.; Kimyonok, A.; Weck, M., *Chem. Commun.* **2006**, 3933-3935.
13. Yount, W. C.; Loveless, D. M.; Craig, S. L., *Angew. Chem. Int. Ed.* **2005,** 44, 2746-2748.
14. Abu-Lai, N. I.; Kaholek, M.; Loveless, D. M.; Craig, S. L.; Zauscher, S., *Polymer Preprints* **2005,** 46, 9-10.
15. Huck, W. T. S.; Prins, L. J.; Fokkens, R. H.; Nibbering, N. M. M.; van Veggel, F. C. J. M.; Reinhoudt, D. N., *J. Am. Chem. Soc.* **1998,** 120, 6240-6246.
16. Higley, M. N.; Pollino, J. M.; Hollembeak, E.; Weck, M., *Chem. Eur. J.* **2005,** 11, 2946-2953.
17. Gerhardt, W. W.; Zucchero, A. J.; South, C. R.; Bunz, U. W. F.; Weck, M., *Chem. Eur. J.* **2007,** 13, 4467-4474.
18. Yount, W. C.; Loveless, D. M.; Craig, S. L., *J. Am. Chem. Soc.* **2005,** 127, 14488-14496.
19. Fujita, M.; Fujita, N.; Ogurra, K.; Yamaguchi, K., *Nature* **1999,** 400, 52-55.
20. Yang, H.-B.; Ghosh, K.; Das, N.; Stang, P. J., *Org. Lett.* **2006,** 8, 3991-3994.
21. Tarkanyi, G.; Jude, H.; Palinkas, G.; Stang, P. J., *Org. Lett.* **2005,** 7, 4971-4973.
22. Yang, H.-B.; Das, N.; Huang, F.; Hawkridge, A. M.; Muddiman, D. C.; Stang, P. J., *J. Am. Chem. Soc.* **2006,** 128, 100014-10015.
23. Suzuki, K.; Iida, J.; Sato, S.; Kawano, M.; Fujita, M., *Angew. Chem. Int. Ed.* **2008,** 47, 5780-5782.
24. Nishioka, Y.; Yamaguchi, T.; Yoshizawa, M.; Fujita, M., *J. Am. Chem. Soc.* **2007,** 129, 7000-7001.
25. Nakabayashi, K.; Ozaki, Y.; Kawano, M.; Fujita, M., *Angew. Chem. Int. Ed.* **2008,** 47, 2046-2048.
26. Hall, J. R.; Loeb, S. J.; Shimizu, G. K. H.; Yap, G. P. A., *Angew. Chem. Int. Ed.* **1998,** 37, 121-123.
27. Jeon, S. L.; Loveless, D. M.; Yount, W. C.; Craig, S. L., *Inorg. Chem.* **2006,** 45, 11060-11068.
28. Roll, C. P.; Donnio, B.; Weigand, W.; Bruce, D. W., *Chem. Commun.* **2000**, 709-710.
29. Donnio, B.; Bruce, D. W., *New J. Chem.* **199**, 275-286.
30. Huck, D. M.; Nguyen, H. L.; Coles, S. J.; Hursthouse, M. B.; Donnio, B.; Bruce, D. W., *J. Mater. Chem.* **2002,** 12, 2879-2886.
31. Huck, D. M.; Nguyen, H. L.; Horton, P. N.; Hursthouse, M. B.; Guillon, D.; Donnio, B.; Bruce, D. W., *Polyhedron* **2006,** 25, 307-324.
32. Albrecht, M.; Hovestad, N. J.; Boersma, J.; van Koten, G., *Chem. Eur. J.* **2001,** 7, 1289-1294.
33. Albrecht, M.; Lutz, M.; Spek, A. L.; van Koten, G., *Nature* **2000,** 406, 970-971.
34. de Ruiter, G.; Gupta, T.; van der Boom, M. E., *J. Am. Chem. Soc.* **2008,** 130, 2744-2745.
35. Shukla, A.; Das, A.; van der Boom, M. E., *Angew. Chem. Int. Ed.* **2005,** 44, 3237-3240.

36. Lo, K. K.-W., *Struct. Bond.* **2007,** 123, 205-245.
37. Lo, K. K.-W.; Hui, W.-K.; Chung, C.-K.; Tsang, K. H.-K.; Ng, C. H.-C.; Zhu, N.; Cheung, K.-K., *Coord. Chem. Rev.* **2005,** 249, 1434-1450.
38. Dulcic, A.; Flytzanis, C.; Tang, C.; Pepin, D.; Fetizon, M.; Hoppilliard, Y., *J. Chem. Phys.* **1981,** 74, 1559-1563.
39. Papper, V.; Likhtenstein, G. I., *J. Photochem. Photobiol. A* **2001,** 140, 39-52.
40. Papper, V.; Pines, D.; Likhtenstein, G.; Pines, E., *J. Photochem. Photobiol. A* **1997,** 111, 87-96.
41. Vijayakumar, T.; Hubert Joe, I.; Reghunadhan Nair, C. P.; Jayakumar, V. S., *Chemical Physics* **2008,** 343, 83-99.
42. Batema, G. D.; Lutz, M.; Spek, A. L.; van Walree, C. A.; de Mello Donega, C.; Meijerink, A.; Havenith, R. W. A.; Perez-Moreno, J.; Clays, K.; Buchel, M.; van Dijken, A.; Bryce, D. L.; van Klink, G. P. M.; van Koten, G., *Organometallics* **2008,** 27, 1690-1701.
43. Batema, G. D.; van de Westelaken, K. T. L.; Guerra, J.; Lutz, M.; Spek, A. L.; van Walree, C. A.; de Mello Donega, C.; Meijerink, A.; van Klink, G. P. M.; van Koten, G., *Eur. J. Inorg. Chem.* **2007**, 1422-1435.
44. Slagt, M. Q.; Rodriguez, G.; Grutters, M. M. P.; Klein Gebbink, R. J. M.; Klopper, W.; Jenneskens, L. W.; Lutz, M.; Spek, A. L.; van Koten, G., *Chem. Eur. J.* **2004,** 10, 1331-1344.
45. Albrecht, M.; van Koten, G., *Angew. Chem. Int. Ed.* **2001,** 40, 3750-3781.
46. Singleton, J. T., *Tetrahedron* **2003,** 59, 1837-1857.
47. van der Boom, M. E.; Milstein, D., *Chem. Rev.* **2003,** 103, 1759-1792.
48. Terheijden, J.; Van Koten, G.; Grove, D. M.; Vrieze, K., *J. Chem. Soc. Dalton Trans.* **1987**, 1359-1366.
49. van den Broeke, J.; Heeringa, J. J. H.; Chuchuryukin, A. V.; Kooijman, H.; Mills, A. M.; Spek, A. L.; van Lenthe, J. H.; Ruttink, P. J. A.; Deelman, B.-J.; van Koten, G., *Organometallics* **2004,** 23, 2287-2294.
50. Steenwinkel, P.; Kooijman, H.; Smeets, W. J. J.; Spek, A. L.; Grove, D. M.; van Koten, G., *Organometallics* **1998,** 17, 5411-5426.
51. Chuchuryukin, A. V.; Chase, P. A.; Mills, A. M.; Lutz, M.; Spek, A. L.; van Klink, G. P. M.; van Koten, G., *Inorg. Chem.* **2006,** 45, 2045-2054.
52. Suijkerbuijk, B. M. J. M.; Aerts, B. N. H.; Dijkstra, H. P.; Lutz, M.; Spek, A. L.; van Koten, G.; Klein Gebbink, R. J. M., *Dalton Trans.* **2007**, 1273-1276.
53. Schmülling, M.; Grove, D. M.; van Koten, G.; van Eldik, R.; Veldman, N.; Spek, A. L., *Organometallics* **1996,** 15, 1384-1391.
54. Terheijden, J.; van Koten, G.; Vinke, I. C.; Spek, A. L., *J. Am. Chem. Soc.* **1985,** 107, 2891-2892.
55. Amijs, C. H. M.; Berger, A.; Soulimani, F.; Visser, T.; van Klink, G. P. M.; Lutz, M.; Spek, A. L.; van Koten, G., *Inorg. Chem.* **2005,** 44, 6567-6578.
56. Jude, H.; Krause Bauer, J. A.; Connick, W. B., *Inorg. Chem.* **2002,** 41, 2275-2281.
57. van der Ploeg, A. F. M. J.; van Koten, G.; Schmitz, J. E. J.; van der Linden, J. G. M., *Inorg. Chim. Acta* **1982,** 58, 53-58.
58. Cauzzo, G.; Galiazo, G.; Mazzucato, M.; Mougiat, M., *Tetrahedron* **1966,** 22, 589-593.
59. Haroutounian, S. A.; Scribner, A. W.; Katzenellenbogen, J. A., *Steroids* **1995,** 60, 636-645.
60. Pregosin, P. S., *Coord. Chem. Rev.* **1982,** 44, 247-291.
61. Eaton, D. F., *Pure Appl. Chem.* **1988,** 60, 1107-1114.
62. Crosby, G. A.; Demas, J. N., *J. Phys. Chem.* **1971,** 75, 991-1024.
63. Duisenberg, A. J. M.; Kroon-Batenburg, L. M. J.; Schreurs, A. M. M., *J. Appl. Cryst.* **2003,** 36, 220-229.
64. Sheldrick, G. M. *SADABS: Area-Detector Absorption Correction*, 2.10; Universitaet Goettingen: Goettingen, 1999.
65. Beurskens, P. T.; Admiraal, G.; Beurskens, G.; Bosman, W. P.; Garcia-Granda, S.; Gould, R. O.; Smits, J. M. M.; Smykalla, C. *The DIRDIF99 program system, Technical Report of the Crystallography Laboratory*; University of Nijmegen: Nijmegen, 1999.
66. Sheldrick, G. M., *Acta Cryst.* **2008,** A64, 112-122.
67. Spek, A. L., *Acta Cryst.* **2009,** D65, 148-155.
68. Hutchison, A. J.; Williams, M.; Angst, C.; de Jesus, R.; Blanchard, L.; Jackson, R. H.; Wilusz, E. J.; Murphy, D. E.; Bernard, P. S.; Schneider, J.; Campbell, T.; Guida, W.; Sills, M. A., *J. Med. Chem.* **1989,** 32, 2171-2178.

Chapter 8

Site-Specific Covalent Immobilization of a Racemization Catalyst onto Lipase-containing Beads

The synthesis and application of the novel heterogenized bifunctional catalyst **CALB[5]Cl** for the dynamic kinetic resolution of (*S*)-1-phenylethanol to (*R*)-1-phenylethyl acetate is described. The semisynthetic ruthenium lipase hybrid **CALB[5]Cl** was obtained by inhibiting CALB beads with the novel ruthenium phosphonate complex **[5]Cl** possessing a lipase active site-directed phosphonate group. By partially inhibiting the lipase beads with **[5]Cl**, a multifunctional cascade catalyst was obtained, which was active in the racemization (by the Ru-catalytic site; 0% ee after 24h) and in the kinetic resolution (enzymatic acylation by the uninhibited CALB sites; 37.9% after 3h) of (*S*)-1-phenylethanol. A dynamic kinetic resolution experiment of (*S*)-1-phenylethanol with **CALB[5]Cl** gave the acylated (*R*)-product in 18% yield and with >99% ee.

Introduction

During recent years, enzymes have played an increasingly important role in organic synthesis,[1-7] especially due to their high activities and (enantio)selectivities and their very mild, green reaction conditions.[6] The recent advances in protein modification techniques, *e.g.* directed evolution[8] or site-directed mutagenesis, have enabled chemists to tailor enzymatic performances and to use them as environmentally benign catalysts for the synthesis and production of fine chemicals and pharmaceuticals.[5] Additionally, enzymes or proteins modified by different transition metal complexes have been used as semisynthetic biocatalysts, mostly in hydrogenation and oxidation reactions,[9-19] thereby taking advantage of the chiral surrounding of the embedded catalytic sites and the water-solubility of the protein to obtain synthetic products with, in some cases, high ee's.

An emerging area in this research field is the development of catalytic cascade reactions involving the combination of enzymatic and transition metallic catalysis. By combining the high enantioselectivities and activities of enzymes with the versatility of transition metal complexes, a cascade of reactions can now be performed in one pot, making the sometimes laborious isolation and purification of intermediate products unnecessary.[6] A very well-studied type of cascade reaction is the Dynamic Kinetic Resolution reaction (DKR, Scheme 1), where a transition metal-catalysed racemization reaction is coupled with enzymatic kinetic resolution.[20-23] The DKR has been, among others, successfully applied to resolve racemic secondary alcohols (Scheme 1),[24-28] β-haloalcohols,[29, 30] fluorinated aryl alcohols,[31] allylic alcohols,[32] 1,2-diarylethanols,[33] primary amines[26, 34] and γ-hydroxy amides,[35] often yielding >99% conversion and >99% ee. Various racemization metal catalysts have been developed for the DKR. Among the most successful ones are the ruthenium based catalysts which racemize fast at room temperature (*e.g.* **[8]Cl**, Scheme 1) and are compatible with enzymatic resolution (often performed by lipases on a solid support or hydrolases).[20-23] In one case, a ruthenium racemization catalyst immobilized on a solid polystyrene support has been reported, which possessed the same catalytic activity as its soluble counterpart (Scheme 1, **[9]Cl**).[27] The immobilized catalyst could be used twice without loss of activity (>99% conversion) and enantioselectivity (>99% ee) and, moreover, appeared also active under aerobic conditions.

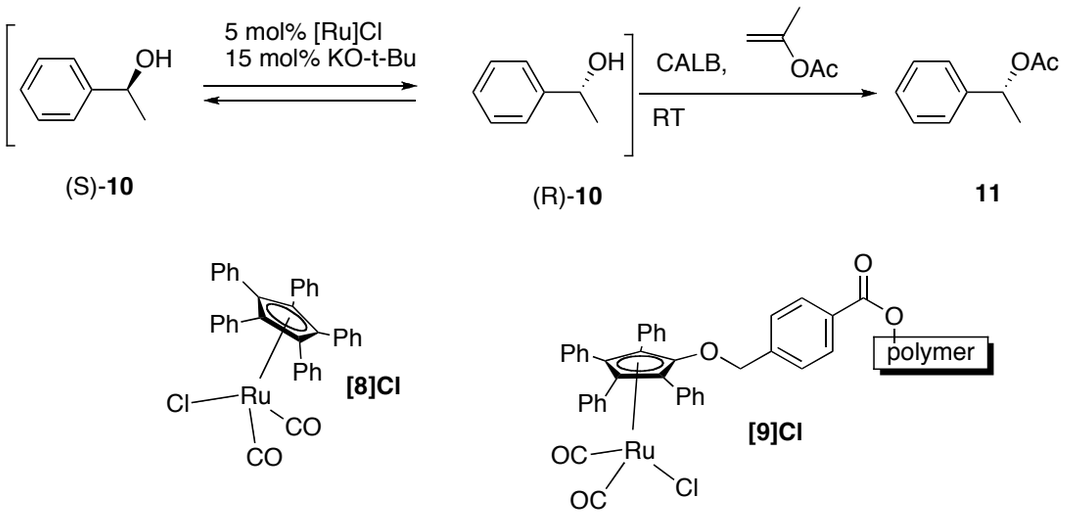

Scheme 1: The ruthenium and CALB catalyzed dynamic kinetic resolution of (*S*)-1-phenylethanol; examples of a highly active (**[8]Cl**)[24, 28] and an immobilized (**[9]Cl**)[27], recyclable racemization ruthenium catalyst used for this DKR reaction are shown.

Recently, our laboratory has successfully modified different lipases, *e.g.* cutinase,[36-40] with synthetic organometallic ECE-pincer metal complexes to generate so-called semisynthetic pincer-metalloenzymes,[36, 40-42] which have been fully structurally analysed, including protein X-ray crystallography. By modifying the organometallic pincer-moiety with a lipase-reactive phosphonate group, the pincer moieties could be irreversibly attached to the active site of the cutinase, with the phosphonate group acting as an active site-selective lipase inhibitor. The developed ECE-pincer metal lipase hybrids have been successfully applied in labelling[36, 39] and coordination studies[38] and proved to be effective catalysts in an abiotic C-C coupling reaction.[37] Using this straightforward active site selective lipase inhibition strategy for the anchoring of an organometallic complex to a heterogenized lipase can be an attractive way to immobilize homogeneous metal catalysts, *i.e.* in the present study we selected the ruthenium based racemization catalysts used in DKR. Due to the ease of the immobilization method, partial inhibition of the lipase sites could even provide a DKR system where both the racemization metal catalyst and the enzyme are recyclable and combined on one type of support. Furthermore, no purification of the product would be necessary, since the catalyst can be separated by filtration. To the best of our knowledge, a site-directed immobilization of a transition metal catalyst onto heterogenized enzymes has not been reported before.

Here, we report the synthesis of a novel organometallic phosphonate inhibitor **[5]Cl** (Figure 1), as well as its use in the irreversible modification of both a free lipase (cutinase), and CALB on a solid support. The inhibition procedures for both cutinase and supported CALB are described, including an estimation of the metal catalyst loading on the lipase support. The immobilized bifunctional catalyst **CALB[5]Cl** is

tested in the racemization of (*S*)-1-phenylethanol and a proof-of-principle study for its use in DKR is described.

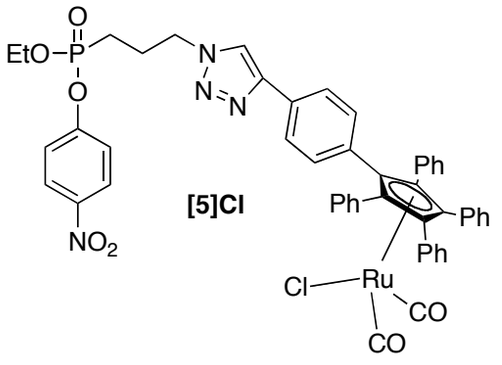

Figure 1: The target molecule of this study, racemization precatalyst **[5]Cl**.

Results and Discussion

*Synthesis of ruthenium complex **[4]Cl** and click reaction to form **[5]Cl***

It was anticipated that the organometallic and the phosphonate moiety of **[5]Cl** could be easily linked together via the well-established click-chemistry,[43] which would enable us to synthesize **[5]Cl** under the mild conditions required to keep the reactive phosphonate moiety intact. First, the acetylene functionalized organometallic complex **[3]Cl** was synthesized in three steps (Scheme 2), starting from (4-bromophenylethynyl)trimethylsilane, which was lithiated and subsequently reacted with tetraphenylcyclopentadienone to form TMS-protected **1** (70% yield).

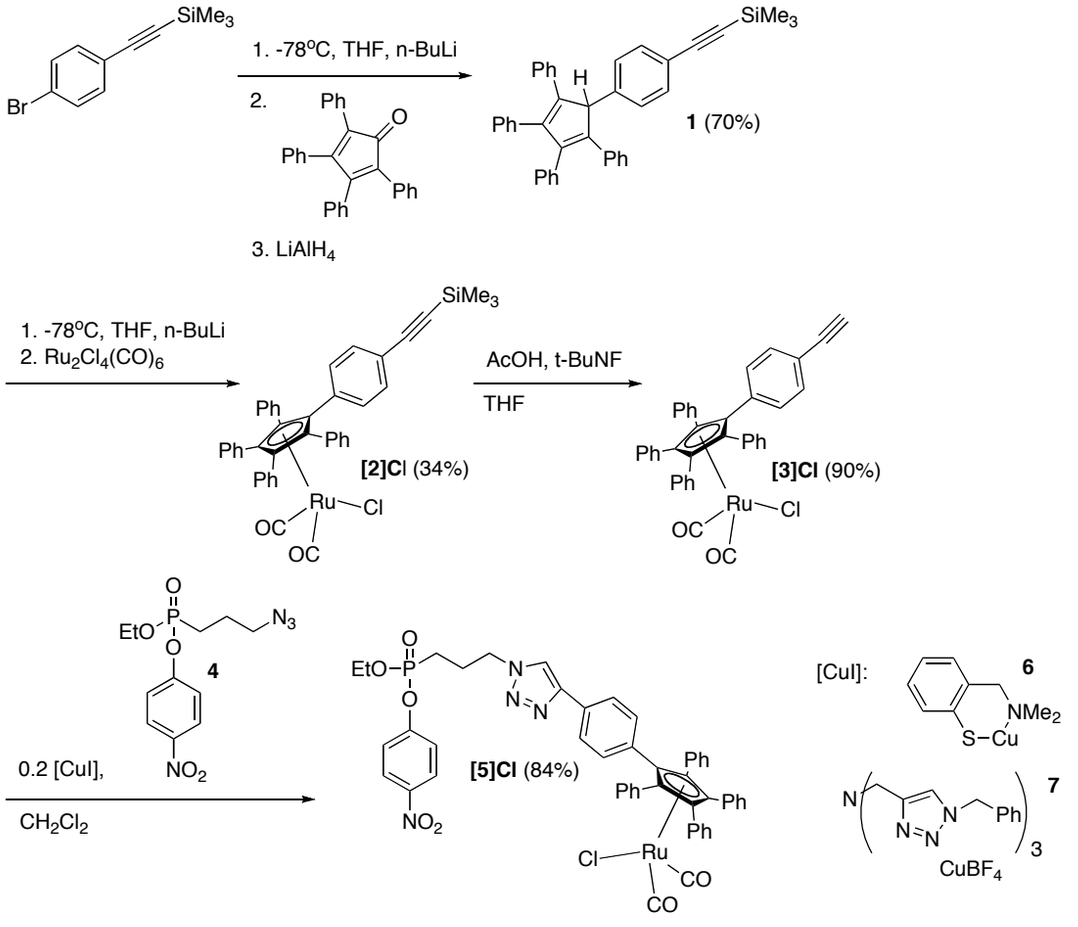

Scheme 2: Synthesis of ruthenium complex **[5]Cl**.

Compound **1** was subsequently lithiated to form the cyclopentadienyl anion, after which a transmetalation reaction with $Ru_2Cl_4(CO)_6$ was performed to give the protected ruthenium complex **[2]Cl** in 34% yield. Finally, **[2]Cl** was deprotected to give **[3]Cl** (90%), which then was used in the click reaction with azide-functionalized phosphonate **4**.[39] For the click reaction between phosphonate **4** and the ruthenium acetylene complex **[3]Cl**, the conditions were optimized first, by performing a screen with different solvents (MeCN, CH_2Cl_2), reactant concentrations and two different catalysts (**6**[44, 45] and **7**,[43] Scheme 2). It was found that the shortest reaction times and highest yields could be obtained with the Cu(I) amino arenethiolate catalyst **6**[44, 45] in dichloromethane. Consequently, these optimized reaction conditions were used to perform the click reaction while monitoring the progress by ^{31}P NMR spectroscopy. After 4 days full conversion was reached, and after workup **[5]Cl** was isolated in 84% yield. The long reaction time, which is rather uncommon for click reactions,[43, 46] might be caused by the special electronic and steric properties of the acetylene ruthenium complex, as azide-functionalized phosphonates have been proven earlier to be very reactive.[47] Ruthenium phosphonate complex **[5]Cl** was fully characterized by ^{1}H, ^{13}C and ^{31}P NMR spectroscopy, IR and high-resolution ES-MS spectrometry.

*Inhibition of cutinase with **[5]Cl***

To assay the inhibitory activity of **[5]Cl** towards lipases in general, an inhibition study with cutinase was performed, following the straightforward protocol we developed earlier (Scheme 3).[36, 41, 42, 47-52]

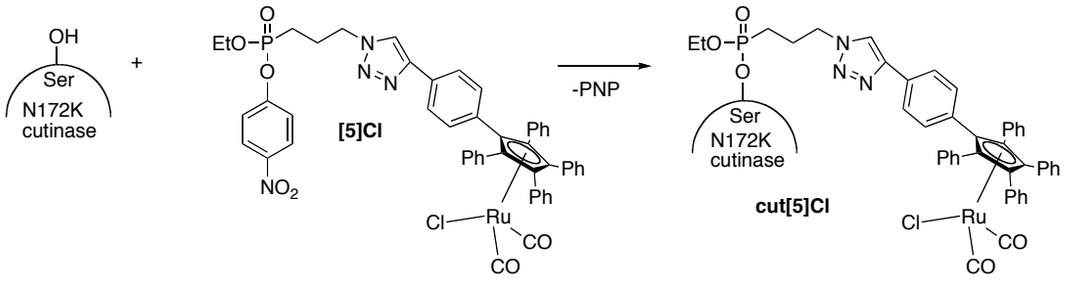

Scheme 3: Inhibition of cutinase with complex **[5]Cl** (PNP = *p*-nitrophenolate anion).

To this purpose, a solution of cutinase in Tris/Triton buffer (pH 8.0) was incubated with a solution of **[5]Cl** in MeCN (8 eq.), after which the solution was dialysed to remove the excess of inhibitor **[5]Cl**. A subsequent activity test with *p*-nitrophenyl butyrate[41] as substrate after 18h reaction time confirmed 70% inhibition of cutinase by **[5]Cl** (Figure 2). Although this indicates a very slow inhibition rate, it unambiguously proves that lipases can be modified with **[5]Cl**.

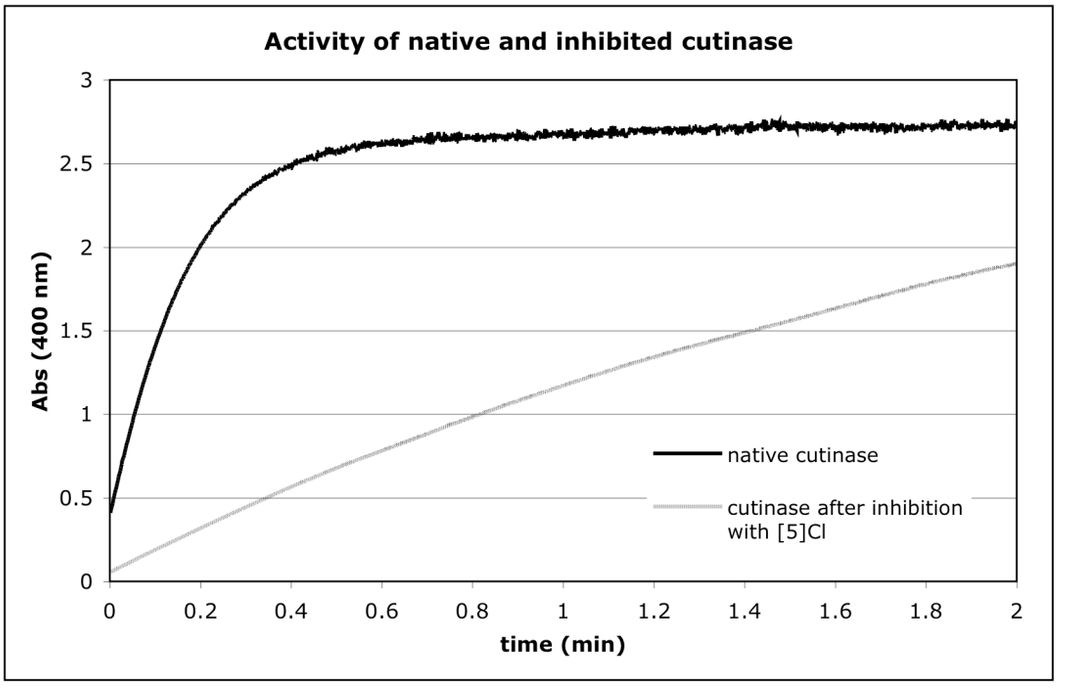

Figure 2: Activity tests with free cutinase and cutinase after inhibition with **[5]Cl**.

*Immobilisation of **[5]Cl** onto Novozym® 435 beads*

For the immobilization of **[5]Cl** onto CALB beads (Scheme 4) a slightly different strategy had to be followed as the number of accessible CALB sites on the surface of the commercially available CALB beads (Novozym® 435) used in this study was unspecified.

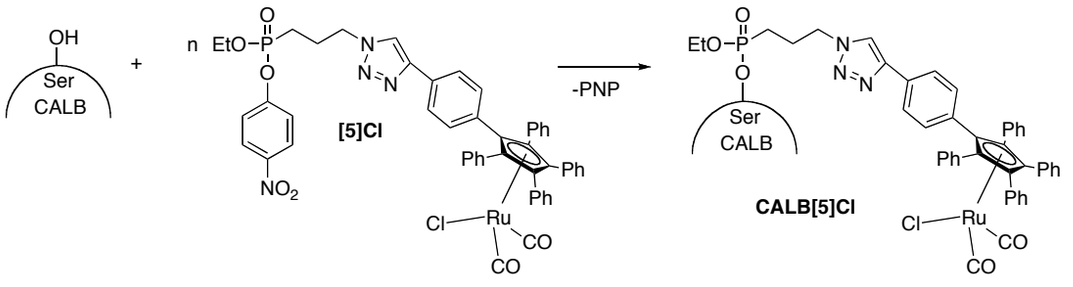

Scheme 4: Immobilization of **[5]Cl** onto Novozym® 435 beads.

In the case of our studies with cutinase solutions being inhibited by ECE-pincer metal phosphonates, the progress of the inhibition could be nicely quantified by following the release of the *p*-nitrophenolate anion during inhibition with UV-vis spectroscopy. However, as the CALB beads used in this study were not water-soluble, this analysis method proved to be unsuccessful. In order to get a reliable estimate of the amount of accessible CALB active sites on the beads, a calibration study was performed first. For this purpose, various batches of Novozym® 435 beads (20.2 mg) suspended in Tris/Triton buffer were incubated overnight with different amounts of a solution of **[5]Cl** (10 mM) in MeCN (see Experimental Section for details). After 18 hours the batches were washed with water and dichloromethane (to remove formed *p*-nitrophenolate (PNP) and unreacted **[5]Cl**) and then freeze-dried. Subsequently, activity tests with the various batches of the (partially) inhibited beads were performed, using *p*-nitrophenyl butyrate as substrate (Scheme 5). The remaining hydrolytic activity of the inhibited Novozym® 435 beads was determined by mixing a suspension of the beads (3.0 mg) with a *p*-nitrophenyl butyrate solution and filtering off the beads after exactly 2 minutes. The absorbance of released *p*-nitrophenolate anion in the remaining solution at 400 nm was measured and correlated to the amount of **[5]Cl** added (Scheme 5).

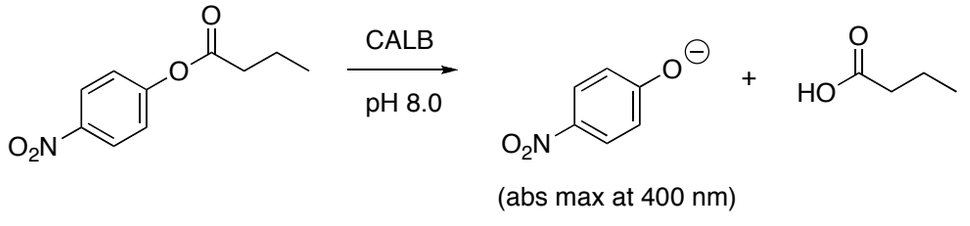

CALB: Novozym™ 435 (CALB on solid support)

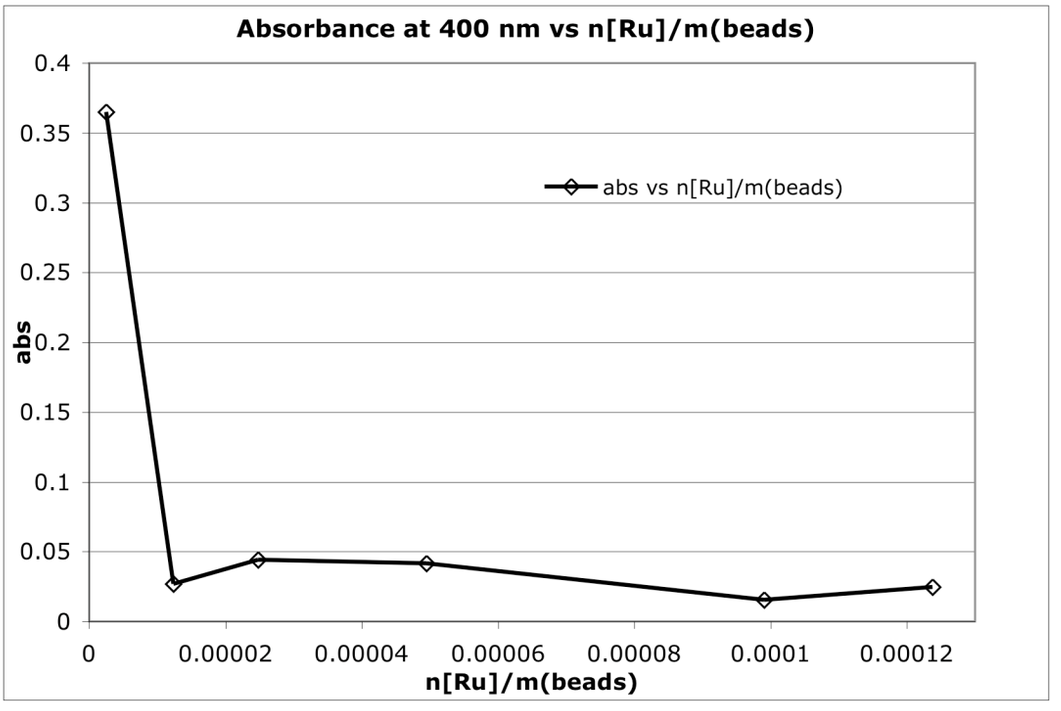

Scheme 5: Determination of the remaining hydrolytic activity of different batches of Novozym® 435 beads, which had been inhibited by **[5]Cl**; the measured release of *p*-nitrophenolate anion (y-axis, at 400 nm) is plotted versus the amount of **[5]Cl** added (x-axis, mol[Ru] added/g(beads)).

The curve in Scheme 5 shows that the hydrolytic activity of the beads did decrease upon addition of increasing amounts of **[5]Cl**. When the amount of added ruthenium complex had reached 0.025 mmol[Ru]/g(beads) or higher, the residual activity of the beads remained relatively constant.

The surface loading of the heterogenized ruthenium racemization catalyst obtained via this procedure was estimated to be 0.0125 mmol[Ru]/g(beads), thereby taking into account that only one enantiomer of the racemic phosphonate complex **[5]Cl** would bind to the active site of the enantioselective lipase **CALB**. The surface loading of 0.0125 mmol[Ru]/g(beads) is lower than for the heterogenized catalyst described by Kim and Park (**[9]Cl**, Scheme 1),[27] who achieved a loading of 0.3 mmol[Ru]/g(support) (3.37 wt % [Ru]), by using a functionalized polystyrene support. However, the ease and the mild reaction conditions of the immobilization method described here show the straightforwardness of our approach, as no pretreatment of the polymeric support or elevated temperatures during a prolonged period of time[27] are required. Furthermore, side effects of the support material are not expected, as the support itself (CALB on beads) acts as a catalyst in the cascade reaction, providing one catalytic material catalyzing two different reactions (*vide infra*). By using the described inhibition method, the amount of available catalytic

sites of the CALB beads can be controlled relative to the amount of ruthenium sites, enabling us to vary and fine-tune the composition of the catalytic material.

Catalytic studies

To investigate, whether **CALB[5]Cl** would be active as racemization catalyst, it was tested in the racemization of (*S*)-1-phenylethanol (Table 1), as this is a very well-studied substrate in various Dynamic Kinetic Resolution studies.[24-28, 53-55] For comparison, a racemization study with soluble **[5]Cl** and **[8]Cl** (Schemes 1 and 2) was performed as well, where **[8]Cl** is the standard catalyst for the metal catalysed racemization of (*S*)-1-phenylethanol.[24, 28, 55]

Table 1: Racemization of (*S*)-1-phenylethanol (**10**) with different **[Ru]Cl** catalysts.

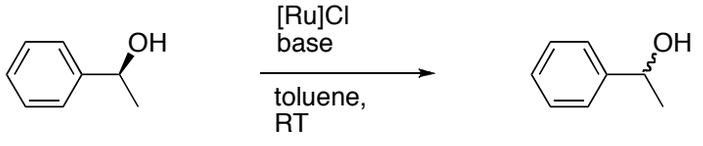

(S)-**10** rac-**10**

entry	**[Ru]Cl** catalyst (mol%)	Base used	c(M) of **10**	Time (h)	ee [a]
1	**[8]Cl**[b] (1)	KO-*t*-Bu	0.25	1	0.0%
2	**[8]Cl**[b] (5)	KO-*t*-Bu	0.25	1	0.0%
3	**[8]Cl**[b] (1)	K_3PO_4	0.25	1	0.0%
4	**[5]Cl**[c] (5)	KO-*t*-Bu	0.2	5	0.0%
5	**CALB[5]Cl**[d] (1)	K_3PO_4	0.125	18	45.2%
6	**CALB[5]Cl**[d] (1)	K_3PO_4	0.125	24	0.0%

[a] analysis by chiral GC; [b] 1 mol% **[8]Cl**, 10 mol% KO-*t*-Bu, 0.1 mmol (*S*)-**10**; [c] 5 mol% **[5]Cl**, 33 mol% KO-*t*-Bu, 0.1 mmol (*S*)-**10**; [d] 1 mol% **CALB[5]Cl**, 1 eq. K_3PO_4, 0.025 mmol (*S*)-**10**.

Firstly, the activation of the racemisation catalyst **[8]Cl** by two different bases known from literature (K_3PO_4 and KO-*t*-Bu)[24, 27] was studied. For this purpose, **[8]Cl** was activated with the respective base in toluene, after which the substrate was added. After 1h, the racemisation of (*S*)-1-phenylethanol catalyzed by **[8]Cl** was complete (entries 1, 2 and 3), indicating similar activation behaviour of the K_3PO_4 and KO-*t*-Bu base for **[8]Cl**.

As Kim and Park had used K_3PO_4 in the activation of heterogenized racemisation catalyst **[9]Cl** (Scheme 1),[27] it was decided to use the same base for the activation of the heterogenized catalyst **CALB[5]Cl** (entries 5 and 6). Racemisation with **CALB[5]Cl** gave 45.2% ee after 18h and full racemisation after 24h.

The racemisation of **[5]Cl** in solution gave full racemisation after 5h (entry 4). As no samples had been taken at shorter time intervals, it is not known whether full racemisation was achieved after a shorter period of time.
The longer reaction times of catalyst **CALB[5]Cl** in comparison to the standard racemisation catalyst **[8]Cl** are most probably due to the heterogenization of the racemisation catalyst onto a solid support, *e.g.* the reduced accessibility or the effect of site isolation of the ruthenium metal centres on the support might cause the reaction time increase. The decrease in activity for heterogenized catalysts has been observed for other catalyst systems before.[56, 57] Nevertheless the semisynthetic, immobilized biocatalyst **CALB[5]Cl** shows reasonable activity in this racemisation reaction.

In order to assay the remaining lipase activity of the uninhibited lipase active sites in **CALB[5]Cl**, a kinetic resolution of a racemic alcohol was performed. To this purpose, a kinetic resolution was run with **CALB[5]Cl** and *rac*-1-phenylethanol with isopropenyl acetate as acyl donor (Table 2).

Table 2: Results of the kinetic resolution of *rac*-**10** catalyzed by **CALB[5]Cl** and **CALB**.[a]

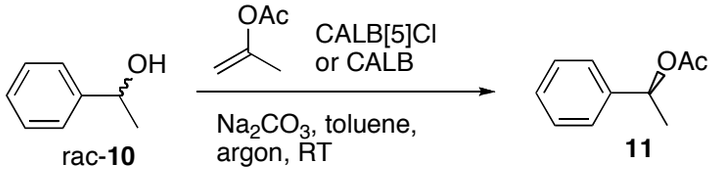

catalyst	time (h)	conversion (%)[b]	ee (%)[c]
CALB[5]Cl	0.5	5	4.9
	1	9	9.9
	3	28	37.9
CALB	0.5	35	52.5
	1	46	84.7
	3	50	>99

[a] Na_2CO_3 (0.5 mmol), enzyme beads (3.0 mg), toluene (1.0 mL), *rac*-**10** (0.5 mmol), isopropenylacetate (0.75 mmol); [b] calculated values; [c] *ee* of (*R*)–alcohol determined by chiral GC.
The **CALB** batch (without any inhibition by **[5]Cl**) gave full acylation of (*R*)-**10** within 3 hours. The partially inhibited **CALB[5]Cl** beads gave 28% acylation of (*R*)-**10** after 3 hours, indicating that the uninhibited lipase active sites on the beads were still accessible and catalytically active in the kinetic resolution.

Based on these results, an explorative DKR experiment was run using **CALB[5]Cl** as both a racemization and an enzymatic resolution catalyst. First, a racemization of

(*S*)-**10** catalyzed by **CALB[5]Cl** (1 mol%) was performed during 24h (Table 1), after which isopropenyl acetate (1.8 eq.) was added. After 24h a sample was taken, showing 18% conversion towards the acylated product **11** (>99% ee of the (*R*)-enantiomer, no (*S*)-product observed) and 14% ee of the remaining alcohol **10** ((*S*)-enantiomer). This proof-of-principle experiment shows that the used **CALB[5]Cl** beads both function as racemization and as enantioselective acylation catalyst, *i.e* through the partial inhibition of the lipase active sites with ruthenium catalyst **[5]Cl** a single supported catalyst system can be designed combining both activities.

As a general condition for successful DKR, the resolution rate of the enzyme should not exceed the racemization rate of the ruthenium catalyst too much to avoid depletion of the resolved enantiomer, meaning that a fast racemisation reaction is required.[24, 28] For the bifunctional heterogenized catalytic system **CALB[5]Cl** described here, the racemisation reaction is rather slow (Table 1) in comparison to the esterification reaction, yet we did not observed the acylated (*S*)-product. However, due to the bifunctional nature of the catalytic system, the ratio of the ruthenium catalyst versus the lipase catalyst can be easily altered, by varying the amount of ruthenium phosphonate during the lipase inhibition (Scheme 5).

Conclusions

The synthesis of ruthenium-serine hydrolase inhibitor **[5]Cl** and its use to construct the first example of a bifunctional immobilized artificial inhibitor metalloenzyme combining ruthenium racemization and lipase esterification catalytic properties is reported. **[5]Cl** was synthesized by linking an enzyme-reactive phosphonate group to an organometallic ruthenium complex *via* Cu(I) catalyzed click chemistry. Complex **[5]Cl** could be irreversibly anchored to the lipases cutinase and to CALB beads, thereby demonstrating the reactivity of **[5]Cl** even towards heterogenized lipases, which had not been described in the literature before. A study estimating the surface loading for the ruthenium complex on the beads was performed, thereby giving a good measure of inhibited and uninhibited lipase sites on the beads. A racemization study of (*S*)-1-phenylethanol catalyzed by **CALB[5]Cl** showed that the beads were catalytically active with complete racemization after 24h. A kinetic resolution study revealed that the uninhibited lipase sites on the **CALB[5]Cl** beads were catalytically active in the enantioselective acylation of 1-phenylethanol. A DKR experiment with the bifunctional heterogeneous catalytic material **CALB[5]Cl** gave 18% product formation of the acylated enantiopure product (>99% ee) after 3 hours. By changing the ratio between ruthenium inhibitor complex **[5]Cl** and **CALB** beads, the properties of the bifunctional catalytic material can be changed, thereby optimizing the catalytic system, which can potentially be recycled.

Experimental Section

General Comments: Azide exchange resin on Amberlite IRA 400 16-50 mesh (surface loading 3.8 mmol/g), diethyl 3-bromopropylphosphonate and Triton X-100 were purchased from Sigma Aldrich. Tris(hydroxylmethyl)aminomethane (Tris) was purchased from J.T. Baker, and aqueous HCl (35%) from Interchema. MeCN and CH_2Cl_2 were distilled over CaH_2 prior to use. All syntheses and the catalysis studies were performed under an inert atmosphere using Schlenk techniques and distilled solvents, unless stated otherwise. The cutinase and CALB inhibition studies were performed in air. Purification of water for buffer solutions was performed with the Milli-Q filtration system (Millipore, Quantum Ultrapure). The dialysis membranes were purchased from Pierce. Cutinase mutant N172K was provided by Unilever. Novozyme^{TM} 435 was purchased from Sigma-Aldrich and used as received. The Cu(I) amino arenethiolate catalyst **6**,[44, 45] **7**[43] and **[8]Cl**[24, 28, 55, 58] were prepared according to literature procedures. The synthesis of phosphonate **4** is described elsewhere.[39] The racemization and catalytic studies were performed under a dry argon atmosphere.

Trimethyl((4-(2,3,4,5-tetraphenylcyclopenta-2,4-dienyl)phenyl)ethynyl)silane (1): (4-Bromophenylethynyl)trimethylsilane (2.53 g, 10 mmol) was dissolved in dry THF (20 mL) under argon atmosphere and the solution was cooled to -78 °C. *n*-Butyl lithium (1.6 M in hexanes, 6.3 mL, 10 mmol) was added dropwise and the resulting yellow solution was stirred 20 minutes at -78 °C. Next, tetraphenylcyclopentadienone (3.84 g, 10 mmol) was added in one portion resulting in a beige precipitate. The suspension was allowed to reach ambient temperature and then stirred 16 h before it was cooled to 0 °C. $LiAlH_4$ (0.76 g, 20 mmol) was added in portions and the reaction mixture was stirred at ambient temperature for 3 h and then quenched with saturated aqueous NH_4Cl-solution. Et_2O was added and the organic layer was then washed with 1 M HCl, H_2O, brine and then dried over $MgSO_4$. The precipitates were filtered off and the solvent was evaporated. Purification by column chromatography (CH_2Cl_2/Pentane 1:4, silica gel) yielded 3.78 g of a yellow solid, yield 70%. ^{1}H NMR (400 MHz, $CDCl_3$) δ 7.21-6.86 (m, 24 H), 5.06 (2 singlet peaks due to the isomeric mixture, 1 H), 0.22-0.18 (3 singlets due to the isomeric mixture, 9H).

Complex [2]Cl: 1 (1.22 g, 2.24 mmol) was dissolved in dry THF (20 mL) under argon atmosphere and cooled to -78 °C. *n*-Butyl lithium (1.6 M in hexanes, 1.40 mL, 2.24 mmol) was added slowly to the solution at -78 °C. The red solution was stirred at -78 °C 25 min before $Ru_2Cl_4(CO)_6$ (573 mg, 1.12 mmol) was added in one portion. The reaction mixture was allowed to reach ambient temperature and then stirred at this temperature for 3 days before the solvent was evaporated. Purification by column chromatography (CH_2Cl_2/Pentane 1:1, silica gel) yielded 558 mg pure product as a yellow solid, Yield 34%. ^{1}H NMR (400 MHz, $CDCl_3$) δ 7.24-7.16 (m, 6H), 7.14-

7.06(m, 8H), 7.04-6.98 (m, 8H), 6.98-6.94 (m, 2H), 0.22 (s, 9H); ^{13}C NMR (100 MHz, $CDCl_3$) δ 196.67, 132.11, 131.93, 131.36, 129.96, 129.37, 129.31, 128.46, 128.42, 127.95, 127.85, 122.95, 106.40, 106.22, 106.07, 104.45, 95.67, -0.16.

Complex [3]Cl: [2]Cl (49 mg, 0.067 mmol) was dissolved in THF (0.6 mL). Glacial acetic acid (7.6 μL, 0.13 mmol) followed by TBAF·3H_2O (32 mg, 0.10 mmol) was then added. Note: addition order is very important. The reaction mixture was stirred for 1 h at ambient temperature and then put directly onto a silica gel column (CH_2Cl_2/pentane 1:1). The product was eluated with CH_2Cl_2/pentane 1:1 to yield 40 mg of a yellow solid. Yield 90%. ^{1}H NMR (400 MHz, $CDCl_3$) δ 7.27-7.20 (m, 6H), 7.17-7.09 (m, 8H), 7.08-6.98 (m, 10H), 3.11 (s, 1H); ^{13}C NMR (100 MHz, $CDCl_3$) δ 196.89, 132.36, 132.27, 131.76, 130.60, 129.60, 129.52, 128.76, 128.69, 128.22, 128.11, 122.27, 106.75, 106.47, 83.35, 78.56.

Optimization of the click reaction: To different solutions of ruthenium complex **[3]Cl** (0.02 mmol) in degassed CH_2Cl_2 or MeCN were added solutions of phosphonate **4** (0.02 mmol) in degassed CH_2Cl_2 or MeCN. The final concentrations of the reactants were 0.03-0.14 M. To these solutions was added Cu(I) catalyst **6**[44, 45] (0.1 eq.) or catalyst **7**[43] (0.1 eq) in combination with sodium ascorbate (0.5 eq.). The reaction mixtures were stirred at room temperature. The progress of the reactions was monitored by taking samples at different time intervals and subsequent analysis by ^{31}P NMR.

Complex [5]Cl: To a solution of ruthenium complex **[3]Cl** (0.1326 g, 0.2 mmol, 1.0 eq.) in degassed CH_2Cl_2 (5 mL) was added a solution of phosphonate **4** (0.0628 g, 0.2 mmol, 0.4 M, 1.0 eq.) in degassed CH_2Cl_2. To this solution was added Cu-thiolate catalyst **6**[44, 45] (0.0046 g, 0.02 mmol, 0.1 eq.) and the solution was stirred at RT. The progress of the reaction was followed by ^{31}P NMR spectroscopy. After 3 days more Cu-thiolate catalyst **6** (0.0046 g, 0.02 mmol, 0.1 eq.) was added. After 4 days full conversion was reached, all volatiles were evaporated *in vacuo* and the solid was dissolved in CH_2Cl_2 (30 mL). The organic layer was washed with 1M K_2CO_3 (2 x 50 mL), brine (2 x 50 mL) and MQ-H_2O (2 x 50 mL) and dried on Na_2SO_4, after which all volatiles were removed *in vacuo* to give a yellow solid (0.1642 g, 84%). ^{1}H NMR (CD_2Cl_2, 300 MHz) δ: 1.33 (app t, 3H, $^3J_{H\text{-}H}$ = 7.0, P-O-CH_2-CH_3), 1.94-2.06 (m, 2H, P-CH_2-CH_2-CH_2-N-), 2.29-2.44 (m, 2H, P-CH_2-CH_2-CH_2-N-), 4.12-4.33 (m, 2H, P-O-CH_2-CH_3), 4.55 (t, 2H, $^3J_{H\text{-}H}$ = 6.6 Hz, P-CH_2-CH_2-CH_2-N-), 7.05-7.28 (br m, 22H, 5 Ph, Cp-*Ar*-triazole), 7.42 (d, 2H, $^3J_{H\text{-}H}$ = 9.3 Hz, P-O-*Ar*-NO_2), 7.61 (d, 2H, $^3J_{H\text{-}H}$ = 8.4 Hz, Cp-*Ar*-triazole), 7.84 (s, 1H, triazole H), 8.26 (d, 2H, $^3J_{H\text{-}H}$ = 9.0 Hz, P-O-*Ar*-NO_2). ^{13}C NMR (CD_2Cl_2, 100 MHz) δ: 16.3 (d, $^3J_{C\text{-}P}$ = 5.7 Hz, P-O-CH_2-CH_3), 23.2 (d, $^1J_{C\text{-}P}$ = 142.7 Hz, P-CH_2-CH_2-CH_2-N-), 23.7 (d, $^2J_{C\text{-}P}$ = 4.5 Hz, P-CH_2-CH_2-CH_2-N-), 50.1 (d, $^3J_{C\text{-}P}$ = 16.5, P-CH_2-CH_2-CH_2-N-), 63.5 (d, $^2J_{C\text{-}P}$ = 7.0 Hz, P-O-CH_2-CH_3), 106.6, 107.0, 107.4, 120.6 (triazole), 121.2 (d, $^3J_{C\text{-}P}$ = 4.5 Hz, P-O-*Ar*-NO_2), 125.0, 125.8 (P-O-*Ar*-NO_2), 128.0, 128.1, 128.6, 128.7, 129.7, 129.8, 129.9, 130.8, 132.4,

132.5, 132.9, 144.8, 147.1, 155.8 (d, $^{2}J_{C\text{-}P}$ = 8.3 Hz), 197.4 (*C*=O). ^{31}P NMR (CD_2Cl_2, 298 K, 121 MHz) δ: 28.8. ^{31}P NMR (CD_3CN, 298K, 162 MHz) δ: 29.6. IR (cm^{-1}): 2050 (CO), 1999 (CO), 1613, 1594, 1525, 1494, 1447, 1393, 1347, 1266, 1227, 1162, 1112, 1077, 1034, 972.7, 918.7, 860.8, 795.2, 729.5, 698.7, 660.1. HR MS (ES+, CH_2Cl_2) for $C_{50}H_{41}ClN_4O_7PRu$ (M, 977.1445): *m/z* 977.1555 $[M]^+$ (calcd. 977.1522).

Inhibition of cutinase with complex [5]Cl: To a solution of cutinase (1000.0 μL, 200 μM, 0.2 μmol, 1 eq.) in 0.1% (m/m) Triton, 50 mM Tris buffer (pH 8.0) was added a solution of **[5]Cl** (160.0 μL, 10 mM, 8 eq.) in MeCN. After incubation overnight at 7°C, the mixture was dialysed with NH_4OAc buffer (150 mM) during 24 h (2 x 400 mL).

Activity tests: To different batches of freshly prepared 0.1% (m/m) Triton, 50 mM Tris buffer (1.493 μL, pH 8.0) was added a solution of *para*-nitrophenolbutyrate (7.0 μL, 50 mM) in MeCN. To these substrate solutions were added portions of inhibited and uninhibited cutinase (0.5 μL, 200 μM, 0.1 nmol) and the release of *para*-nitrophenolate was measured at 400 nm during 10 min.

Immobilization of complex [5]Cl onto Novozym® 435 beads (variation of the surface loading): To batches of Novozym® 435 beads (0.0202 g) in 0.1% (m/m) Triton, 50 mM Tris buffer (a: 1.495 mL; b: 1.485 mL; c: 1.475 mL; d: 1.450 mL; e: 1.400 mL; f: 1.350 mL; g: 1.300 mL; h: 1.250 mL) were added different portions of **[5]Cl** (10 mM) in MeCN (a: 5.0 μL, 0.05 μmol; b: 15.0 μL, 0.15 μmol; c: 25.0 μL, 0.25 μmol; d: 50.0 μL, 0.50 μmol; e: 100.0 μL, 1.00 μmol; f: 150.0 μL, 1.50 μmol; g: 200.0 μL, 2.00 μmol; h: 250.0 μL, 2.50 μmol). After incubation at RT overnight, the beads were washed with MilliQ-H_2O (15 mL each) and CH_2Cl_2 (15 mL each) and freeze-dried overnight.

Activity tests with inhibited Novozym® 435 beads (determination of the optimum surface loading): In different cuvettes, different batches of inhibited Novozym® 435 beads were weighed (0.0030 g) and freshly prepared 0.1% (m/m) Triton, 50 mM Tris buffer (1.493 μL, pH 8.0) was added. To the different suspensions a solution of *para*-nitrophenolbutyrate (7.0 μL, 50 mM) in MeCN was added, after which the suspensions were shaken during exactly 2 minutes. Subsequently, the beads were filtered off and a UV-VIS spectrum of the solution was recorded (600-200 nm).

Immobilization of complex [5]Cl onto Novozym® 435 beads (with optimum surface loading): To batches of Novozym® 435 beads (0.6000 g) in 0.1% (m/m) Triton, 50 mM Tris buffer was added **[5]Cl** (3.0000 mL, 30.0 μmol, 10 mM) in MeCN. After incubation at RT overnight, the beads were washed with MilliQ-H_2O (200 mL)

and CH_2Cl_2 (120 mL) and freeze-dried overnight. The obtained beads with an approximal surface loading of 0.05 mmol/g were used in the racemization studies.

Racemization studies with CALB[5]Cl: CALB[5]Cl beads (1 mol%) were weighed into a schlenk and toluene (0.25 mL) was added, after which a solution of K_3PO_4 (50.0 μL, 0.025 mmol, 0.5 M, 1.0 eq.) in THF was added. After 10 minutes of stirring, (*S*)-1-phenylethanol (0.025 mmol) was added and the reaction mixture was stirred at room temperature. After 24h a sample was taken, filtered over cotton with Et_2O as eluent and analysed by chiral GC.

Racemization studies with [5]Cl and [8]Cl: The catalyst powder was weighed into a schlenk and the desired volume of toluene was added, after which a solution of KO*t*-Bu (0.5 M, 10-33 mol%) in THF was added. After 10 minutes of stirring, (*S*)-1-phenylethanol (12.0 μL, 0.1 mmol) was added and the reaction mixture was stirred at room temperature. After a certain time interval a sample was taken, filtered over cotton with Et_2O as eluent and analysed by chiral GC.

Kinetic resolution with CALB or CALB[5]Cl: To Na_2CO_3 (0.5 mmol) were added enzyme beads **CALB** or **CALB[5]Cl** (3.0 mg), toluene (1.0 mL), *rac*-1-phenylethanol (0.5 mmol) and isopropenylacetate (0.75 mmol). All reagents were stirred under Argon at room temperature and after different time intervals samples were taken, filtered over cotton with Et_2O as eluent and analysed by chiral GC.

DKR experiment with CALB[5]Cl: CALB[5]Cl beads (1 mol%) were weighed into a schlenk and toluene (0.25 mL) was added, after which a solution of K_3PO_4 (50.0 μL, 0.025 mmol, 0.5 M, 1.0 eq.) in THF was added. After 10 minutes of stirring, (*S*)-1-phenylethanol (0.025 mmol) was added and the reaction mixture was stirred at room temperature. After 24h a sample was taken, filtered over cotton with Et_2O as eluent and analysed by chiral GC. To the reaction mixture toluene (0.2 mL), (*S*)-1-phenylethanol (0.025 mmol) and isopropenylacetate (0.045 mmol) were added. The mixture was stirred during 24h, after which a sample was taken, filtered over cotton with Et_2O as eluent and analysed by chiral GC.

References

1. Faber, K., *Biotransformations in Organic Chemistry*. 5th ed.; Springer: Berlin, 2004; p 1-454.
2. Bornscheuer, U. T.; Kazlauskas, R. J., *Hydrolases in Organic Synthesis, Regio- and Stereoselective Biotransformations* 2nd ed.; Wiley-VCH: Weinheim, 1999; p 1-368.
3. Drauz, K.; Waldmann, H., *Enzyme Catalysis in Organic Synthesis: A Comprehensive Handbook*. 2nd ed.; Wiley-VCH: Weinheim, 2002; p 1-1500.
4. Wong, C.-H.; Whitesides, G. M., *Enzymes in Synthetic Organic Chemistry*. 1st ed.; Pergamon: Oxford, 1994; p 1-346.
5. Sheldon, R. A., *Biochem. Soc. Trans.* **2007,** 35, 1583-1587.
6. Sheldon, R. A., *Chem. Commun.* **2008**, 3352-3365 and references mentioned therein.
7. van de Velde, F.; van Rantwijk, F.; Sheldon, R. A., *Trends Biotechnol.* **2001,** 19, 73-80.
8. Reetz, M. T.; Rentzsch, M.; Pletsch, A.; Maywald, M.; Maiwald, P.; Peyralans, J. J.-P.; Maichele, A.; Fu, Y.; Jiao, N.; Hollmann, F.; Mondière, R.; Taglieber, A., *Tetrahedron* **2007,** 63, 6404-6414.
9. Wilson, M. E.; Whitesides, G. M., *J. Am. Chem. Soc.* **1978,** 100, 306-307.
10. Yokoi, N.; Ueno, T.; Unno, M.; Matsui, T.; Ikeda-Sato, M.; Watanabe, Y., *Chem. Commun.* **2008**, 229-231.
11. Thomas, C. M.; Letondor, C.; Humbert, N.; Ward, T. R., *J. Organomet. Chem.* **2005,** 690, 4488-4491.
12. Ueno, T.; Abe, S.; Yokoi, N.; Watanabe, Y., *Coord. Chem. Rev.* **2007,** 251, 2717-2731.
13. Ueno, T.; Koshiyama, T.; Abe, S.; Yokoi, N.; Ohashi, M.; Nakajima, H.; Watanabe, Y., *J. Organomet. Chem.* **2007,** 692, 142-147.
14. Ueno, T.; Norihiko, Y.; Abe, S.; Watanabe, Y., *J. Inorg. Biochem.* **2007,** 101, 1667-1675.
15. Panella, L.; Broos, J.; Jin, J.; Fraaije, M. W.; Janssen, D. B.; Jeronimus-Stratingh, M.; Feringa, B. L.; Minnaard, A. J.; De Vries, J. G., *Chem. Commun.* **2005,** 45, 5656-5658.
16. Pierron, J.; Malan, C.; Creus, M.; Gradinaru, J.; Hafner, I.; Ivanova, A.; Sardo, A.; Ward, T. R., *Angew. Chem. Int. Ed.* **2008,** 47, 701-705.
17. Collot, J.; Gradinaru, J.; Humbert, N.; Skander, M.; Zocchi, A.; Ward, T. R., *J. Am. Chem. Soc.* **2003,** 125, 9030-9031.
18. Creus, M.; Pordea, A.; Rossel, T.; Sardo, A.; Letondor, C.; Ivanova, A.; LeTrong, I.; Stenkamp, R. E.; Ward, T. R., *Angew. Chem. Int. Ed.* **2008,** 47, 1400-1404.
19. Davies, R. R.; Distefano, M. D., *J. Am. Chem. Soc.* **1997,** 119, 11643-11652.
20. Ahn, Y.; Ko, S.-B.; Kim, M.-J.; Park, J., *Coord. Chem. Rev.* **2008,** 252, 647-658.
21. Kim, M.-J.; Ahn, Y.; Park, J., *Curr. Opin. Biotechnol.* **2002,** 13, 578-587.
22. Martín-Matute, B.; Bäckvall, J.-E., *Curr. Opin. Chem. Biol.* **2007,** 11, 226-232.
23. Huerta, F. F.; Minidis, A. B. E.; Bäckvall, J.-E., *Chem. Soc. Rev.* **2001,** 30, 321-331.
24. Martín-Matute, B.; Edin, M.; Bogar, K.; Bäckvall, J.-E., *Angew. Chem. Int. Ed.* **2004,** 43, 6535-6539.
25. Boren, L.; Martín-Matute, B.; Xu, Y.; Cordova, A.; Bäckvall, J.-E., *Chem. Eur. J.* **2006,** 12, 225-232.
26. Ko, S.-B.; Baburaj, B.; Kim, M.-J.; Park, J., *J. Org. Chem.* **2007,** 72, 6860-6864.
27. Kim, N.; Ko, S.-B.; Kwon, M. S.; Kim, M.-J.; Park, J., *Org. Lett.* **2005,** 7, 4523-4526.
28. Martín-Matute, B.; Edin, M.; Bogar, K.; Kaynak, F. B.; Bäckvall, J.-E., *J. Am. Chem. Soc.* **2005,** 127, 8817-8825.
29. Träff, A. M.; Bogar, K.; Warner, M.; Bäckvall, J.-E., *Org. Lett.* **2008,** 10, 4807-4810.
30. Haak, R. M.; Berthiol, F.; Jerphagnon, T.; Gayet, A. J. A.; Tarabiono, C.; Postema, C. P.; Ritleng, V.; Pfeffer, M.; Janssen, D. B.; Minnaard, A. J.; Feringa, B. L.; De Vries, J. G., *J. Am. Chem. Soc.* **2008,** 130, 13508-13509.
31. Bogar, K.; Bäckvall, J.-E., *Tetrahedron Lett.* **2007,** 48, 5471-5474.
32. Bogar, K.; Hoyos Vidal, P.; Alcantara Leon, A. R.; Bäckvall, J.-E., *Org. Lett.* **2007,** 9, 3401-3404.
33. Kim, M.-J.; Choi, J.-H.; Kim, S.; Kim, D.; Han, K.; Ko, S.-B.; Park, J., *Org. Lett.* **2008,** 10, 1295-1298.

34. Thalen, L. K.; Zhao, D.; Sortais, J.-B.; Paetzold, J.; Hoben, C.; Bäckvall, J.-E., *Chem. Eur. J.* **2009,** 15, 3403-3410.
35. Fransson, A.-B.; Boren, L.; Pamies, O.; Bäckvall, J.-E., *J. Org. Chem.* **2005,** 70, 2582-2587.
36. Rutten, L.; Wieczorek, B.; Mannie, J.-P. B. A.; Kruithof, C. A.; Dijkstra, H. P.; Egmond, M. R.; Lutz, M.; Klein Gebbink, R. J. M.; Gros, P.; van Koten, G., *Chem. Eur. J.* **2009,** 15, 4270-4280 (Chapter 2 of this thesis).
37. Wieczorek, B.; Klimeck, T.; Dijkstra, H. P.; Egmond, M. R.; van Koten, G.; Klein Gebbink, R. J. M., In manuscript in preparation (Chapter 5 of this thesis).
38. Wieczorek, B.; Snelders, D. J. M.; Dijkstra, H. P.; Versluis, K.; Heck, A. J. R.; Lutz, M.; Spek, A. L.; Egmond, M. R.; Klein Gebbink, R. J. M.; van Koten, G., In manuscript in preparation (Chapter 4 of this thesis).
39. Wieczorek, B.; Lemcke, B.; Dijkstra, H. P.; Egmond, M. R.; van Koten, G.; Klein Gebbink, R. J. M., In manuscript in preparation (Chapter 6 of this thesis).
40. Wieczorek, B.; Dijkstra, H. P.; Klein Gebbink, R. J. M.; van Koten, G., *J. Organomet. Chem.* **2009,** 694, 812-822 (Chapter 1 of this thesis).
41. Kruithof, C. A.; Casado, M. A.; Guillena, G.; Egmond, M. R.; van der Kerk-van Hoof, A.; Heck, A. J. R.; Klein Gebbink, R. J. M.; van Koten, G., *Chem. Eur. J.* **2005,** 11, 6869-6877.
42. Kruithof, C. A.; Dijkstra, H. P.; Lutz, M.; Spek, A. L.; Egmond, M. R.; Klein Gebbink, R. J. M.; van Koten, G., *Eur. J. Inorg. Chem.* **2008,** 28, 4425-4432.
43. Rodionov, V. O.; Presolski, S. I.; Gardinier, S.; Lim, Y.-H.; Finn, M. G., *J. Am. Chem. Soc.* **2007,** 129, 12696-12704.
44. Janssen, M. D.; Donkervoort, J. G.; van Berlekom, S. B.; Spek, A. L.; Grove, D. M.; van Koten, G., *Inorg. Chem.* **1996,** 35, 4752-4763.
45. Knotter, D. M.; Van Maanen, H. L.; Grove, D. M.; Spek, A. L.; van Koten, G., *Inorg. Chem.* **1991,** 30, 3309-3317.
46. Meldal, M.; Tornoe, C. W., *Chem. Rev.* **2008,** 108, 2952-3015.
47. Dijkstra, H. P.; Sprong, H.; Aerts, B. N. H.; Kruithof, C. A.; Egmond, M. R.; Klein Gebbink, R. J. M., *Org. Biomol. Chem.* **2008,** 6, 523-531.
48. Cambillau, C.; Longhi, S.; Nicolas, A.; Martinez, C., *Curr. Opin. Struct. Biol.* **1996,** 6, 449-456.
49. Longhi, S.; Cambillau, C., *Biochim. Biophys. Acta* **1999,** 1441, 185-196.
50. Longhi, S.; Mannesse, M. L. M.; Verheij, H. M.; De Haas, G. H.; Egmond, M.; Knoops-Mouthuy, E.; Cambillau, C., *Protein Sci.* **1997,** 6, 275-286.
51. Longhi, S.; Nicolas, A.; Creveld, L.; Egmond, M.; Verrips, C. T.; de Vlieg, J.; Martinez, C.; Cambillau, C., *Proteins* **1996,** 26, 442-458.
52. Mannesse, M. L. M.; de Haas, G. H.; van der Heijden, H. T. W. M.; Egmond, M. R.; Verheij, H. M., *Biochem. Soc. Trans.* **1997,** 25, 165-170.
53. Choi, J.-H.; Kim, Y. H.; Nam, S. H.; Shin, S. T.; Kim, M.-J.; Park, J., *Angew. Chem. Int. Ed.* **2002,** 41, 2373-2376.
54. Kim, M.-J.; Kim, H.-M.; Kim, D.; Ahn, Y.; Park, J., *Green Chem.* **2004,** 6, 471-474.
55. Csjernyik, G.; Bogar, K.; Bäckvall, J.-E., *Tetrahedron. Lett.* **2004,** 45, 6799-6802.
56. McDonald, A. R.; Muller, C.; Vogt, D.; van Klink, G. P. M.; van Koten, G., *Green Chem.* **2008,** 10, 424-432.
57. Madhavan, N.; Jones, C. W.; Weck, M., *Acc. Chem. Res.* **2008,** 41, 1153-1165.
58. Connelly, N. G.; Manners, I., *J. Chem. Soc., Dalton Trans.* **1989**, 283-288.

English Summary

The modification of biomolecules by transition metal complexes has become an increasingly important area of research in recent years. As transition metal complexes possess a high electron density around the metal centre, they display a wide range of reactivities rendering them extremely useful target molecules in *e.g.* catalysis and coordination studies.[1, 2] When transition metal complexes are used to modify biological molecules such as carbohydrates, peptides and proteins, these special properties can be used to alter the structure and function of the respective biomolecule. This combination of transition metal and biochemistry opens up exciting new possibilities in the structural study of biomolecules and drug targeting, in which the special properties of the metal centre can be exploited to elucidate the structure and the mechanism of action. Furthermore, by synthetic modification with metal complexes, the intrinsic properties of the biomolecule can be altered and novel functionalities can be added, *e.g.* novel spectroscopic or non-natural catalytic features. Transition metal complexes can be attached to biomolecules in a covalent or non-covalent manner, thereby modifying different functional groups in the host molecule in a reversible or irreversible way.

A group of transition metal complexes, which have been studied intensively, are the so-called pincer complexes.[3] These pincer complexes contain a terdentate, monoanionic ligand of the general formula $[2,6\text{-}(ECH_2)_2C_6H_3]^-$, where E is a neutral, two-electron heteroatom donor, mostly NR_2, PR_2, or SR (Figure 1).

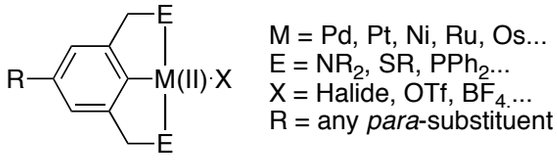

Figure 1: General structure of an ECE-pincer metal complex.

In these complexes, M(II) is a divalent transition metal cation, for example from the d^8 metal series, and X is a monoanion.[3] In these complexes, the bis-*ortho*-chelation of the metal ion by the two E-donating groups provides further stability to the central M-C bond, making some ECE-pincer metal complexes even compatible with aqueous solvent media (acidic, neutral, basic), aerobic conditions and elevated temperatures. Due to their specific structural features[4, 5] and remarkable stability, ECE-pincer metal complexes have found numerous applications, ranging from their uses such as catalysts, organometallic switches, and heavy atom probes to sensoring applications.[3] Until now, different types of ECE-pincer metal complexes have been attached as building blocks to polymers,[6] dendrimers[7] and solid supports (*e.g.* silica surfaces).[8] Those hybrid materials were successfully used as catalysts in various catalytic reactions, as sensor and diagnostic devices, and as supramolecular building blocks. Recently, several ECE-pincer metal complexes substituted by protein-reactive phosphonate groups have been developed in our group (Figure 2).[9]

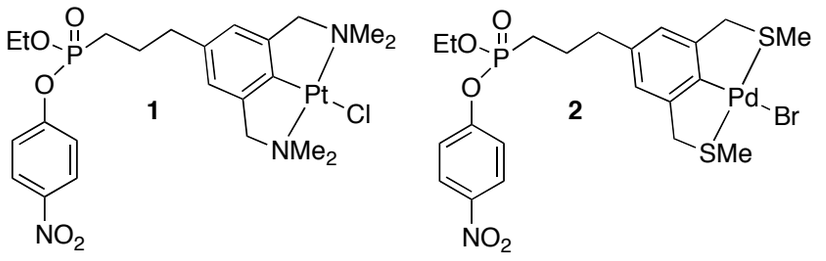

Figure 2: Structures of the single-site reactive ECE-pincer metal complexes described in this thesis.

As phosphonates have been known to be site-selective inhibitors for serine hydrolases binding covalently to the reactive nucleophile serine in the active site of serine hydrolases, the ECE-pincer metal substituted phosphonates in Figure 2 could be used for the single-site covalent labelling of the lipase cutinase (lipases belong to the super family of serine hydrolases), as shown recently (Figure 3).[9]

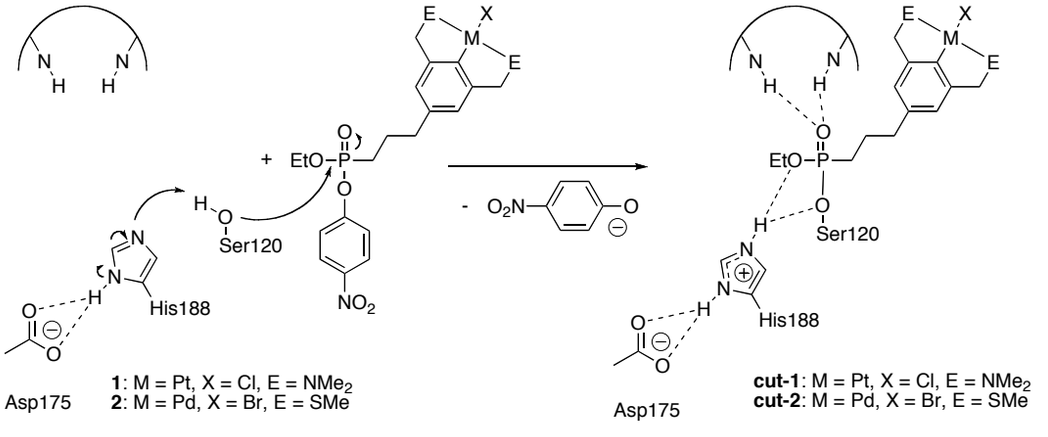

Figure 3: Single-site covalent binding of ECE-pincer metal phosphonate inhibitors to the active site of cutinase.

In this thesis the demonstrated inhibitory activity of organometallic phosphonates[9, 10] towards lipases is exploited further and the constructed organometallic enzyme hybrids are applied in structural (*Chapter 2*), kinetic (*Chapter 3*), coordination (*Chapter 4*), catalytic (*Chapters 5* and *8*) and protein labelling (*Chapter 6*) studies.
In *Chapter 1* a comprehensive overview of bioorganometallic pincer complexes known from literature is given. Due to their excellent stability and versatile properties, ECE-pincer metal complexes have been used as anticarcinogenic agents, as SPR enhancers in the study of carbohydrate protein-interactions, as building blocks in supramolecular chemistry involving carbohydrates and peptides, as peptide biomarkers and catalysts, and in the design of pincer metal protein hybrids. This diverse chemistry and the various application possibilities of bioorganometallic ECE-

pincer complexes were taken as a starting point for the study of the organometallic serine hydrolase hybrids described in this thesis.

In *Chapter 2*, five crystal structures of cutinase covalently modified with two different ECE-pincer metal phosphonate inhibitors (Figure 4) are described. The two ECE-pincer metal complexes had been introduced by site-selective inhibition prior to crystallization and have been shown to bind selectively to the Ser120 residue in the active site of cutinase.

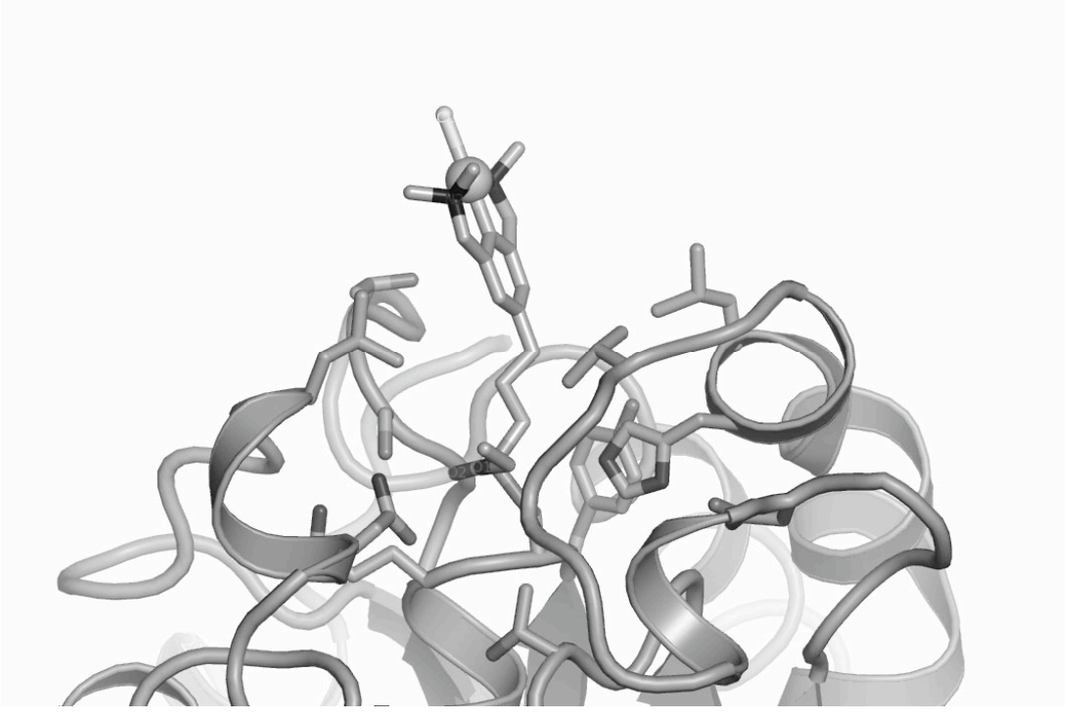

Figure 4: Crystal structure of a NCN-pincer platinum cutinase hybrid (**cut-1**).

For all five presented crystal structures, the ECE-pincer platinum or palladium head group sticks out of the cutinase active site pocket and is exposed to the solvent. Depending on the nature of the ECE metal head group, the ECE-pincer platinum and palladium phosphonate guests occupy different pockets in the cutinase active site, with concomitant different stereochemistries on the phosphorous atom for the NCN-pincer platinum (**1**, S_P) and SCS-pincer palladium (**2**, R_P) cutinase hybrid structures. When the NCN-pincer platinum cutinase hybrid (**cut-1**) was crystallized under halide-poor conditions, a novel metal-induced dimeric structure was formed between two cutinase-bound pincer platinum head groups, which are interconnected via a single μ-Cl bridge. This halide-bridged metal dimer shows that coordination chemistry is possible with protein modified pincer metal complexes. Furthermore, the NCN-pincer platinum complex **1** could be used as site-selective tool for the phasing of raw protein diffraction data, which shows the potential of the pincer platinum complex as heavy-

atom derivative for facilitating the phasing of raw diffraction data in protein crystallography.

In *Chapter 3* a study investigating the binding of the two opposite enantiomers of phosphonate pincer substrates **1** and **2** (Figure 2) to cutinase is described. A ^{31}P NMR spectroscopic study showed that after addition of stoichiometric amounts of either NCN-pincer platinum (**1**) or SCS-pincer palladium (**2**) inhibitor both stereoisomers are formed, whereas a single stereoisomer is formed when 2.5 equivalents of these inhibitors were used. A kinetic study based on the release of the *para*-nitrophenolate group upon inhibition of cutinase showed that racemic inhibitors **1** and **2** display a different kinetic inhibition behaviour, explaining the different stereoisomers observed in the crystal structures in *Chapter 2*.

In *Chapter 4* a coordination study between a cationic NCN-pincer platinum cutinase hybrid and several phosphines is described. NMR spectroscopy and ES mass spectrometry analyses provided evidence that the protein-embedded cationic metal centre is accessible for the coordination of phosphine ligands in aqueous media. The strength and extent of the coordination is highly dependent on the steric bulk and the electronic properties of the phosphine. Even phosphine ligands that are insoluble in water were capable of coordinating to the platinum centre of the hybrid, the resulting **cut-1**-phosphine coordination complex is water-soluble. This study unambiguously shows that the pincer-metal centre in these hybrid constructs is still available for the coordination of ligands, solvent molecules or substrates. This opens up opportunities to apply these pincer-metal-biomolecule adducts among others as abiotic catalysts and for protein diagnosis studies.

Based on the successful coordination studies, a catalytic study with an SCS-pincer palladium cutinase hybrid was performed in *Chapter 5*. An abiotic C-C coupling reaction between a boronic acid and an epoxide was catalyzed by an SCS-pincer palladium-cutinase hybrid in aqueous media yielding both a linear and a branched product (Scheme 1).

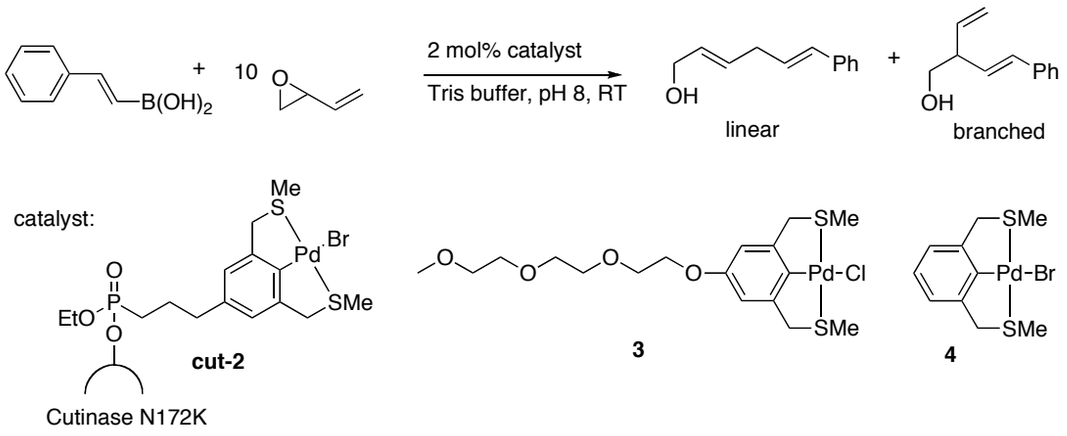

Scheme 1: C-C coupling reaction catalyzed by SCS-pincer palladium cutinase hybrid **cut-2** and SCS-pincer palladium catalysts **3** and **4**.

The selectivities of the pincer-cutinase hybrid catalyst **cut-2** (linear/branched = 4.3) were different for the small molecular SCS-pincer palladium catalysts studied (linear/branched = 0.4 (**3**) and 2.4 (**4**)), demonstrating the influence of the protein backbone on the selectivity of the metal centre. The activities in buffer were highest for catalyst **4** (64% yield), whereas the pincer protein catalyst **cut-2** showed intermediate activity (31%) and the water-soluble catalyst **3** had a low activity (12%).

In *Chapter 6* a novel luminescent organometallic biolabel based on a luminescent NCN-platinum complex is described (Figure 5).

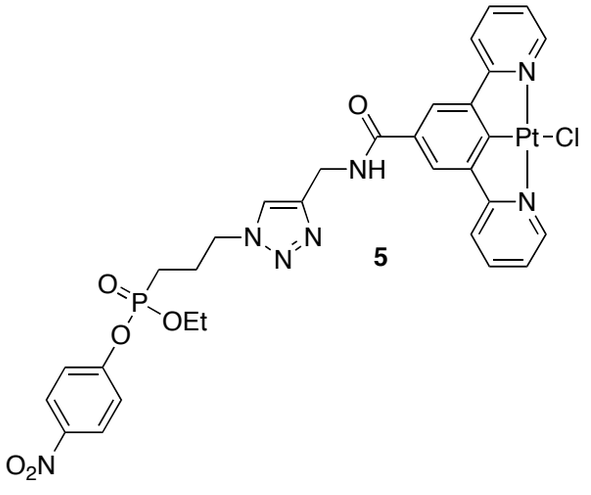

Figure 5: Structure of the luminescent organometallic complex **5** used for lipase labelling.

The luminescent organometallic NCN-platinum moiety was coupled to the phosphonate via click chemistry, leaving the reactive *para*-nitrophenolate moiety intact. Complex **5** was successfully used in the irreversible covalent labelling of various lipases and applied in a SDS PAGE gel experiment. The luminescent NCN-platinum moiety was stable under the electrophoresis conditions applied, showing the versatility of the fluorescent phosphonate **5** and opening up possibilities for further protein diagnosis studies of **5** with other serine hydrolases.

In *Chapter 7* the coordination of a fluorescent stilbazole to a cationic NCN pincer platinum complex is described (Figure 6).

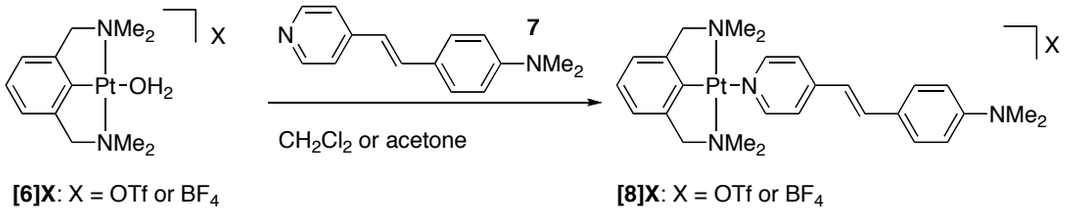

Figure 6: Formation of stilbazole-pincer coordination complex **[8]X**.

The coordination to the pincer metal centre influenced the spectroscopic properties of the stilbazole molecule, which was accompanied by a red-shift of the absorption and emission spectra of the novel coordination complex. The coordination was observed in dichloromethane, methanol and acetone, whereas no coordination complex **[8]X** was formed in acetonitrile. The spectroscopic properties of the stilbazole molecule were changed upon coordination to the pincer complex, which can play a role for the development of novel future luminescent diagnostic or sensor materials.

The synthesis and site-specific immobilization of ruthenium racemization catalyst **[9]Cl** onto lipase beads is described in *Chapter 8* (Figure 7).

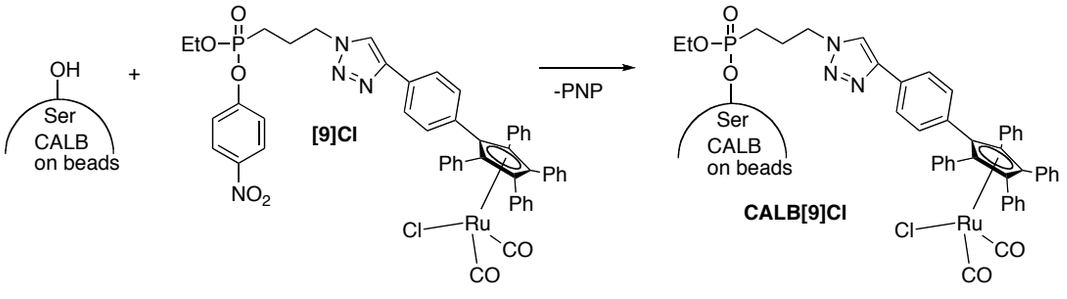

Figure 7: Immobilisation of ruthenium racemization catalyst **[9]Cl** onto lipase-containing beads.

Due to the nucleophilic serine in the active site of supported CALB, complex **[9]Cl** could be immobilized directly onto CALB-containing beads. As the accessibility of the CALB active sites for **[9]Cl** was reduced in comparison to lipases in solution, the achieved inhibition of CALB was incomplete. A determination of the surface loading showed that up to 0.0125 mmol [Ru]/g beads could be achieved. The resulting immobilized semi-synthetic CALB complex **CALB[9]Cl** was subsequently used in the racemization of a secondary alcohol, which gave complete racemization after 24 h. Due to incomplete inhibition of the CALB beads, the lipase activity of the beads was conserved partially, enabling their use as cascade catalyst in a Dynamic Kinetic Resolution (DKR) study. Thereby, the ruthenium inhibited sites of the beads acted as racemization catalyst and the free CALB sites catalyzed the kinetic resolution, which gave the acylated product (99% ee) in 18% yield.

In this thesis various phosphonate functionalized organometallic complexes were immobilized onto the active site of lipases and used in structural, coordination, catalytic and protein labeling studies. The various applications of these transition metal complex lipase hybrids show the versatility of these systems and open up new possibilities for further studies in proteomics, novel catalytic reactions and supramolecular metal-biohybrid systems. By exploiting the unique structural and electronic properties of protein-embedded transition metal complexes, novel protein modification and studying tools are at hand, which can tremendously advance the field of protein science. Based on this work, novel paramagnetic pincer complexes for the mapping of active sites can be developed for example, or cascade reactions leading to green(er) organic synthesis routes or novel materials can be constructed with combined metal-biomolecule properties.

References

1. Crabtree, R. H., *The Organometallic Chemistry of the Transition Metals*. Wiley: New York, 1988; p 1-422.
2. Elschenbroich, C.; Salzer, A., *Organometallics*. VCH: Weinheim, 1992; p 1-495.
3. Albrecht, M.; van Koten, G., *Angew. Chem. Int. Ed.* **2001,** 40, 3750-3781.
4. Slagt, M. Q.; Rodriguez, G.; Grutters, M. M. P.; Klein Gebbink, R. J. M.; Klopper, W.; Jenneskens, L. W.; Lutz, M.; Spek, A. L.; van Koten, G., *Chem. Eur. J.* **2004,** 10, 1331-1344.
5. Stiriba, S.-E.; Slagt, M. Q.; Kautz, H.; Klein Gebbink, R. J. M.; Thomann, R.; Frey, H.; van Koten, G., *Chem. Eur. J.* **2004,** 10, 1267-1273.
6. Slagt, M. Q.; Stiriba, S.-E.; Klein Gebbink, R. J. M.; Kautz, H.; Frey, H.; van Koten, G., *Macromolecules* **2002,** 35, 5734-5737.
7. Kleij, A. W.; Gossage, R. A.; Jastrzebski, J. T. B. H.; Boersma, J.; van Koten, G., *Angew. Chem. Int. Ed.* **2000,** 39, 176-178.
8. Mehendale, N. C.; Sietsma, J. R. A.; de Jong, K. P.; van Walree, C. A.; Klein Gebbink, R. J. M.; van Koten, G., *Adv. Synth. Catal.* **2007,** 349, 2619-2630.
9. Kruithof, C. A.; Casado, M. A.; Guillena, G.; Egmond, M. R.; van der Kerk-van Hoof, A.; Heck, A. J. R.; Klein Gebbink, R. J. M.; van Koten, G., *Chem. Eur. J.* **2005,** 11, 6869-6877.
10. Kruithof, C. A.; Casado, M. A.; Guillena, G.; Egmond, M. R.; van der Kerk-van Hoof, A.; Heck, A. J. R.; Klein Gebbink, R. J. M.; van Koten, G., *Eur. J. Inorg. Chem.* **2008,** 27, 4425-4432.

Nederlandse Samenvatting

De modificatie van biomoleculen met overgangsmetaalcomplexen heeft zich gedurende de afgelopen jaren tot een belangrijk onderzoeksgebied ontwikkeld. Overgangsmetaalcomplexen bezitten door hun specifieke elektronendichtheid op het metaalcentrum een breed activiteitenspectrum hetgeen hen tot bijzonder geschikte doelmoleculen maakt in, onder andere, katalytische en coördinatiestudies.[1, 2] Wanneer overgangsmetaalcomplexen toegepast worden voor de modificatie van biomoleculen zoals koolhydraten, peptides en proteïnen, kunnen deze speciale eigenschappen gebruikt worden om de structuur en functie van het desbetreffende biomolecuul te beïnvloeden. De combinatie van overgangsmetaal- en biochemie opent nieuwe, interessante mogelijkheden voor de structurele studie van biomoleculen en de ontwikkeling van geneesmiddelen. In deze studies worden de speciale eigenschappen van het metaalcentrum gebruikt om bijvoorbeeld de structuren en reactiemechanismen op te helderen.
Verder kunnen door synthetische modificatie met metaalcomplexen de intrinsieke eigenschappen van het biomolecuul veranderd worden en nieuwe functionaliteiten worden toegevoegd, zoals bijvoorbeeld nieuwe spectroscopische eigenschappen of juist niet-natuurlijke katalytische eigenschappen. Overgangsmetaalcomplexen kunnen covalent of niet-covalent aan biomoleculen gebonden worden. Hierdoor kunnen verschillende functionele groepen in het gastmolecuul op een hetzij reversibele of een irreversibele manier gemodificeerd worden.
Een groep organometaalcomplexen, die veelvoudig zijn bestudeerd, zijn de zogenaamde pincercomplexen.[3] Deze pincercomplexen bevatten een terdentaat, monoanionisch ligand met de algemene formule $[2,6\text{-}(ECH_2)_2C_6H_3]^-$, waarbij E een neutrale, twee-elektronen heteroatoomdonor is, zoals bijvoorbeeld NR_2, PR_2, of SR (Figuur 1).

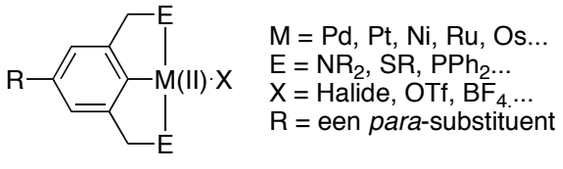

Figuur 1: Algemene structuur van een ECE-pincermetaalcomplex.

Voor deze complexen is M(II) een divalent overgangsmetaalkation van bijvoorbeeld de d^8-metaalserie, en is X een anion.[3] De bis-*ortho*-chelering van het metaalion door de twee electrondonerende E-groepen zorgt voor een verdere stabilisatie van de centrale M-C-binding, wat sommige ECE-pincermetaalcomplexen zo stabiel maakt dat zij zelfs compatibel zijn met waterige (zuur, neutraal, basisch) milieus, aërobische condities en hogere reactietemperaturen.
Door hun specifieke structurele eigenschappen[4, 5] en hun bijzondere stabiliteit worden ECE-pincermetaalcomplexen veelvuldig onderzocht als katalysatoren, moleculaire schakelaars, zware atomen probes voor structuuropheldering, voor de synthese van speciale polymeren en voor sensorische toepassingen.[3] In andere toepassingen worden ECE-pincermetaalcomplexen als bouwstenen gebonden aan polymeren,[6] dendrimeren[7] en aan vaste dragermaterialen, zoals silicaoppervlakken.[8] Deze hybridematerialen

worden met succes gebruikt als katalysatoren in de organische synthese, als sensor- en diagnostische materialen en als supramoleculaire bouwstenen. Recentelijk zijn door onze groep verschillende ECE-pincermetaalcomplexen ontwikkeld die gesubstitueerd zijn met proteïnereactieve fosfonaatgroepen (Figuur 2).[9]

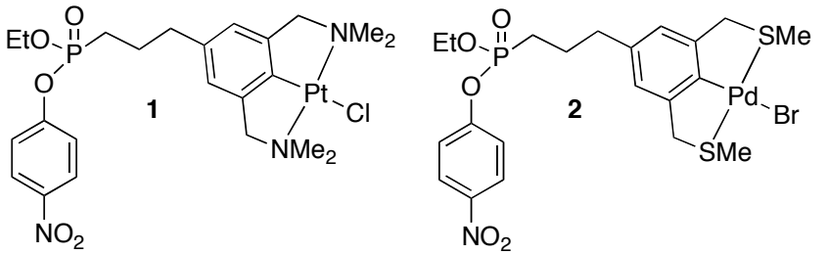

Figuur 2: Structuren van ECE-pincermetaalcomplexen met een proteïnereactieve fosfonaatgroep, zoals beschreven in dit proefschrift.

Fosfonaten staan bekend om hun eigenschappen als selectieve inhibitoren van de katalytische centra van serine hydrolases; hiervan gebruik makend konden ECE-pincermetaalgesubstitueerde fosfonaten (Figuur 2) ingezet worden voor de single-site covalente markering van cutinase (een lipase behorend tot de superfamilie van serine hydrolasen), zoals recentelijk werd aangetoond (Figuur 3).[9]

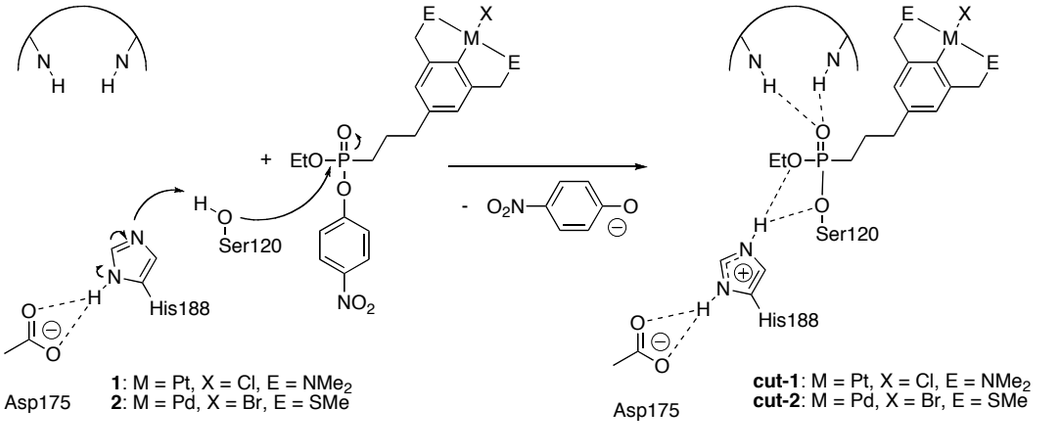

Figuur 3: Single-site covalente binding van ECE-pincermetaal- fosfonaatinhibitoren aan de actieve site van cutinase.

In dit proefschrift wordt deze inhibitieeigenschap van organometaalfosfonaten[9, 10] aan lipasen verder uitgebuit en worden de daaruit resulterende organometaal enzymhybriden toegepast in diverse richtingen: voor structurele studies van de hybriden zelf (*Hoofdstuk 2*), voor kinetische studies van het inhibitieproces (*Hoofdstuk 3*), voor de studie van de coördinatie-eigenschappen van het gebonden organometaalcentrum (*Hoofdstuk 4*), voor de katalytische eigenschappen van de hybriden (*Hoofdstukken 2* en *8*) en tenslotte voor proteïnemarkeringsstudies (*Hoofdstuk 6*).

In *Hoofdstuk 1* wordt een actueel literatuuroverzicht gegeven van bekende bioorganometaalpincercomplexen. Mede op grond van hun excellente stabiliteit worden ECE-pincermetaalcomplexen nu gebruikt als anticarcinogene stoffen, als Surface Plasmon Resonance verbeteraars in studies van koolhydraat-proteïne interacties, als bouwstenen in de supramoleculaire chemie van koolhydraten en peptiden, als peptidebiomarkers en katalysatoren en in de ontwikkeling van pincermetaal-proteïnehybriden. Deze verscheidenheid van chemie en toepassingsmogelijkheden van bioorganometaal ECE-pincercomplexen waren mede de reden om de studie van de organometaal-(serine hydrolase)hybriden als uitgangspunt voor hetgeen in dit proefschrift beschreven staat te kiezen.

In *Hoofdstuk 2* worden vijf kristalstructuren beschreven van covalent gemodificeerde cutinases met twee verschillende ECE-pincermetaal-fosfonaatinhibitoren (Figuur 4). De twee ECE-pincer metaalcomplexen werden in het proteïne geïntroduceerd door site-selectieve inhibitie en de kristalstructuren bevestigen onomstotelijk eerdere studies dat de inhibitoren selectief aan het Ser120 residu van de actieve site van cutinase gebonden zijn.

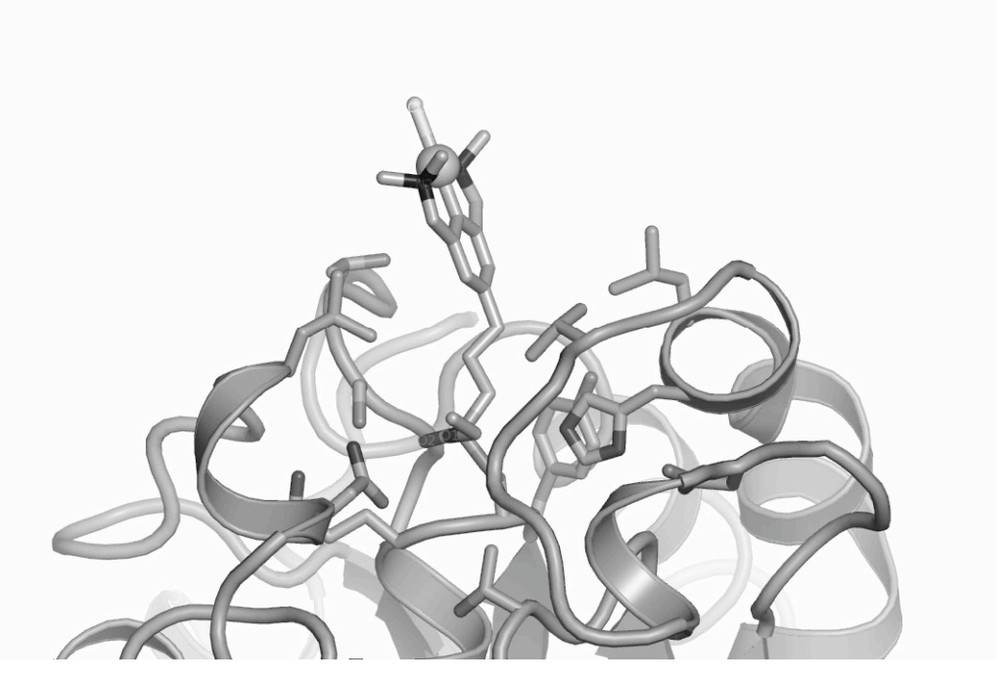

Figuur 4: Deel van de moleculaire structuur van een NCN-pincerplatina-cutinasehybride (**cut-1**) in de vaste stof (X-raystructuuurbepaling).

In ieder van de vijf kristalstructuren bevindt de ECE-pincer platina- of palladiumkopgroep zich aan het oppervlak van de actieve site van het cutinasemolecuul (zie Figuur 4) en is daardoor blootgesteld aan het omringende oplosmiddel. Afhankelijk van de ECE-metaalgroep bezetten de ECE-pincer-platina en palladium fosfonaatgastmoleculen verschillende pockets in de actieve site van cutinase, met de daaruit resulterende, tegengestelde configuratie van het fosforatoom: voor de NCN-pincerplatina hybride (**cut-1**) S_P en voor de SCS-pincerpalladium hybride (**cut-2**) R_P. Kristallisatie van het NCN-pincerplatina cutinasehybride (**cut-1**) onder

halidearme condities resulteerde in de kristallisatie van een nieuwe, metaalgeïnduceerde dimere structuur die bestaat uit twee cutinasegebonden platinakopgroepen, die onderling verbonden zijn door een enkele μ-Cl-brug. Het is spannend om voor het eerst te kunnen zien dat coördinatiechemie met proteïnegemodificeerde overgangsmetaalcomplexen mogelijk is. Verder kon de aanwezigheid van de NCN-pincerplatina kopgroep in **cut-1** als site-selectief faseringspunt in het eiwit gebruikt worden. Hierdoor wordt het faseren van ruwe proteïnediffractiedata vergemakkelijkt, hetgeen de potentie van de pincerplatina kopgroep als zware metalen marker voor het faseren van ruwe diffractiedata in de eiwitkristallografie laat zien.

In *Hoofdstuk 3* wordt het resultaat van het onderzoek van het bindingsproces van de twee verschillende enantiomeren van de fosfonaat-pincerracematen **1** en **2** (Figuur 2) aan cutinase beschreven. Een ^{31}P NMR studie liet zien dat na toevoeging van stoïchiometrische hoeveelheden van de NCN-pincerplatina- (**1**) of de SCS-pincerpalladiuminhibitor (**2**) aan cutinase de beide diastereoisomeren gevormd worden. Daarentegen werd uitsluitend één van de diastereoisomeren gevormd toen 2.5 equivalenten van deze inhibitoren werd toegevoegd. Een kinetische studie gebaseerd op de vorming van de *para*-nitrofenolaatgroep gedurende de inhibitie van cutinase liet zien dat inhibitoren **1** en **2** een verschillend kinetisch inhibitiegedrag vertonen, en de aanwezigheid van de tegengestelde configuratie aan het geïnhibeerde fosforatoom in de kristalstructuren van respectievelijk **cut-1** en **cut-2** in *Hoofdstuk 2* kan verklaren.

In *Hoofdstuk 4* wordt een coördinatiestudie van een kationisch NCN-pincer platinacutinasehybride met verschillende fosfines beschreven. Analyse van NMR-spectroscopische en ES-massaspectrometrische data bewezen dat het metaalcentrum in **cut-1** toegankelijk is voor de coördinatie van fosfineliganden in waterige milieus. De sterkte van de coördinatie en het aantal coördinerende fosfines zijn erg afhankelijk van de sterische hinder en de elektronische eigenschappen van de fosfines zelf en van het omringende cutinase oppervlak. Zelfs fosfineliganden, die niet in water oplosbaar zijn, konden aan het platinacentrum van **cut-1** coördineren; het resulterende **cut-1**-fosfine complex is wateroplosbaar. Deze studie laat duidelijk zien dat het pincermetaalcentrum in deze hybriden beschikbaar is voor de coördinatie van liganden, oplosmiddelmoleculen en dus ook voor substraten. Dit maakt de toepassing van deze pincermetaal-lipasehybriden als, onder andere, abiotische katalysatoren en in diagnostische proteïnestudies mogelijk.

In vervolg op deze coördinatiestudies werd een katalytische studie met de SCS-pincerpalladium-cutinasehybride **cut-2** uitgevoerd, hetgeen wordt beschreven in *Hoofdstuk 5*. Een abiotische C-C koppelingsreactie tussen een boorzuur en een epoxide werd gekatalyseerd met **cut-2** in waterig milieu, waarbij zowel een lineair als een vertakt product werden gevormd (Schema 1).

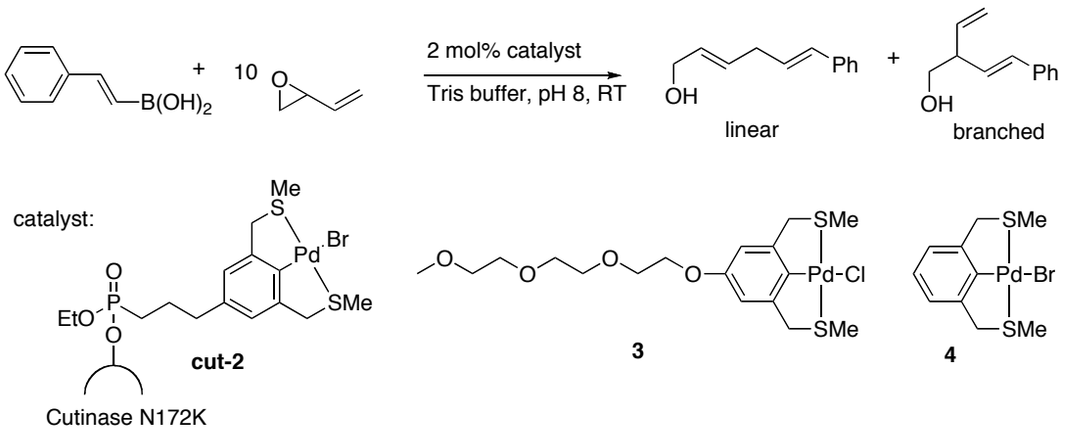

Schema 1: C–C-koppelingsreactie gekatalyseerd door SCS-pincerpalladium-cutinasehybride **cut-2** en SCS-pincer palladiumkatalysatoren **3** and **4**.

De selectiviteit (lineair/vertakt = 4.3) in de reactie gekatalyseerd door de SCS-pincerpalladium-cutinasehybride katalysator **cut-2** was verschillend van de selectiviteiten (lineair/vertakt = 0.4 (**3**) en 2.4 (**4**)) die werden verkregen met de SCS-pincerpalladiumkatalysatoren zelf. Deze resultaten zijn een bewijs voor de invloed die het cutinaseproteïne heeft op de selectiviteit van het gebonden metaalcentrum in **cut-2**. De activiteiten in een gebufferde waterige oplossing waren het hoogst voor katalysator **4** (64% opbrengst). Daarentegen vertoonde de pincer-proteïnehybridekatalysator **cut-2** een gemiddelde activiteit (31%) terwijl de wateroplosbare katalysator **3** een lage activiteit (12%) toonde.

In *Hoofdstuk 6* wordt de synthese van een nieuwe luminescente biomarker beschreven, die gebaseerd is op het gebruik van een luminescent NCN-pincerplatina organometaalcomplex (Figuur 5).

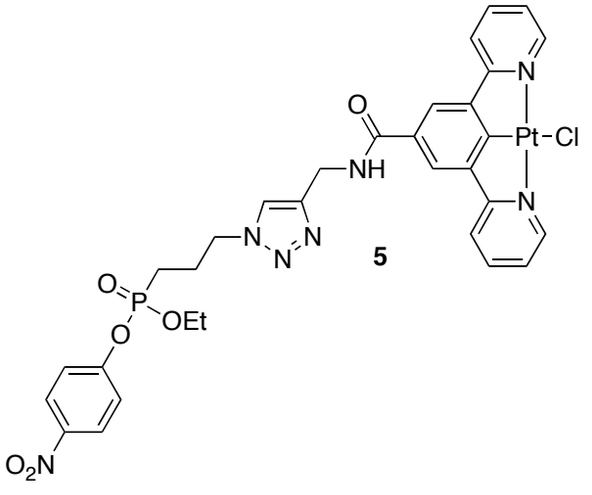

Figuur 5: Structuur van het luminescente organometaalcomplex **5**, dat gebruikt is voor het markeren van lipasen.

Het luminescente organometaal gedeelte werd door middel van clickchemie aan het fosfonaat gekoppeld, met behoud van de reactieve *para*-nitrofenolaatgroep. Complex **5** werd met succes voor het irreversibele, covalente markeren van verschillende lipasen gebruikt en de resulterende hybriden werden geanalyseerd met behulp van SDS PAGE gelelectrophorese. Het luminescente NCN-pincerplatinagedeelte bleek stabiel onder de gebruikte electrophoresecondities. Dit toont de veelzijdigheid van het luminescente fosfonaat **5** die verder het gebruik van **5** in verdere proteïnediagnosestudies met andere serine hydrolasen mogelijk maakt.

In *Hoofdstuk 7* wordt de coördinatie van een fluorescent stilbazool aan de kationisch NCN-pincerplatinacomplexen **[6]X** beschreven (Figuur 6).

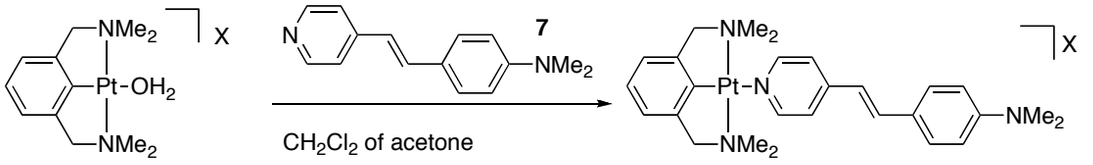

[6]X: X = OTf of BF_4 **[8]X**: X = OTf of BF_4

Figuur 6: Vorming van het stilbazool-pincer coördinatiecomplex **[8]X**.

Door coördinatie aan het pincermetaalcentrum worden de spectroscopische eigenschappen van het stilbazoolmolecuul beïnvloed, hetgeen resulteert in roodverschuivingen in de absorptie- en emissiespectra van het nieuwe coördinatiecomplex. Coördinatie vindt plaats in dichloormethaan, methanol en aceton, maar in acetonitril kon de vorming van **[8]X** niet worden aangetoond. Deze eerste resultaten laten zien dat meetbare veranderingen van de spectroscopische eigenschappen van het stilbazoolmolecuul door coördinatie aan het platinacentrum van **[6]**$^+$ optreden, hetgeen bruikaar zou kunnen zijn bij de ontwikkeling van nieuwe luminescente diagnostische en sensormaterialen.

De synthese en site-specifieke immobilizatie van de racemisatiekatalysator **[9]Cl** op lipasebeads (zie Figuur 7) wordt beschreven in *Hoofdstuk 8*.

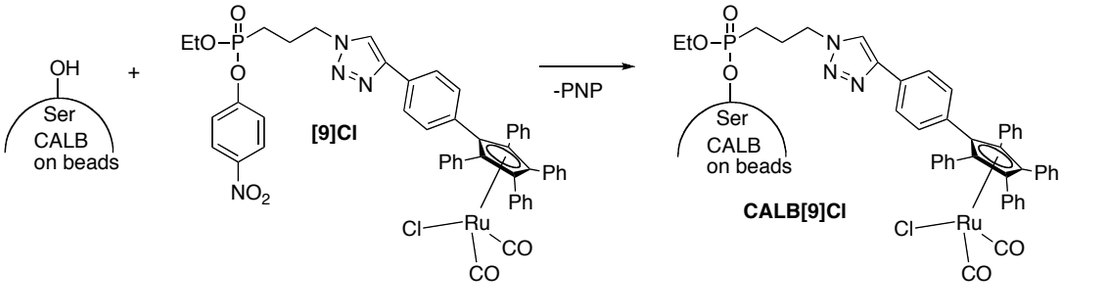

Figuur 7: Immobilisatie van de racemisatiekatalysator **[9]Cl** op lipasebeads resulterend in **CALB[9]Cl**.

Door de aanwezigheid van het nucleofiele serine residu in de actieve site van CALB dat is geïmmobiliseerd op de beads kon complex **[9]Cl** direct op de vaste drager gebonden worden. Omdat de toegankelijkheid van de CALB actieve sites op het dragermateriaal minder is dan voor CALB in oplossing, was de inhibitie niet volledig. Een bepaling van de oppervlaktelading liet zien dat een belading van ongeveer 0.0125 mmol [Ru]/g beads bereikt kon worden. Het verkregen geïmmobiliseerde semi-synthetische CALB complex **CALB[9]Cl** werd vervolgens gebruikt voor de racemisatie van een secundair alcohol: complete racemisatie werd bereikt in 24 uur. Door de onvolledige inhibitie van de CALB beads werd de lipaseactiviteit van de beads gedeeltelijk behouden. Van dit gegeven werd gebruik gemaakt in een cascadereactie waarin het **CALB[9]Cl**-CALB hybridenmateriaal als cascadekatalysator in een Dynamische Kinetische Resolutie studie (DKR) fungeerde: De rutheengeïnhibeerde sites katalyseren de racemisatie terwijl de vrije CALB-sites de enantioselectieve vorming van het geacyleerde product katalyseert hetgeen resulteert in de kinetische resolutie (99% ee) van het racemische alcohol met 18% opbrengst.

In dit proefschrift werd de immobilizatie van verschillende fosfonaatgefunctionaliseerde organometaalcomplexen in de actieve site van lipasen beschreven. De resulterende organometaal-lipasehybride materialen werden toegepast in structurele, coördinatie, katalytische en proteïnemarker studies. De resultaten tonen de veelzijdigheid van deze systemen en wijzen in de richting van nieuwe toepassingsmogelijkheden door verdere studies in proteomics, homogene katalyse en supramoleculaire chemie. Door de unieke stabiliteit en de structurele en elektronische eigenschappen van pincermetaalcomplexen uit te buiten, kan bijvoorbeeld gedacht worden aan paramagnetische pincercomplexen die door inhibitie aan proteïnen gebonden worden voor mapping van active sites, aan cascadereacties die leiden tot "groene(re)" organische syntheseroutes en aan toepassingen voor de constructie van nieuwe materialen met nieuwe combinaties van eigenschappen.

Referenties

1. Crabtree, R. H., *The Organometallic Chemistry of the Transition Metals*. Wiley: New York, 1988; p 1-422.
2. Elschenbroich, C.; Salzer, A., *Organometallics*. VCH: Weinheim, 1992; p 1-495.
3. Albrecht, M.; van Koten, G., *Angew. Chem. Int. Ed.* **2001,** 40, 3750-3781.
4. Slagt, M. Q.; Rodriguez, G.; Grutters, M. M. P.; Klein Gebbink, R. J. M.; Klopper, W.; Jenneskens, L. W.; Lutz, M.; Spek, A. L.; van Koten, G., *Chem. Eur. J.* **2004,** 10, 1331-1344.
5. Stiriba, S.-E.; Slagt, M. Q.; Kautz, H.; Klein Gebbink, R. J. M.; Thomann, R.; Frey, H.; van Koten, G., *Chem. Eur. J.* **2004,** 10, 1267-1273.
6. Slagt, M. Q.; Stiriba, S.-E.; Klein Gebbink, R. J. M.; Kautz, H.; Frey, H.; van Koten, G., *Macromolecules* **2002,** 35, 5734-5737.
7. Kleij, A. W.; Gossage, R. A.; Jastrzebski, J. T. B. H.; Boersma, J.; van Koten, G., *Angew. Chem. Int. Ed.* **2000,** 39, 176-178.
8. Mehendale, N. C.; Sietsma, J. R. A.; de Jong, K. P.; van Walree, C. A.; Klein Gebbink, R. J. M.; van Koten, G., *Adv. Synth. Catal.* **2007,** 349, 2619-2630.
9. Kruithof, C. A.; Casado, M. A.; Guillena, G.; Egmond, M. R.; van der Kerk-van Hoof, A.; Heck, A. J. R.; Klein Gebbink, R. J. M.; van Koten, G., *Chem. Eur. J.* **2005,** 11, 6869-6877.
10. Kruithof, C. A.; Casado, M. A.; Guillena, G.; Egmond, M. R.; van der Kerk-van Hoof, A.; Heck, A. J. R.; Klein Gebbink, R. J. M.; van Koten, G., *Eur. J. Inorg. Chem.* **2008,** 27, 4425-4432.

GRAPHICAL ABSTRACT

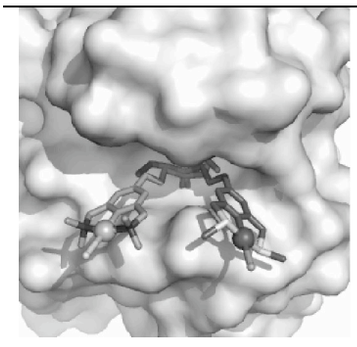

Chapters 2 + 3

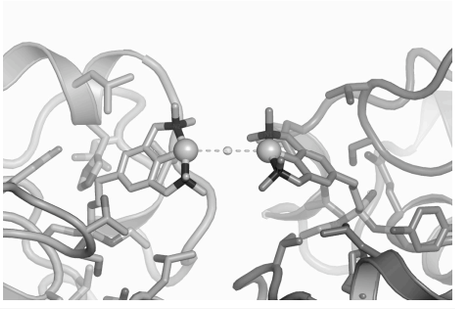

Chapter 4

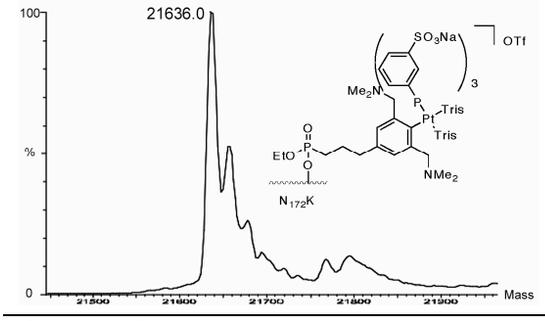

Chapter 7

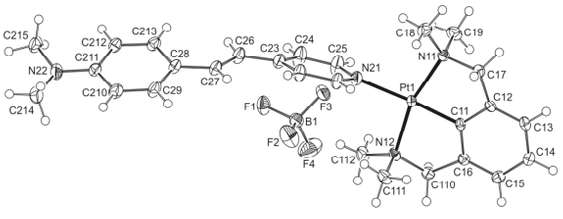

Chapter 5

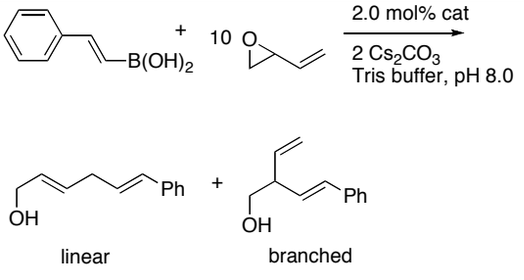

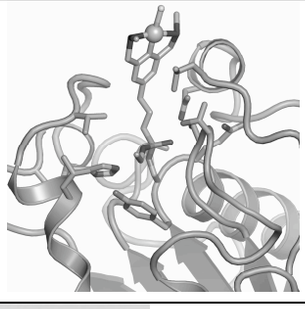

Chapter 6

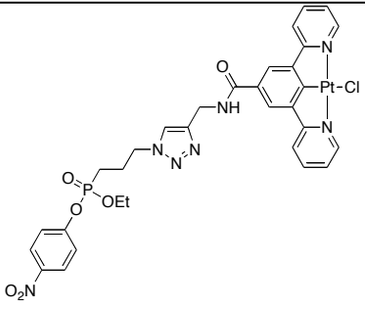

Chapter 8

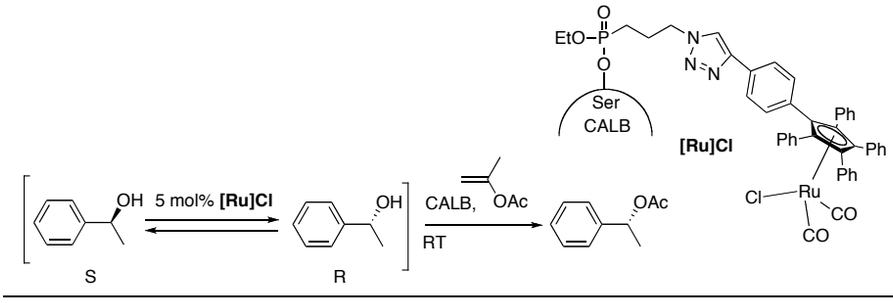

BEDANKT!

Het boekie is af! Na 4 jaar en nog een beetje meer hard werken is het dan eindelijk zover. Gelukkig heb ik niet alles alleen hoeven doen – en bij deze wil ik degenen, die aan dit proefschrift hebben bijgedragen, bedanken.
Allereerst mijn drie promotoren prof. dr. Gerard van Koten, prof. dr. Bert Klein Gebbink, prof. dr. Maarten Egmond en dr. Harm Dijkstra. Het was een erg uitdagende en spannende taak om als organicus het terrein van de proteïnchemie te betreden en jullie expertise en input vanuit verschillende disciplines heeft ervoor gezorgd dat dit onderzoeksproject succesvol is verlopen.
Beste Gerard, jouw inspirerende visie op de chemie van proteïnen heeft me steeds weer gemotiveerd om toch nog die ene extra meting te doen - en nu ben ik blij dat ik het allemaal toch gedaan heb. Je oog voor details en de algehele rode lijn waren een grote hulp gedurende de afgelopen jaren – en ik heb niet alleen op chemisch gebied veel van je geleerd.
Beste Bert, vaak heb jij mijn resultaten vanuit een heel ander perspectief bekeken en mij hierdoor behoorlijk aan het denken gezet. Jouw scherpe kijk op de manuscripten en de opbouw van mijn onderzoek zijn onmisbaar geweest. Gelukkig kon ik altijd kort even binnen komen vallen om het een en ander te vragen, wat van tijd tot tijd erg handig was. Ik wens je veel succes in de toekomst in het leiden van de groep.
Beste Maarten, zonder jouw input en advies over met name enzymactiviteit, -structuur en -kinetiek zou ik nu nog steeds op het lab zitten. Juist door jouw iets andere visie op de wetenschappelijke feiten heb jij mij geïnspireerd tot experimenten en metingen, die ik zelf waarschijnlijk nooit zou hebben bedacht, en dit heeft dit onderzoek stukken sterker gemaakt. De proteïnchemie is en blijft inspirerend en jij was een uitstekende 'gids'.
Beste Harm, jij hebt een erg belangrijke rol gedurende en in de afrondende fase van het onderzoek gespeeld. Jij wist op de belangrijke momenten altijd de knoop door te hakken en had altijd ontzettend handig praktisch advies toen ik het zelf niet meer wist. Dat jij in de laatste maanden naast je nieuwe baan ook nog in je vrije tijd mijn proefschrift ging corrigeren is zeker bijzonder te noemen – jij was onmisbaar en ik ben je erg veel dank verschuldigd!

Interdisciplinair onderzoek is erg afhankelijk van goede samenwerkingen, en gelukkig heb ik er gedurende mijn promotieonderzoek in Utrecht een paar enthousiaste samenwerkingspartners gehad:
Allereerst is er de uiterst succesvolle samenwerking met prof. dr. Piet Gros, dr. Lucy Rutten, dr. Martin Lutz, Jean-Paul Mannie en prof. dr. A.L. Spek te noemen. Door jullie enthousiasme en inzet werden de eerste kristalstructuren van een proteïne gemodificeerd met een pincercomplex verkregen – en dit is toch wel erg speciaal te noemen. Lucy, ik heb van jou erg veel over eiwitkristallografie geleerd en onze gezamenlijke sessies voor de UNIX machines zullen mij nog lang bijblijven, ik wens je in ieder geval veel succes in de toekomst met je nieuwe baan in Utrecht. Martin en Ton, wij kunnen ons in Utrecht erg gelukkig prijzen met de uitstekende kleine moleculen kristalstructuuranalysefaciliteiten – dank voor het oplossen van de diverse structuren.
De groep van prof. dr. Albert Heck wil ik graag bedanken voor de uitstekende samenwerkingen op het gebied van de eiwit-massaspectrometrie, en dan met name Cees Versluys en Anka van der Kerk-van Hoof. Beste Cees, ik heb erg veel over eiwit-MS geleerd van jou en de mooie MS resultaten in hoofdstuk 4 zijn vooral aan jou te danken.

Jag vil gärna tacka prof. dr. Jan-Erling Bäckvall, Annika Träff och Patrik Krumlinde för vårs fantastikt DKR samarbete. Jag fick et varmt välkommen, då jag var i Stockholm och i en relativ kort tid har vi producered manga resultater. Annnika, jag önsker dig mycket succé med fortsättningen av projektet, din licentiat og resten av din PhD – när du er i Skåne eller Köpenhamn de näste gang skal vi dricka lite kaffe.

Een goedgevuld proefschrift is natuurlijk niets zonder de bijdrage van enkele studenten, met name Thijmen van Klei, Thomas Klimeck en Bart Lemcke. Jongens, zonder jullie enthousiasme voor de bioorganometaalchemie en jullie synthetische inzet op het lab was dit boekje een stuk dunner geweest! Ik heb een erg leerzame, intensieve, maar vooral leuke tijd met jullie op het lab doorgebracht en ik wens jullie veel succes met jullie banen en/of vervolgstudies in de toekomst.

Henk, Johann en Ed, jullie hebben ervoor gezorgd dat alle machines, computers en apparatuur vlekkeloos functioneerden en dat de chemicaliën daar te vinden waren waar ze behoorden, jullie hebben ons AIOs het leven stukken makkelijker gemaakt ;). Johann, dankzij jouw enthousiasme heeft deze wereld een Mac-fanaat meer. En Henk, ik mis je grappen aan de koffietafel toch wel een beetje…
Margo, Milka, Hester, Irene zonder jullie secretariële diensten en hulp met alle formulieren was ik waarschijnlijk al lang het overzicht kwijtgeraakt. Bedankt voor jullie hulp en de opbeurende praatjes tussendoor.
Een grote dank gaat ook uit naar de altijd behulpzame en vriendelijke medewerkers van de AV-dienst en de glasblazerij – zonder fatsoenlijke kleurenposters en degelijk glaswerk ben je als AIO verloren ☺.

En nu komt een groot dankjewel aan alle leden van de SOC/FOC/CBOC/TOC groep, die mijn lableven gedurende de afgelopen jaren tot een onvergetelijke ervaring hebben gemaakt. Met sommigen van julllie had ik dagelijks intensief 'chemisch' en persoonlijk contact, anderen ging ik alleen '1e-jaars-student-biochemie-vragen' stellen (lieve mensen van de westvleugel - bedankt voor jullie geduld!) en met anderen had ik vooral leuke gesprekken aan de koffie/borreltafel:
Catelijne, Marianne, Marcella, Preston (miss you, beaver ☺), Alexsandro, Kees (bedankt voor de informatieoverdracht in het 1e jaar), Aidan, Alexey, Monika (good luck in Germany!), Guido, Erwin, Nilesh, Iréna, Bart, Yves (merci pour nos longues conversations, ça m'a motivé de continuer ;)), Sylvestre, Pieter, Silvia, Jeroen, Jérôme, Jie (thanks for accepting somebody doing aqueous chemistry next to your very sensitive lithiations☺), Judith, Kamil, Maaike, Marcel, Peter, Rob K, Thomas, Dennis (de beste wensen voor Lausanne!), Niels (succes met de afronding), Thies, Nesibe (all the best for the future), Berth-Jan, Leo, Jacco, Layo, Jan, prof. dr. Antoinette Kilian, dr. Eefjan Breukink, Erica, Tania, Jacques (le premier français qui boit pas de vin…), Yvonne, Marlies, Martijn, Diana, Chris, Irene, alle studenten en alle anderen, die ik ben vergeten…
Verder wil ik nog alle collega's van de 'pinke' verdieping (= 6 Noord) bedanken voor hun hulp met mijn alledaagse, kleine biochemische probleempjes – jullie wetenschappelijk advies was erg handig en de borrels erg gezellig! Pavel, I wish you all the best in Cambridge & Per, ohne Dich wäre das Gel nie was geworden!
Elena, we have been soul mates (or partners in crime?) during the last few years – grazie mille and all the best for the future. Now that all of this will be over soon, we should have some good wine (or was it Jägermeister?) again. Morgane, après avoir passé plusieurs années au

labo ensemble, ça me fait vraiment plaisir de t'avoir comme paranimf. Je te souhaite bonne chance avec ta propre thèse aussi et j'espère de te revoir tôt ou tard quelquepart en Europe ☺.

En dan nog een bedankje aan de diverse (ex-)protonezen. Lief 'ondersteboven' bestuur, de laatste jaren zagen we elkaar vaker op housewarmings- en verjaardagsfeesten dan op de aloude bestuursetentjes – maar dat maakt ook niet uit. Ik vind het geweldig, dat wij nog steeds contact houden en hoop dat dit lang zo blijft! Rudy, ik vind het geweldig dat je wilt 'paranimferen' en mij moreel gaat supporten op deze belangrijke dag. De afgelopen jaren in de OLC commissie waren erg gezellig – met name de vergaderingen (of waren het borrels?), ik hoop dat wij elkaar nog af en toe terugzien op de diverse activiteiten.

J'aimerais bien remercier tous les gens de Strasbourg – JB, Magno, Alexandre, Sara, Lisa, Lena, Woj, Iris, Kostis, Emilie, Krisztina, Dave et tous les autres pour leur compagnie pendant les dernières années et j'espère de garder le contact avec vous/de vous revoir un de ces jours quelquepart dans le monde ☺.
Lieve Club 14 leden, ik vond de kerstdiners erg gezellig. Maartje, als je de volgende keer op de reis naar Wietske een tussenstop wilt maken, zijn jullie van harte welkom hier.
Katja, ich find's echt enorm mutig von Dir einfach nach Tel Aviv auszuwandern – hoffe, dass wir uns irgendwann mal wieder sehen und bin enorm gespannt, wo das denn sein wird ☺

Marijke, Christiaan, Peter, Tom, Ellen, Mathilde, Diewke en Els – met zulke gezellige huisgenoten was het soms moeilijk om in plaats van in de keuken te gaan zitten naar mijn kamer te gaan en artikelen te lezen of te schrijven – jullie waren de ideale ontspanning ☺. Met de dames hoop ik nog veel chaotische weekendtripjes mee te maken. Van aftandse caravans, over kano's gevuld met kaas tot veganistisch meditatie-eten en vieze Churros hebben we nu zo ongeveer alles al meegemaakt, maar de hamvraag is natuurlijk nog steeds: Waar is die reisgids nou gebleven???

And then a very special thanks to all the guys who have made the last few years in Utrecht so much more bearable when my molecules were refusing to do what I wanted them to. Henri, Pierre-O, Steve, Emil, Marcin, Teemu and Elena, I have learned more about Finnish dance music, French Rugby players, metrosexual shoes, computer games, Polish hair care products & finances, dating women and Swedish people dancing than I ever wanted to know – but I had a great time listening to your stories and enjoying your company. I could always call one of you for a coffee/beer when the chemistry drove me crazy and that meant a lot to me - thanx.

Alex, for fem år siden tog vi den forkerte metro i Sankt Petersborg, og nu er du min vært – yderst usandsynligt rent statistiskt, men sjovt! Du var en stor hjælp i begyndelsen af eventyret i København, mange tak for det. Jeg ønsker dig det bedste i fremtiden (engang imellem kan det *umulige* ske!) og jeg håber at vi snart kan tage en Malmø-tur igen – denne gang uden Mr. TomTom, men til gengæld med øl eller GinT. Og hvis du behøver en printer, nogle hasselnødder eller en ny mobiltelefon igen, så kommer du bare forbi ☺.
Estevao, I can't wait to see Big Rock & Candy Mountain with you again – If not in CPH then in Barceló – Cuándo vienes la próxima vez? Lara, I wish you all the best for the future with your little daughter and work – the next time I'm around Zagreb, I will definitely pass by. Kylli, ik wens je veel succes in Nederland.

Flemming, jeg vidste ikke at renovere en lejlighed kunne være så sjovt – at male var den ideelle og hyggelige afslapning fra alt skriveriet – håber at vi ses snart igen til et glas rødvin ☺. Stefan, Svanhvit, Allan, Lena, Ulrik, Tom, Anne Katrine - tak for den dejlige tid ude i byen – København er meget hyggligere med folk som jer ☺. Og Stefan: Næste år Roskilde igen (men den gang *alle* dager...)!

Und schliesslich für alle 'Daheimgebliebenen': In de letzten Jahren war ich entweder aufm Labor oder auf Achse und deswegen viel zu wenig in Köln, Ludwigshafen, Schwetzingen oder Erlangen und leider wird sich das in der näheren Zukunft auch nich ändern. Es war für euch wahrscheinlich etwas schwer zu verstehen, warum ich denn schon wieder das ganze Wochenende aufm Labor oder vorm Computer sitzen musste, aber dieses Büchlein liess sich eben nicht von selbst schreiben... Danke für die moralische Unterstützung und euer Verständnis während der letzten Jahre. Die Familienfeiern/-grillfeste/-geburtstage waren eine sehr willkommene Abwechslung vom Alltag (auch *ohne* armenischem Cognac...) und ich hoffe, dass wir uns noch regelmässig alle zusammen sehen werden, in Dänemark, Deutschland oder irgendwo.
En tenslotte: Lieve Sip, dankjewel!

Vi ses i København,

Birgit

CURRICULUM VITAE

De schrijfster van dit proefschrift werd geboren op 4 maart 1980 te Mainz, Duitsland. Haar schooltijd bracht zij door in Duitsland en Nederland, waarna zij in 1999 haar eindexamen (Abitur) behaalde aan het Emil-von-Behring Gymnasium in Erlangen-Spardorf, Duitsland. In hetzelfde jaar begon zij met de studie Scheikunde aan de Universiteit Utrecht. Na een Bachelor Thesis in kleine moleculen Kristallografie (Dr. H. Kooijman, Prof. A.L. Spek) en een Master Thesis in de Organometaalchemie (Prof. G. van Koten, Prof. R.J.M. Klein Gebbink) verbleef de schrijfster zes maanden aan de Université Louis Pasteur in Strasbourg, Frankrijk voor een onderzoeksstage in de Bioorganometaalchemie (Dr. M. Pfeffer, Dr. C. Sirlin). In augustus 2004 werd de Master of Science degree behaald met het judicium *cum laude*.

Van september 2004 tot september 2008 verrichtte de schrijfster het in dit proefschrift beschreven promotieonderzoek in de vakgroep Chemische Biologie & Organische Chemie onder supervisie van Prof. G. van Koten, Prof. R.J.M. Klein Gebbink en Prof. M.R. Egmond. Een gedeelte van dit onderzoek bestond uit een gezamenlijk project met de onderzoeksgroep Organische Chemie van de Universiteit Stockholm, Stockholm, Zweden (Prof. J.-E. Bäckvall). Het hier beschreven onderzoek werd op verschillende nationale en internationale bijeenkomsten gepresenteerd, zoals de 'Netherlands' Chemistry and Catalysis' Congressen, het '7th European Symposium of the Protein Society' (Stockholm, Zweden) en '4th International Symposium on Bioorganometallic Chemistry' (Missoula, USA). Sinds 1 April 2009 is de schrijfster werkzaam als PostDoctoral Scientist voor Novo Nordisk A/S in Måløv, Denemarken.

The author of this thesis was born on March 4th, 1980 in Mainz, Germany. After schooling in Germany and the Netherlands, she graduated from high school at the Emil-von-Behring Gymnasium in Erlangen-Spardorf, Germany in 1999. That same year she started studying Chemistry at Utrecht University, the Netherlands. After a Bachelor Thesis in small molecule Crystallography (Dr. H. Kooijman, Prof. A.L. Spek) and a Master Thesis in Organometallic Chemistry (Prof. G. van Koten, Prof. R.J.M. Klein Gebbink), the author spent six months at the Université Louis Pasteur in Strasbourg, France for a research project on Bioorganometallic Chemistry (Dr. M. Pfeffer, Dr. C. Sirlin). In August 2004 she obtained her MSc degree with honours.
From September 2004 until September 2008 the author worked as a PhD student in the Chemical Biology and Organic Chemistry group at Utrecht University under supervision of Prof. G. van Koten, Prof. R.J.M. Klein Gebbink and Prof. M.R. Egmond on the research described in this thesis. Part of this research was performed as a joint collaboration with the Organic Chemistry group at Stockholm University, Stockholm, Sweden (Prof. J.-E. Bäckvall). The research described in this thesis was presented at several national and international Conferences including the 'Netherlands' Chemistry and Catalysis' Conferences, the '7th European Symposium of the Protein Society' (Stockholm, Sweden) and the '4th International Symposium on Bioorganometallic Chemistry' (Missoula, USA). Since April 1st 2009, the author has been working as a PostDoctoral Scientist for Novo Nordisk A/S in Måløv, Denmark.

LIST OF PUBLICATIONS

1. *Incorporating ECE-pincer metal complexes as functional building blocks in semisynthetic metalloenzymes, supramolecular polypeptide hybrids, tamoxifen derivatives, biomarkers and sensors* Wieczorek, B.; Dijkstra, H.P.; Egmond, M.R.; Klein Gebbink, R.J.M.; van Koten, G. *Journal of Organometallic Chemistry* **2009**, 694, 812-822 (Special Issue on Bioorganometallic Chemistry, Chapter 1 of this thesis)
2. *Solid-State Structural Characterization of Cutinase-ECE-Pincer-Metal Hybrids* Rutten, L.; Wieczorek, B.; Mannie, J.-P.B.A.; Kruithof, C.A.; Dijkstra, H.P.; Egmond, M.R.; Lutz, M.; Klein Gebbink, R.J.M.; Gros, P.; van Koten, G. *Chemistry - A European Journal*, **2009**, 15, 4270-4280 (Chapter 2 of this thesis)
3. *A recyclable nanosize aminoarenethiolato copper(I) catalyst for C-C coupling reactions* Arink, A. M.; Van de Coevering, R.; Wieczorek, B.; Firet, J.; Jastrzebski, J. T. B. H.; Klein Gebbink, R. J. M.; van Koten, G. *Journal of Organometallic Chemistry* **2004**, 689, 3813-3819.
4. *Charge-transfer interactions in 4-donor 4'-acceptor substituted 1,1-diphenylethenes* Van Walree, C. A.; Kaats-Richters, V. E. M.; Veen, S. J.; Wieczorek, B.; Van Der Wiel, J. H.; Van Der Wiel, B. C. *European Journal of Organic Chemistry* **2004**, 14, 3046-3056.
5. *The binding mode of the ambidentate ligand dicyanamide to transition metal ions can be tuned by bisimidazoline ligands with H-bonding donor property at the rear side of the ligand* Mohamadou, A.; van Albada, G. A.; Kooijman, H.; Wieczorek, B.; Spek, A. L.; Reedijk, J. *New Journal of Chemistry* **2003**, 27, 983-988.
6. *Site-Selective Ser-Hydrolase Labelling with a Luminescent Organometallic NCN-Platinum Complex* Wieczorek, B.; Lemcke, B.; Dijkstra, H.P.; Egmond, M.R.; Klein Gebbink, R.J.M.; van Koten, G. *submitted for publication* (Chapter 6 of this thesis)
7. *Study on the Chiral Preference of Cutinase in the Reaction with ECE-Pincer Metal Phosphonate Inhibitors* Wieczorek, B.; Dijkstra, H.P.; Klein Gebbink, R.J.M.; van Koten, G.; Egmond, M.R. *to be submitted for publication* (Chapter 3 of this thesis)
8. *Coordination Chemistry in Water of a Free and a Lipase-Embedded NCN-Pincer Platinum Centre with Neutral and Ionic Triaryl Phosphines* Wieczorek, B.; Snelders, D.J.M.; Dijkstra, H.P.; Versluis, K.; Heck, A.J.R.; Lutz, M.; Spek, A.L.; Egmond, M.R.; Klein Gebbink, R.J.M.; van Koten, G. *to be submitted for publication* (Chapter 4 of this thesis)

9. *An Abiotic C-C Coupling Reaction Catalyzed by Semisynthetic Pincer-Metalloenzymes* Wieczorek, B.; Klimeck, T.; Dijkstra, H.P.; Egmond, M.R.; Lutz, M.; Spek, A.L.; Klein Gebbink, R.J.M.; van Koten, G. *to be submitted for publication* (Chapter 5 of this thesis)
10. *Coordination of a Stilbazole to Cationic NCN-Pincer Platinum Complexes* Wieczorek, B.; Batema, G.D.; Dijkstra, H.P.; Egmond, M.R.; Lutz, M.; Spek, A.L.; Klein Gebbink, R.J.M.; van Koten, G. *to be submitted for publication* (Chapter 7 of this thesis)
11. *Site-Selective Immobilization of a Racemization Catalyst onto Lipase-containing Beads* Wieczorek, B.; Träff, A.M.; Krumlinde, P.; Dijkstra, H.P.; Egmond, M.R.; Klein Gebbink, R.J.M.; Bäckvall, J.-E.; van Koten, G. *to be submitted for publication* (Chapter 8 of this thesis)

Hormone, Endorphine, Adrenaline, Enzyme
bestimmen den Ablauf auf der Lebensbühne
sie leiten Deine Gefühle, gib Dir keine Mühe,
rein gar nichts kann Dich retten, wetten,
wir sind alle nur chemische Marionetten,
hängen an Desoxyribonucleinsäureketten

(Jazzkantine, ‘Alles nur Chemie’, Album: Geheimrezept)

No tomorrow
Let us stop here
We did some great things
Didn’t we

(Fever Ray, ‘Dry And Dusty’, Album: Fever Ray)

Full Colour Figures Belonging To Chapter 2

Figures 1a + b

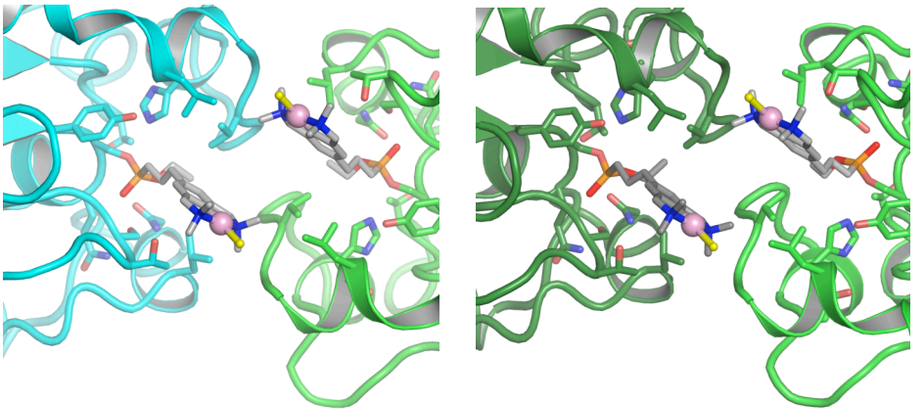

Figure 2

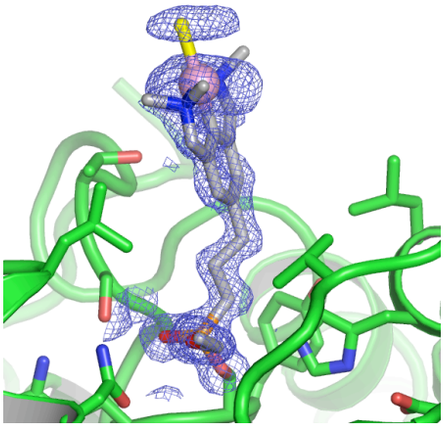

Figure 3

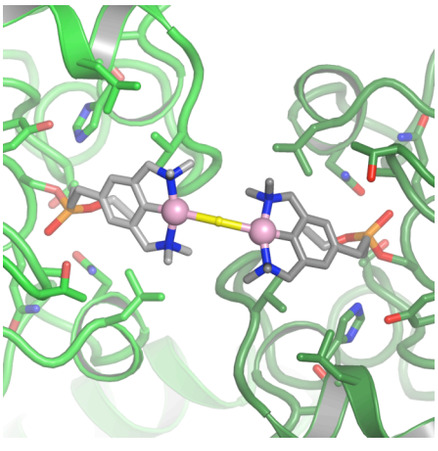

Figure 4

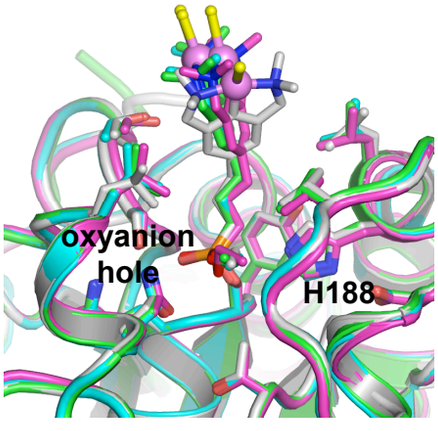

Figure 5

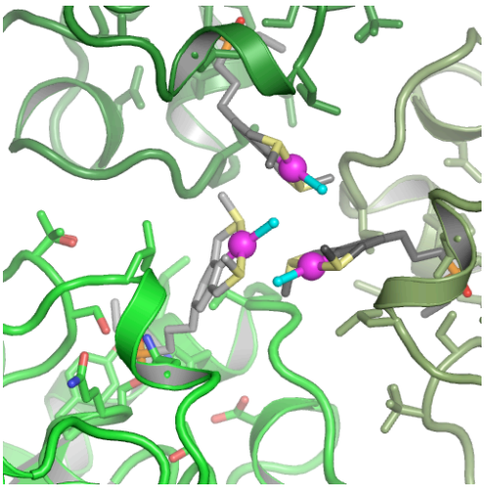

Figures 8 a + b